INTESTINAL ABSORPTION BARRIERS AS MODELLED BY P-GLYCOPROTEIN AND CYTOCHROME P450 3A4 IN CACO-2 CELLS.

CHRISTINE DIEM-CHAU HUYNH TRAN

Doctor of Philosophy

ASTON UNIVERSITY

December 1999

ASTON UNIVERSITY

INTESTINAL ABSORPTION BARRIERS AS MODELLED BY P-GLYCOPROTEIN AND CYTOCHROME P450 3A4 IN CACO-2 CELLS.

CHRISTINE DIEM-CHAU HUYNH TRAN
Doctor of Philosophy
1999

SUMMARY

The passage number and origin of two populations of Caco-2 cells influence their enterocyte-like characteristics. Caco-2 cells of passage number >90 from Novartis pharmaceutical company possess higher levels of expression of alkaline phosphatase and P-glycoprotein and a greater cellular uptake of Gly-L-Pro than those of passage number <40 from the American Type Tissue Culture collection.

High P-gp expressing Caco-2 cells have been developed through stepwise selection of the cells with doxorubicin. This newly-developed cell line (hereafter referred to as Type I) possesses approximately twice as much P-gp protein than non-exposed cells, restricts the transepithelial transport of vincristine in the apical-to-basolateral direction whilst facilitating its transport in the reverse direction and accumulates less vincristine than non-exposed cells. There is no apparent evidence of the co-existence of the multidrug resistance protein (MRP) in Type I cells to account for the above-listed observations. Stopping the exposure for more than 28 days decreases the P-gp protein expression in previously doxorubicin-exposed Type I Caco-2 cells and reduces the magnitude of vincristine transepithelial fluxes in both directions to the levels that are almost similar to those of non-exposed cells.

Exposing Caco-2 cells to 0.25 μM 1α, 25-dihydroxyvitamin D_3 induces their expression of cytochrome P450 3A4 protein to the level that is equivalent to that from isolated human jejunal cells. Under the same treatment, doxorubicin-exposed (Type I) cells metabolise midazolam poorly and less extensively compared to non-exposed cells, suggesting that there is no such co-regulation of P-gp and CYP3A4 in Caco-2 cells. However, there is evidence which suggests CYP3A metabolises midazolam into 1- and 4-hydroxymidazolam, the latter may possibly be a P-gp substrate and is transported extracellularly by P-gp, supporting the hypothesis of P-gp-CYP3A4 synergistic roles in keeping xenobiotics out of the body.

Doxorubicin-exposed (Type I) cells are less effective in translocating L-proline and glycyl-L-proline across the cell monolayers.

Caco-2, P-glycoprotein (P-gp), Vincristine sulphate, Cytochrome P450 3A4 (CYP3A4), Midazolam, L-Proline, Glycyl-L-proline.

ACKNOWLEDGEMENTS

TABLE OF CONTENTS

CHAPTER 2   General materials and methods

CHAPTER 3   Different characteristics of Caco-2 cells as a function of passage number and origin

Chapter 4   Modulation of P-glycoprotein (P-gp) level in Caco-2 cell monolayers: stable and enhanced P-gp expression by doxorubicin

CHAPTER 5   Interplay between intestinal efflux and metabolism as
                   modelled by P-glycoprotein and cytochrome P450 3A in
                   Caco-2 cells

TABLE OF TABLES

TABLE OF FIGURES

CHAPTER ONE

GENERAL INTRODUCTION

ABSTRACT

This chapter provides an overview of intestinal drug absorption, efflux and cytochrome P450 metabolism. The applications of an *in vitro*, enterocyte-like Caco-2 cell model in each of these fields are also reviewed.

1.1 BACKGROUND

The colonic adenocarcinoma (Caco-2) cell model has many applications in drug discovery programmes that are targeted towards the oral route of administration. The cell line not only possesses many structural and functional characteristics similar to those of small intestinal epithelial cells but it is also of human origin which ultimately allows for better prediction of drug absorption in man. In drug discovery process, the Caco-2 cell line has been used to estimate the intestinal permeability of oral drug candidates that are of limited quantities, offers rapid characterisation of new chemical entities (*i.e.* prediction of their oral bioavilability) and are more suitable for automation and for mechanistic studies [Borchardt, 1995]. The cell line, thus, has been used to:

(i)   Elucidate pathways for drug transport in the intestinal mucosa (*i.e.* paracellular *vs.* transcellular transport; passive diffusion *vs.* carrier mediated transport).

(ii)   Determine:

> (a) the structure-transport relationships for carrier-mediated pathways of drug transport and polarised drug efflux
>
> (b) the optimal physical characteristics of drugs for passive diffusion (*i.e.* size, charge, lipophilicity, hydrogen bonding potential, conformation)
>
> (c) the pathways of drug metabolism in the intestinal mucosa
>
> (d) potential toxic effects of drug candidates or formulation components on the intestinal mucosa
>
> (e) how pharmaceutical excipients can influence the transport of drug candidates

(iii)   Evaluate formulation strategies (*i.e.* adjuvants) and chemical strategies (*i.e.* prodrugs)

In addition, this cell line also offers potential for the screening of numerous compounds derived by combinatorial chemistry to select those possessing desirable pharmaceutical (*i.e.* high intestinal permeability) and biological (*i.e.* resistance to enzyme degradation) properties.

However, there are many limitations associated with the Caco-2 cells with regards to their use as a drug absorption model. Firstly, although Caco-2 cells secrete mucins, the level of secretion is low and further reduced upon cellular

differentiation [Niv *et al.*, 1992]. This renders the Caco-2 cell monolayers to be unrealistic model of the gastrointestinal epithelium and is one of many factors which limits the extrapolation of *in vitro* drug permeability to their *in vivo* absorption. Secondly, the electrical resistance and ion-conductance properties of Caco-2 cells resemble those of colonic crypt cells [Grasset *et al.*, 1984]. Drug absorption restricted to the paracellular pathway in Caco-2 cells was found to be lower than in rat ileum [Artursson., 1990]. Thirdly, due to the heterogeneity of Caco-2 cells [Artursson., 1991], different cell origins, passage numbers, culture conditions and previous exposure to drugs lead to different levels of cellular expression of intestinal membrane proteins such as the drug efflux pump P-glycoprotein and an important phase I drug metabolising enzyme, cytochrome P450 3A4 that are associated with the intestinal epithelium *in vivo* [Anderle *et al.*, 1998; Prueksaritanont *et al.*, 1996, Schmiedlin-Ren *et al.*, 1997].

1.2 EPITHELIAL LINING OF THE HUMAN SMALL INTESTINE

The small intestine in humans is a tube about 6.3 m long with a diameter of 2.5 cm. It lies coiled within the abdominal cavity, extending between the stomach and the large intestine, and is arbitrarily divided into three segments: the duodenum (the first 20 cm), jejunum (2.5 m) and the ileum (3.6 m). Structural modifications of the small intestine greatly increase its surface area for absorption. These include:

(i)   Folding of the inner surface of the small intestine which increases the surface area three-fold

(ii)   The presence of villi on the folded surface which gives the lining a velvety appearance and increases the surface area by another 10 times and

(iii)   The hairlike projections microvilli, which arise from the luminal surface of these epithelial cells with each cell having as many as 3,000 to 6,000 of these microvilli.

Altogether, the folds, villi and microvilli provide the small intestine with a luminal surface area 600 times greater than a tube of the same length and diameter lined by a flat surface. The epithelial cells that cover the surface of the villus are joined at the tight junctional complexes which consist of tight junctions where the

adjacent membranes fuse, an intermediate zone and a number of desmosomes. The lateral membranes also infold so that the cells are joined together like a complex jig-saw puzzle [Sherwood, 1997].

Within their luminal brush-border, these epithelial cells possess carriers for absorption of specific nutrients and electrolytes from the lumen as well as intracellular digestive enzymes that digest carbohydrate and protein. Dipping down into the mucosal surface between the villi are shallow invaginations known as the crypts of Lieberkuhn which secrete water and electrolytes. The epithelial cells lining the small intestine slough off and are replaced at a rapid rate as the result of high mitotic activity in the crypts. New cells that are continually being produced at the bottom of the crypts, migrate up the villi and, in the process, push off the older cells at the tip of the villi into the lumen. In this manner, more than 100 million intestinal cells are shed *per* minute. The epithelial lining of the small intestine is replaced approximately every three days [Sherwood, 1997].

1.3   INTESTINAL TRANSPORTERS

The small intestinal transporters are summarised in figure 1.1 [Tsuji and Tamai., 1996]. Of relevance to this project are the human amino-acid transporter, the oligopeptide transporter and P-glycoprotein (MDR1).

FIGURE 1.1 **Intestinal epithelial transporters located on the apical and basolateral membranes identified in animals**

[Adapted from Tsuji and Tamai, 1996]

The transporters shown by square and oval shapes demonstrate active and facilitated transporters respectively. The names of cloned transporters are shown within oval or square shapes. In the case of active transporters, arrows of the same direction represent symport of the substrate and the driving force whilst those going in the reverse direction mean antiport.

Abbreviations: EAAC1: intestinal glutamate transporter (rabbit); PEPT1: di-/tripeptide transporter; SGLT1: human Na^+/glucose transporter; GLUT2 and GLUT5: 2-deoxy-D-glucose and D-fructose transporters respectively; MCT1: monocarboxylic transporter; MDR: multidrug resistance efflux pump (P-glycoprotein), SCFA: short-chained fatty acids.
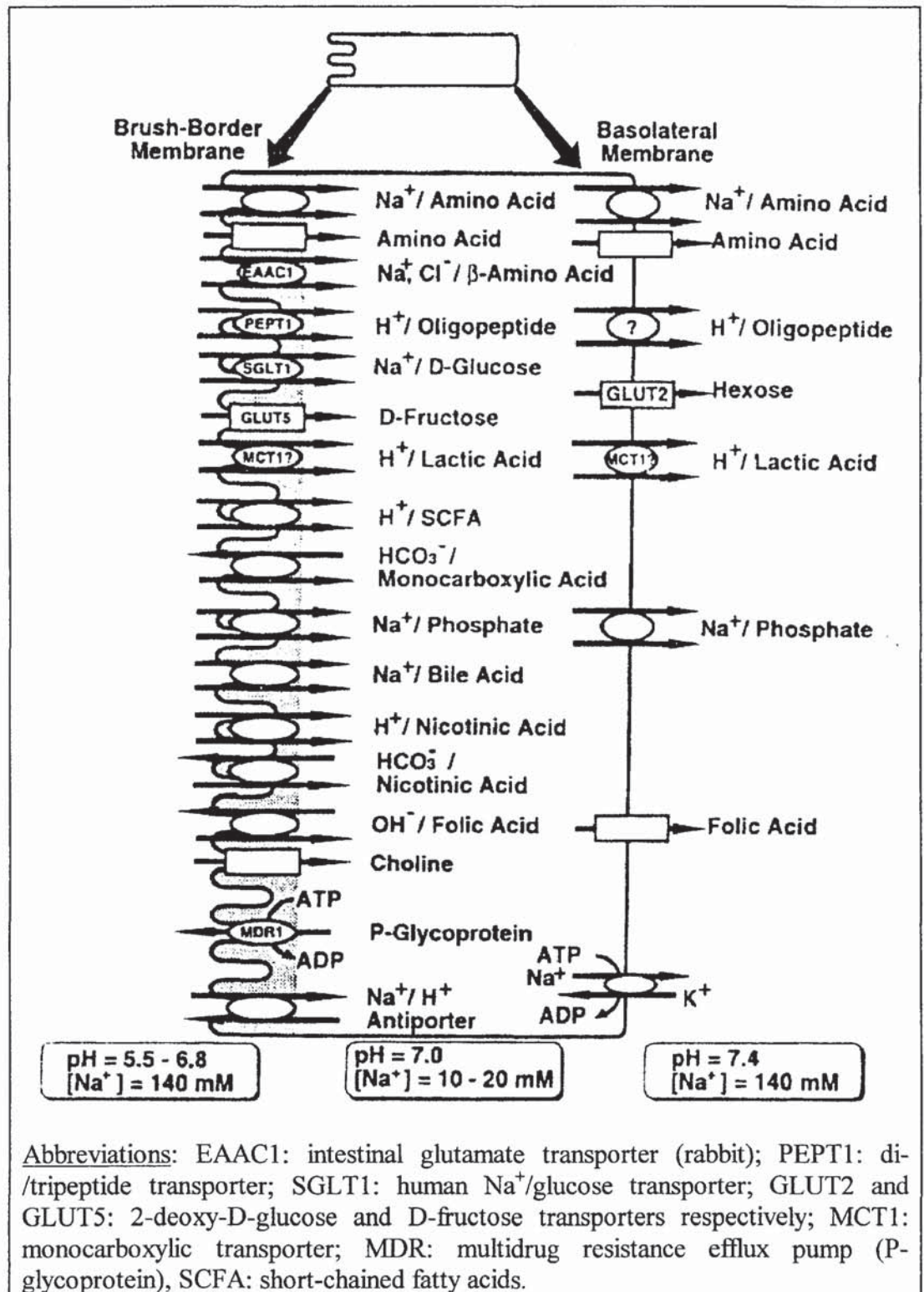
1.4   CLASSIFICATION OF AMINO-ACID TRANSPORTERS

The multiple amino-acid intestinal transport systems are classified according to their substrate specificity, cross inhibition profile with other amino-acids and their position in either the apical or basolateral membrane. A summary of different transport systems for amino-acids in the brush-border and basolateral membranes of the small intestine are presented in tables 1.1 and 1.2 respectively [Ganapathy *et al.*, 1994]

TABLE 1.1   **Different intestinal brush-border transport systems for amino-acids**

[Adapted from Ganapathy *et al.*, 1994]

Transport system	Substrates	Dependence on Na^+ gradient	Involvement of other ions
B	Dipolar α-amino-acids	Yes	None
$B^{0,+}$	Dipolar α-amino-acids	Yes	None
	Basic amino-acids		
	Cysteine		
$B^{0,+}$	Dipolar α-amino-acids	No	None
	Basic amino-acids (i.e. lysine)		
	Cysteine		
Y^+	Basic amino-acid	No	None
IMINO	Imino-acids (proline, hydroxyproline and pipecolic acid)	Yes	Cl^-
β	β-amino-acids	Yes	Cl^-
X^-_{AG}	Acidic amino-acids (i.e. glutamate and aspartate)	Yes	K^+

The imino-acid transporter in rabbit jejunal vesicles exclusively transports imino-acids such as proline, hydroxyproline and N-methylamino-isobutyric acid (MeAIB) [Stevens *et al.*, 1984].

TABLE 1.2   **Intestinal basolateral transport systems for amino-acids**

[Adapted from Ganapathy *et al.*, 1994]

Transport system	Substrates	Dependence on Na$^+$ gradient
A	Dipolar α-amino-acids Imino-acids	Yes
ASC	Three- and four-carbon dipolar amino-acids	Yes
Asc	Three- and four-carbon dipolar amino- acids	No
L	Bulky, hydrophobic, dipolar amino-acids such as leucine, phenylalanine	No
Y$^+$	Basic amino-acids such as lysine, arginine	No

The preferred substrates for the A system are alanine, serine and glutamine whereas those of the ASC systems are alanine, serine and cysteine [Palacin *et al.*, 1998]. One criterion for recognition of the A system is that it also transports N-methylated amino acids such as N-methylamino-isobutyric acid (MeAIB) [Palacin *et al.*, 1998]

1.5   DI-/TRIPEPTIDE TRANSPORTER

The intestinal oligopeptide transporter, PEPT1, couples di-/tripeptide and peptidomimetic drug transport with H$^+$ ions and is pH dependent. It will be discussed in depth later in section (1.8.4).

1.6   INTESTINAL P-GLYCOPROTEIN (P-gp)

P-glycoprotein functions to reduce the apparent intestinal epithelial permeability from lumen to blood for various lipophilic and cytotoxic drugs and will be discussed later in section 1.9.

1.7   INTESTINAL BRUSH-BORDER MEMBRANE
ENZYMES

As part of the make up of intestinal epithelial cells, many different enzymes are found on the brush-border membrane of enterocytes. Some will be typical enzyme markers of the brush-border membrane such as alkaline phosphatase which is located within the microvilli of small intestinal epithelial cells. The majority are digestive enzymes that play important roles in the digestion of nutrients and function as an absorption barrier to therapeutic peptides and proteins.

The terminal digestion of proteins and carbohydrates occurs at the enterocyte-luminal borders by means of numerous peptide and saccharide hydrolases. The distribution of sucrase and lactase activity along the human small intestine showed that their activities were highest in the jejunum whereas glucoamylase activity, which is involved in the digestion of maltose, increased from the jejunum and reached its highest activity near the ilealcecal valve [Triadou *et al.*, 1983]. The distribution of maltase activity was intermediate between that of sucrase and glucoamylase. Maximal digestion of disaccharides thus took place in the jejunum [Triadou *et al.*, 1983]. The brush-border membrane of the intestinal cells contained at least 15 peptidases that together had a broad specificity and can degrade both protein and peptides [Woodley, 1994]. It is these enzymes that represent an enzymatic barrier to therapeutic peptides and proteins. The peptidase enzymes of the intestinal brush border are listed in table 1.3 along with their substrate specificities. Endopeptidases hydrolyse peptide bonds interior to the terminal bonds of the peptide chains whilst exopeptidases hydrolyse the bond linking the N-terminal (aminopeptidases) or the C-terminal acid (carboxypeptidases) to the peptide chain. Enzymes that remove dipeptides from the N-terminus of the peptide chains are termed dipeptidyl peptidases whilst those that remove dipeptides from the C-terminus are called peptidyl dipeptidases [Woodley, 1994].

Cytochrome P450 metabolising enzymes are also found in the human small intestine [Peters and Kremers, 1989; Watkins *et al.*, 1987]. The implication of these enzymes on their own or in conjunction with P-glycoprotein on the bioavailability of orally administered drugs will be discussed later in section (1.10) and in chapter 5.

TABLE 1.3   **Intestinal brush-border membrane peptidases**

[Adapted from Woodley, 1994]

	Enzymes	Specificity
Endopeptidases	Endopeptidase-24.11	Hydrophobic amino-acids
	Endopeptidase-24.18	Aromatic amino-acids
	Enteropeptidase	Peptides containing four aspartyl residues upstream from the lysine
Exopeptidases: Amino-terminus	Aminopeptidase N	N-terminal amino-acid of peptide chains
	Aminopeptidase A	N-terminal aspartate or glutamate residue
	Aminopeptidase P	N-terminal proline residue
	Aminopeptidase W	N-terminal tryptophan, tyrosine or phenylalanine residue
	γ-glutamyl transpeptidase	N-terminal γ-glutamic acid
	Dipeptidyl peptidase IV	N-terminal dipeptide from the peptide chain with the second amino-acid of the dipeptide being either proline or alanine
Exopeptidases: Carboxy-terminus	Peptidyldipeptidase A	Especially His-leu C-terminal dipeptide
	Carboxypeptidase P	C-terminal proline, glycine or alanine
	Carboxypeptidase M	C-terminal lysine or arginine
	γ-glutamyl carboxypeptidase	γ-glutamic acid residues
Dipeptidase	Microsomal dipeptidase	Many, with the second amino acid residue having D-configuration.

1.8   HUMAN COLONIC ADENOCARCINOMA CELL LINE (CACO-2)

Twenty intestinal adenocarcinoma cell lines were classified into four groups depending on their degree of differentiation [Chantret *et al.*, 1988]. Caco-2 cells

are classified as Type I cells whose characteristics include spontaneous differentiation under normal cell culture conditions with polarisation of cells and the formation cell dome, well-developed apical brush-border membrane with several hydrolases. The growth pattern, structural and functional characteristics of Caco-2 cells were well documented by Pinto *et al.*, (1983).

1.8.1 GROWTH PATTERN OF CACO-2 CELLS *IN VITRO*

When grown on a plastic surface, cellular proliferation began after a lag period of 24 hours. Confluency was reached on day 6 and the stationary phase on day 9. During the phase of active growth, the cells grew as semi-spheroid clusters of polygonal cells and confluency was characterised by cellular dome formation [Pinto *et al.*, 1983]. The domes were randomly distributed all over the monolayer and increased in size with the time in culture, from 100-800 μm in diameter and 80-140 μm in depth. The cells could not be maintained for more than 25-30 days on plastic supports as the monolayers started to detach from the edges of the flasks [Pinto *et al.*, 1983].

At confluency, the cells were covered by typical brush-border microvilli projecting perpendicular to the apical cell membrane surface only. The microvilli were lined by a plasma membrane showing double leaflets, the outer one being coated by filamentous material. Each microvillus contained a core of bundled microfilaments which extended into the cytoplasm. The microvilli showed either a carpet-like pattern or flower-like clusters which seemed to join at the apical ends. Junctional complexes were also present with tight junctions and desmosomes being visible [Pinto *et al.*, 1983].

Different supports influence the morphology and characteristics of Caco-2 cells [Hidalgo *et al.*, 1989]. When cultured on permeable membranes, there was no sign of cellular deterioration at day 32. Cells grew rapidly on permeable supports from day 3 to day 16 with cell-height increased by 489% and cell-width decreased by 42% as observed from the cross-sections of cell monolayers by transmission electron microscopy. The cells formed occluding junctional complexes as early as day 3 in culture and by day 16, Caco-2 cell monolayers consisted of cells ~30 μm in height that possessed a morphology similar to that of simple, columnar epithelium of the small intestine [Hidalgo *et al.*, 1989].

The functional differentiation of Caco-2 cells is a growth-related phenomenon [Pinto *et al.*, 1983]. The activities of brush-border marker enzymes such as alkaline phosphatase, sucrase-isomaltase and aminopeptidase of cells on plastic supports were detected at a low level as early as day 5 in culture medium and increased regularly with time [Pinto *et al.*, 1983]. On day 19 when the cells were fully confluent, the activities of alkaline phosphatase and sucrase-isomaltase were nearly half those observed in human small intestinal mucosa and that of aminopeptidase was about 10% of the value observed for the human small intestine [Pinto *et al.*, 1983]. On permeable inserts, functional expression of alkaline phosphatase activity at the apical membrane was achieved faster and could be detected as early as day 3 in cell culture with increment of two-to-threefold from day 5 to 20 [Hildago *et al.*, 1989]. The transepithelial electrical resistance which serves as an indication of the barrier property of Caco-2 cells ranged from 96.6 ± 22.0 at day 3 to 173.5 ± 10.9 $\Omega.cm^2$ at day 17 on permeable membrane. This value was higher than that reported for rat intestine (60 $\Omega.cm^2$) but lower than that of the colon (300 $\Omega.cm^2$) [Hildago *et al.*, 1989].

Several functional transporters are expressed in confluent Caco-2 cells which are also identified in the human and animal small intestine brush border membrane vesicles (table 1.4).

TABLE 1.4 **Identified transporters in Caco-2 cells**

Transporter	References
Amino-acid transporter	[Nicklin *et al.*, 1992; Thwaites *et al.,* 1993 b, c]
Di-/tripeptide transporter	[Nicklin *et al.*, 1996]
Bile acid	[Hildago and Borchardt, 1990]
Monocarboxylic acid transporters	[Tsuji *et al.*, 1990]
Tranporters for sugar	[Blais *et al.*, 1987]
Vitamin B_{12} transporter	[Muthiah and Seetharam., 1987]

The di-/tripeptide and amino-acid tranporters are of relevance to the project and will be reviewed in depth in the relevant sections (1.4, 1.8 and chapter 6).

Recently, P-glycoprotein, an apically polarised drug efflux pump and intestinal cytochrome P450 metabolising enzymes have also been identified in Caco-2 cells [Anderle *et al.*, 1998; Schmiedlin-Ren *et al.*, 1997]. They play crucial roles in determining the bioavailability of orally administered drug candidates and will be discussed extensively later in section 1.9 and chapters 4 and 5.

Since confluent Caco-2 cells exhibit enterocyte-like morphology and express structural and functional characteristics similar to those of human intestinal epithelial cells, they have been widely used as model of the intestinal mucosa [Hildago *et al.*, 1989; Artursson 1990; Artursson, 1991a]. Scientists in the pharmaceutical industry have used this specific cell-culture model to estimate the intestinal permeability of oral drug candidates, thus conserving compounds only available in limited quantities. The determined Caco-2 cell permeability coefficients are useful to rank order a series of structurally similar compounds and allow intelligent selection of "lead" candidates for more extensive animal studies which are designed to determine their absolute oral bioavailability.

1.8.2 DRUG PERMEATION ROUTES ACROSS THE CACO-2 CELL MONOLAYER

Drug molecules travel across the Caco-2 cell monolayer by different routes (figure 1.2), namely:

(i)   The transcellular route which consists of three different mechanisms:

- Passive diffusion (predominant mechanism of absorption for most drugs)

- Carrier mediated transport

- Transcytosis

(ii)   Paracellular route

Lipophilic drugs such as metoprolol, propranolol, hydrocortisone, and testosterone are passively absorbed predominantly across the cell membrane by the transcellular route whereas small hydrophilic molecules such as those of mannitol are absorbed mainly *via* the tight junctions (paracellular route).

A few drugs like the peptidomimetic drugs utilise the transport systems for nutrients which are located in the apical membrane (the carrier-mediated route).

Macromolecules can be transported across the cell monolayer in endocytosed vesicles (the transcytosis route) which can either be fluid phase or receptor-mediated endocytosis. The transport of horse-radish peroxidase (HRP) in Caco-2 cells has been shown to be mediated by fluid phase transcytosis along two functional pathways: a minor pathway allowing the transport of the intact protein and a major lysosomal degenerative pathway [Hayman *et al.*, 1990]. In the absorptive direction, HRP was transported mainly by a degenerative pathway and was inhibited at low temperature. In contrast, the transport of vitamin B_{12} (VB_{12}) occurs *via* receptor-mediated endocytosis [Muthiah and Seetharam, 1987] where VB_{12} first binds to an intrinsic factor which in turn binds to an intrinsic factor receptor on the surface of Caco-2 cells. The vitamin B_{12}-intrinsic factor complex is subsequently transported across the cells

FIGURE 1.2 **Drug permeation routes across the Caco-2 cell monolayer** (1: passive diffusion (major component of the transcellular route), 2: paracellular route, 3: carrier-mediated transport, C: substrate carrier, 4: transcytosis)

26
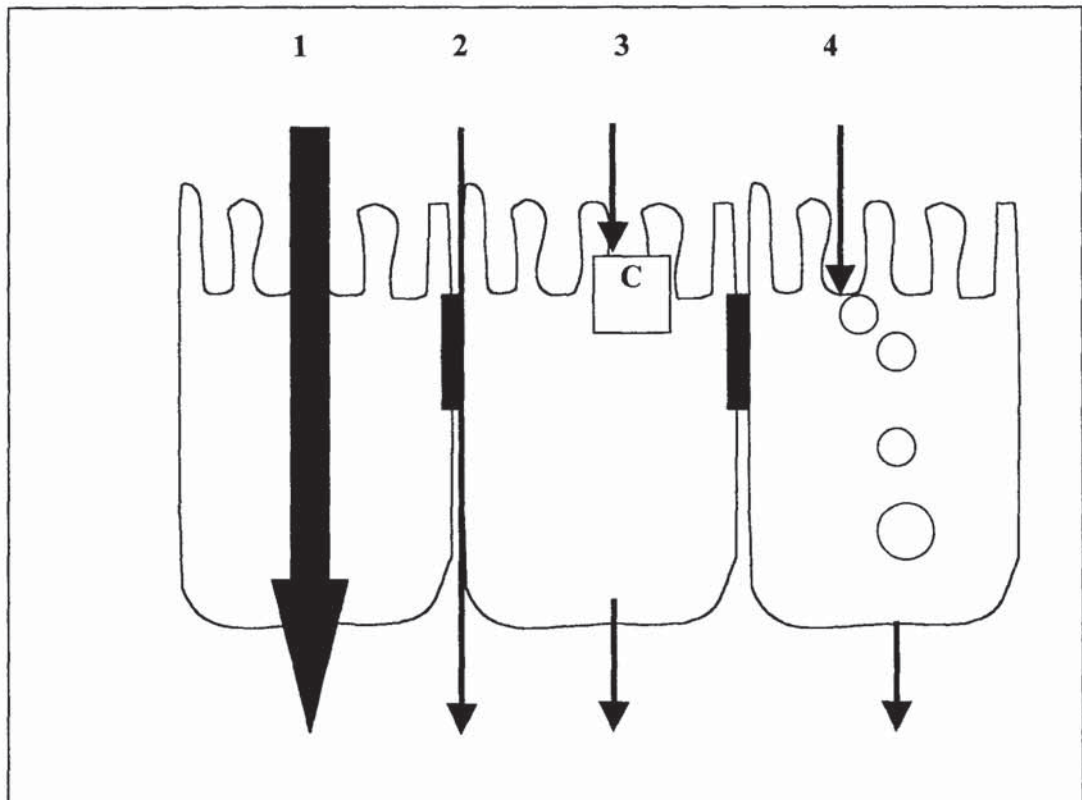
1.8.3 ANALYSIS OF DRUG PERMEATION ACROSS THE CACO-2 CELL MONOLAYER AND PREDICTION OF *IN VIVO* DRUG ABSORPTION

Simultaneous assessment of structure-permeability relationships as well as structure-activity relationships can expedite the selection of a drug candidate with good oral absorption. Traditional measures such as lipophilicity and the pH-partition hypothesis only give an approximate indication of the extent of drug absorption [Chong *et al*., 1996]. A better correlation was obtained when the percentage of absorbed drugs after oral administration was expressed as a function of apparent permeability coefficients *via* Caco-2 cell monolayers [Artursson and Karlsson, 1991b]. By determining the permeability coefficients of a series of drugs and peptides and comparing those to their percentage absorption in humans, a general conclusion was reached that completely absorbed drugs had permeability coefficients of greater than 1×10^{-6} cm/s. Drugs which were absorbed > 1% but < 100% had permeability of 0.1-1.0×10^{-6} cm/s whilst peptides and drugs that were absorbed < 1% had permeability coefficients of $\leq 1 \times 10^{-7}$ cm/s [Artursson and Karlsson, 1991b]. This finding was supported by Lennernas *et al*., (1996) who reported that rapidly and passively transported drugs such as naproxen, antipyrene and metoprolol had comparable apparent permeability coefficients in Caco-2 cells and in human jejunum. However, the carrier-mediated transport rates of L-dopa, L-leucine and D-glucose were much lower in Caco-2 cells than in human jejunum, prompting care and precaution in extrapolating the results obtained *in vitro* to predict the *in vivo* absorption rates of carrier-mediated compounds [Lennernas *et al*., 1996]. Indeed, the findings by Chong *et al*., (1996) indicated that *in vitro* permeability through Caco-2 cells was not quantitatively predictive of *in vivo* absorption for peptide-like drugs which were absorbed *via* the di-/tripeptide transport system. Based on the current permeability-absorption relationship for passively absorbed drugs, the predicted *in vivo* absorption for the four carrier-mediated drugs (amoxycillin, cephalexin, lisinopril and SQ 29852) was ten-fold lower than their actual *in vivo* absorption values [Chong *et al*., 1996]. Another draw back of the relationship between permeability coefficient and % absorption *in vivo* curve was that the curve was predictive for poorly and well-absorbed compounds but less accurate for those in its middle steeper part [Brayden, 1997].

1.8.4 INTESTINAL DI-/TRIPEPTIDE TRANSPORTER IN CACO-2 CELLS

1.8.4.1 DI-/TRIPEPTIDE TRANSPORTERS, PEPT1 AND PEPT2

Two di-/tripeptide transporters which are responsible for the transport processes of intact di-/tripeptides in intestinal and renal absorptive epithelial cells have been cloned and termed PEPT1 and PEPT2 respectively [Leibach and Ganapathy, 1996]. Comparison of the amino acid sequences between PEPT1 and PEPT2 revealed 50% identity and 70% similarity. PEPT2 is 21 amino acids longer than PEPT1 and the extent of similarity is much higher in the transmembrane domains than in the hydrophilic regions between the transmembrane domains [Leibach and Ganapathy, 1996]. PEPT1 in Caco-2 cells is relevant to this project and will be discussed extensively hereafter.

1.8.4.2 THE CLONING AND STRUCTURE OF INTESTINAL DI-/TRIPEPTIDE TRANSPORTER PEPT1

Caco-2 cells express PEPT1 but not PEPT2 [Ganapathy and Leibach, 1996]. The cloning of PEPT1 has been reported [Fei *et al.*, 1994]. Starting from poly $(A)^+$ mRNA isolated from the rabbit small intestinal mucosa and injected in to *Xenopus laevis* (frog) oocytes, the di-/tripeptide transport activity was assessed by measuring the uptake of a radiolabelled dipeptide [^{14}C]Glycyl-sarcosine (Gly-Sar). Size fractionation of mRNA indicated that the functional expression of the activity was associated with the mRNA 1.8-3.6 kb in size and, therefore, the selected RNA-pool containing the message was used for constructing a cDNA library in a bacterial vector. Individual cDNA clones of the library were then transcribed into the corresponding cRNAs which were injected individually into oocytes. Oocytes containing different cRNAs were then assayed for induced transport activity. By this procedure, the library of cDNA was screened for a single clone encoding the transport activity of interest. Sequencing the clone-cDNA finally allowed the amino acid sequence of the transport protein to be determined and hydropathy analysis allowed some first predictions of the PEPT1 transporter arrangement within the cell membrane [Fei *et al.*, 1994]. The predicted protein consisted of 708 amino acid residues with 12 membrane-spanning domains, 2 putative sites for

protein kinase C-dependent phosphorylation and several N-glycosylation sites in the extracellular domain [Liang *et al.*, 1995]. By using a combination of molecular modelling which included the protein structure prediction algorithms and site-directed mutagenesis, specific amino acids which were involved in the substrate interaction with PEPT1 were identified [Bolger *et al.*, 1998]. Mutation of tryptophan 294 or glutamine 595 into alanine reduced Gly-Sar uptake by 80% and 95% respectively by human embryonic kidney cells that had been transfected with human PEPT1 cDNA. Compared to PEPT1 expressed in other animals, the human H^+/peptide co-transporter exhibited a high degree of homology (81% identity and 92% similarity) with that of the rabbit [Liang *et al.*, 1995]. The driving force for the uptake of dipeptides required proton binding [Adibi, 1997] and an inside negative transmembrane potential [Amashed *et al.*, 1997], a mechanism which will be elaborated on in section 1.8.4.3.

1.8.4.3 MECHANISMS AND TRANSPORT CHARACTERISTICS OF DI-/TRIPEPTIDES BY THE INTESTNAL PEPTIDE TRANSPORTER PEPT1

Using the available results from the literature and also their collected results, Ganapathy and Leibach, (1985) first hypothesised that dipeptides and protons were co-transported across the intestinal brush-border membrane by a H^+/dipeptide transporter. This was because an inward proton gradient stimulated peptide transport and that the stimulation was reduced when the proton gradient was rapidly dissipated by a protonophore. A model depicting the mechanism of di-/tripeptide absorption is illustrated in figure 1.3.

FIGURE 1.3   **Mechanisms of di-/tripeptide absorption in the small intestinal epithelial cells**

[Adapted from Ganapathy and Leibach, 1985]
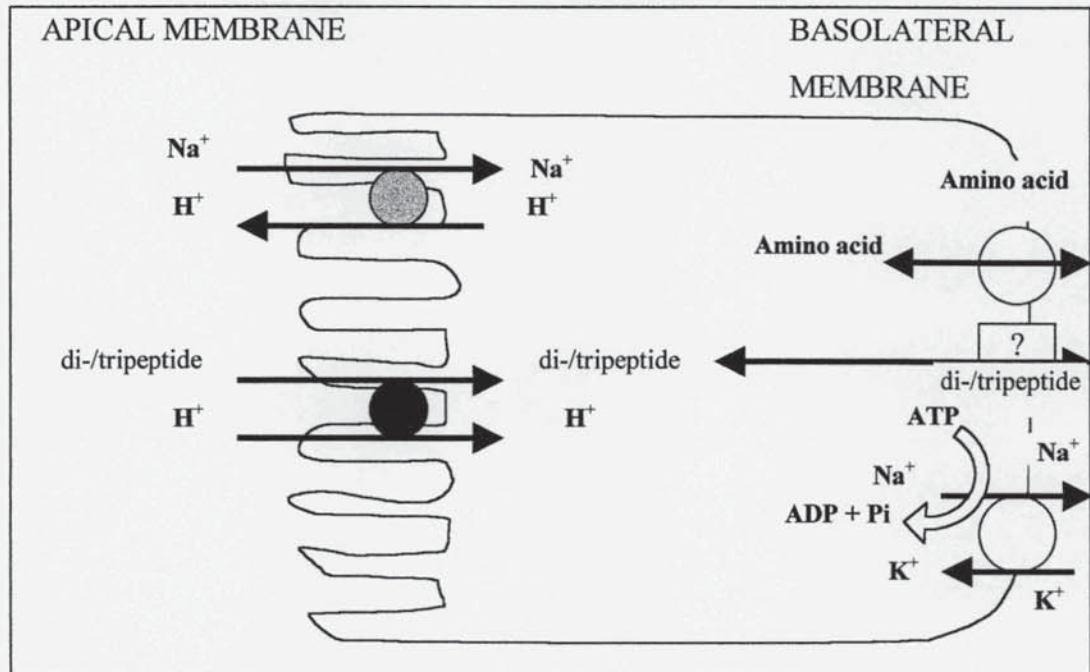
The proton gradient was generated and maintained by the Na^+/H^+ exchanger in the brush-border membrane in response to an inward Na^+ gradient. The Na^+- K^+-ATPase, located in the basolateral membrane, actively pumped Na^+ out of the cells and this process lowered the intracellular concentration of Na^+ and consequently resulted in an inward proton gradient across the brush-border membrane. Depending on their susceptibility, the peptides entering the mucosal cells might be hydrolysed to a varying degree into their constituent amino-acids which were then absorbed. [Ganapathy and Leibach, 1985]. The hypothesis was later proven correct by Thwaites *et al.*, (1992 and 1993a) who demonstrated that the intake of a dipeptide Gly-Sar at pH 6.0 caused a decrease in the intracellular pH of Caco-2 cells, providing the first direct evidence that dipeptides were indeed co-transported with H^+ ions. The stoichiometry of proton : dipeptide co-transport varied with the nature of di-/tripeptides. Neutral, acidic and basic peptides all induced intracellular acidification in *Xenopus laevis* oocytes in which rabbit PEPT1 was expressed [Steel *et al.*, 1997]. The rates at which they induced intracellular acidification and the ratios of their initial rates of uptake (at pH 5.5) over the associated charge fluxes, gave different proton- substrate coupling ratios of 1:1, 2:1 and 1:1 for neutral, acidic and basic peptides respectively [Steel *et al.*, 1997]. In the light of these newly found results, a model for the coupled transport of

30

neutral and charged dipeptides was proposed by Steel *et al.*, (1997) as illustrated in figure 1.4.

According to this model, PEPT1 had a peptide site and a cation site which contained a histidine residue being responsible for the coupling of proton(s). The second histidine residue was predicted to lie adjacent to the peptide site at the extracellular face of the transporter. Following proton binding to the cation site, peptides were predicted to bind to the peptide site. The negatively charged glycylglutamate (Gly-Glu) was co-transported with two protons, one of which was involved in H^+ coupling whilst the other was predicted to neutralise the charge on the dipeptide substrate creating a zwitterionic species. A single proton was co-transported with a positively charged glycyllysine (Gly-Lys) and its apparent affinity to PEPT1 was shifted towards more basic values (*i.e.* from pH 4.8 to pH 6.2). To account for this, a histidine residue located near the peptide site was predicted to be deprotonated at or above pH 6 to allow binding and translocation of positively charged dipeptides [Steel *et al.*, 1997].

FIGURE 1.4   **Mechanisms of peptide/H^+ coupling process by PEPT1**

[Adapted from Steel *et al.*, 1997]

Abbreviations. C: cation site; P: peptide site; His^+: histidine amino-acid residue

31
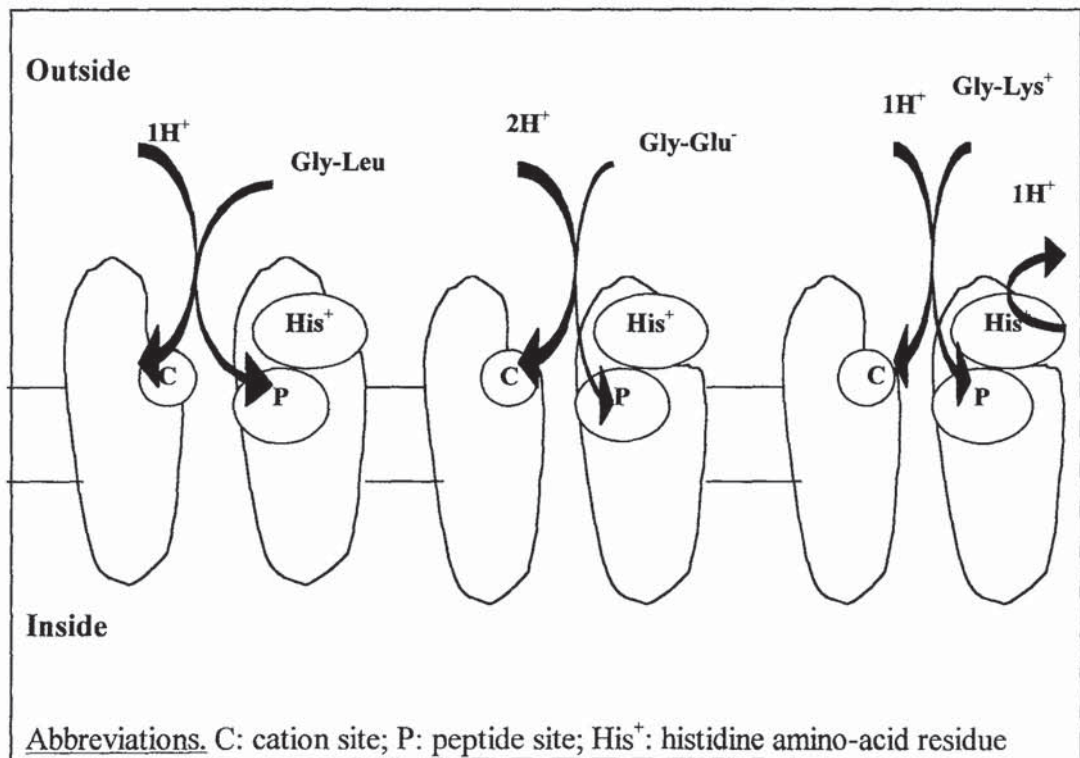
A wide spectrum of substrates is transported by the intestinal di-/tripeptide transporter and are of nutritional and pharmacological importance. Some examples representing different classes of substrates are mentioned in section 1.8.4.4.

1.8.4.4 SUBSTRATES OF THE INTESTINAL DI-/TRIPEPTIDE TRANSPORTER IN CACO-2 CELLS

The di-/tripeptide transporter PEPT1 in Caco-2 cells recognises a variety of substrates ranging from natural peptides to peptide-derived peptidomimetic drugs. Uptake of natural peptides such as [^{3}H]glycylproline (Gly-L-Pro) in Caco-2 cells by the intestinal di-tripeptide transporter was time-, pH- and concentration-dependent at both neutral (7.4) and acidic (6.0) pH [Eddy et al., 1993]. Moreover, an excess of unlabelled Gly-L-Pro (5mM) inhibited the uptake of its radioactive counterpart up to 92% [Eddy et al., 1993] indicating that the uptake was actively mediated by the di-/tripeptide transporter. Thwaites et al., (1993a) also demonstrated the uptake of Gly-Sar into Caco-2 cells by a H$^+$/ di-/tripeptide transporter which coupled dipeptide uptake and intracellular acidification. Angiotensin-converting enzyme inhibitors (ACEs) are widely used in the treatment of high blood pressure. The transport of quinapril, an ACE inhibitor, across Caco-2 cells was pH- and temperature-dependent with the net apical-to-basolateral transport in the presence of a proton gradient (apical pH 6.0 and basolateral pH 7.4) being five times faster than in its absence. Quinapril transport was also inhibited by natural peptides such as Gly-Pro and Phe-Pro, indicating that they shared the same di-/tripeptide transport system [Hu et al., 1995b]. Ceronapril (SQ 29852) is another ACE inhibitor which was reported to be a specific, chemically and metabolically stable probe for the di-/tripeptide transporter [Marino et al., 1996]. At a low concentration (1 mM), the majority of its uptake (90%) in Caco-2 cells was predominantly by a carrier-mediated pathway, which was competitively inhibited by dipeptides such as L-Ala-L-Pro and L-Gly-Phe [Nicklin et al., 1996]. Uptake of cephalosporin antibiotics, as represented by cephalexin, by a dipeptide transport carrier in human intestinal Caco-2 cells has also been reported [Dantzig and Bergin, 1990]. In sodium-free buffer of pH 6.0, Caco-2 cells accumulated cephalexin against the concentration gradient with a distribution ratio of 3.5 within 180 minutes. The drug uptake was maximal at pH 6.0 and reduced in the presence of metabolic inhibitors, ionophores and in the presence of Gly-L-Pro, leading to the

conclusion that Caco-2 cells took up cephalexin by a proton dependent di-/tripeptide transporter. Thyrotropin-releasing hormone (TRH) was also found to be a substrate for PEPT1 [Walter and Kissel, 1994] as reflected by pH- and temperature-dependent transport in addition to an inhibition of its transport in the presence of Gly-Pro and cephradine.

Because there was such a wide range of therapeutic compounds being transported by PEPT1, attempts have been made to understand the relationship between the diverse structures of the substrates and their affinity to/recognition by PEPT1. Such an understanding would facilitate the synthesis of more highly-absorbed pharmacophores. However, there is no straight-forward conclusion but the following essential structural features have been noted as described in section 1.8.4.5.

1.8.4.5 STRUCTURAL REQUIREMENTS FOR INTERACTION WITH THE DI-/TRIPEPTIDE TRANSPORTER PEPT1

The structures of various compounds were modified in different ways to improve their interaction with the di-/tripeptide transporter. The presence of an α-amino group in cephalosporins increased their PEPT1-mediated transepithelial transport in Caco-2 cells [Raeissi et al., 1998]. The permeability ratio (Papp (pH 6.0)/ Papp (pH 7.4)) of a series of cephalosporins was calculated as a measurement of PEPT1 involvement of their transport across Caco-2 cells monolayers. For those with an α-amino group such as cephalexin, cefaclor, cefadroxil, cephradine and cephaloglycin, the permeability ratios ranged between 1.77 and 2.77. In contrast, cephalosporins without an α-amino group, such as cefuroxim, cefamandole and cefazolin had a permeability ratio in the range of 0.74 -1.26 [Raeissi et al., 1998], indicating that an α-amino group of cephalosporins improved their intestinal transport. Other structural features which were of relevance for the recognition of β-lactam antibiotics by the intestinal di-/tripeptide transporter included a steric resemblance to the tripeptide backbone, an N-terminal bond with a α-amino group, a C-terminal peptide bond in the lactam ring and stereoselective L-isomers [Bretschneider et al., 1999; Wenzel et al., 1995]. For the ACE inhibitors, PEPT1 could transport substrates without the N-terminal nitrogen atom [Hu and Gordon, 1988]. The carbonyl group in ACE inhibitors was essential for recognition and translocation of the substrates by PEPT1

[Schoemakers *et al.*, 1999]. This was illustrated by the reduction of the peptide bond of enalapril to form enamipril which, although it still retained the ability to interact with the di-/tripeptide transporter but it was not transported. For natural peptides, cyclisation of the dipeptide backbone might abolish their ability to interact with the di-/tripeptide transporter and the availability of a free carboxylic group was shown to enhance their performance as competitive inhibitors of other peptidomimetic drugs administered simultaneously [Hidalgo *et al.*, 1995].

1.8.5 AMINO-ACID TRANSPORTER IN CACO-2 CELLS

The first evidence of an electrogenic transport pathway for amino acids was provided by Grasset *et al.*, (1984). When L-alanine was added to Caco-2 cells being cultured on permeable inserts and mounted in an Ussing chamber, it caused a concentration-dependent increase in cellular transmembrane potential and short-circuit current as a result of the co-transport of L-alanine and sodium ions. Large neutral amino acids such as phenylalanine were also taken up by a sodium-dependent, saturable, carrier-mediated process with a Km value of 2.7 mM in Caco-2 cells. The uptake of L-proline was carrier-mediated, saturable, sodium- and pH-dependent with the maximum uptake observed at pH 5 and accounted for about two-thirds of the observed flux over a nanomolar concentration range at 37°C and pH 7.4 [Nicklin *et al.*, 1992]. Since it was a carrier-mediated process, the uptake was reduced when protein synthesis, Na^+/K^+ ATPase or cellular metabolism was inhibited. L-proline uptake was also inhibited in the presence of other amino acids such as L-alanine, L-serine or α-aminoisobutyric acid. In contrast, the net absorptive transport of L-proline across Caco-2 cells monolayers was H^+-dependent only and associated with intracellular acidification at both neutral (7.4) and acidic pH (6.0) [Thwaites *et al.*, 1993c]. Absorption of β–alanine by the human intestinal Caco-2 cell monolayers was also shown to be sodium-independent and H^+-coupled which resulted in intracellular acidification at both neutral and acidic pH although the effect was marked at pH 6.0 [Thwaites *et al.*, 1993b].

1.9 EXPRESSION OF P-GP IN DIFFERENT SPECIES

P-glycoprotein belongs to the ABC (ATP-binding cassette) transporter superfamily which is responsible for the drug tolerance towards a variety of

cytotoxic agents in different species ranging from bacteria to man. In humans, infection in immunodeficient patients is often caused by the pathogenic yeast *Candida albicans,* which expresses Cdr1p, an ABC transporter which confers antifungal resistance [Prasad *et al.,* 1995]. In bacteria such as in the *Streptomyces* strains, a transporter such as DrrAB mediates the excretion of specific antibiotics to ensure self-resistance to the antibiotics that they produce [Guilfoile and Hutchinson, 1991]. In man, P-gp isoforms are encoded by two genes, MDR1 and MDR2, and have distinct physiological roles associated with specialised cell functions [Ng *et al.,* 1989; Georges *et al.,* 1990]. MDR1-encoded P-gp is responsible for the multidrug resistance in cancerous cells and of relevance to the project and thus, it will be discussed in more details in section 1.9.1.

1.9.1 STRUCTURE OF HUMAN P-GP

The complete primary structure of human P-gp in multidrug-resistant cancer cells has been determined from its cDNA sequence. The protein has 1280 amino acids and consists of two homologous parts of approximately equal length [Chen *et al.,* 1986]. Each half of the protein includes a hydrophobic domain with six predicted transmembrane segments and a hydrophilic nucleotide-binding domain (NBD) [Chen *et al.,* 1997]. The two halves of the molecule are joined by a linker region which is phosphorylated at several sites by protein kinase C [Chambers *et al.,* 1993]. Phosphorylation of this linker region, however, does not appear to be required for drug transport [Goodfellow *et al.,* 1996]. The integral membrane domains form a pathway through which solutes are translocated across the membranes and provide amino-acid residues for direct interactions with the P-gp substrates [Higgins *et al.,* 1997]. Because of the wide spectrum of structurally unrelated substrates transported by P-gp, the exact amino acid sequences in the transporter's primary structure which interact with the substrates are matters of controversy. It was found, however, that the substitution of glycine[185] by valine[185] in P-glycoprotein led to an increase in resistance to colchicine and epidophyllotoxin and a decrease in resistance to vinblastine and vincristine [Safa *et al.,* 1990].

FIGURE 1.5 **Topological map and domain organisation of P-gp as predicted from its primary sequence**

[Adapted from Higgins *et al.*, 1997]
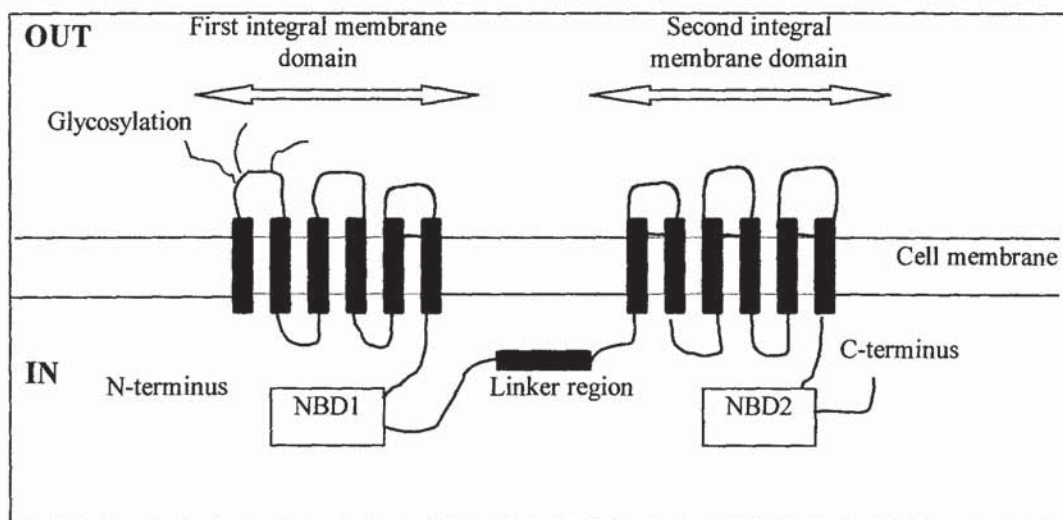
Mutational changes of the amino-acid composition of P-gp leads to a reduction in its ability to confer drug resistance to certain cytotoxic drugs. Loo and Clarke, (1993) found that mutation of either Pro^{223} in the transmembrane segment 4 or Pro^{223} in the transmembrane segment 10 drastically reduced the ability of the mutant protein in murine cells to confer any resistance to colchicine, doxorubicin, or actinomycin D.

The precise number of substrate-binding sites and their exact location in P-gp have been the subject of some contention as a result of the diversity of P-gp substrates and many published studies are hard to interpret. More than one substrate-binding site has been reported. By studying the binding affinity of a photoaffinity analogue of a P-gp substrate such as iodoarylazidoprazosin (IAAP) in the presence of a P-gp modulator, cis (Z) flupenthixol, Dey *et al.*, (1997) found different binding affinities between the two halves with a higher affinity for the C half of the molecule. In addition, the concentration of vinblastine and cyclosporin A required to inhibit 50% of the binding of IAAP to the C-site (Ki values) was increased to 5-6 fold in the presence of cis (Z) flupenthixol whereas there were no effects on the N terminal half. The authors concluded that there were two non-identical drug-interaction sites in P-gp. This was supported by Greenburger, (1993) who photolabelled the binding sites in P-gp using the same substrate and reported that there were two binding sites residing in each half of the molecule. One was situated within or close to the putative transmembrane domains 4-6 in the

N-terminal half and the other in the C-terminal half within or close to transmembrane domains 11-12. Another study by Ferry *et al*., (1992) concluded that P-gp possessed a 1,4-dihydropyridine selective drug-acceptor site which was allosterically coupled to a vinca alkaloid selective drug binding site. In contrast, Bruggermann *et al*., (1992) showed that by using photoactive azidopine to label P-gp, two distinct locations could be identified in the N- and C-halves and that vinblastine inhibited the azidopine labelling to approximately the same extent at each label site of P-gp. This led to the conclusion that the two halves of P-gp approached each other to form a single binding site for these drugs.

The two nucleotide binding domains (NBDs) of P-gp share 30-40% amino-acid sequence identity with each other [Higgins *et al*., 1997]. They bind and hydrolyse ATP and couple the hydrolysis of ATP to the solute translocation across the membranes. Various P-gp conformations are associated with different stages of substrate transport and the binding and hydrolysis of ATP [Mechetner *et al*., 1997].

Recently, a 25-Å resolution secondary structure of P-gp was obtained by electron microscopy and single-particle image analysis of both detergent-solubilised and lipid-reconstituted P-gp [Rosenberg *et al*., 1997]. When viewed from the extracellular face of the membrane, the protein was toroidal with a protein ring of diameter about 10 nm surrounding a large central pore. The protein rings exhibited six-fold symmetry, a model in which the six lobes corresponded to the six extracellular loops between pairs of α-helices. The pore appeared to be aqueous as it stained intensively with uranyl acetate and phosphostungstate. The pore was large, about 5 nm in diameter and was the entrance to a cup-shaped chamber within the membrane, presumably formed by the twelve membrane-spanning α-helices. This chamber narrowed as it passed through the membrane and was closed at the cytoplasmic site of the membrane, presumably by sequences from the nucleotide binding domains and the cytoplasmic loops separating the transmembrane α–helices. Although this secondary structure of P-gp was obtained as a static conformation, an awareness of its structure is essential for understanding of its mode of action.

FIGURE 1.6 **Projection map of P-gp**
[Adapted from Higgins *et al.*, 1997]

As viewed from above the extracellular face of the membrane showing a protein ring surrounding a large central aqueous pore with six-fold symmetry. The putative gaps in the protein ring provide access between the central pore and the lipid phase.
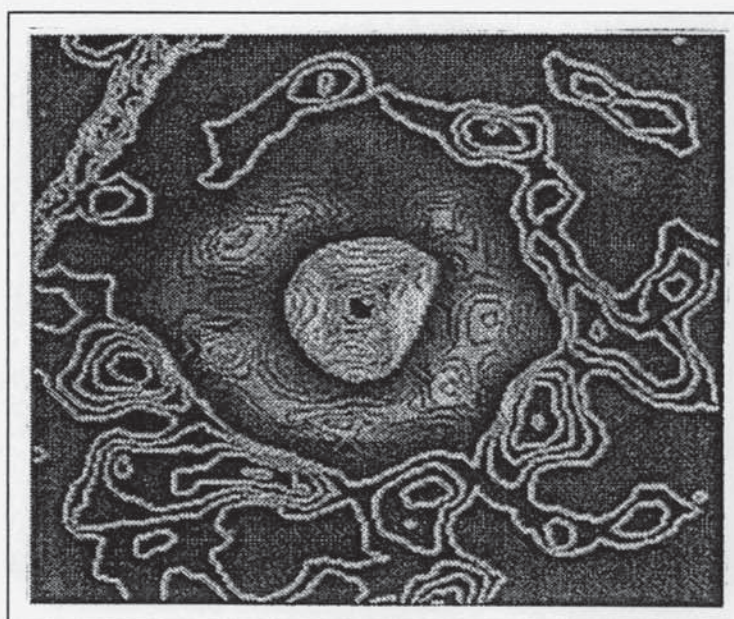
1.9.2 MOLECULAR MECHANISMS OF ACTION OF P-GP

The most consistent observation in cancerous cells which over-express P-gp is the low cellular accumulation of cytotoxic drugs. How P-gp actually operates to achieve this outcome is open to debate and different hypotheses have been proposed with regard to its mode of action. P-gp could function as a transmembrane pore-forming protein leading to an energy-dependent outward drug efflux [Higgins et al., 1997]. In this case, the drug molecules in the cytoplasm which interact with the transport protein from the aqueous phase are pumped across the bilayer and released directly into the aqueous phase on the outside of the cells. P-gp could also act as a hydrophobic vacuum cleaner which transports drugs from the membrane to the extracellular surrounding [Raviv *et al.*, 1990] or as a flippase which transports drugs from the inner to the outer leaflet of the phospholipid bilayer of cell membranes [Higgins and Gottesman, 1992] (figure 1.7). These last two hypotheses require drugs to be in contact with the lipid bilayer before they interact with the transporter protein. They are supported by the

fact that P-gp substrates are primary cationic, lipid-soluble planar molecules which are expected to intercalate between the phospholipid molecules in the bilayer [Higgins and Gottesman, 1992]. The hydrophobic vacuum cleaner and the flippase models emphasise the substrate binding site of P-gp being accessible from the lipid phase. They are consistent with the findings that major binding sites are in transmembrane domains 4-6 and 11-12 as mentioned previously [Greenburger, 1993].

FIGURE 1.7   Molecular model for drug extrusion by P-gp
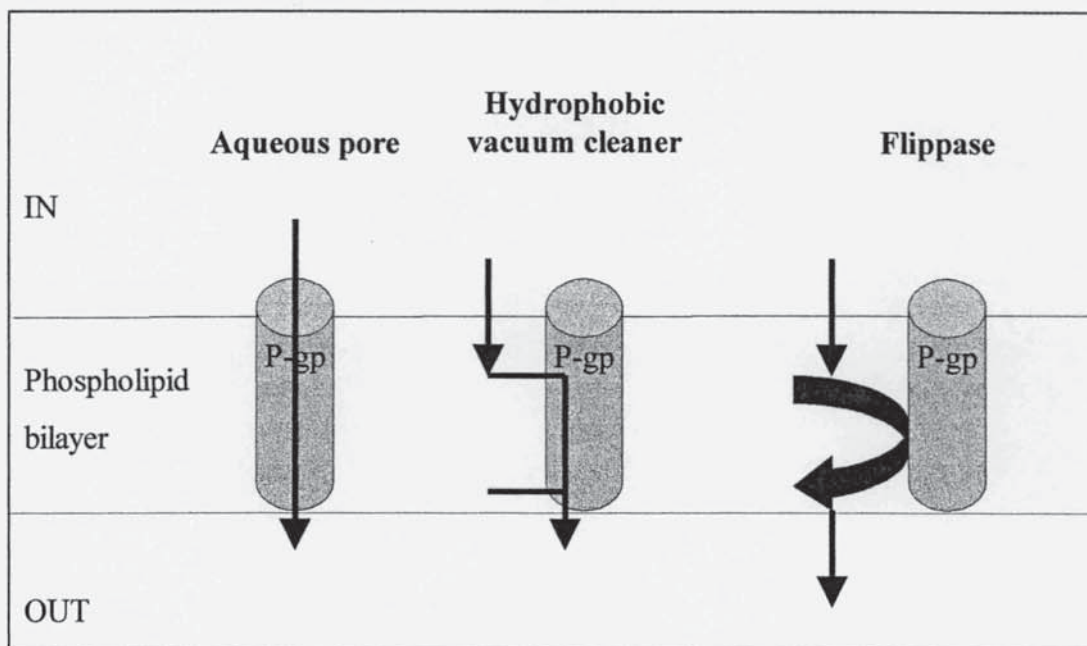
ATP hydrolysis by ATPase in the presence of Mg^{2+} ions is required for P-gp function. Optimum P-gp-ATPase activity was observed at an ATP:Mg^{2+} molar ratio of 0.75: 1 for partially purified P-gp from multidrug-resistant Chinese hamster ovary cells [Doige and Sharom, 1992]. Binding of macrolides FK 506 and FK 520 to P-gp in membrane-enriched fractions of insect cells that had been transfected with human MDR1 cDNA stimulated a P-gp-ATPase activity [Rao and Scarborough, 1994]. The latter proved to be useful in identifying the type of interaction between P-gp substrates and modulators at the drug binding site(s) [Litman et al., 1997b]. In P-gp, both NBD1 and NBD2 bound MgATP or Mg-8-azido-ATP and the two sites showed approximately the same apparent nucleotide binding affinity [Liu et al., 1997]. Experiments with the inhibitor orthovanadate (Vi) (general ATPase inhibitor) demonstrated that in intact P-gp in mammalian cell membranes, both NBDs had the capacity to hydrolyse MgATP and that there was

39

a strong interaction between these two sites [Urbatsch *et al.*, 1995a; Urbatsch *et al.*, 1995b]. This was supported by the fact that strapping of adenosine diphosphate as the P-gp MgADP.Vi complex in either NBD was sufficient to prevent the other site being active. A postulated alternating catalytic sites cycle of ATP hydrolysis by P-gp is illustrated in figure 1.8

FIGURE 1.8 **Alternating catalytic cycle of P-gp hydrolysis**

[Adapted from Senior *et al.*, 1995]
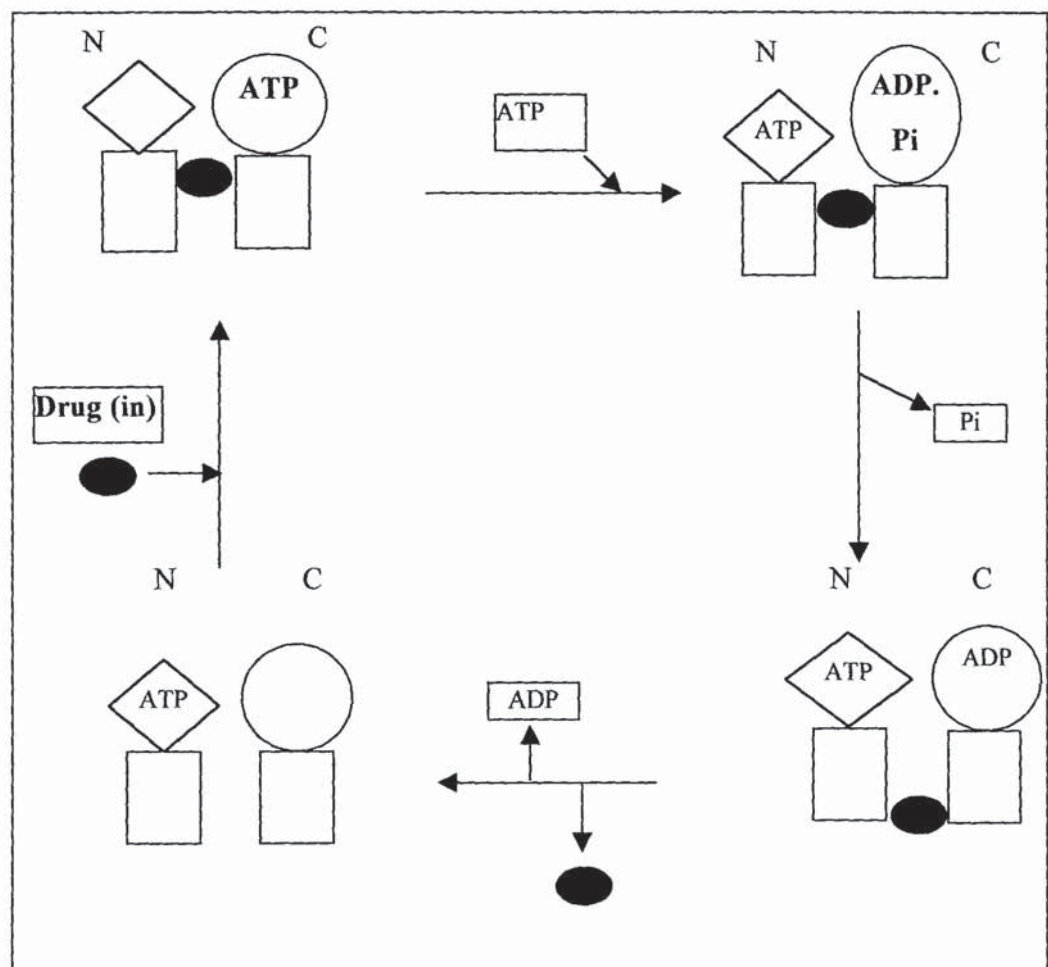
The rectangles represent the P-gp transmembrane domains (TDMs), circles, oval and diamonds represent different conformations of the NBDs labelled "N" and "C" for NBD1 and NBD2. Starting at top left of the figure, drug is bound on the inner surface to the inside-facing drug-binding site(s) in the TMD, the N-catalytic site is empty, the C-catalytic site binds ATP. Top right, ATP binding to the N-site promotes ATP hydrolysis at the C-site, inducing a conformation of the C-site which prohibits hydrolysis at the N-site. ATP hydrolysis in the C-site induces a high chemical potential state with bound ADP.Pi shown as an oval. Bottom right, relaxation of the C-site conformation occurs, coupled to drug movement from inside-facing, higher drug affinity binding site to outside-facing, lower drug affinity binding site and Pi is released. Bottom left, drug dissociates from the outside surface, ADP dissociates. Drug binds from the inner surface, and in top left, the molecule is poised for another cycle of ATP hydrolysis except that the N and C-sites have reversed their relationship, and the next hydrolysis event occurs in the N-site instead of the C-site [Senior *et al.*, 1995].

1.9.3   STRUCTURAL REQUIREMENTS FOR P-GP SUBSTRATES

The ability of P-gp substrates to interact with so many structurally diverse compounds has generated much controversy about the number and nature of the substrate-binding sites.   It is possible that all P-gp substrates including drugs, chemosensitisers and peptides interact with different overlapping regions of a flexible binding site that is large enough to accommodate more than one compound.   On the other hand, multiple drug binding sites could be just as feasible an explanation for the binding of a diverse range of substrates.

Hydrophobicity of the compounds has been shown to be one of the requirements for P-gp interactions [Sharom *et al.*, 1996; Sharom *et al.*, 1998].   A series of hydrophobic peptides ranging from linear tripeptides to cyclic peptides was shown to interact with P-gp using a fluorescence quenching assay and blocked colchicine transport into plasma membrane vesicles prepared from multidrug resistance Chinese Hamster Ovary (CHO) cell lines.   In addition, beauvericine (a cyclic peptide) and a linear peptide such as pepstatin A were able to restore the level of daunorubicin accumulation in the multidrug resistant cells to that observed in drug sensitive cells [Sharom *et al.*, 1998].

Using a series of pesticides, Bain *et al.*, (1996) indicated that both lipophilicity and molecular weight were major determinants in dictating peptide binding to P-gp as measured by the inhibition of efflux of P-gp substrate doxorubicin in murine melanoma cells transfected with the human MDR1 gene (B16/hMDR1 cells).   None of the pesticides having calculated octanol/water partition coefficients (ClogP) of less than 2.5 inhibited P-gp whilst maximum binding occurred amongst those having values of C log P of 3.6 – 4.5.   In addition, pesticides having a molecular weight of 391-490 had a greatest average affinity towards P-gp [Bain *et al.*, 1996].   Binding of drugs to P-gp was also found to be positively correlated with their molecular surface area [Litman *et al.*, 1997a].

With a series of anthracycline analogues with different positive charges, Lampidis *et al.*, (1997) demonstrated that positively charged analogues were recognised better than their neutral counterparts.   Moreover, analogues with increasing lipophilicity, regardless of the charge were able to inhibit drug binding to P-gp with more efficiency [Lampidis *et al.*, 1997], agreeing with the findings of Sharom *et al.*, (1998).

1.9.4 TISSUE DISTRIBUTION OF P-GP AND ITS POSSIBLE FUNCTIONS

P-gp was first discovered by its association with multidrug resistance in cancerous cells [Kartner *et al.*, 1983]. The human MDR1 gene which encodes P-gp was also detected in several tumours [Fojo *et al.*, 1987]. P-gp was found to be highly concentrated in the apical plasma membrane of human carcinoma cell line KB-C4 [Willingham *et al.*, 1987] although it was also found on the luminal side of Golgi apparatus stack membranes, in the endoplasmic recticulum in small amounts [Willingham *et al.*, 1987] and in the cell cytoplasm and nucleus [Baldini *et al.*, 1995]. Non-functional P-gp was expressed intracellularly in human colonic cancer cells [Duensing and Slate, 1994]. The predominant expression of P-gp in the plasma membrane was consistent with its role as a drug efflux pump at the cell surface.

In normal tissues, P-gp was detected in the liver, pancreas, kidneys, colon, jejunum, adrenal gland, skeletal and cardiac muscle fibres and in the blood brain barrier [Thiebaut *et al.*, 1987; Thiebaut *et al.*, 1989; Schinkel *et al.*, 1994]. In the liver, P-gp was located exclusively on the biliary canalicular front of hepatocytes [Thiebaut *et al.*, 1987]. Human liver P-gp is encoded by MDR2 gene (also called MDR3) and although it was unable to transport hydrophobic anticancer drugs, it is a phospholipid transport protein and has an essential role in the secretion of phosphatidylcholine into bile [Smit *et al.*, 1993]. In mice, where the mdr2 gene (an equivalent of human MDR2 gene) was homozygously disrupted, a liver disease that appeared to be caused by the complete inability of the liver to secret phospholipids into the bile was observed [Smit *et al.*, 1993].

In the kidneys, P-gp is located on the apical surface of the proximal tubules. Cultured Madin-Darby canine kidney epithelial cells showed a net secretive flux of cytotoxic drugs across the cell monolayers, suggesting that the function of renal P-gp is to protect the organ against toxins [Horio *et al.*, 1988].

In the adrenal glands, P-gp is distributed on the surface of cells in the medulla and the adrenal cortex. This led to the suggestion that P-gp was linked with hormonal transport in the hormone-producing gland, especially when there was evidence that human MDR1 P-gp could transport the corticosteroid hormones cortisol, aldosterone and dexamethasone [Ueda *et al.*, 1992]. Alternatively, it

might protect steroid-secreting cells against the potentially damaging high local concentration of steroids in the membranes of these cells [Yang et al., 1989].

In the brain, P-gp was detected in the brain capillary endothelial cells and acted as a detoxifying against foreign drugs [Schinkel et al., 1994, Asperen et al., 1997]. Disruption of the mouse mdr1a P-gp gene led to an increased sensitivity to the centrally neurotoxic pesticide ivermectin and vinblastine as a result of the deficiency in the blood-brain barrier [Schinkel et al., 1994].

Intestinal P-gp also plays an important role in the excretion of transported drugs and in limiting drug uptake since it acts as an absorption barrier and protects the body against xenobiotics. A wide spectrum of drugs as P-gp substrates had been reported [Terao et al., 1996]. Quinidine was reported to be a substrate for intestinal P-gp [Emi et al., 1998] and it was exorbed from the blood into the intestinal lumen in rats in addition to passive diffusion [Bair et al., 1992]. Limited oral bioavailability and active excretion of paclitaxel (Taxol) caused by P-gp in rat intestine has also been observed [Sparreboom et al., 1997]. In mice whose mdr1 gene encoding the drug transporting P-gp was homozygously disrupted, there was an increased oral bioavailability from 11% to 35% whereas the drug excretion from the systemic circulation was decreased from 87% to less than 3% of the dose [Sparreboom et al., 1997]. Differences in the clearance of cyclosporin A amongst patients of up to 17% was attributed to variation in intestinal P-gp levels [Lown et al., 1997b].

1.9.5   P-GP IN CACO-2 CELLS

Evidence of a polarised efflux system capable of modulating cyclosporin A (CsA) transport in Caco-2 cells has been reported [Augustijns et al., 1993]. The apical-to-basolateral (A-B) transport of cyclosporin A was non-linear at low concentrations (0.25-5.0 µM) and was lower than that in the reverse (B-A) direction. The presence of P-gp inhibitors such as chlorpromazine and progesterone increased the absorptive flux of CsA whereas its secretory flux was decreased. These results indicated the possibility of P-gp existence in Caco-2 cells which functions as a drug efflux pump and thus, contributing to the ability of existing intestinal transporters in limiting the absorption of xenobiotics [Hunter et al., 1993a]. Indeed, the functional expression of P-gp in the apical membranes of Caco-2 cells which limited the net transepithelial transport of vinblastine had been

identified [Hunter *et al.*, 1993b]. P-gp was found to be located in the apical brush border, approximately 20 μm above the base of the cells and mediated the secretion of vinblastine in the basolateral-to-apical direction with an affinity of 18.99 ± 5.55 μM and a maximum velocity of 1285.9 ± 281.2 pmol/cm^2/h [Hunter *et al.*, 1993b]. There was a direct correlation between the expression of P-gp and the net secretory vinblastine flux which was reduced in the presence of P-gp modulators such as verapamil (R- and S-isomers with equal affinity), nifedipine, taxotere and 1, 9-dideoxyforskolin. Since vinblastine secretory flux was mediated by an active transporter in Caco-2 cells, it was temperature- and energy-dependent [Wils *et al.*, 1994]. Active apical secretory efflux of other drugs such as the HIV protease inhibitors saquinavir and ritonavir [Alsenz *et al.*, 1998], azasetron, a 5-hydroxytryptamine receptor antagonist [Tamai *et al.*, 1997] and linear peptides [Nerurkar *et al.*, 1996] in Caco-2 cells has also been reported.

Variable levels of functional P-gp expression in Caco-2 cells were observed depending on the time in culture, culture conditions and previous exposure to drugs [Hosoya *et al.*, 1996; Anderle *et al.*, 1998]. P-gp was expressed as early as day 7 in Caco-2 cells cultured on permeable inserts but it might not be fully functional until day 17 in culture. Its expression was time-dependent with 1 week > 3 week > 2 weeks based on Western blot analysis [Hosoya *et al.*, 1996]. Trypsinising the cells before they reached confluence resulted in an increase in P-gp expression whereas culturing Caco-2 cells in plastic polystyrene flasks decreased its expression over time [Anderle *et al.*, 1998]. Previous exposure to drugs such as verapamil, celiprolol, and vinblastine induced P-gp expression whereas metkephamid decreased its expression compared to the control value [Anderle *et al.*, 1998]. Continuous exposure of Caco-2 cells to cytotoxic drug such as desacetylvinblastine sulphate (DAVBL sulphate) resulted in an increase in the level of expression of P-gp as confirmed by Western blot analysis and cross resistance of the cell line to various anticancer drugs such as colchicine and doxorubicin [Hoskin *et al.*, 1993]. In parallel with its protein expression, the amount of MDR1 mRNA also increased with continuous DAVBL sulphate exposure. However, in the absence of selective pressure, the cytotoxic drug resistance of Caco-2 cells and their MDR1 mRNA declined whilst P-gp protein expression remained the same [Hoskin *et al.*, 1993]. Since P-gp is expressed in the apical membranes of the cells as well as intracellularly [Willingham *et al.*, 1987;

Duensing and Slate, 1994], it could be that the unchanged P-gp expression of Caco-2 cells as mentioned above was contributed predominantly by non- functional intracellular P-gp.

1.9.6 OTHER MODELS TO STUDY P-GP FUNCTION

The reconstitution of partially purified P-gp from the multidrug resistant CHO cell line into liposomes to make proteoliposomes has been reported [Sharom *et al.*, 1993]. This *in vitro* model displayed an ATP-dependent [^{3}H]colchicine uptake over 4 minutes. No drug uptake was observed for liposomes of lipid alone or liposomes reconstituted with similar extracts from drug-sensitive cells. The uptake of colchicine into the proteoliposomes was inhibited by verapamil, daunorubicin and vincristine. The proteoliposomes showed a high level of ATPase activity which was stimulated over two-fold by verapamil and trifluoperazine. Taken together, the results suggested that P-gp functioned as an active drug transporter with constitutive ATPase activity in proteoliposomes [Sharom *et al.*, 1993]. However, there were a numbers of limitations with this model. Firstly, the lipid composition of the liposomes was chosen on the basis of the stimulation and/ or preservation of the ATPase activity of P-gp from thermal inactivation. Therefore, it does not reflect the true characteristics of the natural semi-fluid, phospholipid bilayers of cell membranes in which P-gp is embedded and functions. Secondly, due to method limitations, P-gp was inserted in such a way that approximately 55% of the reconstituted protein faced inward so that ATP was accessible to the ATP-binding domains on the external surface and the protein could mediate the uptake of colchicine into the proteoliposomes. Therefore, the uptake of a P-gp substrate (*i.e.* colchicine) as a result of P-gp activity was assessed instead of its efflux activity, making the interpretation and direct comparisons of the results obtained from such studies to deduce the true kinetic parameters for drug transport by P-gp not possible. In addition, a limited quantity of proteoliposomes containing the correctly inserted P-gp poses a problem for large-scale investigation of the initial rates of drug transport. Moreover, ATPase activity appeared to be uncoupled from drug binding in such a system which, in turn, makes it more difficult to distinguish the specific P-gp interactions from those of non-specific origin.

A radioligand–binding assay employing P-gp over-expressing cells to test drug affinity to P-gp has been reported [Doppenschmitt et al., 1998]. In this assay, concentration-dependent displacement of [³H]verapamil as a radioligand by various non-labelled ligands was carried out and the affinity constants for P-gp binding were calculated. Although this method offers quick screening to detect compounds whose absorption might be affected by P-gp excretion, it does not offer the insight into the drug absorption process which comprises many affecting parameters in addition to drug efflux by P-gp.

The improved rat everted gut sac system where good tissue viability was achieved by incubating the inverted sacs in tissue culture medium had been used as a tool to evaluate the role of P-gp in the intestinal absorption of drugs, and to screen P-gp inhibitors that might improve the bioavailability of drugs susceptible to transport by P-gp [Barthe et al., 1998]. However, the model is of non-human origin, inter-animal variation which may make result interpretation difficult, a large quantity of drugs may be required in the study and the cost of maintenance of the animals are but a few limitations with this approach.

1.9.7 OTHER DRUG EFFLUX TRANSPORTERS

There are two other identified membrane-bound drug efflux pumps that belong to the ABC (ATP-binding cassette) superfamily of transporters, namely multidrug-resistance proteins (MRP) 1 and 2. MRP1 is a plasma membrane glycoprotein of molecular weight 180-195 kDa, found predominantly in tumour cells, and acts a drug efflux pump to reduce cellular accumulation of cytotoxic drugs such as daunorubicin, vincristine and VP-16 [Zaman et al., 1994]. Another isoform of MRP1 has been cloned and termed MRP2 or canalicular MRP or canalicular multispecific organic anion transporter (cMOAT). It is located predominantly in the hepatocyte canalicular membrane and transports glutathione-S-conjugates and glucuronide conjugates from the liver into the bile [Keppler and Konig, 1997]. Human MRP1 and MRP2 share an overall 49% identity in the amino acid sequence with each other with the highest degree of amino acid identity in the carboxy-terminal domain and in the nucleotide binding domains [Buchler et al., 1996]. Comparison between MRP1 and P-glycoprotein indicates an amino acid sequence identity of 15% whereas MRP2 shares 24% amino acid sequence identity with hepatocyte P-gp (a product of the MDR2 gene) [Cole et al., 1992]

46

Although MRP1 and P-gp share some similarities, such as they are both localised in the plasma membrane of multidrug-resistance cells, both act as a barrier to and reduce the intracellular concentration of cytotoxic drugs and both require ATP for their function, their substrate specificities differ. Specific substrates with high affinity for MRP1 (and also for MRP2) include glutathione (GSH)- or glucuronide conjugate anions such as leukotriene C_4, estradiol 17 β-glucuronide and other amphiphilic anionic conjugates [Leier *et al.*, 1994; Loe *et al.*, 1996; Loe *et al.*, 1998]. However, the glutathione moiety is not a structural determinant of the substrate properties of MRP1 as it was demonstrated by Loe *et al.*, (1998) that MRP actively co-transported GSH and unmodified vincristine (*i.e.* no conjugation) and that vincristine uptake was accompanied by a drug dependent-accumulation of the GSH.

1.10 INTESTINAL CYTOCHROME P450

Xenobiotic metabolism is a process by which the molecular structures of easily absorbed lipophilic compounds are converted to a more hydrophilic nature and their absorption, therefore, is minimised or avoided. There are two stages of metabolism namely phases I and II. Amongst phase I biotransformation, the cytochrome P450 system ranks first in terms of catalytic versability and the sheer number of xenobiotics it detoxifies or activates to reactive intermediates.

1.10.1 GENERAL INTRODUCTION OF CYTOCHROME P450 ENZYMES (P450s)

P450s belong to a group of similar proteins (or isozymes) that have the same porphyrin-haem complex as the catalytic centre but different amino acid sequences which alter the conformation of the active sites. The haem iron in cytochrome P450 is usually in the ferric state (Fe^{3+}) and when reduced to its ferrous state (Fe^{2+}), the enzymes can bind to ligands such as oxygen (O_2) or carbon monoxide (CO). The complex between ferrous P450 and CO absorbs light maximally at 450 nm from which P450s derive their names [Parkinson, 1996]. Since P450s are mono-oxygenases, they oxidise compounds on the carbon atom or on hetero atoms such as nitrogen and sulphur [Parkinson, 1996]. A typical reaction of P450s is shown below:

$$\text{Substrate (RH)} + O_2 + \text{NADPH} + H^+ \xrightarrow{\text{P450s}} \text{ROH (product)} + H_2O + \text{NADP}^+$$
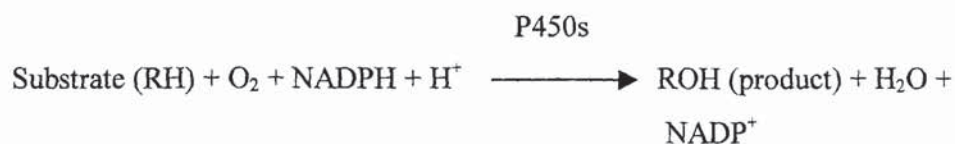
A reducing co-enzyme nicotinamide adenine diphosphate (NADP) is required to relay electrons to P450s *via* another protein. The nature of the protein varies depending on the subcellular location of P450s [Parkinson, 1996]. In the endoplasmic reticulum where most P450s involved in the metabolism of xenobiotics are located, a flavoprotein called NADPH-cytochrome P450 reductase is involved. However, in the mitochondria which house many of the P450s involving in steroid hormone synthesis and vitamin D metabolism, electrons are transferred onto P450s *via* two proteins called ferrodoxin (an iron-sulphur protein) and ferridoxin reductase. NADPH-cytochrome P450 reductase must be imbedded in the phospholipid bilayer of the endoplasmic reticulum in order for it to function. When the C- terminal region that anchors it is cleaved by trypsin, the truncated flavoprotein can no longer support P450 reactions [Parkinson, 1996]. As P450s exist as a family of enzymes, their amino-acid sequences form the basis of their classification and naming. In general, if P450s exhibit more than 40 % amino acid sequence homology, they belong to the same family whilst those displaying more than 60 % amino-acid sequence homology belong to the same subfamily [Spatzenegger and Jaeger, 1995]. Of several human P450 enzymes, those of the CYP3A sub-family have major importance since

- they are by far the most abundant of all the human CYP isoforms
- their substrate specificity is extremely broad
- they are localised in organs of particular relevance to drug disposition such as the GI tract, kidney and the liver
- their catalytic activity is readily modulated by a variety of compounds

1.10.2 TISSUE LOCALISATION OF CYTOCHROME P450 3A (CYP3A)

There are at least three existing functional CYP3A proteins in humans, namely CYP3A4, CYP3A5 and CYP3A7. CYP3A4 is universally found in the liver where it constitutes a major isoform, on average about 30% of the total CYP protein [Shimada *et al.*, 1994]. CYP3A3 is a very closely related isoform to CYP3A4 (>98% cDNA sequence similarity) but its is not known whether this reflects a separate genetic product or an allelic variant [Thummel and Wilkinson., 1998]. Therefore, the term CYP3A4 is generally taken to indicate a collective

contribution of the two isoforms. Apart from the liver, relatively high levels of CYP3A (about 50% of hepatic levels and 70% of total CYP protein) are also present in the GI tract, particular in the region of mature enterocytes [Kolars et al., 1992a, b]. In the kidney, CYP3A4 is present in only 30% of renal tissue samples, mainly in the collecting ducts [Schuetz et al., 1992; Haehner et al., 1996], the reasons for such polymorphic expression is not currently understood.

CYP3A5 is distinct from CYP3A4 and their similarities and differences will be discussed later in section 1.10.6. It is expressed in about 10-30% of hepatic samples and at levels of 10-30% of CYP3A4 [Wrighton et al., 1989; Wrighton et al., 1990]. CYP3A5 is the predominant 3A isoform that is universally expressed in the kidney [Schuetz et al., 1992]. It is also expressed heterogeneously in the GI tract but in lower amounts than CYP3A4 except in the parietal cells of the stomach [Kolars et al., 1992a; McKinnon et al., 1992] and in the colon [Gervot et al., 1996]. The third functional CYP3A isoform is CYP3A7 which was originally found in foetal liver but may also be selectively expressed in adult liver at lower amounts than CYP3A4 and CYP3A5 [Schuetz et al., 1994].

1.10.3 SIGNIFICANT DRUG INTERACTIONS MEDIATED BY CYP3A

In the treatment of certain diseases such as HIV infection and cancer, a combination of many drugs from different therapeutic classes is often used instead of one. In such cases, there exists a significant potential for drug interactions. HIV-infected patients receive, in addition to a combination of HIV drug therapy, concomitant therapeutic treatment for prophylaxis against possible opportunistic infections. Amprenavir is a novel, potent HIV protease inhibitor and is metabolised primarily by CYP3A4 in human liver microsomes [Decker et al., 1998]. The presence of terfenadine and astemizole inhibited amprenavir metabolism by 75% by human liver microsomes and likewise, the disappearance of terfenadine and astemizole, both of which are CYP3A4 substrates, was partially inhibited following the addition of amprenavir to human liver microsomal preparations [Decker et al., 1998]. In addition, it also inhibited the oxidative metabolism of other HIV protease inhibitors such as nelfinavir, saquinavir and indinavir with IC_{50} values of 10, 5.5 and 15.7 μM respectively [Decker et al., 1998], indicating the need for careful evaluation of co-administration of drugs to avoid undesirable interactions.

Terfenadine is a non-sedating H_1 antagonist which is extensively metabolised by CYP3A4 to form azacyclonol and terfenadine alcohol at a ratio of the rate of terfenadine alcohol formation to that of azacyclonol being 3:1 [Ling *et al.*, 1995]. Macrolide antibiotics such as troleandomycin and an azole antifungal agent such as ketoconazole, both of which are CYP3A4 substrate inhibitors, inhibited terfenadine alcohol formation [Ling *et al.*, 1995] and can produce serious cardiac arrythmias, a side-effect of terfenadine, leading to some instances to death [Woosley, 1996].

Midazolam is a short-acting benzodiazepine used prior to diagnostic procedures such as endoscopy as a premedicant which can interact with omeprazole and cimetidine given chronically to patients with chronic peptic ulcer disease. Formation of midazolam metabolites have been shown to be inhibited in a concentration-dependent fashion by omeprazole and cimetidine with IC_{50} values ranging from <0.2 to 3.75 mmol/l in man [Li and Klotz, 1990].

Cyclosporine A (CsA) is a widely used immunosuppressive agent. Initially, it was thought that the low bioavailability of oral cyclosporin formulation was due to its poor oral absorption. However, Wu *et al.*, (1995) demonstrated that Sandimune™ is at least 65% absorbed when administered orally. CsA is known to be metabolised by CYP3A4 and to a lesser extent CYP3A5 [Kolars *et al.*, 1991a, Gromez *et al.*, 1995]. Since both enzymes exist in the intestine [Lown *et al.*, 1994] as well as in the liver, it would be reasonable to assume that the metabolism of CsA would also occur at both sides. An increase in CsA plasma concentration leads to its detrimental side effect such as nephrotoxicity and equally important, a low therapeutic plasma concentration level as a result of drug interaction leads to graft rejection. A combination of a low dose of either ketoconazole or diltiazem with CsA has some therapeutic use to deliberately reduce the latter's metabolism by CYP3A to optimise transplantation success [Thummel and Wilkinson, 1998]

A table enlisting therapeutic agents that are involved in clinically important drug interactions by modulating the activity of CYP3A is presented in table 1.5.

TABLE 1.5   **Therapeutic agents modulating CYP3A activity**

[Adapted from Thummel and Wilkinson, 1998]

Therapeutic agents	CYP3A inhibitor	CYP3A inducer
Azole antifungal agents		
Ketoconazole	+	
Itraconazole	+	
Fluconazole	+	
Macrolide antibiotics		
Erythromycin	+	
Troleandomycin	+	
Calcium channel blockers		
Verapamil	+	
Diltiazem	+	
Serotonin re-uptake inhibitors		
Nefazodole	+	
Fluvoxamine	+	
Sertraline	+	
Paroxetine	+	
Venlafaxine	+	
Anticonvulsants		
Carbamazepine		+
Phenytoin		+
Primidone		+
Phenobarbitone		+

1.10.4 INTESTINAL CYTOCHROME P450s

Phase I metabolism of xenobiotics starts as soon as they cross the intestinal epithelial cells. The distribution of cytochrome P450s along the GI tract is not uniform. In the oesophagus, stomach and colon, there are minimal amounts of cytochrome P450 3A (CYP3A), 2E1 (CYP2E1), 2D6 (CYP2D6), 1A2 (CYP1A2) and 2C (CYP2C) whilst the small intestine contains much higher amounts of CYP3A, CYP2D6 and CYP2C. Microsomal enzymes of the small intestine

contain ~50 % CYP3A4 and 10-20 % CYP2D6 of their respective levels in human liver [deWazier *et al.*, 1990]. Both enzymes metabolise a wide variety of therapeutic drugs and only a few selected examples are presented in the table 1.6

TABLE 1.6   **Therapeutic drugs metabolised by CYP2D6 and 3A4**

[Adapted from Spatzenegger and Jaeger, 1995]

CYP2D6		CYP3A4	
Amitriptyline	Lidocaine	Alfetanil	Glyceryl trinitrate
Brofaromine	Maprotiline	Amiodarone	Ifosfamide
Bufuralol	Propranolol	Benzphetamine	Ketoconazole
Bunitrolol	Metoprolol	Caffeine	Lidocaine
Captopril	Mexilitine	Cannabidiol	Lovastatin
Citalopram	Minaprine	Carbamazepine	Mephenytoin
Clomipramine	Nortryptiline	Cocaine	Miconazole
Clozapine	Omeprazole	Codeine	Midazolam
Codeine	Ondansetron	Corticosterone	Nifedipine
Debrisoquine	Paroxitine	Cortisol	Oxodipine
Amiflamine	Perphenazine	Zonisamide	Paracetamol
Desipramine	Phenformin	Cyclosporin A	Prednisone
Remoxipride	Propafenone	Dantrolene	Propafenone
Encainide		Dapsone	Quinidine
Ethylmorphine		Dextramethorphan	Rapamicin
Flecainide		Diazepam	Retinoic acid
Fluperlapine		Digitoxin	Tamoxifen
Haloperidol		Etoposide	Paclitaxel
Imipramine		Diltiazem	Teniposide
Indoramine		Enalapril	Terfenadine
Fluphenazine		Ethylmorphine	Testosterone
Guanoxan		Erythromycin	Theophylline
Spartein		Estradiol	Toltrzuril
Thebaine		Estrogens	Trazolam
Thioridazine		Flutamide	Verapamil
Timolol		Ethinyl oestradiol	Vinblastine
Tomoxetine		Ethosuximide	Warfarin
Trifluperidol		Etoposide	
Trimipramine			

Within the small intestine, there are higher total mucosal P450 contents in the duodenum and jejunum compared to that in the ileum. Transition from the ileal to colonic mucosa results in a further drop of total P450 content [deWazier *et al.*, 1990]. Therefore, therapeutic drugs which are absorbed at different sites in the small intestine are metabolised to different extents; this is one of many factors which contribute to their variable oral bioavilability.

1.10.5 EXPRESSION OF INTESTINAL CYP3A

Cytochrome P450 3A enzymes (CYP3A) account for approximately 70% of total P450 enzymes in the jejunal mucosa [Watkins *et al.*, 1987]. Their distribution along the small human intestine is such that the level of microsomal CYP3A content is greatest in the duodenum and lowest in the ileum (931 *vs.* 17 pmol/mg of protein) [Paine *et al.*, 1997]. Similarly, CYP3A catalytic activity as reflected the metabolism of midazolam decreases from the duodenum to the jejunum to the ileum (644 *vs.* 426 *vs.* 68 pmol/min/mg of protein) [Paine *et al.*, 1997]. In the human intestine, there are two different but closely related intestinal CYP3A isoforms, namely CYP3A4 and CYP3A5 [Lown *et al.*, 1994]. CYP3A5 was found in 70% of the intestinal biopsies [Lown *et al.*, 1994] but cytochrome P450 3A4 was the most abundant CYP3A enzyme by far in the GI tract [deWazier *et al.*, 1990]. CYP3A4 is located in mature enterocytes [Kolars *et al.*, 1992a, b] but not in crypt cells. Its cellular distribution is such that it is prominent at the villus tip and forms an intense band at the apex of the cells as revealed by immunohistochemistry [Kolars *et al.*, 1992a]. In parallel with protein expression, its gene is also detected in human enterocytes and is inducible by rifampicin [Kolars *et al.*, 1992c, Lown *et al.*, 1996].

The interpatient heterogeneity in the expression of CYP3A4 and CYP3A5 in the small bowel has been well documented [Kolars et al., 1991b; Lown *et al.*, 1994, Watkins, 1994]. There was a 6-fold variation in CYP3A catalytic activity as illustrated by midazolam hydroxylation, an 11-fold variation in the CYP3A4 protein content and an 8-fold variation in CYP3A4 mRNA content in human intestinal biopsies [Lown *et al.*, 1994]. Expression of CYP3A4 as reflected by the formation of 1-hydroxy/4-hydroxymidazolam, CYP3A4 protein and CYP3A4 mRNA varies with gender, with females having a higher expression than males [Lown *et al.*, 1994]. Diseases and diet contribute to the variability in intestinal

CYP 3A expression and function. Lang *et al.*, (1996) reported that patients with coeliac disease exhibited a diminished level of immunoreactive CYP3A protein in the jejunal mucosa and this aberration could be reversed with a gluten-free diet. Catalytic activity of CYP3A4 can be up-regulated with dietary flavones [McKinnon *et al.*, 1992] and intestinal CYP3A protein expression is decreased by grapefruit juice in the diet down to 62% of the control value [Lown *et al.*, 1997a]. The bioavailability of orally administered felodipine in humans increased if it was taken together with grapefruit juice with the effect increased with prolonged administration of the juice [Lown *et al.*, 1997a]. Surprisingly, whilst there was a change in CYP3A protein expression, there was no corresponding change in CYP mRNA level [Lown *et al.*, 1997a], suggesting that post-translational factors may play an important role in the expression of CYP3A.

1.10.6 SIMILARITIES AND DIFFERENCES BETWEEN CYP3A4 AND CYP3A5

Cytochrome P450 3A5 contains 502 amino acid residues with a calculated mass of 57, 115 Da and displays 84% similarity with the amino-acid sequence of CYP3A4, the molecular weight of which is 52, 000 Da [Aoyama *et al.*, 1989; Wrighton *et al.*, 1989]. Due to very similar molecular weights and amino acid sequences, it is very difficult to distinguish CYP3A4 from CYP3A5 by Western blotting. However, they differ in some of their catalytic properties. In contrast to CYP3A4 which metabolises erythromycin and quinidine, CYP3A5 does not catalyse erythromycin-N-demethylation, quinidine-N-oxidation or 3-hydroxylation, or 17α-ethynylestradiol 2-hydroxylation at significant rate [Wrighton *et al.*, 1990]. The anxiolytic drug midazolam is converted into 1- and 4-hydroxymidazolam by CYP3A enzymes [Schmiedlin-Ren *et al.*, 1997]. Microsomal samples containing CYP3A5 in addition to CYP3A4 exhibited a significant greater ratio of 1-hydroxymidazolam to 4-hydroxymidazolam compared with samples containing only CYP3A4 [Gorski *et al.*, 1994]. In addition, CYP3A5 also differs from CYP3A4 in that its expression does not appear to be up-regulated by agents that are well-established inducers for CYP3A4 [Wrighton *et al.*, 1989]

1.10.7 SUITABILITY OF CACO-2 CELLS AS AN *IN VITRO* MODEL FOR DRUG METABOLISM STUDIES

In vitro approaches to studying CYP3A activity have the advantage that conditions can be more closely controlled and altered than *in vivo* methods. On the other hand, the selected *in vitro* conditions may not be representative of those *in vivo*, particularly when the level of cellular integrity and organisation decrease and therefore, experimental findings cannot be readily extrapolated quantitatively.

A major problem for *in vitro* studies of human CYP3A-catalysed reactions is the lack of availability of suitable tissues. Postmortem sources are of little value since the materials must be as fresh as possible and appropriately preserved. Human tissues can be obtained from surgery or from organs that are unsuitable for transplantation. However, the organ conditions that cause its rejection including interrupted blood flow or physical damage, in addition to possible previous drug exposure, may compromise the *in vitro* cell viability and actual metabolic function. As a consequence of the rapid functional deterioration of hepatocytes and liver slices, procedures involving cold preservation (0-4°C) and cryopreservation (-70°C or below) have been investigated with increasing success [Skett *et al.*, 1995].

The closer the origin, architectural and cellular integrity of the tissue preparation relative to that *in vivo*, the more closely the findings relate to those in the whole organ. Caco-2 cells are of human origin [Fogh *et al.*, 1977] and differentiate into enterocyte-like cells upon confluence [Pinto *et al.*, 1983]. However, under conditions similar to those used for conventional transport studies, Caco-2 cells have no measurable P450 activities [Prueksaritanont *et al.*, 1996]. In contrast, Gan *et al.*, (1996) reported a CYP3A-like metabolic activity in Caco-2 cells under normal cell culture conditions. The reason behind the conclusion of detectable "CYP3A-like activity" was because complete metabolism of cyclosporin A by intestinal CYP3A enzymes yielded three different products, namely M1, M17 and M21 [Kolars *et al.*, 1991a] and that only M17 was detected in Caco-2 cells [Gan *et al.*, 1996]. To add to the conflicting evidence, Gervot *et al.*, (1996) showed that CYP3A5 was the major cytochrome P450 3A expressed in Caco-2 cells at the protein and mRNA level. These discrepancies may be caused partly by differences in the cell-line population, culture media and/or conditions used [Prueksaritanont *et al.*, 1996]. In addition, different detection methods used in distinguishing the presence of CYP3A4 from that of its closely related member

CYP3A5 may contribute to different findings, especially when the amino-acid sequences of CYP3A4 and CYP3A5 have 84% identity [Aoyama et al., 1989] and that they shown similar substrate specificity [Aoyama et al., 1989; Wrighton et al., 1989].

Different methods have been used to enhance the expression of CYP3A in Caco-2 cells. They included the use of an extrachromosomal factor to express CYP3A4 cDNA in Caco-2 cells [Crespi et al., 1996], Caco-2 cell subclone TC7 [Carriere et al., 1994, Raeissi et al., 1997] and different cell modulators [Schuetz et al., 1996]. Schmiedlin-Ren et al., (1997) reported the use of 1α, 25-dihydroxyvitamin D_3 and an extracellular matrix, Matrigel®, as means to enhance the expression of CYP3A4 in a Caco-2 cell clone. Treatment of Caco-2 cells with 1α, 25-dihydroxyvitamin D_3 at the beginning of their confluence resulted in a dose- and duration-dependent increase in CYP3A4 mRNA and protein as a result of transcriptional activation of the native CYP3A gene using 1α, 25-dihydroxyvitamin D_3 [Schmiedlin-Ren et al., 1997]. For cells which had been treated for two weeks postconfluence, there was an increased CYP3A4 mRNA expression at all concentrations of 1α, 25-dihydroxyvitamin D_3 used (0.05-1.00 μM). In addition, increased CYP3A protein was evident at 0.05 μM and reached a maximum at 0.25-0.5 μM. Compared to untreated cells, which contained ~7.9 pmol of total CYP3A/mg cell protein, the maximal expression of CYP3A was 20.6 pmol/mg cell protein for those which had been treated with 0.5 μM 1α, 25-dihydroxyvitamin D_3. In cells that had been treated with 0.25 μM 1α, 25-dihydroxyvitamin D_3 for two weeks post-confluence, the rate of formation of 1-hydroxymidazolam (1-OH midazolam) being 75.9 pmol/min/g of cells. Interestingly, one subclone of Caco-2 cells, subclone 5, still possessed a higher rate of 1-OH midazolam formation than the parent cells without any treatment.

There was additional evidence that in treated cells, 1-hydroxymidazolam was preferentially sorted in the apical compartment regardless of the administration chamber [Schmiedlin-Ren et al., 1997; Fisher et al., 1999b] which might indicate an apically-directed transport process for the metabolite. However, co-administration of verapamil, a substrate for CYP3A and P-glycoprotein (P-gp) with midazolam in both compartments resulted in the same observation, suggesting that the 1-hydroxymidazolam sorting mechanism was not controlled by the apically-directed P-gp pump that was expressed in those cells even though there

was a parallel increase in P-gp protein with an increase in CYP3A [Schmiedlin-Ren *et al.*, 1997]. The presence of human serum albumin (4 g/l) in the basolateral chamber reduced the 1-hydroxymidazolam formation rate by 20% when midazolam was administered apically. This value was to increase to 86% when both midazolam and human serum albumin were administered in the basolateral chamber, indicating that extra protein binding of the parent drug did have an effect on its first-pass metabolism in an *in vitro* model such as in Caco-2 cells [Fisher *et al.*, 1999a].

Thus, as reported above, it should now be possible to study the role and importance of CYP3A in the vectorial transport of substrates analogous to that occurring during intestinal absorption as well as the interaction of this process with P-gp mediated efflux since Caco-2 cells constitutively express this transporter.

1.11   OBJECTIVES OF THE THESIS

The aims of the project are:

(i)   To develop a Caco-2 cell line that expresses a higher level of P-gp than the original cells through a multistep cytotoxic drug (doxorubicin) selection

(ii)   To characterise this high P-gp-expressing cell line in terms of cellular morphology and the expression of di/tripeptide and amino acid transporters

(iii)   To promote the expression of CYP3A enzymes in Caco-2 cells by means of cellular exposure to 1α, 25-dihydroxyvitamin D_3 followed by their characterisation

(iv)   To investigate if there is any co-regulation of the expression of CYP3A and P-gp in Caco-2 cells

These studies will hopefully develop a Caco-2 cell model that expresses a stable, high level of P-gp and CYP3A and will contribute to an understanding of the roles of these systems in drug absorption. This model may be useful in the high throughput screening of a wide range of drug candidates in the early phase of their development to select lead compounds. In addition, the current work also sheds some very interesting light on the nature of existence of P-gp as well as to provide an answer to the speculation that there may be a co-regulation of CYP3A and P-gp, at least in Caco-2 cells.

CHAPTER TWO

MATERIALS AND METHODS

ABSTRACT

The materials and methods used routinely for the work of this thesis are presented here. Supplementary and modified experimental procedures are described in the relevant sections of subsequent chapters.

2.1. MATERIALS

2.1.1 CELL CULTURE REAGENTS

Caco-2 cells were classified into two groups: i) cells of lower passage number ranging from 18-40 and ii) those of higher passage number at 90 or above. They were obtained from the American Type Tissue Culture Collection (ATCC) (MD, USA) and Novartis (Horsham, UK) respectively. Type I and II cells were Caco-2 cells of passage number >90 which had been exposed to increasing concentrations of doxorubicin (1-2 μM) and will be described in chapter 4 in the relevant sections.

Dulbecco's Modified Eagle Medium (DMEM), foetal calf serum (FCS), trypsin/EDTA, glutamine (200 mM), penicillin/streptomycin, non-essential amino acids (NEAA) (100x), N-2-hydroxyethylpiperazine-N'-2-ethansulphonic acid (HEPES) powder, phosphate-buffered saline (PBS) tablets and ethylenediaminetetraacetic acid (EDTA) powder were obtained from Gibco (Paisley, UK). The bicinchoninic acid (BCA) protein assay reagent and Neubauer haemocytometer were purchased from Sigma (Poole, UK). Doxorubicin (2mg/mL, Pharmacia) was supplied by City Hospital (Birmingham, UK) every other week. 1α, 25-dihydroxyviatmin D_3 (1μg/μL) was purchased from Calbiochem (Nottingham, UK). Tissue-culture vented flasks, plastic 24- and 6-well plates, clear polyester and collagen-coated Costar™ inserts (3.0 μm pore-size membrane) were purchased from Costar (Bucks, UK).

2.1.2 TRANSPORT STUDIES

Radiolabelled [^{3}H]vincristine sulphate (7.9 Ci/mmol) and D-[^{14}C]mannitol (56 Ci/mmol) were purchased from Amersham (Buckinghamshire, UK). [^{3}H]Gly-L-Pro (50 Ci mmol^{-1}), [^{3}H]L-Proline (50 Ci/mmol^{-1}) and [^{3}H]leukotriene C_4 (110.5 Ci/mmol) were obtained from Dupont New England Nuclear (NEN) Research Products (Hertfordshire, UK). SQ 29852 powder was from Bristol-Myers Squibb Research Institute (Moreton, UK). Midazolam (MDZ), 1-hydroxymidazolam (1-OH MDZ) and 4-hydroxymidazolam (4-OH MDZ) were generously donated by Roche Pharmaceutical Company (Hertfordshire, UK). ($\pm$)Verapamil, proline and Gly-L-Pro of 99% purity, 2,4-dinitrophenol (2,4-DNP), sodium azide, 2-[N-morpholino]ethanosulphonic acid (MES), sucrose powder and dimethylsulphoxide

(DMSO) were purchased from Sigma (Poole, UK). Hank's balanced salt solution powder (HBSS), with and without phenol red (0.01 g/L) was purchased from Gibco (Paisley, UK). Optiphase HiSafe III scintillant was from Fisher (Leicestershire, UK). The radioactivity of ^{3}H and ^{14}C was measured by Hewlett Packard Tricard 2000 CA liquid scintillation analyser.

2.1.3 REVERSED PHASE HPLC

HPLC-grade acetonitrile and methanol were obtained from Fisher (Leicestershire, UK). Ammonium acetate powder was purchased from Sigma (Poole, UK). Lunar(2) octadecyl silane-2 (ODS-2), 3 μm guard column (75 x 4.6 mm) and Lunar(2) analytical octadecyl silane-2 (ODS-2), 5 μm reversed-phase column (150 x 4.6 mm) were purchased from Phenomenex (Cheshire, UK).

2.1.4 EFFLUX OF VINCRISTINE SULPHATE

[^{3}H]Vincristine sulphate (7.9 Ci/mmol) was purchased from Amersham (Buckinghamshire, UK). 2,4-DNP, (±)verapamil, anhydrous $CaCl_2$, KCl, KH_2PO_4, anhydrous $MgSO_4$, NaCl, $NaHPO_4$, sucrose powder and DMSO were obtained from Sigma (Poole, UK). HBSS powder without phenol red was purchased from Gibco (Paisley, UK).

2.1.5 P-GLYCOPROTEIN AND CYTOCHROME P450 3A4 EXTRACTION

Dithiothreitol, benzydamine, aprotinin, Tris-HCl, L-histidine, sucrose and phenylmethylsulphonyl fluoride (PMSF) were purchased from Sigma (Poole, UK).

2.1.6 GEL ELECTROPHORESIS AND WESTERN BLOTTING

Ready Gel 10% Tris-HCl, polyvinylidene difluoride (PVDF) membrane (0.2 μm pore size), blot absorbent filter paper (thick) sheets, gel-running and blotting buffers, sodium dodecyl sulphate (SDS) and blocking grade blotter, non-fat milk powders, broad range pre-stained molecular weight standards (28.8-203 kDa), Laemlii sample buffer and 2-mercaptomethanol solution were obtained from Biorad (Hertfordshire, UK). Human polyclonal anticytochrome P450 3A4 raised in rabbit, anti-rabbit IgG, heavy-and-light chain (goat) alkaline phosphatase conjugate, recombinant human cytochrome P4503A4 expressed in *E.Coli*, anti-

mouse IgG, γ chain specific, (goat) F (Ab')₂ fragment alkaline phosphatase conjugate, lyophilised goat serum powder and the colour development reagent 5-bromo-4-chloro-3-indolyl phosphate/nitroblue tetrazolium (BCIP/NBT) were from Calbiochem (Nottingham, UK). Monoclonal primary antibody for Pgp, C219 raised in mouse was from Signet (Glasgow, UK).

2.1.7 FLUORESCENCE MICROSCOPY

Rhodamine 123 dye was obtained from Sigma (Poole, UK). Lab-Tek® chamber slide systems were obtained from Costar (Buckinghamshire, UK).

2.2 METHODS

2.2.1 CELL CULTURE

All cell culture procedures were carried out under aseptic conditions in a Gelaire, biohazard level II, laminar flow cabinet from ICN (Oxfordshire, UK)

2.2.1.1 MEDIA

Caco-2 cells of low (<40) and higher passage number (>90), Type I and II were maintained in cell growth medium (M1) which consisted of 4.5 g/L glucose, 10 % v/v FCS, 1 % v/v NEAA, 2 mM glutamine, 100 U/mL penicillin, 100 μg/mL streptomycin and HEPES buffer solution (5mM). Transport medium consisted of HBSS (prepared according the manufacturer's instructions) plus 25 mM MES (pH 6.0) or 25 mM HEPES (pH 7.4). Efflux medium (M3) was freshly prepared from the individual ingredients found in M2 (pH 7.4) and to the same concentration except that it contained, in addition, 2 mM 2,4-DNP, no glucose and phenol red. The transport medium (M4) had the same composition as M2 (pH 7.4) but without phenol red. Sodium hydroxide (1M) or hydrochloric acid (1M) were used to adjust the media to the appropriate pH values. M2, M3 and M4 transport media were sterilised by filtration after preparation using a 0.22 μm cellulose acetate bottle-top filter system purchased from Costar (Buckinghamshire, UK). All media were stored at 4°C, and with the exception of cell culture medium which was discarded after 2 weeks, were disposed off after 1 month from the date of preparation.

2.2.1.2 CELLULAR STOCK CULTURES

The cells were cultured in plastic tissue-culture T-flasks, with a non-wetting 0.22 µm hydrophobic microporous membrane vent and an area of 75 cm². Caco-2 cells of different passage numbers (>90 or <40) and origins were seeded at 1,000,000 cells/12 mL per flask whilst the seeding density for Type I and II cells was 2,500,000 cells/12 mL per flask. The cells were grown as monolayers in M1 at 37°C in a humidified atmosphere of 5% CO_2 / 95% air. Type I and II cells were supplemented with 1-2 µM doxorubicin dissolved in M1 immediately after seeding, once every other cell passage. Cell culture medium was replaced every 48 hours. The cells in the flasks were trypsinised/passaged once they reached confluence (4 days for low and higher passage number Caco-2 cells or 4-7 days for Type I and II cells). They were first washed with pre-warmed 0.25% w/v PBS/EDTA solution followed by the addition of 0.25% w/v trypsin/EDTA for 30 seconds. The latter was aspirated and the cells were left to detach for 5 minutes at room temperature before the addition of fresh cell culture medium.

In order to check viable-cell density, a trypan-blue exclusion test was performed when seeding cells on plastic 24-well plates or inserts. A volume of 100 µL of trypan-blue (4 mg/mL) was mixed with 400 µL of cell suspension following trypsinisation. The mixture was added to the counting chamber of a Neubauer haemocytometer, with a depth of 0.1 mm and an area of 1/400 mm². Viable cells appear with clear cytoplasm whereas dead cells absorb the stain and appear blue. The cell density was calculated according to the following equation (As *per* manufacturer's instructions included with the Neubauer haematocytometer):

EQUATION 2.1

Cells/mL = [(number of cells counted)/5] x 10^4 x 1.25 (dilution factor of trypan

blue)

Cell suspensions where the viable cells accounted for less than 96% of the total number were discarded.

2.2.2 LIQUID SCINTILLATION COUNTING

Beta-emitting radionuclides [³H] and [¹⁴C] were quantified using liquid scintillation spectrophotometry. When both radionuclides were present in the samples, they were quantified by dual scintillation counting. Optiphase Hisafe III

63

(Fisher, Leicestersher, UK) was added to each of the samples (10mL) and mixed well prior to counting by the Packard-Tricarb 2000 CA liquid scintillation analyser. The counting times for $[^3H]$ and $[^{14}C]$ radionuclides were 5 and 10 minutes respectively. In all cases, counts per minute (CPM) were converted to decays per minutes (DPM) by comparison with standard quench-correction curves

2.2.3 UPTAKE STUDY OF GLY-L-PRO

Caco-2 cells were seeded on plastic 24-well plates at a density of 80,000 cells/cm^2 and used on the seventh day post-seeding. The cells were first washed with pre-warmed PBS (0.5 mL/well) and incubated with M2 (pH 6.0) for 5 minutes at 37°C. Gly-L-Pro of various concentrations (0.02 - 1.4 mM) was dissolved in M2 (containing in addition, 10 mM L-proline) and 50 nM of $[^3H]$Gly-L-Pro was used to spike each of its non-radiolabelled concentrations. A total volume of 200 µl of the mixture was added to the apical side of the cells and they were then incubated at 37°C for 3 minutes. The uptake of Gly-L-Pro was terminated by adding ice-cold PBS-azide (0.05% w/v) to the cells (0.5 mL/well) which were subsequently washed twice with PBS-azide and the washings were collected separately. The cell monolayers were solubilised with Triton X-100 (1% v/v) (1 mL/well) for at least an hour at 37°C. The radioactivity of Gly-L-Pro associated with the washings and cells was detected by scintillation counting.

2.2.4 TRANSPORT STUDIES

2.2.4.1 TRANSPORT OF VINCRISTINE SUPHATE AND LEUKOTRIENE C$_4$

Caco-2 cells of cell passage number >90, hereafter referred to as parent Caco-2 cells and Type I cells were used as models to assess the transport of vincristine sulphate. All transport media were incubated at 37°C prior to the experiments. The existing cell culture medium was aspirated and replaced with M2 (pH 7.4) for 15 minutes. For apical-to-basolateral (A-B) transport, M2 was added to the wells of another plastic 6-well plate and the inserts, filled with M2 containing 10 nM $[^3H]$vincristine sulphate were immediately laid down into the wells to initiate transport at 37°C. Every minute for 10 minutes, the plate containing the inserts was removed from the incubator and placed on a rotating platform to encourage uniform distribution of vincristine in the receiver chamber.

A volume of 1 mL was removed from the basolateral chamber and immediately replaced with an equivalent volume of M2. At the last sampling point, the total volumes in both apical and basolateral chambers were removed. The cells on the inserts were washed twice with PBS-azide (0.05%w/v) (2 x 2mL in both apical and basolateral chambers) and collected separately. They were then solubilised by adding Triton-X 100 (1% v/v) (2mL/insert) and incubated overnight at 37°C. The cell-associated activity of vincristine, the donor solution, the collected samples at different time points and in the PBS-azide washes were determined by liquid scintillation counting. The cells on another three different inserts cultured at the same time and under the same conditions as those used in the experiments were scraped off the cell membranes using Costar cell scrapers, washed twice by centrifugation (MSE Mistral 3000I, Hitachi, Middlesex, UK) and resuspended in PBS (200μL/insert). The samples were sonicated using Soniprep 150 (Northern Media Supplied Ltd, Birmingham, UK) operating at 56 W for 20 seconds and the protein content in the cell homogenates (n=3) was determined by the BCA assay for each experimental condition. Cumulative transport was calculated by adding the current substrate accumulation in the receiver phase with that obtained previously before normalising for an average cellular protein on inserts (n=3) for each experimental condition; the results were expressed as fmol/mg protein. The apparent permeability coefficients of vincristine sulphate (Papp values) were calculated from the slopes of the plots of its cumulative transport *vs.* time according to the equation:

EQUATION 2.2

$$Papp = (dQ/dt)/(A*C_o)$$

Where

dQ/dt: the drug permeation rate (fmol/sec/mg protein)

A: the nominal surface area of the cell monolayers (4.71 cm^2)

C_o: the initial drug concentration of the donor solution (fmol/mL)

For basolateral-to-apical transport (B-A), the same procedure was applied except that [^{3}H]vincristine sulphate was added to the wells and the inserts contained M2 only.

The procedure for the transport of [³H]leukotriene C₄ was similar to that of vincristine transport except that the apical donor concentration was 1 nM.

Similarly, the same procedure was followed when vincristine was transported in the presence of a P-gp inhibitor. (±)Verapamil (100 μM) was dissolved in M2 containing 1% v/v DMSO. This solution was used to make stock solution containing 10 nM [³H]vincristine sulphate as well as to top-up both the apical and basolateral chambers throughout the experiment. In addition, the cells were pre-incubated with M2 containing 100 μM (±)verapamil for 10 minutes before the transport studies began. One-way analysis of variance (ANOVA) (Dunnett multiple comparison test) (Instat 3, Graph-pad) was used to determine the significance between (i) Papp values of vincristine or leukotriene C₄ of parent *vs.* Type I and II Caco-2 cells in the presence or absence of 100 μM (±)verapamil at $p < 0.05$ or $p < 0.01$.

2.2.4.2 TRANSPORT AND METABOLISM OF MIDAZOLAM

Midazolam transport was carried out as described in 2.2.4.1 with the following modifications: the concentration of midazolam in the donor solution (M4) was 4 μM and samples (0.5 mL/time point) were taken at 15, 30, 45, 60 and 90 minutes. A volume of 200 μL was subjected to reversed phase HPLC analysis whilst 150 μL of each sample was distributed into 96-well fluorescence plates. The fluorescence intensity was measured by the fluorescence plate reader (Excitation λ: 485 nm, emission λ: 535 nm with a plate shaking duration of 2 seconds before fluorescence measurement). After the PBS/azide washes, the cells that had been used for each experimental condition (n=3) were scraped off the membranes and their average protein content from three inserts was determined by the BCA assay. Fluorescein transport in each experiment was calculated from a series of its standard concentrations and normalised for an average cellular protein expression on inserts (n=3). The results were expressed as cumulative nmol fluorescein/mg protein/unit time. The rate of transport and accumulation of midazolam and its metabolites in the receiver chambers were expressed as nmol/min/mg protein and nmol/mg protein respectively. Transport and metabolism of midazolam in the presence and absence of an inhibitor (±)verapamil (100μM) was similar to that described previously (section 2.2.4.1) except the latter was dissolved in the donor solution containing no DMSO.

2.2.4.3 TRANSPORT OF GLY-L-PRO

The procedure for the transport of Gly-L-Pro was similar to that described in section 2.2.4.1. The donor solution was M2, pH 6.0, and consisted of 50 nM [^{3}H]Gly-L-Pro, 10 mM L-proline and 1 µM D-[^{14}C]mannitol. The solution in the receiver chamber was of pH 7.4. When Gly-L-Pro was transported in the presence of a competitive inhibitor, SQ 29852, the latter (1mM) was dissolved in the donor solution prior to it being added to the cells.

2.2.4.4 TRANSPORT OF L-PROLINE

This was carried out using a similar procedure as that described in section 2.2.4.3. L-Alanine (1µM) was added to the donor solution as a competitive amino-acid transport inhibitor.

2.2.5 REVERSED PHASE HPLC ANALYSIS OF MIDAZOLAM AND ITS METABOLITES

A Hewlett Packard (Series 1100) HPLC system with a dual-piston reciprocating pump, controlled temperature thermostat, degaser and UV detector was used. The mobile phase consisting of HPLC grade acetonitrile, methanol and 0.01 M ammonium acetate buffer, pH 7.4 in a ratio of 21: 35: 44 % v/v was filtered using a Costar bottle top filter (0.22µm pore size) and sonicated for 15 minutes before use. Both guard and analytical columns were conditioned before each use by first equilibrating them with 100 % acetonitrile for 10 minutes followed by 50 % v/v aqueous acetonitrile for 15 minutes. They were then left to equilibrate with the mobile phase for at least an hour at a flow rate of 1mL/min. An isocratic run was performed under the following conditions: flow rate of 1mL/min, the temperature of the analytical column was kept at 23°C, the UV detector was operated at 220 nm and the mobile phase was constantly degased by the degaser unit. A total volume of 200µL for each sample containing 20 ng of diazepam as an internal standard, was injected onto the column manually each time. For each HPLC run of the samples, standard midazolam and its metabolites were also analysed at the end of the experiment and the data were used to construct calibration graphs. The resolution (R_s) which measures the degree of separation of parent from metabolite peaks and between metabolite peaks themselves was quantified according to equation [Holbrook, 1989]:

EQUATION 2.3

$$R_s = 2 \times (t_B - t_A)/(W_A - W_B)$$

Where

t$_A$, t$_B$:   retention times of adjacent peaks A and B

W$_A$, W$_B$:   width of peaks A and B in unit time

Both guard and analytical columns were washed with 50 : 50 % v/v acetonitrile : water for 15 minutes followed by 100 % acetonitrile for 10 minutes after each run.

2.2.6 EFFLUX OF VINCRISTINE SULPHATE

M2 and M3 were pre-warmed to 37°C prior to the experiment. The cells on the inserts were washed with pre-warmed M3 (2 x 2ml x 5 minutes in both the apical and basolateral chambers). A solution of M3 containing 10 nM [^{3}H]vincristine sulphate was prepared and added to both chambers and the cells were loaded with vincristine at 37°C, 95% air, 5% CO_2 for 15 minutes. This solution was then withdrawn and Caco-2 cells were washed twice with M3 (2x2mL apically/basolaterally) and the washes were collected separately. M2 was added to both apical and basolateral (2mL/each) chambers in the presence and the absence of 100 μM (±)verapamil and [^{3}H]vincristine sulphate was allowed to be effluxed from the cells in both directions at 37°C for 15 minutes. The cells on inserts were washed twice with PBS-azide (0.05% w/v) in both the apical and basolateral compartments and the washes were collected separately. A volume of 2 mL of Triton-X 100 (1% v/v) was added to the cells apically and they were incubated overnight at 37°C. The radioactivity associated with the PBS-azide washes and solubilised cells was determined by scintillation counting. The cells on another three different inserts cultured at the same time and under the same conditions as those used in the experiments were scraped off the cell membranes using Costar cell scrapers, washed twice by centrifugation (MSE Mistral 3000I, Hitachi, Middlesex, UK) and resuspended in PBS (200μL/insert). The samples were sonicated using Soniprep 150 (Northern Media Supplied Ltd, Birmingham, UK) operating at 56 W for 20 seconds and the average protein content of the cell homogenates (n=3) was determined by the BCA assay for each experimental condition. Cellular accumulation of vincristine was expressed as fmol/mg protein. One-way analysis of variance (ANOVA) (Dunnett multiple comparison test) was used to determine the significant difference between the mean cellular

accumulation of vincristine in the parent *vs.* Type I cells in the presence and absence of μM (±)verapamil at $p < 0.05$.

2.2.7 P-GLYCOPROTEIN AND CYTOCHROME P450 3A4 EXTRACTION

All homogenates and microsomal extractions were stored at $-70°C$ and used within two weeks from the date of preparation.

2.2.7.1 PREPARATION OF P-GP HOMOGENATE

Caco-2 cells in plastic flasks were trypsinised as described previously (section 2.2.1.2) and washed twice with PBS by centrifugation. Cell pellets were resuspended in 0.5 mL of homogenising buffer (pH 7.4) consisting of 100 mM Tris-HCl, 1 mM dithiothreitol, 1 mM PMSF, 1 mM benzydamine, 100 μg/mL aprotinin, 10 mM EDTA and sonicated as descibed in 2.2.4.1.

2.2.7.2 EXTRACTION OF CYTOCHROME P450 3A4 ENZYMES

Caco-2 cells were scraped off the insert membranes using Costar cell scrapers and washed twice with PBS by centrifugation. Each cell pellet was resuspended in 0.5 mL of homogenising buffer and sonicated as described in section 2.2.7.1. After sonication, the cell suspension was centrifuged at 450 x g for 10 minutes to remove any unlysed cells and nuclei. The supernatant was collected and centrifuged again at 15,000 x g for 10 minutes. This was then mixed with an equal volume of 52 mM ice-cold $CaCl_2$ and was left on ice for 30 minutes to aggregate microsomes. The solution was sedimented at 2000 x g for 15 minutes and the microsomal pellet was resuspended in 50 μL homogenising buffer.

2.2.8 GEL ELECTROPHORESIS AND WESTERN BLOTTING

All samples were quantified for their protein content using the BCA assay prior to gel electrophoresis and Western blotting.

2.2.8.1 BCA ASSAY

Bicinchoninic acid (BCA) is a chromogenic reagent for Cu^{1+}. The purple coloured reaction product is formed by the chelation of two molecules of BCA

with one cuprous ion (Cu^{1+}). This water-soluble complex exhibits strong absorbance at 562 nm that is linear with increasing protein concentration. The reaction can be presented as followed:

1. Protein (peptide bonds) $+ Cu^{2+}$ $\xrightarrow{\text{OH-}}$ tetradentate-Cu^{1+} complex

2. Cu^{1+}-complex + BCA $\longrightarrow$ BCA-Cu^{1+}complex (purple red colour)

The protein determination reagent was produced by adding 1 mL of copper (II) sulphate pentahydrate 4% w/v solution to 49 mL of BCA reagent solution, mixed thoroughly and distributed into different tubes (2mL/tube). Increasing amounts of bovine serum albumin (0-50 μg) were added to the tubes from a concentrated aqueous stock (1mg/mL) as a standard. Equivalent volumes of samples were also distributed into different tubes (20 μL/tube). All tubes were incubated at 60°C for 1 hour and left to cool at room temperature for 15 minutes. Their UV absorbance was determined at 562 nm.

2.2.8.2 GEL ELECTROPHORESIS

Proteins (10-20 μL) were subjected to gel electrophoresis on Ready-Gel Tris-HCl polyacrylamide gel (10%) at a fixed voltage of 200 V for 30 minutes as per Biorad's standard protocol. Reference and test samples were added to Laemlii's sample buffer containing 0.05% v/v 2-mercaptomethanol and were heated at 70°C for 5 minutes. They were then kept on ice and were loaded in equal volume into each well.

2.2.8.3 WESTERN BLOTTING

Blotting cassettes, Scotch brite pads, PDVF membranes (after their wetting with 100 % methanol) and filter papers were soaked in blotting buffer containing an additional concentration of sodium dodecyl sulphate (SDS) (0.025 w/v) for 15 minutes at room temperature. The gel and the PDVF membrane were sandwiched first between the filter papers and then Scotch brite pads before the whole assembly was inserted into a blotting cassette. The proteins were transferred onto PDVF membranes overnight at a fixed 25V at room temperature. Tris-buffered saline (TBS) and Tris-buffered saline-Tween (TBST) solutions were prepared. TBS consisted of 0.01 mM Tris-HCl and 150 mM NaCl buffered to pH 7.4 with

Tris base whilst TBST's composition was similar to that of TBS except that it contained in addition 0.05% v/v Tween-20 and was of pH 8.0. Throughout the blotting procedure, the membrane was placed on a rotating platform to ensure even distribution of the solution and that there was no air trapped underneath the membrane. It was first soaked in TBS containing 5 % w/v non-fat milk powder for three hours. Primary antibody (C219 for P-gp) or (anti-P450 3A4 for CYP3A4) in TBS containing 0.5% w/v non-fat milk powder was then added for 90 minutes. The concentration of C219 used was 0.1 µg/mL and that of anti-P450 3A4 was 1: 1000 dilution. The membrane was then washed with TBS (pH 7.4) containing 0.5 % Tween 20 three times (10mL x 3) and immersed in TBST containing the secondary antibody for 90 minutes. The secondary antibody for P-gp was anti-mouse IgG, γ-chain specific (goat) F (Ab')$_2$ fragment alkaline phosphatase conjugate and that for CYP3A4 was anti-rabbit IgG, heavy and light chain (goat) alkaline phosphatase conjugate. The dilution factor for both secondary antibodies was 1: 1000. BCIP/NBT was added for 15-30 minutes to develop the purple bands of the relevant proteins.

2.2.9   FLUORESCENCE MICROSCOPY

Type I (#25 after their first exposure to 1 µM doxorubicin) and parent Caco-2 (#111) cells were seeded in 8-well chamber slide systems at a density of 8,000 cells/well. On day 3 post-seeding, they were incubated with rhodamine 123 laser dye (10 µg/mL) in M1 for 30 minutes in a 5%CO_2 incubator at 37°C. The cells were then washed three times with pre-warmed PBS and quickly viewed under the fluorescence microscope (Axiovert 2, Zeiss, West Gemany) using a UV lamp as a light source, FITC (fluorescein isothyanate) filter set 09 (excitation 450-490nm), beam splitter (510 nm) and emission (520 nm). The objective magnification was set at 400 x and the pictures were captured manually using a Nikon (5536694, Nikkomat, Japan) connected to the microscope.

CHAPTER THREE

DIFFERENT CHARACTERISTICS OF CACO-2 CELLS AS A FUNCTION OF PASSAGE NUMBER AND ORIGIN

ABSTRACT

Caco-2 cells of different passage numbers and origin were compared in terms of their intestinal differentiation. Under identical culturing conditions, those of passage number >90 from Novartis exhibited the following characteristics:

- an initial faster growth rate for the first three days on plastic supports

- higher alkaline phosphatase activity (0.564 ± 0.012 *vs.* 0.163 ± 0.038 U/mg protein) and protein content (311.066 ± 11.548 *vs.* 227.666 ± 16.363 mg/L)

- higher intrinsic tolerance to doxorubicin (40 *vs.* 30 nM), and

- higher expression of the di-/tripeptide transporter (Km: 0.153 ± 0.065 mM, Vmax: 1.924 ± 0.478 nmol/min/mg protein *vs.* Km: 0.085 ± 0.02 mM, Vmax: 0.761 ± 0.104 nmol/min/mg protein for Gly-L-Pro uptake).

Compared to those of passage number <40 from the American Tissue Culture Collection (ATCC, MD, USA).

3.1 INTRODUCTION

Caco-2 cell culture has been used as a model to simulate the gastrointestinal absorption of a wide range of compounds and is a useful mechanistic tool [Artursson *et al.*, 1996]. These adenocarcinoma cells are of human origin and were originally isolated by Fogh and coworkers in 1977 [Fogh *et al.*, 1977]. When grown *in vitro* under standard culture conditions in the absence of the inducers of differentiation, they spontaneously exhibit signs of intestinal morphology and functional differentiation [Pinto *et al.*, 1983]. The cell line possesses several intestinal carrier transport systems upon reaching confluence and these have been listed in table 1.4, chapter 1 and in section 1.9. Inter-laboratory differences such as passage number and origin, cell passaging procedure, different types of supports, the presence of extracellular matrices, cell culture medium composition and additional vitamins and minerals all influence the morphological and functional differentiation which contribute to the heterogeneity of Caco-2 cells [Pinto *et al.*, 1983; Hidalgo *et al.*, 1989; Anderle *et al.*, 1997; Schmiedlin-Ren *et al.*, 1997]. The transport of thyrotropin-releasing hormone (TRH) in Caco-2 cell monolayers was reported to be dependent on the passage number and origin of the cells [Walter *et al.*, 1994]. TRH transport (apical-to-basolateral direction) in low passage number Caco-2 cells (30-34) was mediated by the paracellular route, not inhibited by excess concentration of Gly-Pro and cephradine and not pH-dependent. In contrast, its transport in higher passage number Caco-2 cells (89-99) and of different origin showed a carrier-mediated component which operated in parallel with a paracellular pathway. The optimum pH for TRH transport in higher passage number Caco-2 cells was 6.0 and the Michaelis-Menten parameters of the active, saturable transport component were: $Km = 1.59$ mM and $Vmax = 1.84$ μM/min respectively [Walter *et al.*, 1994].

In the screening of new chemical entities using the Caco-2 cell model to select lead compounds with predictive good oral bioavailability, the accuracy and reproducibility of the results will shorten the discovery and characterisation of therapeutic drugs and therefore, contribute to their successful, cost-effective and rapid production. In this chapter, Caco-2 cells of different number and origin were characterised in terms of their morphology, growth rates, levels of intrinsic resistance to the cytotoxic drug doxorubicin and functional expression of the di-/tripeptide transporter (DTS). The findings will contribute toward the rational

73

selection of Caco-2 cells to best model the intestinal absorption of different drugs by different mechanisms as well as to optimise the reproducibility of reliable results.

3.2 MATERIALS AND METHODS

3.2.1 MATERIALS

Caco-2 cells of low passage number (<40) were obtained from ATCC (American Type Tissue Culture Collection-MD, USA) and those of high passage (>90) were from Novartis (Horsham, UK). For convenience purposes, they will be abbreviated as A-Caco-2 cells and N-Caco-2 cells respectively. Cell culture reagents were as described in section 2.1.1. Biocinchoninic (BCA) solution and alkaline phosphatase kit were obtained from Sigma (Poole, UK). Doxorubicin (2mg/mL, Pharmacia) was acquired from City Hospital (Birmingham, UK). Radiolabelled [^{3}H]Gly-L-Pro (50 Ci mmol^{-1}) was purchased from Dupont (NEN) Research products (Hertfordshire, UK).

3.2.2 METHODS

3.2.2.1 CELL GROWTH AND MORPHOLOGY ON PLASTIC SUPPORTS

A- and N-Caco-2 cells were seeded on plastic 24-well plates at a density of 80,000 cells/cm^2. The number of viable cells was counted on day 1, 2, 3, 4, 5, and 7 post-seeding using the trypan blue exclusion method (section 2.2.1.2). In addition, they were photographed on day 7 post-seeding by light microscopy.

3.2.2.2 DETERMINATION OF PROTEIN CONTENT AND ALKALINE PHOSPHATASE (ALP) ACTIVITY

On the seventh day post-seeding, A- and N-Caco-2 cells on plastic 24-well plates were trypsinised by incubating them with 0.4 mL of 0.25 % w/v PBS/EDTA/well for 5 minutes following by the addition of 0.2 mL of 0.25 % w/v trypsin-EDTA/well for 2 minutes. Detached cells and their washings from three groups of six wells were pooled and centrifuged at 1000 x g for 3 minutes. The supernatant was discarded. Cell pellets from each group were re-suspended in 2 mL of pre-warmed PBS and sonicated (Soniprep 150 sonicator) for 20 seconds at 56 W. The protein content of each cell type (n=3) was determined by BCA assay

74

(section 2.2.8.1) and the alkaline phosphatase activity was determined according to the manufacturer instructions.

Cellular alkaline phosphatase metabolises p-nitrophenyl phosphate at alkaline pH to form p-nitrophenol and inorganic phosphate. The absorbance of p-nitrophenol is maximum at 405 nm and is directly proportional to the ALP activity of the samples. Briefly, the alkaline phosphatase reagent (ALP) containing p-nitrophenyl phosphate was prepared according to the manufacturer's instruction and was warmed at 37°C. A volume of 20 μL of Caco-2 cellular sample was added to a cuvette containing 1 mL of the prepared, pre-warmed ALP (37°C) and was incubated for 30 seconds. Its absorbance was read at 405 nm *vs.* PBS as a reference and was recorded. This was the initial absorbance A. The cuvette was further incubated at 37°C and the absorbance was read after exactly 2 minutes following the initial absorbance reading. The change in absorbance per minute was calculated by substracting initial A from final A and dividing by 2. The ALP activity was calculated according to the following equation (Sigma's protocol):

EQUATION 3.1

ALP (Units/L)=(change in absorbance/min x TV x 1000)/18.45 x SV x LP

where:

TV: Total volume (1.02 mL)

SV: Sample volume (0.02 mL)

18.45: Millimolar absorptivity of p-nitrophenol at 405 nm

LP: Light path (1 cm)

1000:   Conversion of units per mL to units per litre

3.2.2.3 INTRINSIC RESISTANCE TO DOXORUBICIN

The ability of Caco-2 cells to pump (efflux) doxorubicin out of the cells and continue to grow after exposure to the drug is termed their intrinsic resistance. To determine the intrinsic resistance of both A- and N-Caco-2 cells to doxorubicin, they were first seeded on plastic 24-well plates at a density of 80,000 cells/cm^2. The following day, cell culture medium containing a range of concentrations of doxorubicin (0-0.2 μM) was freshly prepared. The existing cell culture medium in the wells was aspirated and immediately replaced by that containing doxorubicin to the total volume of 1 mL per well. This was done in triplicate for each doxorubicin concentration (n=3). The process was repeated

75

every other day (*i.e.* 48 hour doxorubicin exposure after each change of cell culture medium) and the number of viable cells was counted on day 7 using the trypan blue exclusion method (section 2.2.1.2). The concentration of doxorubicin which decreased 50% of the population of viable cells that are responding to doxorubicin cytoxicity was determined to evaluate the intrinsic doxorubicin drug resistance of Caco-2 cells of different passage numbers and origins.

N-Caco-2 cells were also seeded on plastic 24-well plates at a density of 80,000 cells/cm^2. Immediately after seeding, they were exposed to 0, 0.5 and 1 μM doxorubicin for 24 hours. Viable cells were counted on day 1, 3 and 6 post-seeding using the trypan blue exclusion method (section 2.2.1.2).

3.2.2.4 UPTAKE STUDIES OF GLY-L-PRO

The uptake of Gly-L-Pro by A- and N-Caco-2 cells was carried out as described in section 2.2.3. The uptake (velocity) of Gly-L-Pro was described by:

EQUATION 3.2

$$V = Vmax[S]/(Km + [S]) + k_d[S]$$

Where V: The uptake rate (nmol/min/mg protein)

Vmax: The maximum uptake rate (nmol/min/mg protein)

[S]: Concentration of Gly-L-Pro (mM)

Km: Half maximal uptake concentration (mM)

k_d: Coefficient for non-mediated and passive uptake (nmol/min/mg protein/mM)

Computer modelling with a non-linear least squares regression analysis programme, Fig P, (Biosoft) was used to determine the three model parameters V, Vmax and Km.

3.3   RESULTS AND DISCUSSION

3.3.1   CELL GROWTH AND MORPHOLOGY OF CACO-2 CELLS ON PLASTIC SUPPORTS

Figure 3.1 illustrates the growth pattern of Caco-2 cells on plastic 24-well plates. Within a confined surface area of the wells, N-Caco-2 cells multiplied faster and reached confluence on day 3 (observed by light microscopy) as

76

compared to A-Caco-2 cells which grew at a slower rate and achieved confluence on day 4 post-seeding. This difference in growth pattern was reflected by different cell morphology on day 7 post-seeding as viewed at 250 and 1000 x magnification (figure 3.2). N-Caco-2 cells seemed to possess more well-defined tight junctional complexes as compared to A-Caco-2 cells at 1000 x magnification (figure 3.2)

FIGURE 3.1 **Cell growth of N-/A-Caco-2 cells on plastic supports**

Both N- and A-Caco-2 cells were seeded at 80,000 cells/cm^2 on plastic 24-well plates. Viable cells (mean ± sd, n=3) were counted on day 7 post-seeding.
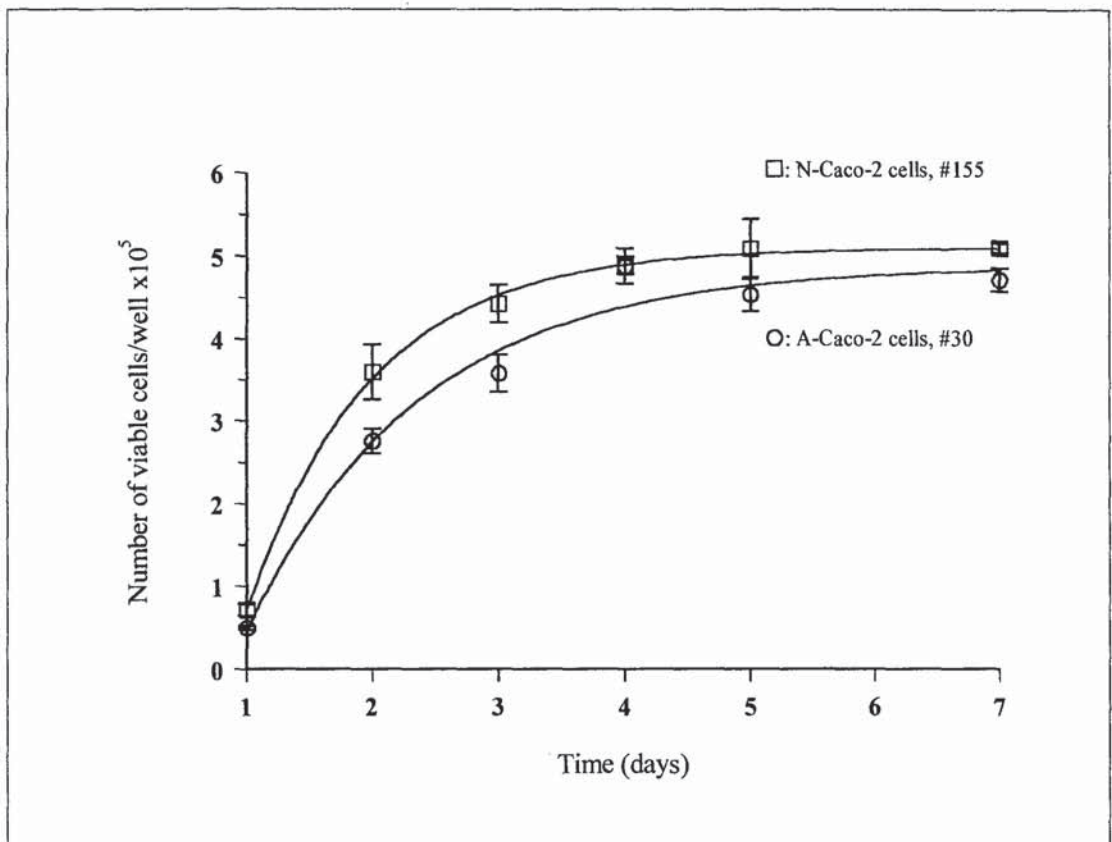
FIGURE 3.2   N-/A-Caco-2 cells on plastic supports, 7 days post-seeding

A and B: N-Caco-2 cells, #111, 250 and 1000 X magnification respectively.
C and D: A-Caco-2 cells, #29, 250 and 1000 X magnification respectively.
A- and N-Caco-2 cells have different cell morphology with the latter seeming to possess more well-defined tight junctional complexes under the light microscope.
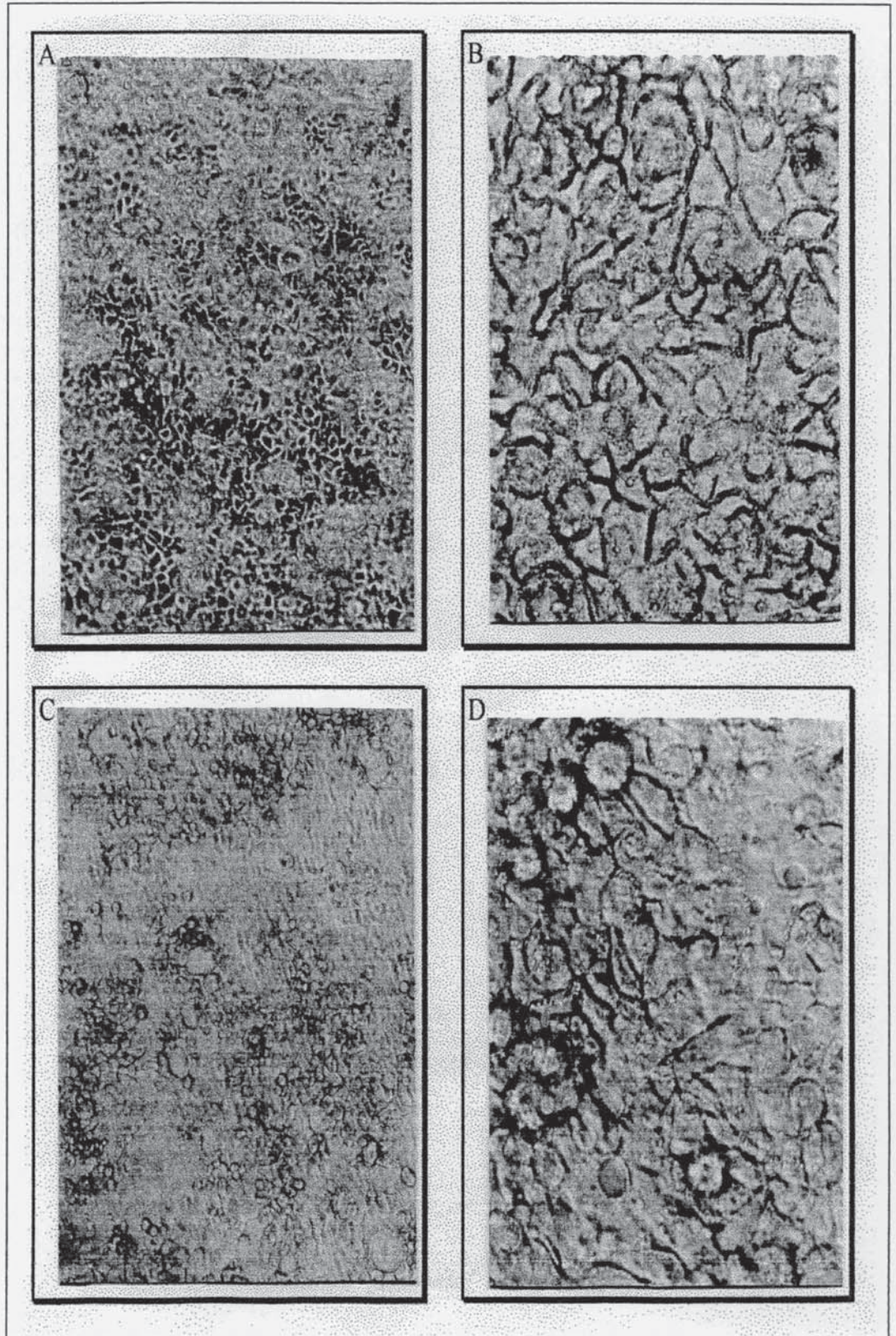
3.3.2 ALKALINE PHOSPHATASE (ALP) ACTIVITIES AND PROTEIN CONTENTS OF CACO-2 CELLS ON PLASTIC SUPPORTS

The ALP activity was approximately three and a half folds higher in N-Caco-2 cells compared to that in A-Caco-2 cells (a value of 0.564 ± 0.021 *vs.* 0.163 ± 0.038 U/mg protein respectively) for the same period of culturing time (figure 3.3). The functional differentiation of Caco-2 cells is a growth-related phenomenon [Pinto *et al.*, 1983]. Therefore, the cells will not differentiate morphologically and functionally into intestinal-like cells before they reach confluence. The cells' intestinal differentiation is reflected by their expression of an intestinal brush-border enzyme marker such as alkaline phosphatase. The results implied that the extent of cellular differentiation was higher in N-Caco-2 cells. Similarly, the total cellular protein as measured by the BCA assay was higher in N-Caco-2 cells (figure 3.4). In a confined environment of the wells, cellular confluency was quickly reached which allowed N-Caco-2 cells to have a longer time to differentiate as compared to their counterparts. This contributed partly to a higher alkaline phosphatase activity of N-Caco-2 cells than A-Caco-2 cells. Alternatively, since Caco-2 cells are of heterogeneous origin [Artusson, 1991a], the differences in alkaline phosphatase activities and protein contents of both cell lines simply reflect different intrinsic characteristics contributed by many sub-populations of cells.

FIGURE 3.3 **Alkaline phosphatase activities in N-/A-Caco-2 cells**

Caco-2 cells were seeded on plastic 24-well plates. Their alkaline phosphatase activities (Unit/mg protein, mean $\pm$ sd, n=3) were assessed 7 days post-seeding.
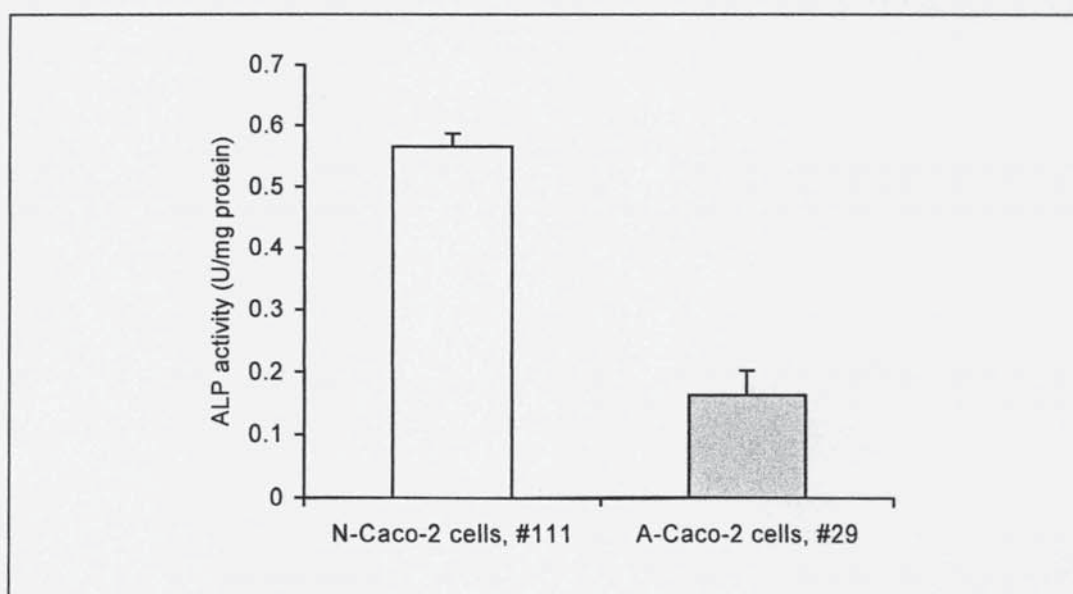
FIGURE 3.4 **Protein contents of N-/A-Caco-2 cells**

Caco-2 cells were seeded on plastic 24-well plates. Their protein contents (mg/L, mean ± sd, n=3) were assessed 7 days post-seeding.
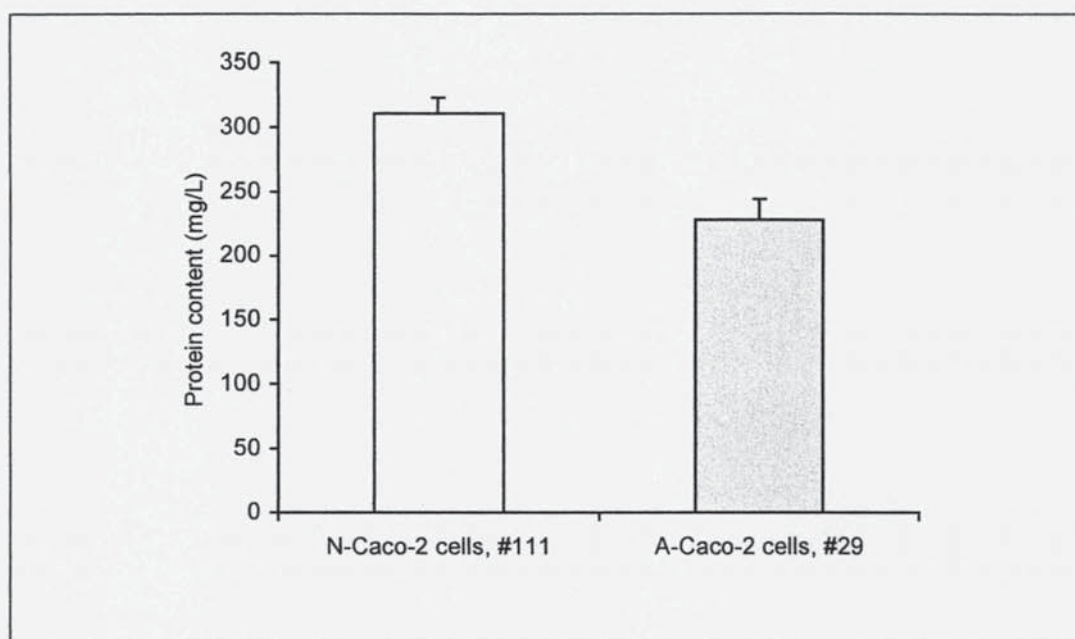
3.3.3 INTRINSIC CELLULAR RESISTANCE TO DOXORUBICIN

The concentration of doxorubicin which decreased 50% of the population of viable cells that were responding to doxorubicin cytoxicity was determined to evaluate the intrinsic doxorubicin drug resistance of Caco-2 cells of different passage numbers and origins. It was 0.03 μM (30 nM) for A-Caco-2 cells and 0.040 μM (40 nM) for N-Caco-2 cells, indicating that the latter were more tolerant to doxorubicin than the former (figure 3.5). There are several possibilities as to why the N-Caco-2 cells should be more tolerant to doxorubicin. Garrido *et al.*, (1995) reported that resistance to cytotoxic drugs could be achieved by the confluent stage of the cells, a phenomenon called confluence-dependent resistance (CDR). N-Caco-2 cells achieved confluence faster than A-Caco-2 cells and therefore, their early confluency might contribute to a higher intrinsic resistance to doxorubicin. However, this was not the case as illustrated by figure 3.6. With the exception of day 1 where seeded cells were mainly attaching themselves to the plastic supports, doxorubicin exposure reduced the number of viable cells regardless of the state of cellular confluency on day 3 and 6, indicating that the existence of CDR, if present, was minimal in N-Caco-2 cells. P-gp is an energy-dependent drug efflux pump in Caco-2 cells and it functions to decrease the

intracellular accumulation of cytotoxic drugs [Gottesman and Pastan, 1988]. It is possible that N-Caco-2 cells have a higher P-gp level than that of A-Caco-2 cells which results in more viable cells under identical drug exposure conditions. This latter possibility was proven to be correct as more P-gp was immunologically detected in Caco-2 cells of passage number >90 obtained from Novartis as reported in section 4.3.1, chapter 4.

FIGURE 3.5 **Cell growth as a function of intrinsic cellular resistance to doxorubicin**

N-/A-Caco-2 cells were exposed to doxorubicin of different concentrations every 48 hours immediately after their seeding on plastic 24-well plates. Viable cells (mean ± sd, n=3) were counted on day 7 post-seeding.
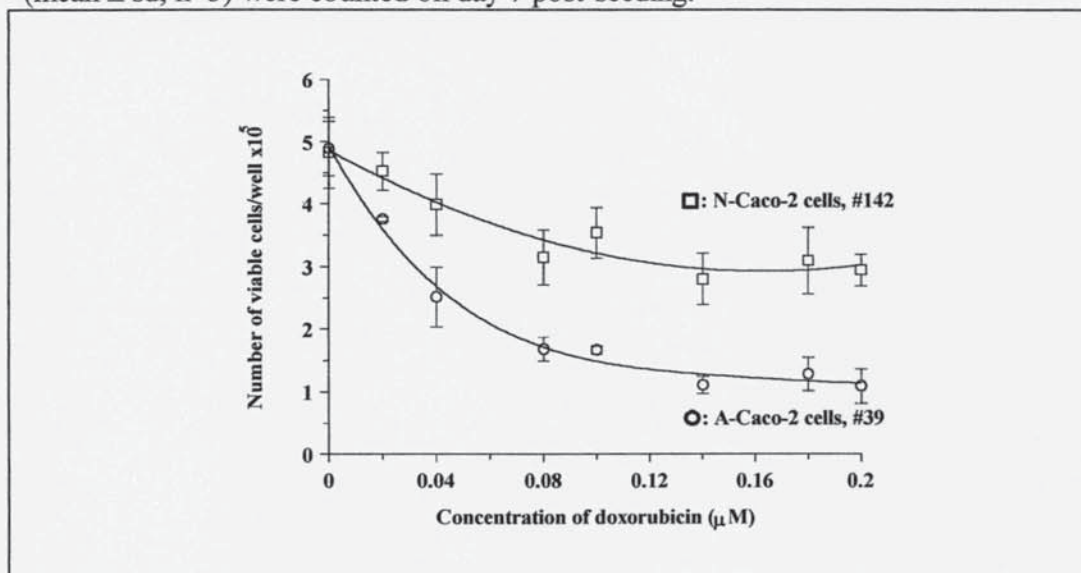
FIGURE 3.6 **Cell viability at different levels of confluence as a function of doxorubicin concentration**

Doxorubicin (□: 0; ■: 0.5; and ▨: 1.0 μM) was added to the wells on 0, 2 and 5 d post-seeding for 24 h. Each bar represents mean ± sd.
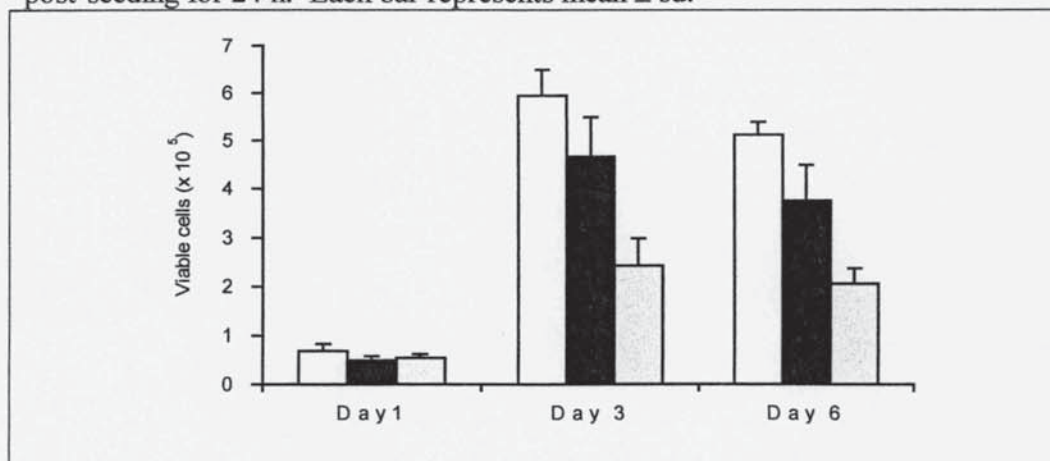
3.3.4   UPTAKE OF GLY-L-PRO

The uptake of Gly-L-Pro is a saturable, carrier-mediated process and is influenced by the passage numbers and origins of Caco-2 cells. All uptake studies were deliberately done at pH 6 because:

i)   It has been demonstrated that the uptake of di-/tri-peptides and peptide-like drugs is coupled with an influx of protons [Ganapathy and Leibach, 1985; Thwaites *et al*., 1992, Thwaites *et al*., 1993a], hence, a proton-gradient will facilitate the uptake process and

ii)   pH 6 is closest to the range of microclimate pHs found on the surface of villous jejunal cells [Shimada and Hoshi, 1988], therefore the uptake of Gly-L-Pro at pH 6 in Caco-2 cells would closely model its *in vivo* absorption by enterocytes.

The uptake of Gly-L-Pro by Caco-2 cells was determined at 3 minutes because preliminary studies had shown that its uptake at 3 minutes was linear and a short incubation period minimised the chance of Gly-L-Pro being hydrolysed. Caco-2 cells have been reported to produce prolidase, an enzyme which cleaves the peptide bond between the penultimate amino acid and proline and which has an apparent Km of 200μM [Hu *et al*., 1995a]. Nicklin *et al*., (1992) reported an apical imino-acid proline transport system in Caco-2 cells with a Km of 5.28 mM. [^{3}H]Gly-L-Pro may be hydrolysed by prolidase during the uptake process and the [^{3}H]proline may enter the cells by the imino-acid transport system, thus misleading the result of the uptake of [^{3}H]Gly-L-Pro by the DTS. For this reason, 10 mM of non-radioactive proline was added to the solution of Gly-L-Pro prior to its addition to the cells so that should hydrolysis occur, then the non-radioactive proline, being of much higher concentration than the Km value, would most likely to saturate the imino-acid transport system. Thus, any radioactivity detected in the cells was most probably due to the active uptake of the radiolabelled dipeptide Gly-L-Pro. The results obtained under such conditions, therefore, are more likely to provide a more accurate prediction of Gly-L-Pro absorption *in vivo*.

Figure 3.7 presents the uptake of Gly-L-Pro by A- and N-Caco-2 cells. The Michaelis-Menten kinetic parameters for Gly-L-Pro uptake are presented in the table 3.1 below:

82

TABLE 3.1 **Michaelis-Menten kinetic parameters of Gly-L-Pro uptake in Caco-2 cells.**

Results are expressed as mean ± se. Asterisk denotes 95% significance difference between the corresponding data of N and A-Caco-2 cells, two-tailed Student t-test for unpaired mean sample data.

Parameters (mean ± se)	Caco-2 cells of passage number >90 from Novartis (N-Caco-2 cells)	Caco-2 cells of passage number <40 from ATTC (A-Caco-2 cells)
Km (mM)	0.153 ± 0.065*	0.085 ± 0.02*
Vmax (nmol/min/mg protein)	1.924 ± 0.478*	0.761 ± 0.104*
k_d (nmol/min/mg protein/mM)	1.560 ± 0.318	1.122 ± 0.081

The half maximal uptake concentration (mM) (Km value) of Gly-L-Pro in N-Caco-2 cells was in good agreement with what had been reported (0.19mM) previously by Moore *et al.*, (1996) using the Caco-2 cell model. Its maximum velocity (Vmax) value was close to that obtained by using human intestinal brush border membrane vesicles (1.53 ± 0.07 nmol/0.5 min/mg protein) [Rajendran *et al.*, 1985]. In contrast, Km of Gly-L-Pro in A-Caco-2 cells was approximately half of that of N-Caco-2 cells. Assuming that Gly-L-Pro binds to the DTS prior to its translocation across the apical cell membrane during uptake, the process can be represented schematically below:

$$\text{Gly-L-Pro + DTS} \underset{k_2}{\overset{k_1}{\rightleftharpoons}} \text{Gly-L-Pro-DTS complex} \xrightarrow{k_3} \text{Uptake}$$
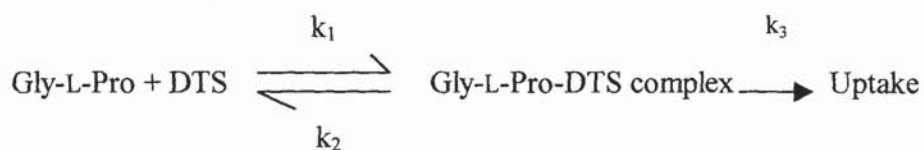
At steady state, Km is the equilibrium constant and is calculated as: $Km = (k_1 + k_3)/ k_2$ [Stryer, 1988] where k_1, k_2 and k_3 are rate constants of the individual steps as outlined in the above schematic representation. If N-Caco-2 cells possessed a higher expression of the DTS (which was presumably represented by the same protein in both groups of cells) than A-Caco-2 cells, then both k_1 and k_2 would be the same in both cell lines due to similar binding of Gly-L-Pro to the same protein. However, k_3 for the uptake would be higher in N-Caco-2 cells as reflected in this case by a higher maximum velocity of Gly-L-Pro uptake (table 3.1). Since the value of Km is depending partly on k_3, a higher k_3 contributed to a

larger Km as observed in N-Caco-2 cells (table 3.1). Uptake of Gly-L-Pro by passive diffusion as represented by k_d was similar in both groups of cells.

FIGURE 3.7 **Uptake of Gly-L-Pro in N-/-A-Caco-2 cells**

Gly-L-Pro of different concentrations was incubated with N-/ A-Caco-2 cells for 3 minutes. Uptake is expressed as nmol/mg protein/min, mean ± sd, n=3.
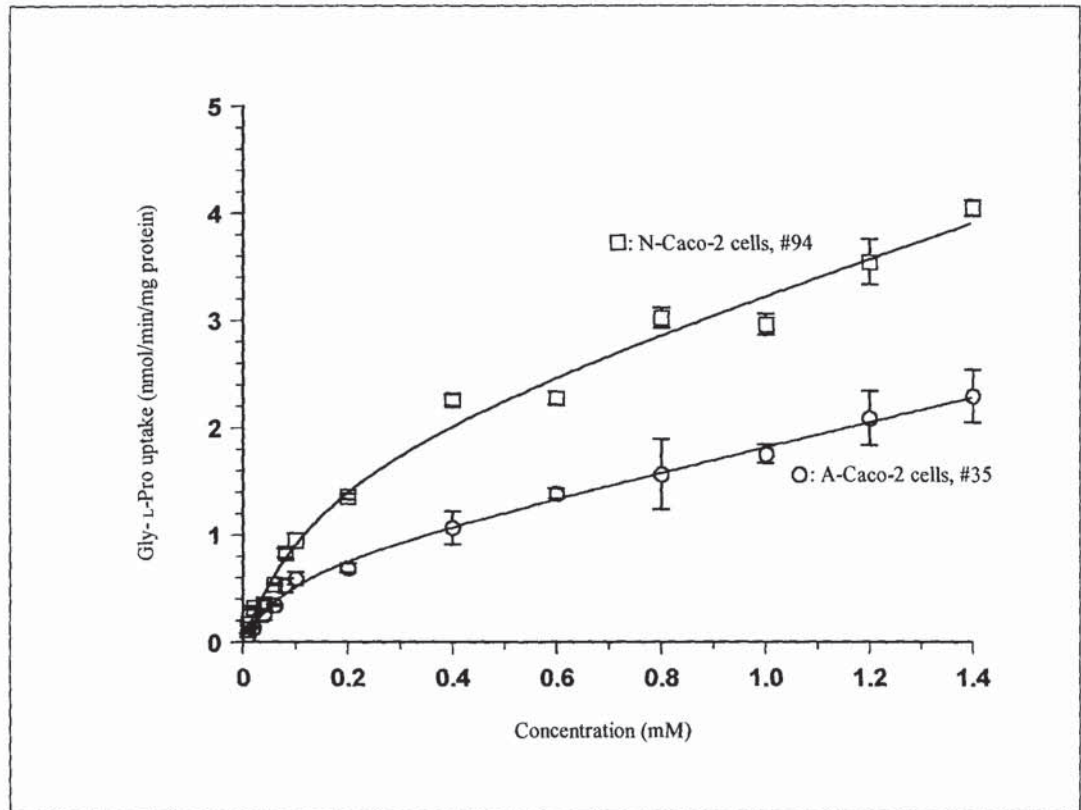
The heterogeneity of Caco-2 cells has been reported [Artusson, 1991a] so that, within a population of cells, there are many sub-populations. This was reflected in this study by different patterns of cell growth, enzyme expression, intrinsic resistance to doxorubicin and different kinetic parameters of Gly-L-Pro uptake. Competition between the sub-populations of cells will lead to the fastest-growing sub-population becoming the predominant cells and thus, their morphological and functional characteristics will give the overall characteristics of the whole cell population. It is probable that N-Caco-2 cells in this case may intrinsically have a higher expression of ALP, DTS transporter and P-gp than A-Caco-2 cells.

3.4 CONCLUSIONS

Caco-2 cells of different origins and passage numbers have different morphological and functional characteristics. Therefore, in the screening process of orally administered drug candidates using the Caco-2 cell model, care should be taken to rationally select a population of Caco-2 cells which best model the intestinal absorption of different drugs by different mechanisms. This allows non-specific interactions to be easily picked up from specific ones as well as to optimise the reproducibility of reliable results.

CHAPTER FOUR

MODULATION OF P-GLYCOPROTEIN (P-GP) LEVEL IN CACO-2 CELL MONOLAYERS: STABLE AND ENHANCED P-GP EXPRESSION BY DOXORUBICIN

ABSTRACT

Caco-2 cells of passage number >90 were exposed to 1 and 2 μM doxorubicin once every other cell passage. Increase in total P-gp expression was assessed at both protein level by Western blotting and functionally by (i) transepithelial transport of $[^3H]$vincristine and (ii) its efflux from the cells in the presence or absence of 100 μM (±)verapamil. For comparative purposes, the transepithelial transport of a multidrug resistance protein (MRP)-specific substrate, $[^3H]$leukotriene C_4 (LTC_4), was also assessed. The stability of P-gp expression in exposed cells was investigated by growing them in drug-free cell culture media with characterisation 28 days later. In addition, the cellular distribution of P-gp and surface characteristics of non-exposed and exposed Caco-2 cells were also explored by fluorescence and scanning electron microscopy.

Higher levels of P-gp expression, both functionally and at the protein level ($p<0.05$) were seen in Caco-2 cells being exposed to doxorubicin and was stable for at least 28 days under drug-free conditions. Cellular location of P-gp by a fluorescent P-gp substrate, rhodamine 123, was observed in both exposed and non-exposed cells, mainly around the periphery of the cells.

Stepwise selection of Caco-2 cells with doxorubicin of increasing concentrations could be used to develop an intestinal cell model with an enhanced P-gp expression that was retained for at least 28 days in drug-free medium.

4.1 INTRODUCTION

Multidrug resistance (MDR) has become progressively more common in cancer chemotherapy. One of its main causes has been identified as the action of P-glycoprotein (P-gp) in tumour cells [Kartner *et al.*, 1983; Endicott and Ling, 1989]. P-gp exists as a transmembrane protein in the apical cell membrane and has a molecular weight of ~170 kDa [Higgins *et al.*, 1997]. It mediates luminal-directed secretion of a variety of lipophilic, structurally unrelated anticancer drugs [Bellamy, 1996] which results in decreased intracellular concentrations vital for their actions. P-gp can also be found in normal tissues such as the intestinal epithelial cells, the capillaries of some human brain samples, the liver, the pancreas, the colon, the kidneys, the adrenal cortex and medulla [Thiebaut *et al.*, 1987; Thiebaut *et al.*, 1989]. In the small intestine, P-gp serves as one of the biological barriers, limiting the absorption of a variety of drugs which are prone to P-gp-mediated intestinal secretion in addition to indirectly enhancing their intestinal metabolism [Gan *et al.*, 1996].

Various resistant cancerous cell lines have been used to study the absorption kinetics of compounds which may interact with P-gp [Watanabe *et al.*, 1989; Hamilton *et al.*, 1993]. Currently, a wide spectrum of orally administered drugs has been identified as P-gp substrates [Arimori and Nakono, 1998]. The Caco-2 cell culture system has been used extensively as an *in vitro* model to predict and characterise the mechanisms of oral absorption of drug candidates [Artursson, 1991; Morrison *et al.*, 1996]. This is because, upon confluence, they are able to differentiate into enterocyte-like cells and form tight junctions [Pinto *et al.*, 1983], together with the development of many transporters normally found in the small intestine [Tsuji and Tamai, 1996; Nicklin *et al.*, 1996]. Drug permeability through the Caco-2 cell monolayer, therefore, gives an indication of the potential extent of drug absorption *in vivo* and is a useful tool for the screening process in the early phase of drug development. However, for the Caco-2 cell line to be used as a biological model to predict the absorption of compounds that are potential substrates for P-gp, further development of the model is required. This is because, first of all, the level of P-gp expression in Caco-2 cells is variable depending on their age in culture [Hosoya *et al.*, 1996]. Secondly, the inconsistent extent of P-gp expression in Caco-2 cell line due to different culture conditions and previous exposure to drugs [Anderle *et al.*, 1998] has made data interpretation and

87

comparison between experiments difficult. Thirdly, to be a good screening model, it should have a stable, enhanced level of P-gp so that specific P-gp-mediated pharmacokinetic activities can be easily differentiated from non-specific interactions, thus identifying accurately any absorption-limiting factors of the tested compounds so that they can be further developed.

An intact, stable, enhanced P-gp expression Caco-2 model not only satisfies the above requirements but also provides a wider view of the drug absorption profile as it represents mixed parameters affecting drug permeability in addition to P-gp interaction. The aim of this work was to investigate the modulation of P-gp expression in Caco-2 cells by cytotoxic drug (doxorubicin) exposure. The outcome of such investigation contributes towards the knowledge of developing an intestinal Caco-2 cell model with a stable and enhanced P-gp expression. Such cell model will provide a comprehensive understanding of the oral absorption process of drug candidates more akin to *in vivo* conditions than the conventional Caco-2 cell model in drug screening and will be useful in quantitative structure activity relationship (QSAR) studies of new chemical entities.

4.2   MATERIALS AND METHODS

4.2.1   MATERIALS

Doxorubicin (2mg/mL) (Pharmacia, Milton Keynes, UK) was obtained from City Hospital (Birmingham, UK). [^{3}H]Vincristine sulphate (7.9 Ci/mmol) and D-[^{14}C]mannitol (56 Ci/mmol) were obtained from Amersham Company (Buckinghamshire, UK). [^{3}H]Leukotriene C$_4$ (110.5 Ci/mmol) was obtained from Dupont New England Nuclear (Hertfordshire, UK). P-gp primary monoclonal antibody C219 was obtained from ID labs (Glasgow, UK). (±)Verapamil powder was obtained from Sigma (Poole, UK). Caco-2 cells of passage number >90 were donated by Novartis (Horsham, UK) and those of passage number <40 were obtained from the American Type Tissue Culture collection (ATTC, MD, USA).

4.2.2 METHODS

4.2.2.1 CELL CULTURE

Caco-2 cells of different cell passage numbers were cultured and passaged/trypsinised every 4 days as described previously (section 2.2.1.2) unless specified otherwise. Experiments in which only cells of passage number >90 were used (hereafter referred to as parent or control cells) will be stated so in the appropriate sections.

4.2.2.2 EXPOSURE OF PARENT CACO-2 CELLS TO DOXORUBICIN IN PLASTIC FLASKS

The seeding density was 2.5 x 10^6 cells/12 mL per 75 cm^2 base flask. Immediately after seeding, Caco-2 cells were exposed to 1 μM of doxorubicin for 48 hours. Under this condition, the cells reached confluence on day 4 for three consecutive cell passages. They were then exposed to 1 μM doxorubicin every other cell passage at the same cell seeding density. The time taken for them to reach confluence was 4 days in plastic flasks. After 46 cell passages under this condition, previously exposed cells with the same seeding density *per* flask were exposed to an increasing concentration of 2 μM doxorubicin once every other cell passage. The time taken for them to reach confluence in plastic flasks was 6 days for the first ten cell passages under the new conditions and 4 days thereafter.

4.2.2.3 PREPARATION OF WHOLE CELL LYSATE

Briefly, the cells in the plastic flasks were passaged as previously described (section 2.2.1.2) whereas those on inserts were scraped off using Costar cell scrapers. Loose cells were collected and washed twice by centrifugation (1000 x g x 5 minutes) with pre-warmed PBS. The cell pellets were resuspended in a homogenisation buffer consisting of 0.01 M Tris-HCl, 0.25 M sucrose, 0.2 mM CaCl$_2$, 1 mM EDTA, phenylmethylsulphonyl fluoride (1mg/mL), aprotinin (1μg/mL) and benzydamine (1 mM), pH 7.3. The cells in suspension were sonicated for 20 seconds (Soniprep 150, Northern Media Supply Limited) operating at a power of 56W. Cell lysates were then centrifuged at 1000 x g for 10 minutes to remove any unlysed cells and nuclei. The supernatant was stored at -70°C and used within one week. Preparation of a whole cell lysate of rat liver

cells from a male Wistar rat (230-250g) was similar to the method described above except that only soft tissues of liver were washed twice in ice-cold PBS and cut into pieces before sonication.

4.2.2.4 PROTEIN DETERMINATION ASSAY AND WESTERN BLOTTING

Protein concentration of whole cell lysate was determined by the BCA assay using bovine serum albumin as a standard as *per* Sigma procedure (section 2.2.8.1). Proteins (10-20 μl) were subjected to gel electrophoresis on Ready-Gel Tris-HCl polyacrylamide gel (10%, Biorad) (section 2.2.8.2) and transferred onto PDVF membranes overnight at a fixed voltage of 25V. Immunoblotting procedure was performed as described in section 2.2.8.3 except that the general blocking of non-specific binding sites of PDVF membranes was carried out with 5% w/v skimmed milk in Tris-buffered saline, pH 7.4 (TBS) which also contained 2% v/v goat serum. P-gp was detected qualitatively by a colourimetric assay using 5-bromo-4-chloro-3-indolyl phosphate/nitroblue tetrazolium (BCIP/NBT) as a colouring reagent and the intensity was analysed quantitatively by a computer operated densitometry software package (Gelworks 1D- Intermediate, Ultra Violet Products, Cambridge, UK). Two-tailed Student's t-test (for unpaired mean data) was used to determine the significance of difference between the mean P-gp intensities of exposed and non-exposed cells at $p < 0.05$.

4.2.2.5 TRANSEPITHELIAL TRANSPORT STUDIES OF VINCRISTINE SULPHATE IN THE PRESENCE OR ABSENCE OF 100 μM (±) VERAPAMIL AND LEUKOTRIENE C_4

Transport studies were carried out in (i) parent Caco-2 cells (ii) parent cells which had been exposed to doxorubicin (1 and 2 μM) (hereafter referred to as type I cells) and (iii) Type I cells where doxorubicin exposure (1 μM/every other cell passage) was stopped after 28 passages and they were grown in drug-free medium afterwards (hereafter referred to as Type II cells).

The cells were seeded at a density of 400,000 cells per insert, cultured for 3 weeks and were used between 21 and 28 days. No doxorubicin was added to the cells when they were growing on the inserts. Vectorial transport studies of [^{3}H]vincristine in the presence or absence of 100 μM (±)verapamil were performed

as described in section 2.2.4.1. The transport of 1 nM [^{3}H]leukotriene C$_4$ was carried out similarly to [^{3}H] vincristine. One-way analysis of variance (ANOVA, with Dunnett multiple comparison post-test, Instat 3, Graphpad) (vincristine sulphate transport) or two-tailed Student t-test (leukotriene C$_4$ transport) was used to analyse the significant difference between the Papp of vincristine or leukotriene C$_4$ of parents *vs.* those of Type I or II Caco-2 cells at $p<0.05$ or $p<0.01$.

4.2.2.6 EFFLUX STUDIES OF VINCRISTINE SULPHATE IN CACO-2 CELLS

Cells were cultured on clear polyester inserts (section 4.2.2.5) and were used between 3-4 weeks post-seeding. Efflux studies were carried out as described in section 2.2.6. The radioactivities associated with the PBS-azide washes and solubilised cells were determined by scintillation counting and the results were expressed as fmol/mg protein. One-way ANOVA (with Dunnett multiple comparison post-test, Instat 3, Graphpad) was used to determine the significance of difference between the mean cellular accumulations of vincristine in the parent *vs.* Type I and II cells at $p<0.05$.

4.2.2.7 LABELLING OF P-GP IN PARENT AND TYPE I CACO-2 CELLS BY ITS FLUORESCENT SUBSTRATE, RHODAMINE 123

Rhodamine 123 was used as a fluorescent substrate to label P-gp in the parent and Type I Caco-2 cells. P-gp distribution was assessed by fluorescence microscopy as described in section 2.2.9.2.

4.3   RESULTS AND DISCUSSION

The objective of this study was to investigate the modulation of P-gp expression in the intestinal Caco-2 cell model through cytotoxic (doxorubicin) exposure. The screening of drug candidates that are potential substrates for P-gp using such cell model may provide a thorough understanding of their oral absorption process more akin to that *in vivo* than the conventional Caco-2 cell model. In addition, such a model would also facilitate the prediction of drug bioavailability *in vivo* and would also be useful in studies of *in vitro* drug interactions and quantitative structure-activity relationships (QSAR).

4.3.1 IMMUNOLOGICAL DETECTION OF P-GP IN CACO-2 CELLS

For each condition, a total number of three flasks of each cell type were used (n=3) and each lane represents the P-gp protein level from each flask. Parent Caco-2 cells possessed a higher P-gp expression than those of passage number <40 as shown by Western blot analysis (figure 4.1, row A). Clear, visible bands (n=3) were detected in the region of ~170 kDa molecular weight, with those of parent cells having a higher intensity ($130 \pm 18.83\%$, lanes 3, 4 and 5, row A) compared to cells with passage number <40 ($100 \pm 15.31\%$, lanes 6, 7, and 8, row A) as revealed by densitometric analysis. Total P-gp expression in Type I and II cells was higher than in parent Caco-2 cells as reflected by more intense P-gp bands as shown in rows B and C (figure 4.1). Densitometric analysis revealed that, compared to the intensity of P-gp protein expression in parent cells, $100 \pm 16.05\%$ (row B, lanes 3, 4 and 5) and $100 \pm 13.34\%$ (rows C, lanes 3, 4 and 5) respectively, those of Type I cells were $213 \pm 54.35\%$ (row B, lanes 6, 7 and 8) and $135 \pm 20.03\%$ (row C, lanes 6, 7 and 8) respectively. Two-tailed Student's t-test for unpaired mean data showed that there was a significant difference in P-gp protein expression between Type I and the parent cells ($p<0.05$) in rows B and C.

FIGURE 4.1 **Western immunoblots of P-gp expression in Caco-2 cells.**

All rows: Lane 1: molecular weight markers 115 and 208 kDa, lane 2: rat liver cell lysate. *Row A*: Lanes 3, 4, 5: cell lysate of Caco-2 cells of parent cells; lanes 6, 7, 8: cell lysate of cells of passage number <40. *Row B*: Lanes 3, 4, 5: cell lysate of parent Caco-2 cells; lanes 6, 7, 8: cell lysate of Type I Caco-2 cells. *Row C*: Lanes 3, 4, 5: cell lysate of parent Caco-2 cells; lanes 6, 7, 8: cell lysate of Type II Caco-2 cells. The loading capacity was 20 µg protein/well for lanes 2-8 for all rows.
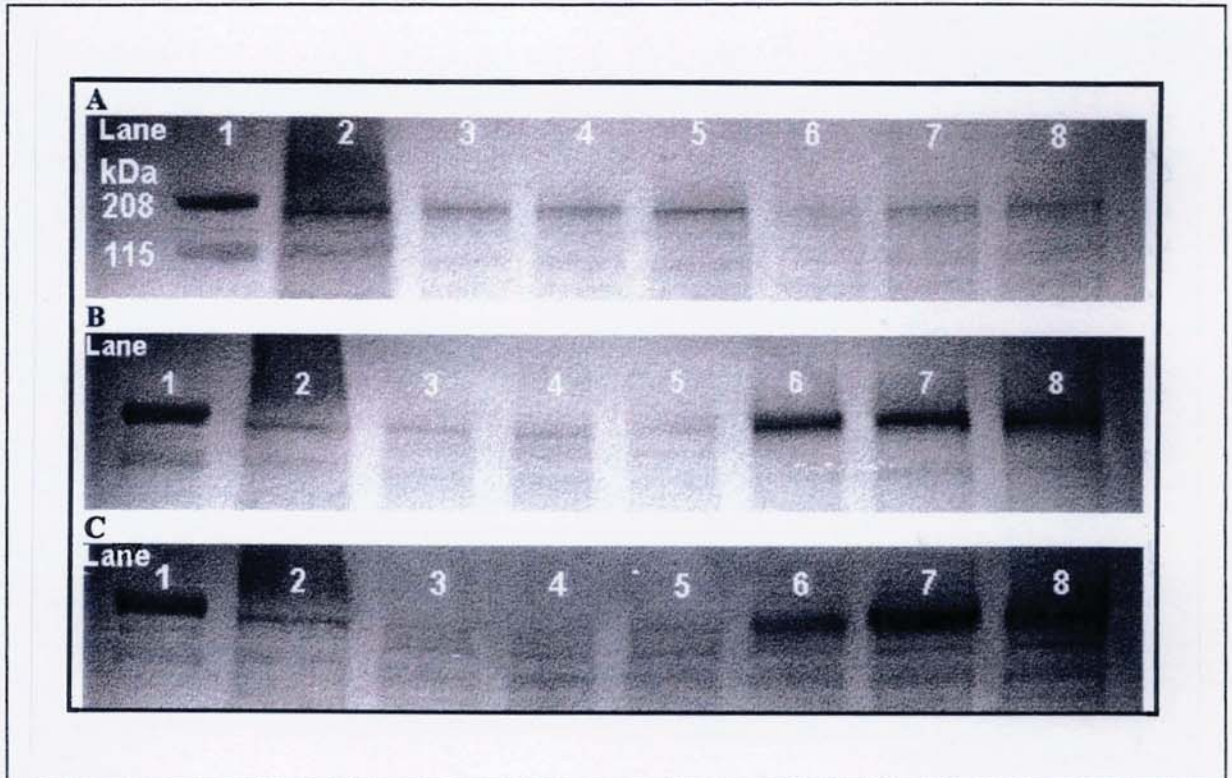
4.3.2 TRANSEPITHELIAL TRANSPORT OF VINCRISTINE SULPHATE AND LEUKOTRIENE C_4 IN CACO-2 CELLS

The observed vincristine accumulation in the receiver phase is a net result of its transcellular and paracellular transport minus its efflux and non-specific binding (in this case, it was ~27%, calculated by dividing the sum of vincristine radioactivity in the receiver phase, washes and cells after the experiment by that of the donor phase before the start of the experiment.

The apparent permeabilities of vincristine (A-B direction) in Type I and II cells were significantly less than that in the parent cells at $p<0.05$ (figure 4.2), (a value of $7.49 \pm 0.21 \times 10^{-6}$ and $7.25 \pm 0.29 \times 10^{-6}$ vs. $8.53 \pm 0.18 \times 10^{-6}$ cm/sec/mg protein respectively), implying the contribution of P-gp in forming a transport barrier to vincristine influx. In contrast, vincristine transport was faster in the reverse (B-A) direction in both Type I (p<0.05) and II cells (figure 4.2) as compared to that in the parent cells ($29.20 \pm 0.72 \times 10^{-6}$ and $27.40 \pm 0.95 \times 10^{-6}$ vs. $25.40 \pm 0.10 \times 10^{-6}$ cm/sec/mg protein), indicating the enhanced functional P-pg activity and/or expression in assisting the secretory transport of vincristine. While stopping doxorubicin exposure for up to 7 cell passages or 28 days resulted in a small loss of total P-gp expression (135 ± 20.03 % vs. 100 ± 13.34 %, figure 4.1, row C), its longer absence (i.e. an additional 21-28 days whilst the cells were growing on inserts) caused the exposed Type II cells to start reverting to their original state as reflected by a smaller difference (A-B) or no change (B-A) between the Papp values of vincristine in Type II and parent cells (figure 4.2 and table 4.1).

A big increase in total P-gp expression in both Type I (~2 folds) and II (~1.5 fold) Caco-2 cells (213 ± 54.35% for Type I and 135 ± 20.03 % for Type II cells, figure 4.1) did not translate proportionally to the differences of vincrsitine transport in either direction in both Type I and II Caco-2 cells. This indicates the likely contribution of non-functional intracellular P-gp that contributes to the total P-gp expression as proposed by Hosoya et al (1996) and as observed in figure 4.1. Different cell monolayers on permeable inserts were formed from heterogeneous cell colonies which might display different permeabilities to mannitol transport as observed in table 4.1. This in turn could affect the quantity of vincristine molecules traversing across the cell monolayer by the paracellular route and could therefore, over/underestimate the transepithelial transport of vincristine in both A-

B and B-A directions by P-gp. However, the surface area represented by the tight junctional complexes for passive diffusion of vincristine is relatively much smaller than that contributed to the total surface area of the monolayer by the cells themselves. Therefore, the reduced A-B transport and enhanced B-A export of vincristine in Type I cells was likely to be due to an increase in P-gp activity. In addition, another study (*i.e.* efflux) to confirm an enhanced P-gp activity in Type I Caco-2 cells is reported in section 4.3.4.

The presence of 100 μM ($\pm$)verapamil caused an increase in the apparent permeabilities of vincristine in the A-B direction in Types I and II and parent cells whilst decreasing them in the reverse direction (figure 4.3). With Type I cells, these changes were highly variable with over three times differences in the apparent permeabilities of vincristine in the A-B and B-A directions respectively (24.10 $\pm$ 0.40 x 10^{-6} and 3.82 $\pm$ 0.22 x 10^{-6} cm/sec/mg protein) (table 4.1). The presence of DMSO in the transport medium had no effect on the mean loss of vincristine by non-specific adsorption (23.65 %), therefore the majority of vincristine transport across cell monolayers should be predominantly by passive diffusion and P-gp activity. The marked differences of vincristine permeability coefficients in Type I cells (A-B and B-A) were more likely to be attributed to differences in the integrity of cell monolayers which required more investigation (Papp of mannitol, A-B, being 38.3 $\pm$ 3.24 x 10^{-6} cm/s/mg protein *vs.* 6.32 $\pm$ 0.58 x 10^{-6} cm/s/mg protein, mannitol permeability in B-A direction), but not due to the cytotoxicity of DMSO to the cells. This is because the permeability coefficients of mannitol in type II and parent cells in the presence of DMSO were comparable to, if not smaller than those in its absence (table 4.1).

FIGURE 4.2 **Transepithelial transport of vincristine sulphate in Type I, II and parent cells**

Caco-2 cells: #99, Type I and II (44 cell passages after their first exposure to doxorubicin) were grown on clear polyester inserts and were used betweeen 21-28 days post-seeding. Results are expressed as fmol/mg protein , mean ± sd, n=3.
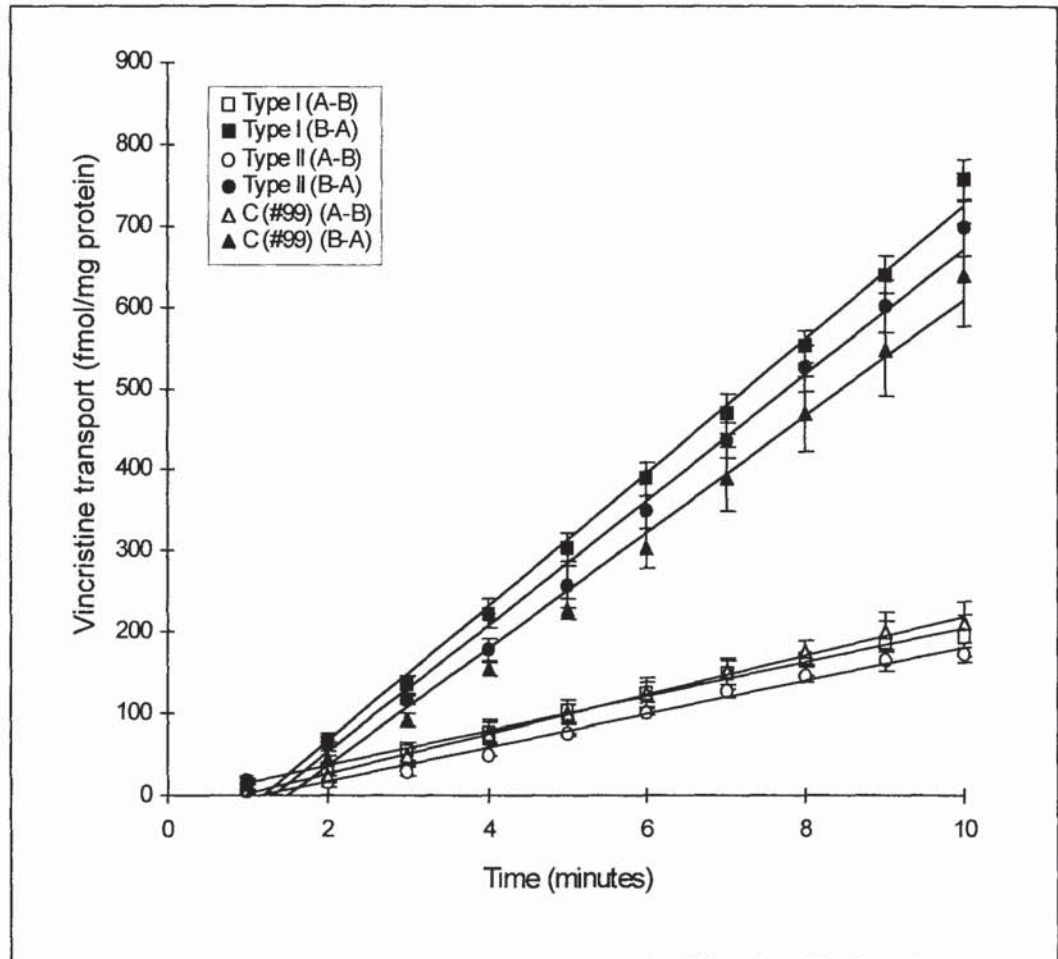
FIGURE 4.3   **Transepithelial transport of vincristine sulphate in Type I, II and parent Caco-2 cells in the presence of 100 μM (±)verapamil**

Type I and II cells were 44 cell passages after their first exposure to doxorubicin. Results are expressed as fmol/mg protein, mean ± sd, n=3.
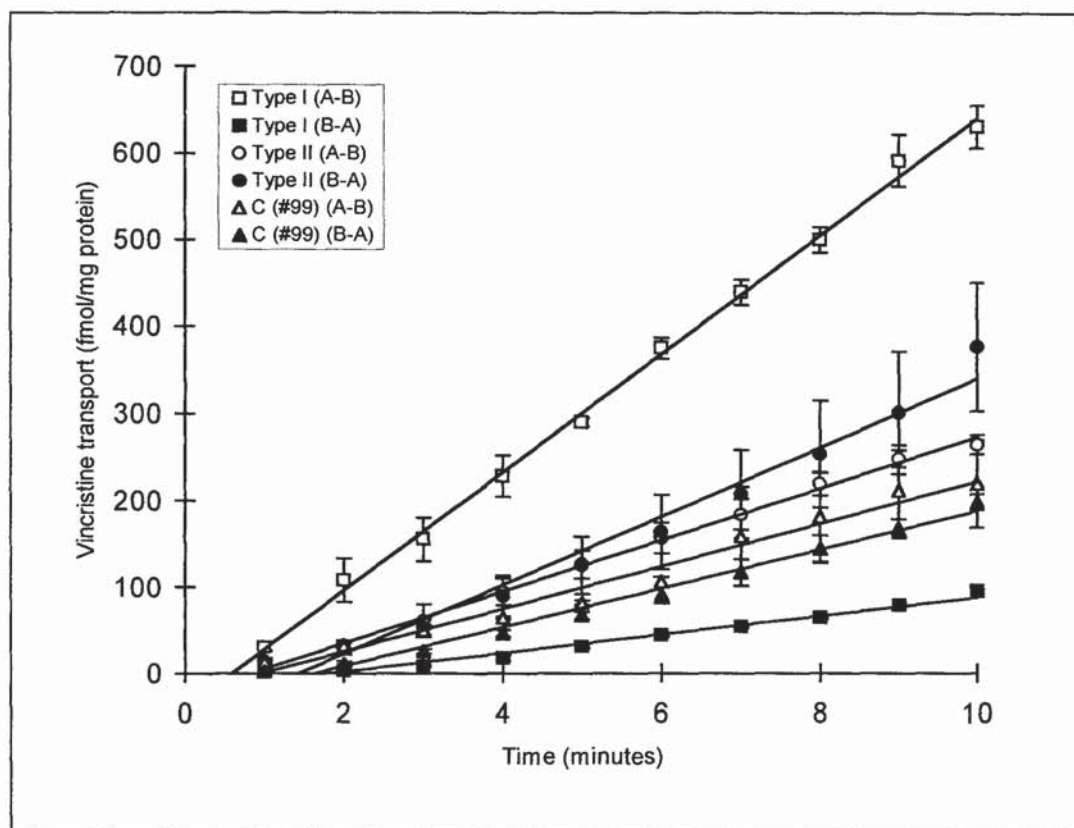
Leukotriene C_4 was reported to be a specific substrate for the multidrug resistance protein (MRP) [Loe *et al.*, 1998] which also transports vincristine. The transport of leukotriene C_4 was conducted in both cell lines and was linear in both directions over 10 minutes. The apical-to-basolateral rate through Type I cells (17.38 ± 2.57 fmol/mg protein/min) was significantly greater (p<0.05) than the reverse direction (B-A, 14.29 ± 0.37 fmol/mg protein/min) but was lower than that for parent cells (A-B, 21.86 ± 0.92 fmol/mg protein/min) (p<0.01) (figure 4.4). However, there was no difference between the two cell lines in the B-A direction (parent cells, B-A, 14.51 ± 0.9 fmol/mg protein/min). The absence of vectorial transport (B-A) of leukotriene C_4 confirmed the absent activity of MRP and that the lower apparent permeability of vincristine in the A-B direction and its higher value in the reverse direction in Type I cells were, indeed, mediated by P-gp.

FIGURE 4.4 **Transepithelial transport of leukotriene C₄ in parent and Type**

Caco-2 cells

Type I cells were 88 cell passages after their first exposure to doxorubicin. Results are expressed as fmol/mg protein, mean ± sd, n=3.

FIGURE 4.5 **Transepithelial transport of mannitol in parent and Type I**

Caco-2 cells

Results are expressed as pmol/mg protein, mean ± sd, n=3.

TABLE 4.1   **Apparent permeability coefficients (Papp values) of vincristine and mannitol with/without 100 μM (±)verapamil in Caco-2 cells**
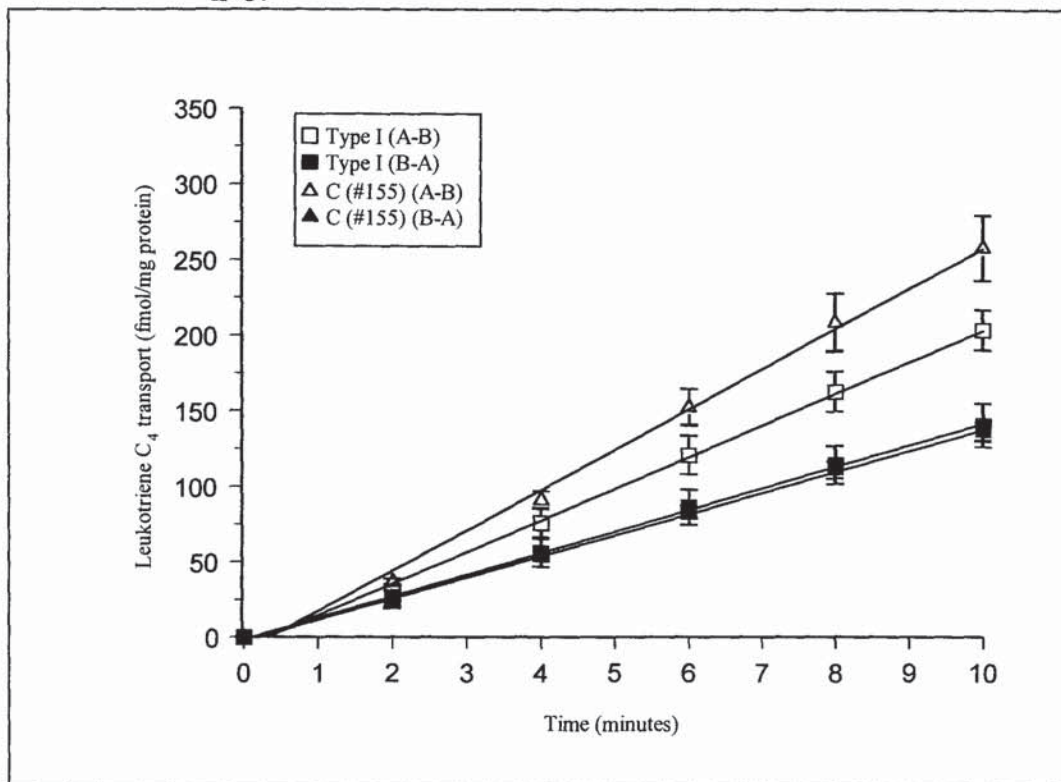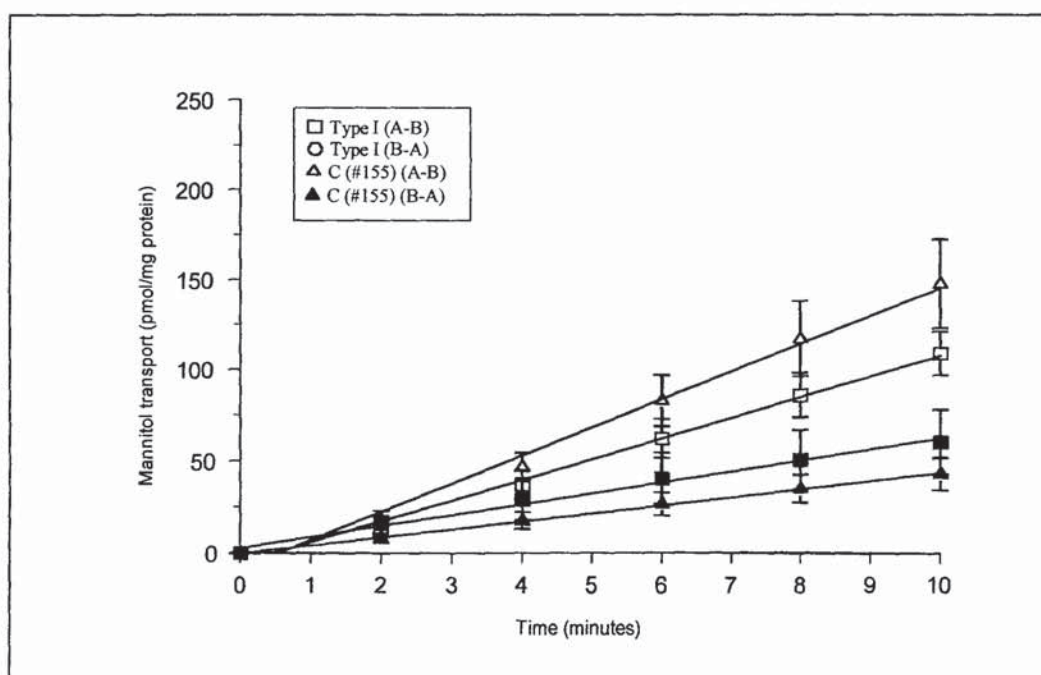
Type I cells in this experiment were 44 cell passages after their first exposure to 1 μM doxorubicin once every other cell passage. Results are expressed as mean ± sd, n=3. Single and double asterisk (*, **) denotes statistical significance from the control values of parent cells at $p<0.05$ and $p<0.01$ respectively (One-way ANOVA with Dunnett multiple comparison post-test).

Cell types	± Vera-pamil	Trans-epithelial direction	Papp vincristine x 10^6 (cm/sec/mg protein)	Papp mannitol x 10^6 (cm/sec/mg protein)
I		A-B	7.49 ± 0.36*	17.8 ± 0.72**
		B-A	29.20 ± 1.24*	15.40 ± 0.96
II	None	A-B	7.25 ± 0.51*	12.10 ± 0.90
		B-A	27.40 ± 1.64	15.60 ± 1.50
#99		A-B	8.53 ± 0.30	10.90 ± 0.48
		B-A	25.40 ± 1.74	15.10 ± 0.93
I		A-B	24.10 ± 0.69**	38.3 ± 3.24**
		B-A	3.82 ± 0.38**	6.32 ± 0.58
II	100 μM	A-B	10.60 ± 0.35*	13.9 ± 1.03*
		B-A	14.10 ± 1.41**	15.6 ± 1.96**
#99		A-B	8.75 ± 0.87	10.10 ± 0.41
		B-A	7.94 ± 0.59	7.86 ± 0.59

4.3.3   CELLULAR ACCUMULATION OF VINCRISTINE SULPHATE AFTER ITS TRANSEPITHELIAL TRANSPORT

Within the cells, new P-gp was synthesised and stored in the cell cytoplasm and/or transported to the plasma membrane where its function was influenced by verapamil Hosoya *et al*, (1996). That means that once inside the cells, total vincristine was the sum of unassociated and bound vincristine (to the stored P-gp). In the absence of verapamil, P-gp in the apical cell membrane of Type I and II cells limited the permeation of vincristine, therefore no significant difference ($p>0.05$) with regards to vincristine cellular accumulation was observed between the three types of cells (table 4.2) in the A-B direction. In contrast, when vincristine was transported in the reverse (B-A) direction, the cellular accumulation of vincristine was highest in Type I cells (table 4.2), most probably in the bound form of vincristine-Pgp complexes. In the presence of verapamil, there was a decrease in

all the values with greatest reduction in Type I cells in both (A-B and B-A) directions. This indicated that verapamil, by binding to both membrane and non-functional intracellular P-gp, prevented the binding and hence cellular accumulation of vincristine. This effect was markedly seen in Type I cells, implying their higher quantity of P-gp being expressed intracellularly.

TABLE 4.2 **Cellular accumulation of vincristine at 10 minutes in the presence or absence of 100 μM ($\pm$)verapamil**

Type I cells in this experiment were 44 cell passages after their first exposure to 1 μM doxorubicin once every other cell passage. Results are expressed as mean $\pm$ sd, n=3. Single and double asterisk (*, **) denotes statistical significance from the control values of parent cells at $p<0.05$ and $p<0.01$ respectively (One-way ANOVA with Dunnett multiple comparison post-test).

Cellular accumulation	Direction of transepithelial transport	Type I cells	Type II cells	Parent cells
Without Verapamil	A-B	211.95 ± 40.25	169.52 ± 14.69	260.39 ± 88.92
	B-A	5687.46 ± 362.46**	4469.68 ± 226.15	4151.82 ± 215.97
With Verapamil	A-B	226.52 ± 8.34**	212.09 ± 15.44**	322.17 ± 22.57
	B-A	471.72 ± 18.59**	967.07 ± 20.61*	1095. 54 ± 76.81

4.3.4 EFFLUX OF VINCRISTINE SULPHATE IN PARENT AND TYPE I CACO-2 CELLS

Since only Type I cells display an undiminished P-gp protein expression and function with time, further studies concentrated on characterising P-gp activity in this cell line in comparison with the parent cells.

In the absence of 100 μM ($\pm$)verapamil, only Type I cells retained significantly less vincristine than that of the parent cells after 15 minutes, $p<0.05$, (figure 4.6). If the mean vincristine retention after efflux (n=3) in the parent cells was converted to percentage and expressed as 100 $\pm$ 16.2% (mean $\pm$ sd), then that retained in Type I cells was 72 $\pm$ 3.1%, nearly one third less than that in the parent cells. In the presence of 100 μM ($\pm$)verapamil, this figure increased to 87.8 $\pm$ 3.1% that of the parent cells. Significantly lower retention of vincristine found with Type I cells after its efflux for 15 minutes in the absence of verapamil

(p<0.05) suggested a higher proportion of functional P-gp in Type I cells than in type II and parent Caco-2 cells. In the presence of verapamil, higher vincristine retention was observed compared with that in its absence. This was because verapamil bound to the functional P-gp and prevented it from effluxing vincristine out of the cells (figure 4.6).

The second PBS-azide washes from both apical and basolateral chambers (figure 4.7) showed that there was significantly less vincristine associated with the cellular surface compared with that found with solubilised cells in all cases (p<0.05), supporting the suggestion that the radioactivity of vincristine associated with solubilised cells was indeed reflecting its presence intracellularly.

FIGURE 4.6 **Cellular retention of vincristine after its efflux for 15 minutes.**

The amounts of vincristine associated with solubilised cells are expressed as fmol/mg protein (mean ± sd). Asterisk (*) denotes 95% significant difference between the mean cellular accumulation of vincristine in parent *vs.* Type I cells (One-way ANOVA, Dunnett multiple comparison test). Type I cells were 48 and 63 cell passages after their first exposure to doxorubicin.
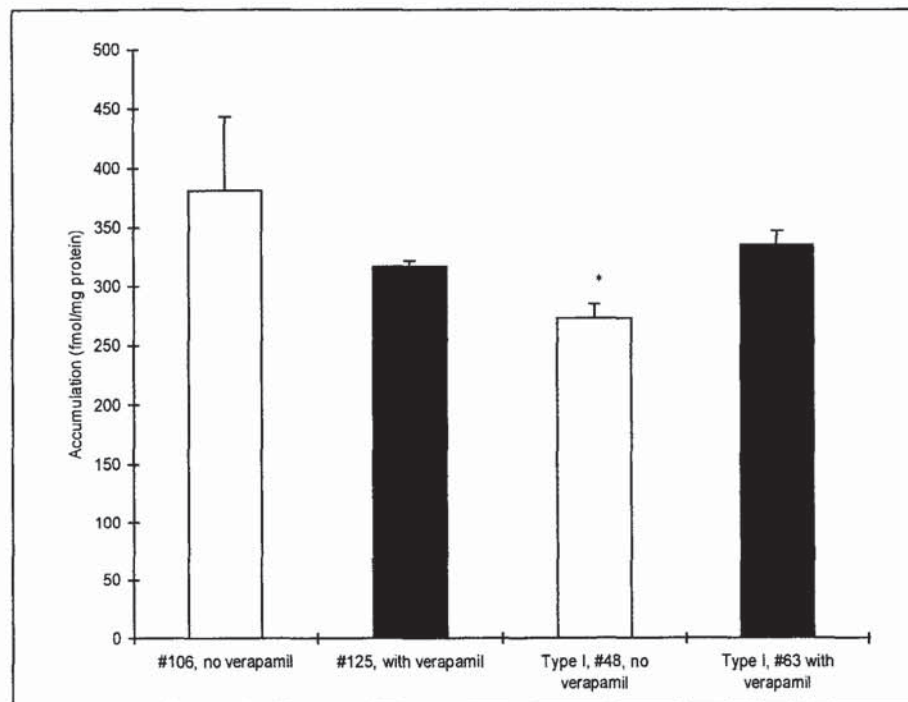
FIGURE 4.7 **Vincristine sulphate associated with the second PBS-azide wash before cellular solubilisation.**

Results are expressed as fmol/mg protein (mean ± sd). 1, 2, 5, 6: in the apical chambers; 3, 4, 7, 8: in the basolateral chambers. C and I: parent and Type I cells respectively. (+) and (-): with and without 100 µM (±)verapamil respectively.
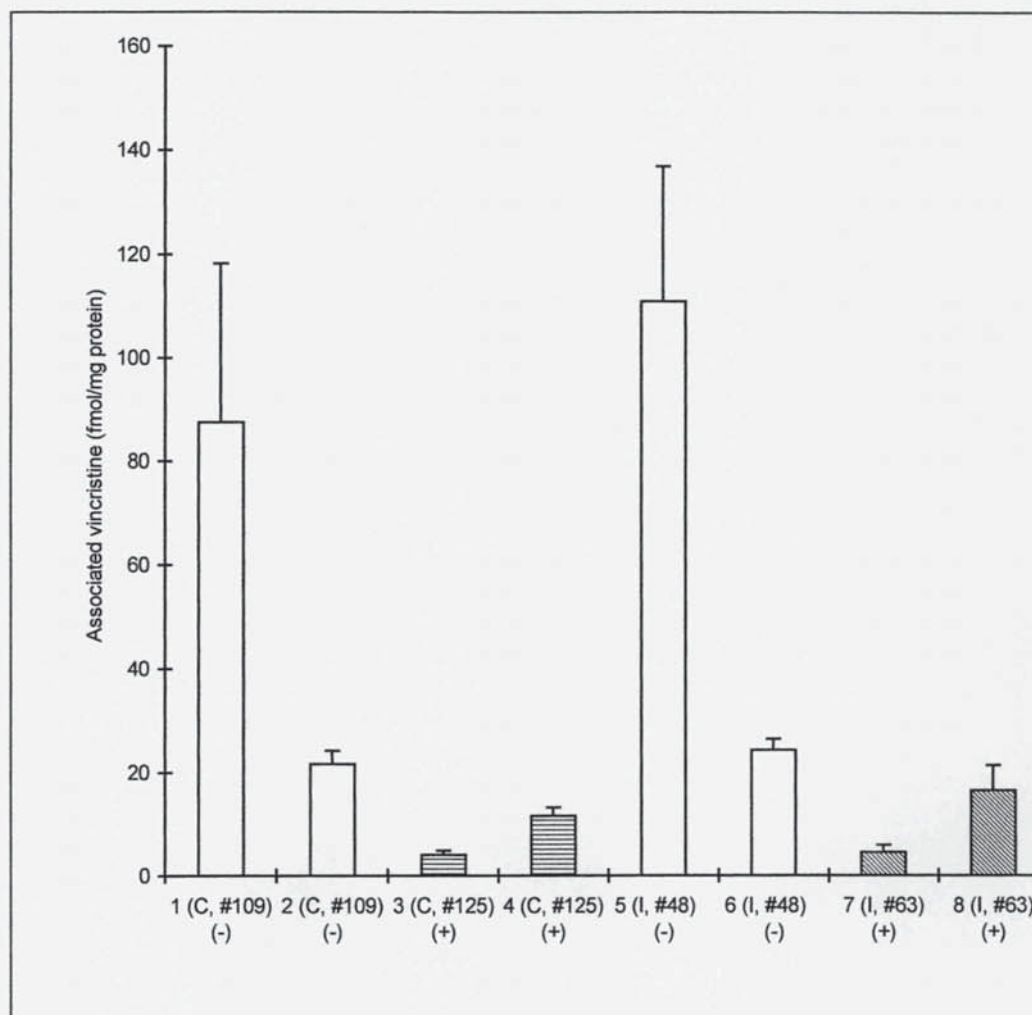
4.3.5 LOCATION OF P-GP IN PARENT AND TYPE I CACO-2 CELLS

Labelling P-gp by its fluoresent substrate rhodamine 123 revealed its distribution around the periphery of parent Caco-2 cells. In P-gp enriched Type I Caco-2 cells, the intensity of fluorescence was much less than that seen in parent Caco-2 cells, presumably because there was less binding of rhodamine 123 to the cell membrane due to the activity of P-gp in effluxing rhodamine 123.

FIGURE 4.8   **Labelling of P-gp in parent Caco-2 cells by its fluorescent substrate, rhodamine 123**
Caco-2 cells of passage number 111, viewed at magnification 400 X
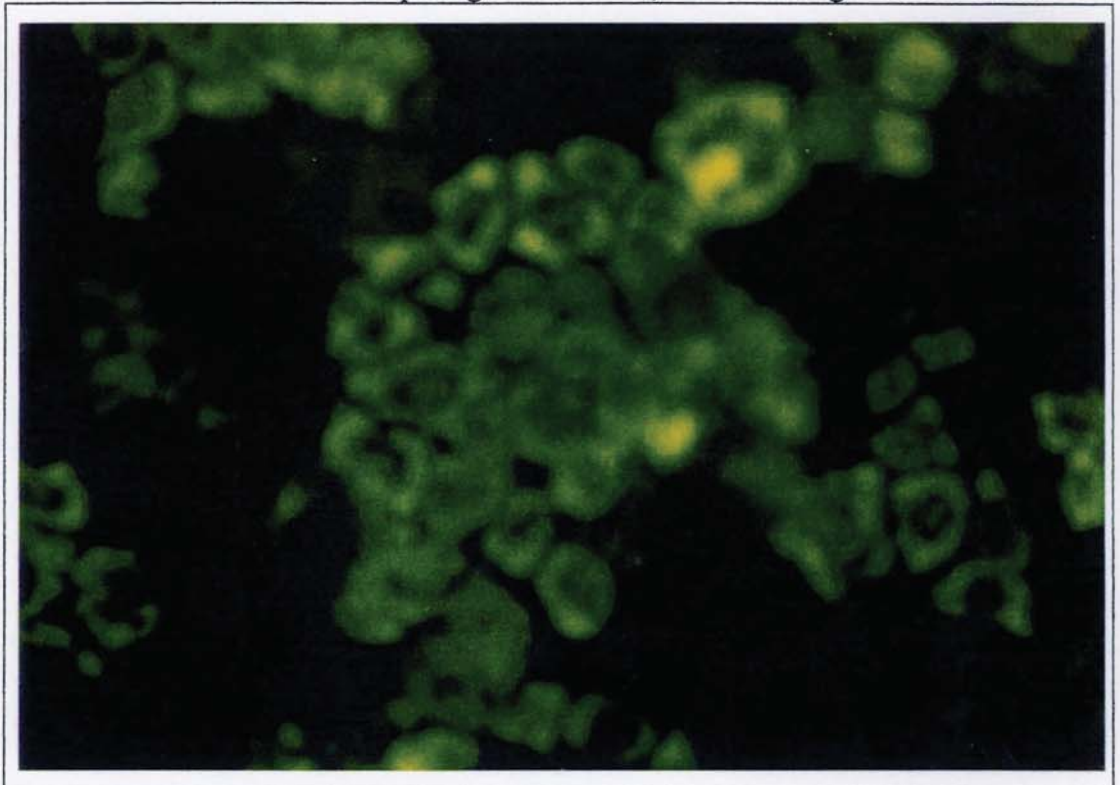
FIGURE 4.9   **Labelling of P-gp in Type I Caco-2 cells by its fluorescent substrate, rhodamine 123**
Type I cells after 25 cell passages of exposure to 1μM doxorubicin viewed at magnification 400 X.
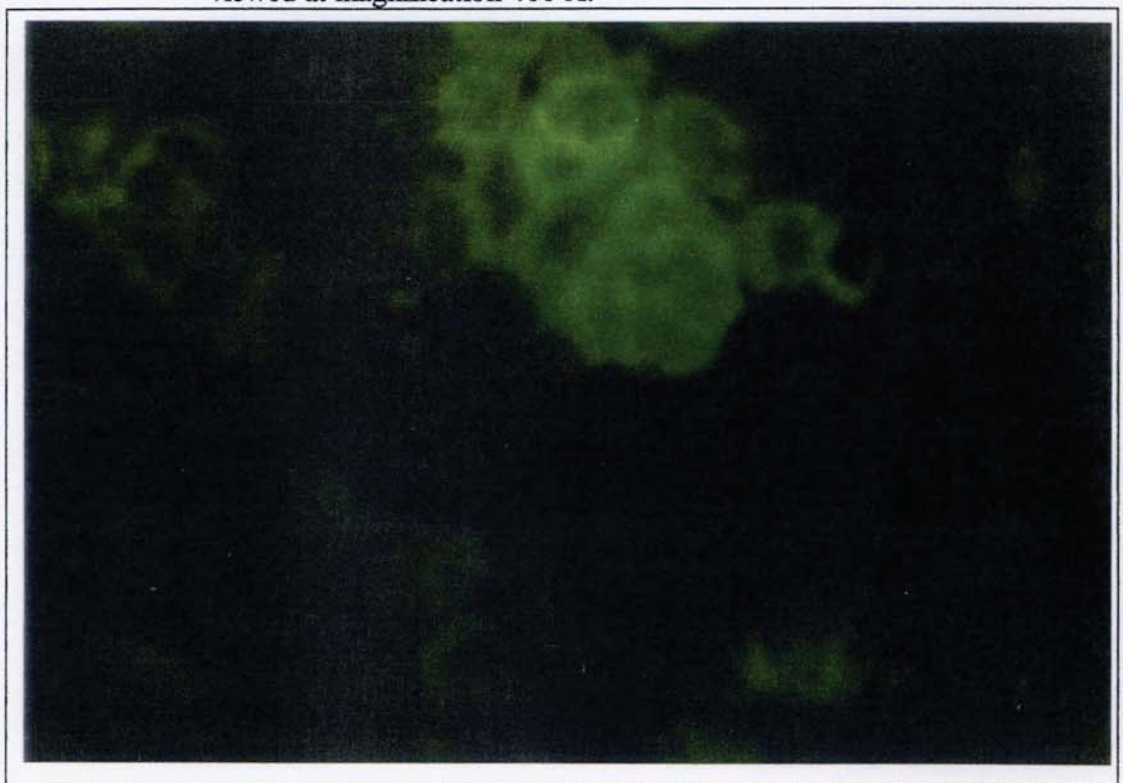
4.4 CONCLUSIONS

In conclusion, exposing Caco-2 cells of passage >90 from Novartis to doxorubicin caused an increase in their total P-gp expression (indicated by P-gp immunoblotting) which can be attributed to an increase in the amount of both non-functional intracellular P-gp and functional P-gp in the apical cell membrane. The increased functional P-gp expression was stable for at least 28 days (*i.e.* when Type I cells were culture on inserts for transport or efflux study) in drug-free medium as indicated by predominant secretory of vincristine and less vincristine cellular retention in Type I cells than in Type II or parent cells. How much functional P-gp contributes to the increase in total cellular P-gp has yet to be determined. Furthermore, how comparable this is to the level of P-gp expression in human intestine remains to be discovered, in addition to the characterisation of the enterocytically functional differentiation of exposed Caco-2 cells.

CHAPTER FIVE

INTERPLAY BETWEEN INTESTINAL EFFLUX AND METABOLISM AS MODELLED BY P-GLYCOPROTEIN AND CYTOCHROME P450 3A IN CACO-2 CELLS*

ABSTRACT

Confluent Caco-2 cells of passage number >90 (parent cells) and those which have been exposed to 2 μM doxorubicin to enhance P-gp expression (Type I cells) were exposed to 0.25 μM 1α, 25-dihydroxyvitamin D_3 for one to two weeks. CYP3A4 immunoprotein which was detected in the parent cells after two weeks of treatment (76.2 ± 7.6 pmol/mg protein) was comparable with the quantity of CYP3A4 found in human jejunal enterocytes (70.0 ± 20.0 pmol/mg protein). For both cell types, the rates of 1-hydroxylation of midazolam (1-OH MDZ) by CYP3A in treated cells ranged from 257.0 ± 20.0 to 1057.0 ± 46.0 pmol/min/mg protein and closely mirrored those achieved when using human small intestinal tissues. In the absence of 100 μM (±)verapamil, preferential apical accumulation of 4-hydroxymidazolam (4-OH MDZ) only was observed, and in its presence, no 4-OH MDZ metabolite was formed in both cell types, implying that 4-OH MDZ might possibly be a substrate for P-gp. The results support the hypothesis that intestinal CYP3A enzymes generate products that are better substrates for P-gp than the parent drugs and together they function to keep xenobiotics out of the body.

In conclusion, both *in vitro* cell models offer comparable intestinal CYP3A-metabolising capacity to that *in vivo* as well as being useful in the studies of P-gp-CYP3A interactions.
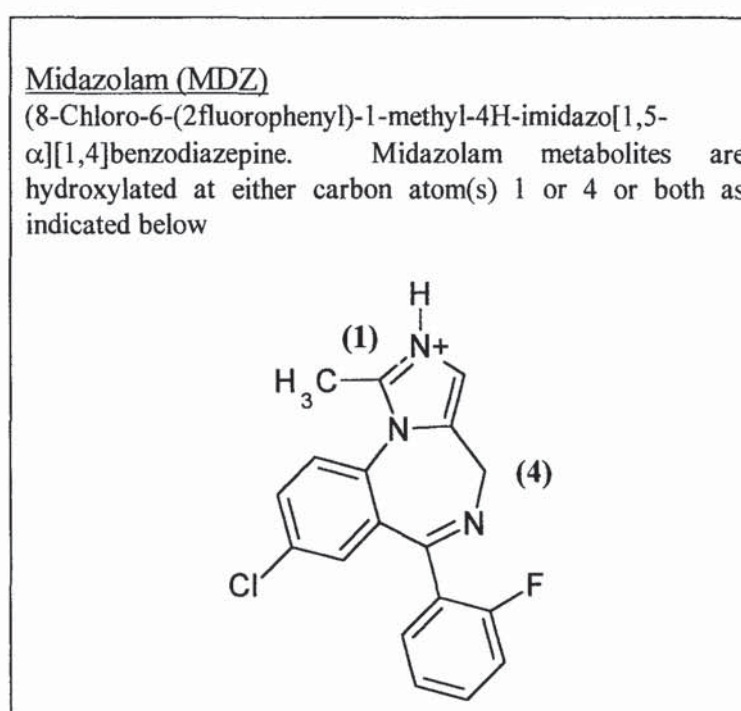
5.1 INTRODUCTION

Drug metabolism can significantly reduce the efficacy of otherwise potent molecules and therefore, affects the progression of potential lead compounds. For orally administered drugs, phase I drug metabolism can start as soon as the molecules cross the intestinal epithelial layer. Intestinal oxidative metabolism of many xenobiotics is mediated predominantly by a sub-family of enzymes called cytochrome P450 3A (CYP3A) which are located in the apex of the enterocytes [Kolars et al., 1992c]. Details of intestinal CYP3A enzymes have been discussed elsewhere (section 1.10). There are many isoforms of intestinal CYP3A of which cytochrome P450 3A4 (CYP3A4) has the highest concentration [de Waziers et al., 1990, Kolars et al., 1992a] and is responsible for significant "first-pass" metabolism of orally administered substrates [Kolars et al., 1991a; Lown et al., 1994; Kolars et al., 1992c]. The expression and catalytic activities of intestinal CYP3A show inter-variation [Kolars et al., 1991b; Lown et al., 1994] and are affected by diet, age and disease [Wilkinson, 1997].

The hydroxylation of midazolam (MDZ), the structure of which is depicted in figure 5.1, has been widely regarded as a proto-typical CYP3A-catalysed reaction [Haehner et al., 1996]. Metabolites of midazolam as mediated by CYP3A enzymes include 1-hydroxymidazolam (1-OH MDZ), 4-hydroxymidazolam (4-OH MDZ) and 1, 4-hydroxymidazolam (1, 4-OH MDZ) [Vree et al., 1981].

Midazolam is rapidly metabolised *in vivo* and its metabolism is affected by many CYP3A inducers/inhibitors. Following an intraveneous (IV) injection of MDZ (1.71 mg/kg) into beagle dogs, free 1-OH MDZ was quickly distributed and conjugated with glucuronic acid to form glucuronide conjugates (1-OH MDZ glucuronide) in the blood plasma, the latter had a plasma elimination half-life of 53 minutes. The minor metabolite, 4-OH MDZ, was only present as the glucuronide conjugate whilst the 1,4-OH MDZ in both free and conjugate form was not detected at all [Vree et al., 1981]. In man, MDZ was rapidly absorbed after an oral administration with a bioavilability between 30-70% and a plasma half-life of about 2 hours [Moffat, 1986]. A dose of 10 mg of midazolam given by IV route yielded only 1-OH MDZ glucuronide which had an elimination half-life of 80 minutes [Vree et al., 1981]. The metabolism of MDZ by human liver microsomes followed simple Michaelis-Menten kinetics with an apparent Km value of 9.7 ± 0.5

μM and a Vmax value of 2212 ± 27 pmol/min/mg protein as estimated by linear regression analysis [Wrighton and Ring, 1994]. In rats, the apparent bioavilability of MDZ after intrajejunal administration was 11.6 % of the given dose (10 μmol). Co-administration of ketoconazole with MDZ increased its plasma concentration from 11.6 % to 52.6 % [Higashikawa et al., 1999]. Three days pre-treatment of rats with different P450 3A inducers decreased MDZ bioavailability to different extent with clotrimazone (44%), phenobarbital (75%), pregnenolone-16α-carbonitrile (81%) and dexamethasone (82%) [Higashikawa et al., 1999].

FIGURE 5.1   **Structure of midazolam**

Midazolam (MDZ)
(8-Chloro-6-(2fluorophenyl)-1-methyl-4H-imidazo[1,5-α][1,4]benzodiazepine.   Midazolam   metabolites   are hydroxylated   at   either   carbon   atom(s)   1   or   4   or   both   as indicated below

P-glycoprotein (P-gp) is a transmembrane protein of molecular weight ~ 170 kDa which was first discovered in cancer cells [Kartner et al., 1983]. Details of P-gp can be found in section 1.9. Like CYP3A enzymes, P-gp is situated in the apical membrane of mature epithelial cells but not in crypt cells [Thiebault et al., 1987]. Their co-location in the small intestine has led to the suggestion of their synergistic roles in keeping xenobiotics out of the body. There are a number of studies supporting the above hypothesis. Firstly, there are overlapping substrates between CYP3A and P-gp [Watcher et al., 1995] and the expression of both proteins is up-regulated after treatment with many drugs, including rifampicin, phenobarbital, clotrimazole, reserpine and isosafrole [Schuetz et al., 1996].

Secondly, it has been reported previously that P-gp causes an increase in the metabolism of cyclosporin A by effectively slowing down its transport and repeatedly recycling it into the cells, therefore increasing the time during which the parent drug is exposed to intracellular CYP3A for metabolism [Gan *et al*., 1996]. The synergistic roles of intestinal CYP3A4 and P-gp are depicted in figure 5.2. P-gp minimises the absorption of xenobiotics by enhancing the efflux of both parent compounds and/or their metabolites out of the cells. Meanwhile, the parent compounds are metabolised by CYP3A4 to form more polar metabolites, which are less likely to traverse the lipophilic basolateral intestinal cell membranes.

Such interesting interrelationships between CYP3A and P-gp and their determining roles in the bioavailability of orally administered drugs have led to the search of an *in vitro* human intestinal cell model that expresses both enzymes in quantities similar to those *in vivo* for use in drug screening. This has many advantages including: fast, high-throughput screening of newly discovered drug candidates which are available in limited quantities, an insight to drug metabolism and interactions which provides not only an in-depth understanding of the compounds but also a selection of the best possible drug candidates for later clinical phase of development. In addition, a cellular system of human origin offers a full complement of the absorption process of oral drug candidates which is more akin to the *in vivo* situation. It is, therefore, a better predictive model than those in which cellular organelles or sub-organelles are used, to try to predict each absorption parameter of drugs orally *in vivo*.

FIGURE 5.2   The synergistic roles of intestinal CYP3A and P-gp

LUMINAL SIDE   SEROSAL SIDE

ENTEROCYTE

P: parent drug   M: metabolite(s) 1: smooth endoplasmic reticulum which houses CYP3A
2: microvilli   N: nucleus
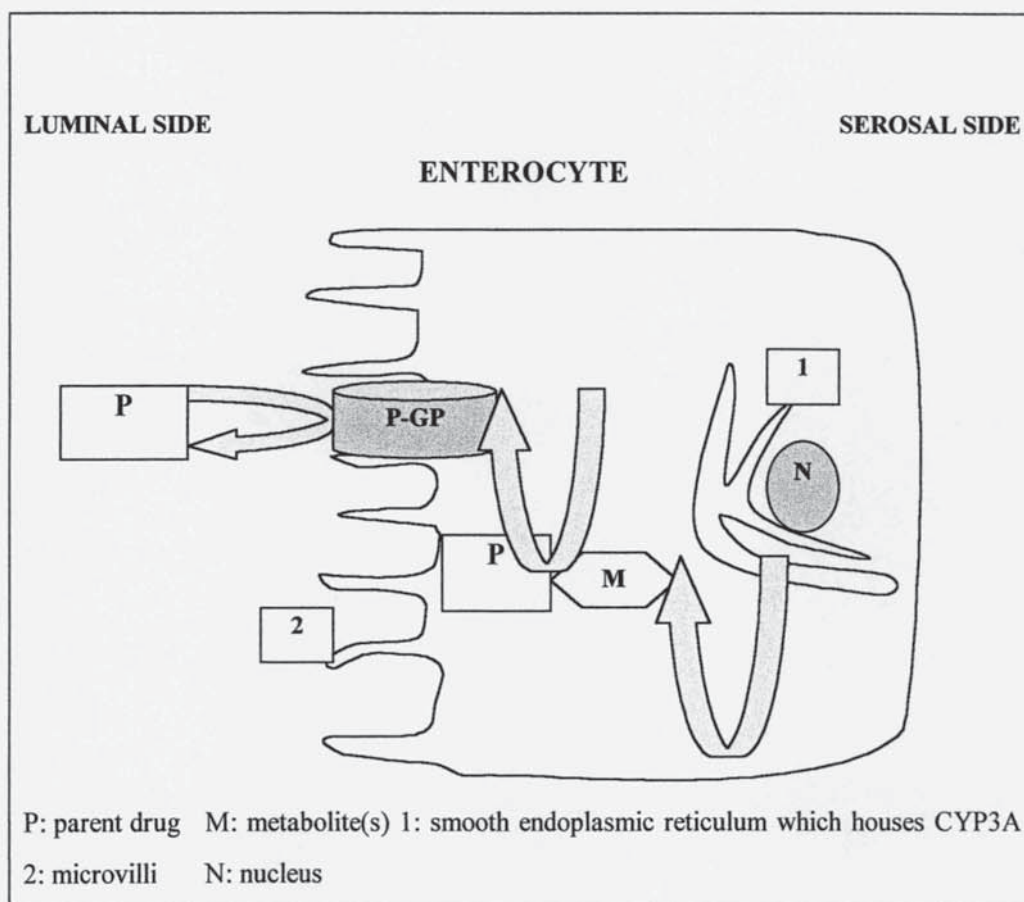
The Caco-2 cell model has been widely used as a means to predict *in vivo* drug absorption [Artursson, 1990]. However, due to very low quantity of CYP3A in Caco-2 cells, attempts have been made to improve it including the transfection of CYP3A4 cDNA into the cells [Crespi *et al.*, 1996], the use of a subclone [Raeissi *et al.*, 1997] and exposure of Caco-2 cells to 1α, 25-dihydroxyvitamin D_3 to increase CYP3A4 expression [Schmiedlin-Ren *et al.*, 1997]. The aims of this study were:

-   to develop and characterise Caco-2 cell culture systems that express CYP3A from two different types of Caco-2 cells namely: 1) a highly P-gp expressing Type I cells that were continuously exposed to doxorubicin and 2) non-exposed Caco-2 cells (parent cells)

-   to assess the metabolising capacities of both cell lines based on their ability to metabolise MDZ, a proto-type CYP3A substrate

- to study the interactions between P-gp and CYP3A in the oral absorption of MDZ.

5.2   MATERIALS AND METHODS

5.2.1   MATERIALS

1α, 25-dihydroxyvitamin D_3 was purchased from Calbiochem (Nottingham, UK). MDZ, 1-OH MDZ and 4-OH MDZ were kindly donated by Roche Pharmaceutical (Hertfordshire, UK). HPLC solvents and columns were as described in section 2.1.3. Cell culture materials were as mentioned previously (section 2.1.1). All other chemicals were of highest purity grade.

5.2.2   METHODS

5.2.2.1 OPTIMISATION OF CELL CULTURE MEDIA AND SEEDING DENSITY

Preliminary experiments have led to an observation that Type I Caco-2 cells have a poorer attachment to the permeable supports than the parent cells in cell culture medium supplemented with 0.1 μM sodium selenite, 3 μM zinc sulphate, 5 μM ferrous sulphate and 0.25 μM 1α, 25-dihydroxyvitamin D_3. Therefore, the effects of culture components on Type I cells' cytotoxicity were investigated. Caco-2 cells were seeded on plastic 24-well plates at a density of 80,000 cells/cm^2 in three different types of cell culture media, namely:

a)   M1 (section 2.2.1.1)

b)   M1 supplemented (to the indicated final concentration) with (0.1 μM) sodium selenite, (3 μM) zinc sulphate and (5 μM) ferrous sulphate and

c)   M1 supplemented with 0.25 μM 1α, 25-dihydroxyvitamin D_3.

The media were changed every other day and the total number of viable cells/well in triplicate was counted on day 7 post-seeding using the trypan blue exclusion method (section 2.2.1.2). Results were expressed as the number of viable cells *per* well. In addition, different cell seeding densities per collagen-coated insert were also investigated to achieve maximal cell attachment, as reflected by a smooth,

uniform cellular surface at 5 weeks post-seeding, with optimal conditions applied for both cell types later on.

5.2.2.2 EXPOSURE OF CACO-2 CELLS TO 1α, 25-DIHYDROXYVITAMIN D$_3$

Unless stated otherwise, all collagen-coated inserts were seeded at 170,000 cells/cm^2/insert. At three weeks post-seeding, they were exposed to 0.25 μM 1α, 25-dihydroxyvitamin D$_3$. Briefly, 0.25 μM 1α, 25-dihydroxyvitamin D$_3$ in sterile absolute ethanol was thoroughly mixed with M1 under aseptic conditions before the mixture was added to the cells. The process was repeated every time the medium was changed every two to three days, and the inserts were used for experiments during week 6 post-seeding.

5.2.2.3 IMMUNOLOGICAL DETECTION OF CYP450 3A4 IN CACO-2 CELLS

Parent Caco-2 cells on collagen-coated inserts, 3 weeks post-seeding, (seeding density: 85,000 cells/cm^2/insert) were divided into two groups and exposed to 0 (control) or 0.25 μM 1α, 25-dihydroxyvitamin D$_3$ for two weeks respectively as described previously (5.2.2.2). Each group consisted of three sets of inserts with four inserts per set. At the end of the exposure period, Caco-2 cells were scraped off the inserts and cellular microsomes were prepared (section 2.2.7.2). For each treatment, microsomal aliquots (10 μg protein) were subjected to gel electrophoresis and Western blotting as described previously (2.2.8) using a polyclonal antibody for CYP3A4. The intensities of the CYP3A4 proteins were quantified by densitometric software (Gelworks 1D- Ultra Violet Products, Cambridge, UK).

5.2.2.4 METABOLISM AND TRANSPORT OF MIDAZOLAM

MDZ, 1-OH MDZ and 4-OH MDZ were dissolved in 50:50% v/v water: methanol at a concentration of 3.9 mM (1.28 mg/mL), 3.4 mM (1.16 mg/mL) and 3.5 mM (1.2 mg/mL) respectively and were stored at 4°C as stock solutions. M2 was maintained at 37°C throughout the experiments and used as a vehicle to dissolve MDZ and fluorescein (4 and 26.6 μM respectively). Transport conditions

were as described previously (section 2.2.4.2). Results were expressed as nmol/min/mg protein.

5.2.2.5 DETECTION OF MIDAZOLAM AND ITS METABOLITES BY HPLC

A Hewlett Packard (Series 1100) HPLC system with a dual-piston reciprocating pump, controlled-temperature thermostat, degaser and UV detector was used as described in section 2.2.5.

5.2.2.6 IDENTIFICATION OF MIDAZOLAM AND ITS 1-OH and 4-OH METABOLITES PEAKS

Prior to experimentation, MDZ, 1-OH MDZ and 4-OH MDZ were dissolved in the transport medium to a concentration of 1.28, 1.16, 1.2 μg/mL respectively. Their peaks and retention times were identified by reversed phase HPLC as described in section 2.2.5. In addition, their calibration graphs were constructed after each HPLC run of the samples.

5.2.2.7 ASSESSMENT OF MIDAZOLAM PURITY IN THE DONOR PHASE

Prior to adding the donor phase containing MDZ to the cells, its purity was assessed by reversed phase HPLC as described in the previous section 2.2.5. This was to ensure that the metabolites detected in the receiver phase were, indeed, generated by the cells, and not as a result of the metabolites being the contaminants of the parent drug, which might diffuse through the cell monolayers with time.

5.2.2.8 EXTENT OF MIDAZOLAM METABOLISM AS A FUNCTION OF TIME

Type I and parent Caco-2 cells were cultured and exposed to 0.25 μM 1α, 25-dihydroxyvitamin D_3 as described previously (section 5.2.2.2) except the lengths of exposure was one week. The extent of MDZ metabolism was then assessed by adding it to the apical solution and detecting the parent drug and its metabolites in the receiver solution at 15, 30, 45 and 60 minutes.

5.2.2.9 KINETIC PROFILES OF THE FORMATION OF MIDAZOLAM METABOLITES

Type I and parent Caco-2 cells were cultured and exposed to 0.25 μM 1α, 25-dihydroxyvitamin D_3 for two weeks as described previously (section 5.2.2.2). MDZ was added to either the apical or basolateral chamber in the presence or absence of 100 μM (±)verapamil. The parent drug and its metabolites were detected in the receiver phase at the following time points: 15, 30, 45, 60 and 90 minutes.

5.2.2.10 DETECTION OF FLUORESCEIN

Samples were distributed into 96-well fluorescence black plates (Sigma, Poole, UK) (150 μL/well) and fluorescein was detected using a fluorescence plate reader (1420-Victor[2] Multilabel Counter, Wallac, Milton Keynes, UK) (section 2.2.4.2). A standard calibration graph was constructed for each run.

5.3   RESULTS AND DISCUSSION

It is important to optimise the cell culture conditions to promote cell attachment and growth to maximise the production of cellular CYP3A4.

5.3.1 OPTIMISATION OF CELL CULTURE MEDIA AND SEEDING DENSITY

The optimisation process was carried out with Type I cells only since they have a poorer cellular attachment to both plastic and permeable supports than the parent cells as observed from preliminary experiments. The optimising set of conditions was then applied to both cell types afterwards. The aim here was to find a composition of cell culture medium which would confer the least cellular toxicity and yet promote the cellular expression of CYP3A.

Figure 5.3 indicated that both the supplemented salts and 1α, 25-dihydroxyvitamin D_3 inhibited cell growth with the latter having a greater effect (decreases of 39.4 and 65.8% growth compared to the control). 1α, 25-Dihydroxyvitamin D_3 promoted the expression of CYP3A4 in Caco-2 cells by transcriptional activation of native CYP3A gene [Schmiedlin-Ren et al., 1997] but

at the same time inhibited cell growth as indicated above. Based on the above finding, the elimination of the supplemented salts would diminish, in part, cell toxicity. This, together with doubling the original seeding density (from 85,000 to 170,000 cells/cm^2) allowed Caco-2 cells to grow and form an intact monolayer by week 6 post-seeding. In addition, unlike the culturing conditions described by Schmiedlin-Ren *et al.*, (1997), only cell culture medium containing 10% v/v FCS was used for cell growth and maintenance. The cell culture conditions serve to maintain and/or enhance optimal cell growth and tend to vary with each cell type. With a clone of Caco-2 cells as reported by Schmiedlin-Ren *et al.*, (1997), a combination of permeable inserts with extracellular Matrigel® coating, supplements of mineral salts and DL-α-tocopherol, and a gradient addition of FCS (5-20%v/v) to the cell culture medium was required for optimum CYP3A4 expression. However, for those particular cell types in our laboratories, the reported conditions were modified to best suit their maximal growth and CYP3A4 expression.

FIGURE 5.3   **The effects of cell media composition on cell growth**

Caco-2 cells were seeded at a density of 80,000 cells/cm^2 in three different types of cell culture media, namely 1: normal cell culture medium (M1), 2: M1 supplemented with 0.1 μM sodium selenite, 3 μM zinc sulphate and 5 μM ferrous sulphate, 3: M1 with 0.25 μM 1α, 25-dihydroxyvitamin D$_3$. Results were expressed as mean ± sd, n=3. Asterisk denotes significant difference (p<0.05) of cell growth by ANOVA with Dunnett multiple comparison post-test.
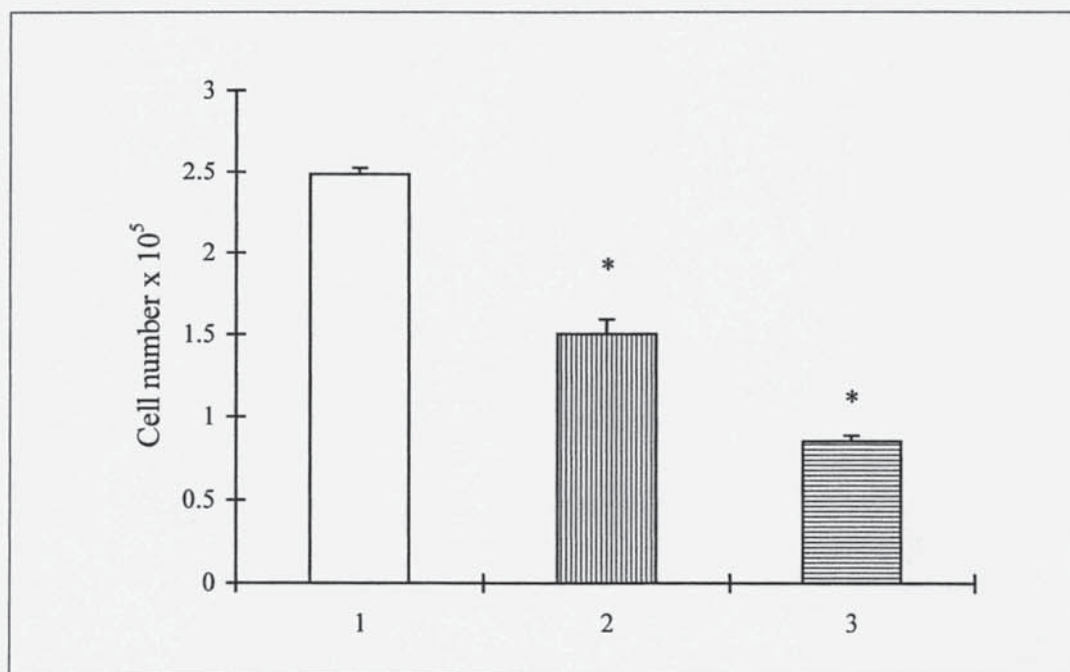
5.3.2 IMMUNOLOGICAL DETECTION OF CYP450 3A4 IN CACO-2 CELLS

Based on the intensity of the positive internal standard (lane 2, figure 5.4) which consisted of 0.88 pmol of purified CYP3A4, the level of CYP3A4 in 1α, 25-dihydroxyvitamin D_3 treated cells was calculated to be 0.762 ± 0.076 pmol per 10 μg protein loading capacity (n=3) or 76.2 ± 7.6 pmol CYP3A4/mg protein. This value was much higher than that reported previously (20.6 pmol CYP3A/mg cells) [Schmiedlin-Ren et al., 1997] but was comparable with the CYP3A4 content of human jejunum (70 ± 20 pmol/mg protein) [Watkins et al., 1987]. In contrast, non-treated cells contained 14.96 ± 8.008 pmol CYP3A4/mg protein and was in good agreement with previously reported value (~ 7.9 pmol/mg cells) [Schmiedlin-Ren et al., 1997]. Thus, the modified cell culture conditions and the origin of parent Caco-2 cells are attributed to their expression of CYP3A4 protein that is equivalent to that found in vivo.

FIGURE 5.4 **Expression of cytochrome P450 3A4 in Caco-2 cells**

Confluent cells (#122) at three weeks post-seeding were treated with 0.25 μM 1α, 25-dihydroxyvitamin D_3 for two weeks. Microsomal proteins (10-20 μg/lane) were subjected to gel electrophoresis and Western blotting using a rabbit polyclonal CYP3A4 primary antibody as described in section 2.2.8.3. Lane 1: rat liver microsomes (20 μg/lane), lane 2: standard purified CYP3A4 (20 μg/lane), lanes 3, 4, 5: non-treated Caco-2 cell microsomes (10 μg/lane), lanes 6, 7, 8: treated Caco-2 cell microsomes (10μg/lane).
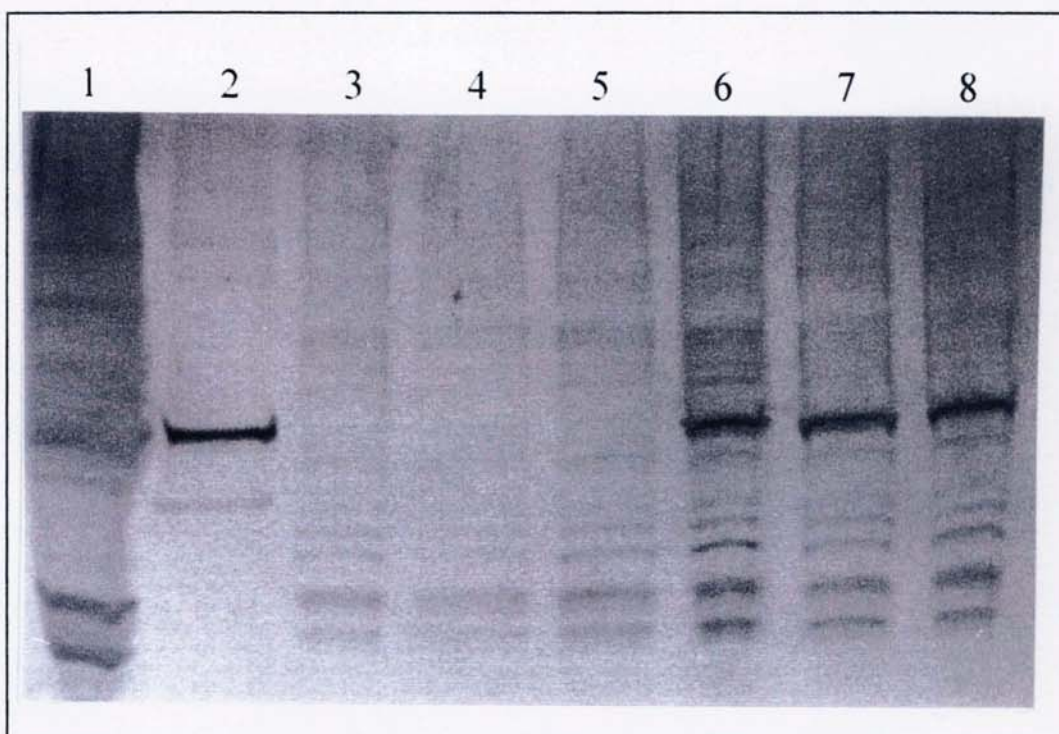
5.3.3 IDENTIFICATION OF MIDAZOLAM AND ITS METABOLITES BY HIGH PERFORMANCE LIQUID CHROMATOGRAPHY (HPLC)

Figures 5.5, 5.6, 5.7 and 5.8 represent the chromatograms of MDZ, 1-OH MDZ, 4-OH MDZ and diazepam (internal standard) of retention times 17.41, 11.40, 9.55 and 19.83 minutes respectively. The resolution of all four compounds in an experimental sample at 90 minutes after the addition of midazolam to the cells is shown in figure 5.9 with the following Rs values:

Rs=   165.3 between 4-OH MDZ and 1-OH MDZ

Rs=   107.2 between 1-OH MDZ and MDZ

Rs=   655.4 between MDZ and diazepam

All values are highly indicative of complete separation of peaks with clarity.

The purity of the donor phase containing MDZ only was assessed by HPLC immediately after its preparation and before it was added to the cells. Figure 5.10 indicates that there was a negligible contamination of 1-OH MDZ in the donor phase but that the contamination was very small as compared with that being produced after 90 minutes incubation (figure 5.9), therefore, high concentrations of midazolam metabolites were predominantly generated by the cells themselves. Figures 5.11, 5.12, 5.13, indicated the standard peaks of MDZ (5.11), 1-OH MDZ (5.12) and 4-OH MDZ (5.13) of the same concentration (0.05 µg/mL) but with each peak showing a different area under the curve. Figures 5.14, 5.15 and 5.16 represent the calibration graphs of MDZ, 1-OH MDZ and 4-OH MDZ respectively.

FIGURE 5.5   **Identification of MDZ by HPLC**
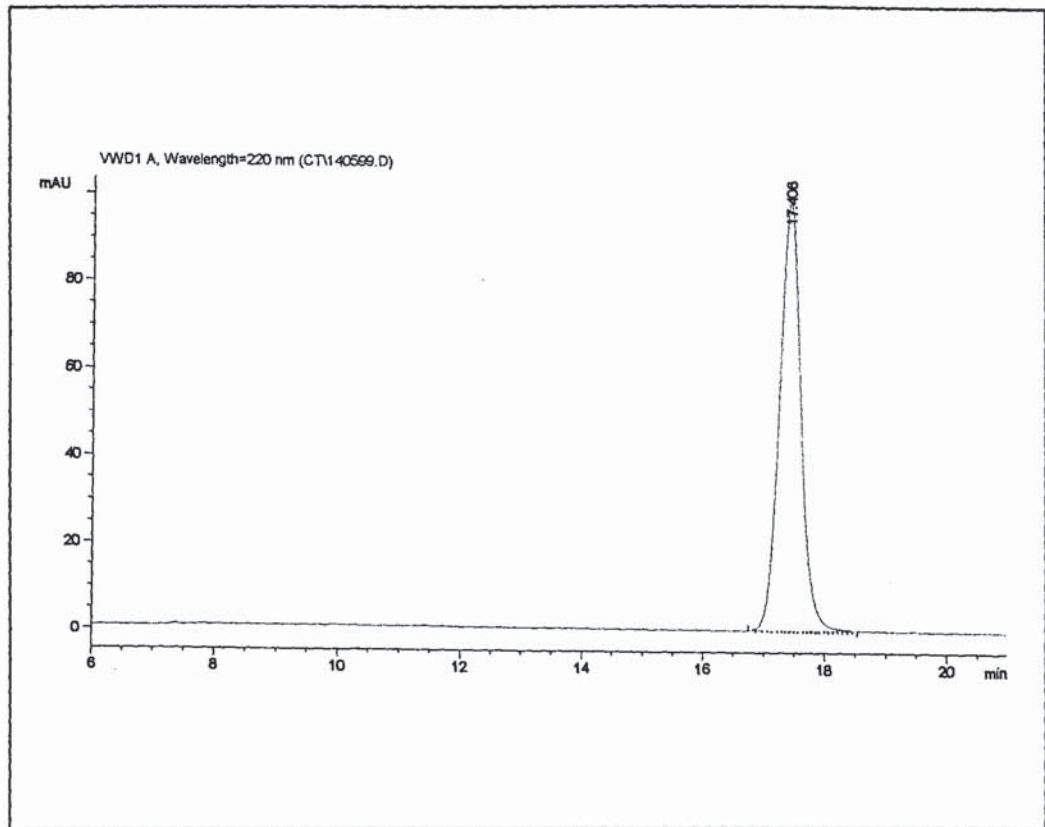
FIGURE 5.6   **Identification of 1-OH MDZ by HPLC**

118
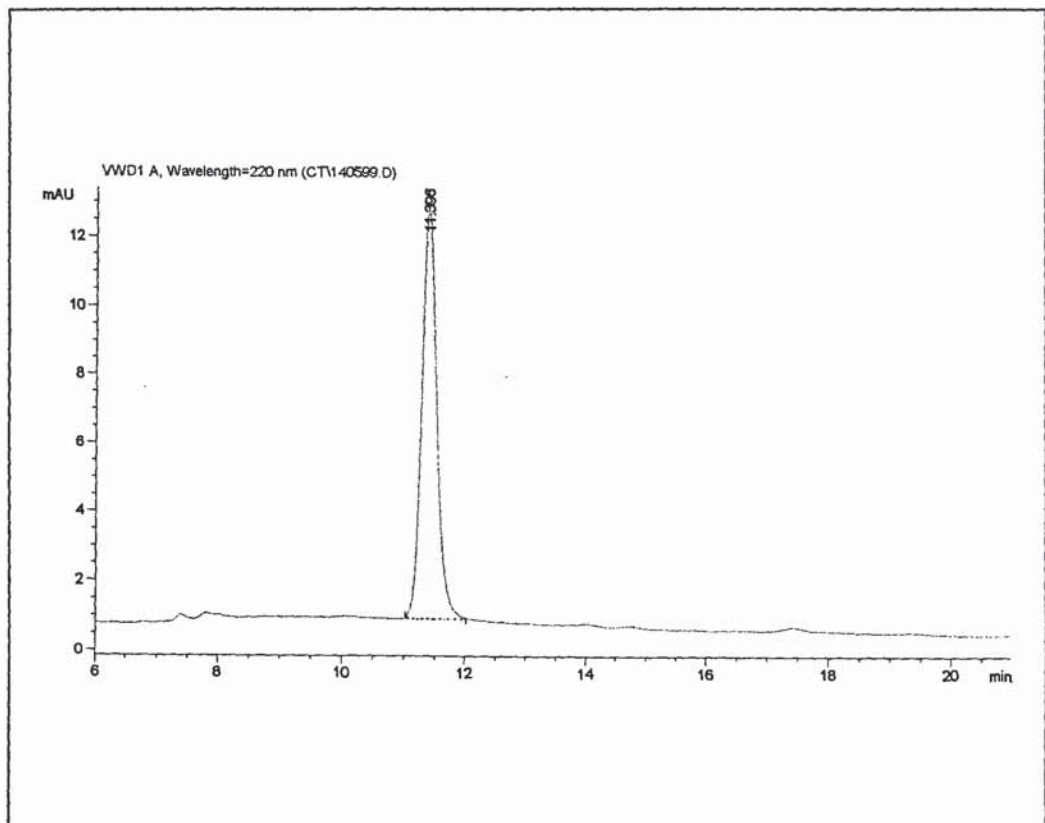
FIGURE 5.7   Identification of 4-OH MDZ by HPLC

VWD1 A, Wavelength=220 nm (CT\080399.D)
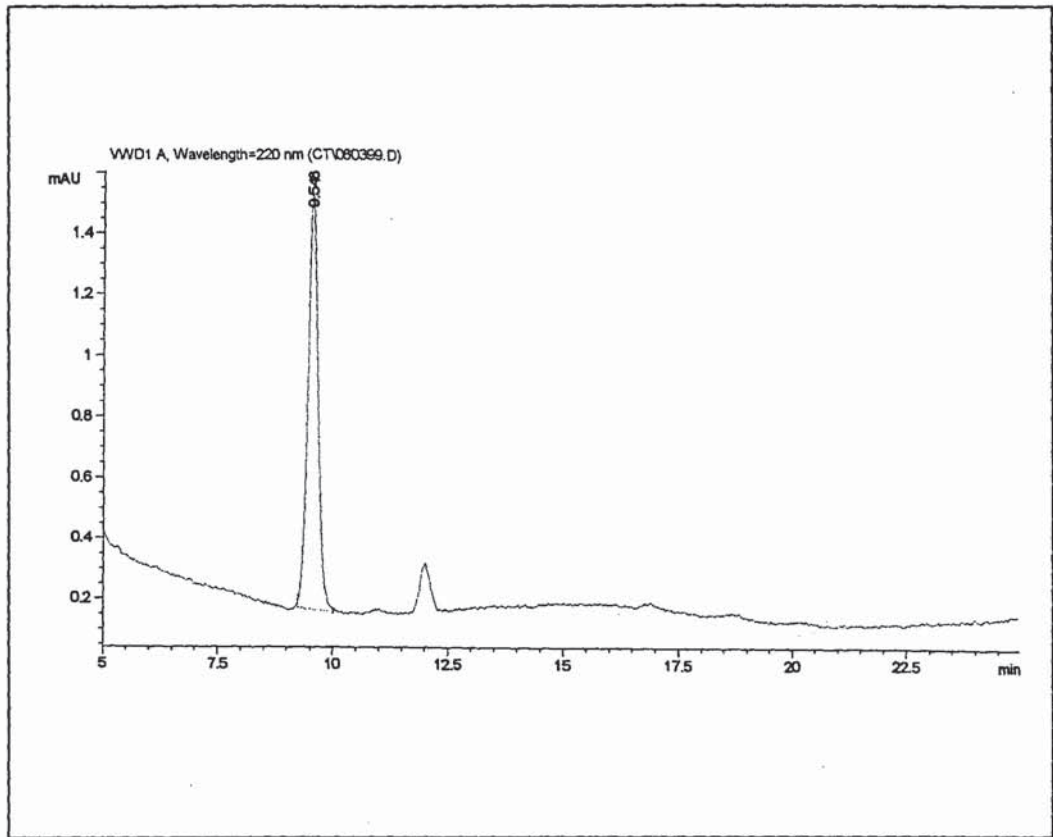
FIGURE 5.8   Identification of diazepam (internal standard) by HPLC

VWD1 A, Wavelength=220 nm (CT\140599.D)
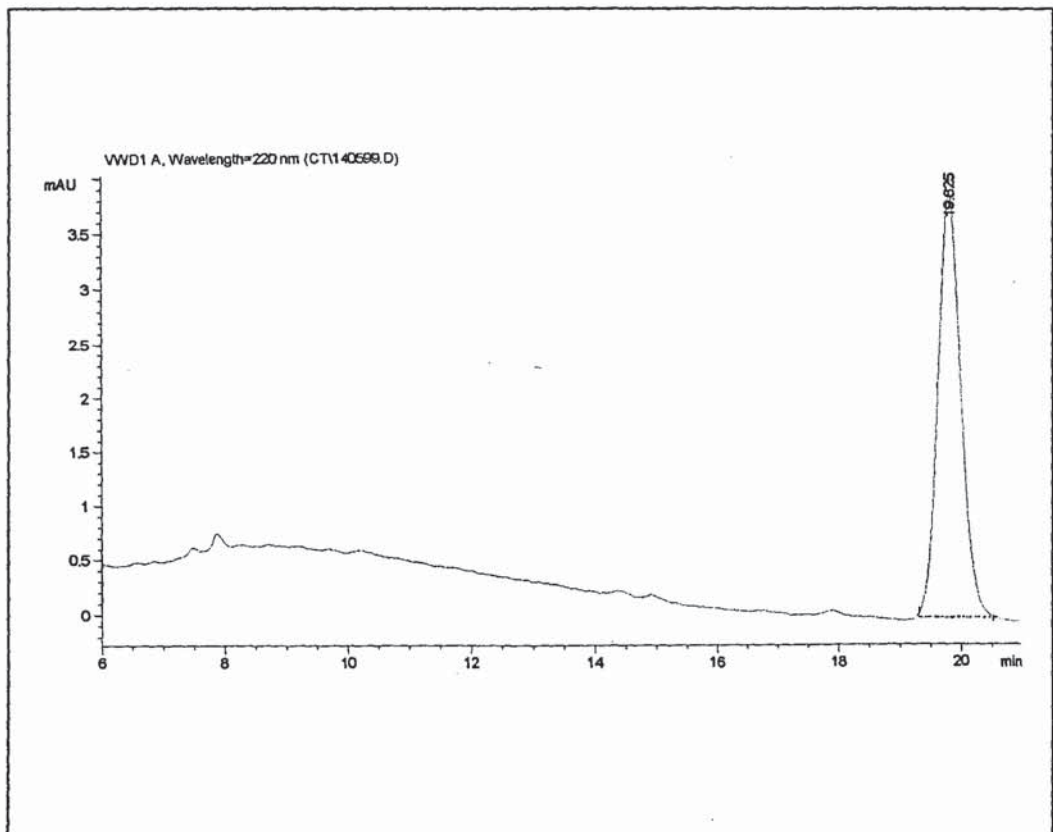
FIGURE 5.9 **Metabolism of midazolam by treated Caco-2 cells after 90 minutes**
From left to right: 4-OH MDZ, 1-OH MDZ, MDZ and diazepam
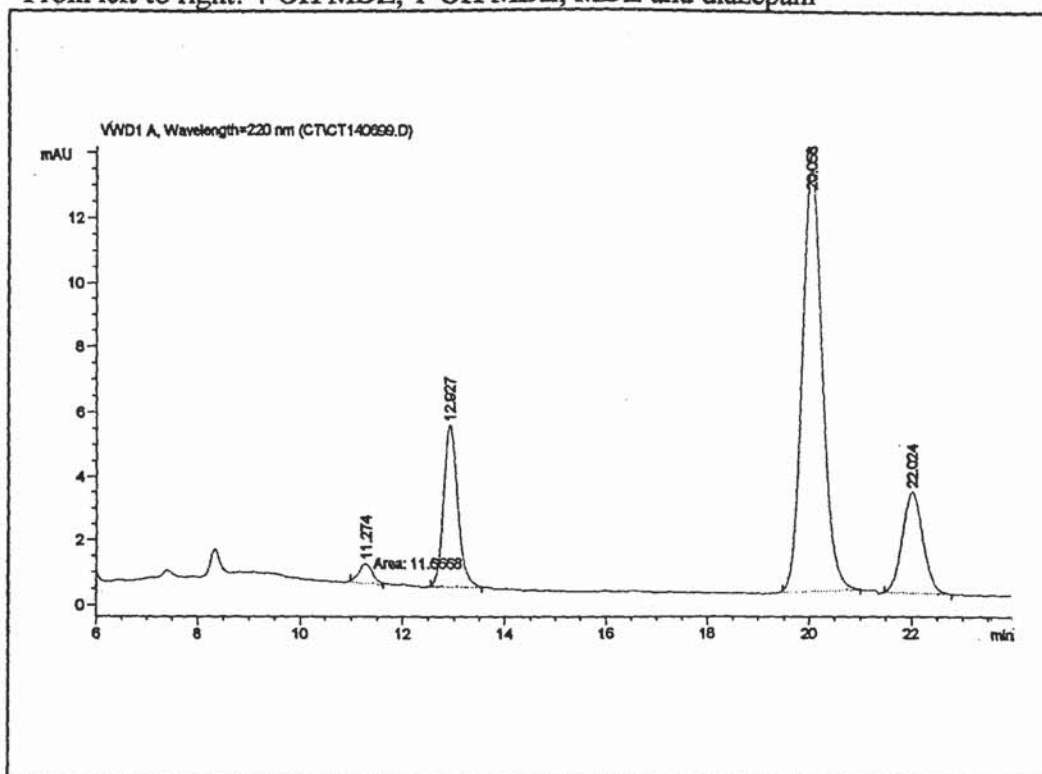
FIGURE 5.10 **MDZ purity in the donor phase (pH 7.42) after its preparation**
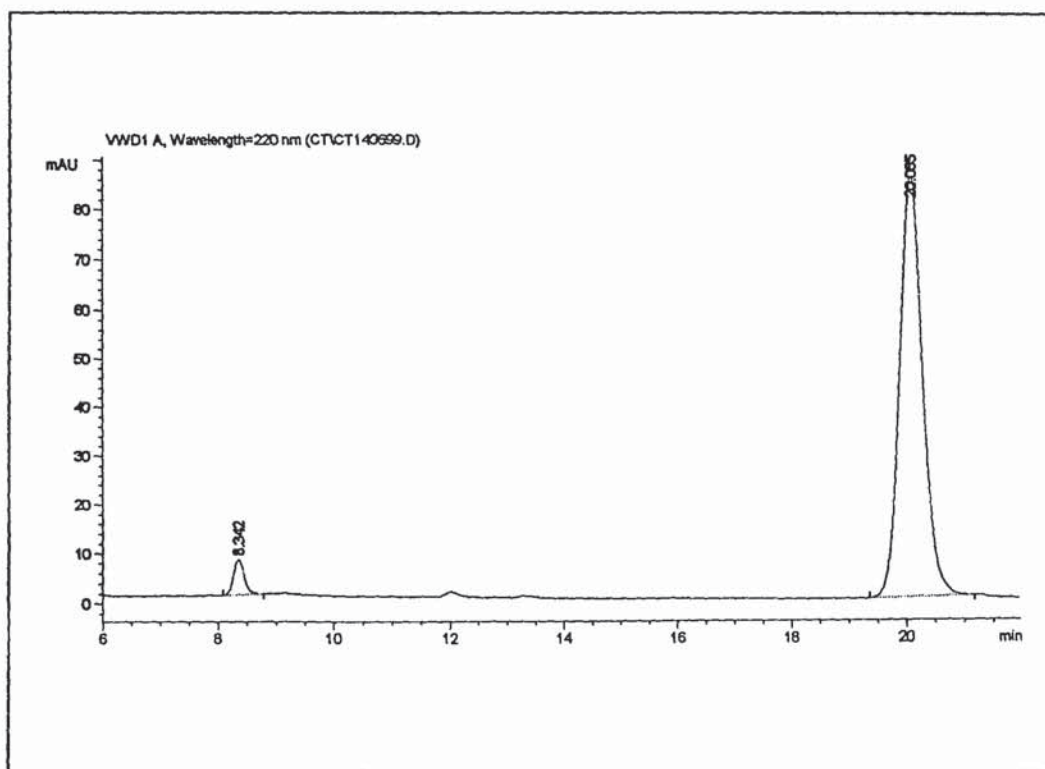
FIGURE 5.11 **MDZ (0.05 μg/mL) and diazepam (20ng/200μL)**
(Injection volume: 200 μL)
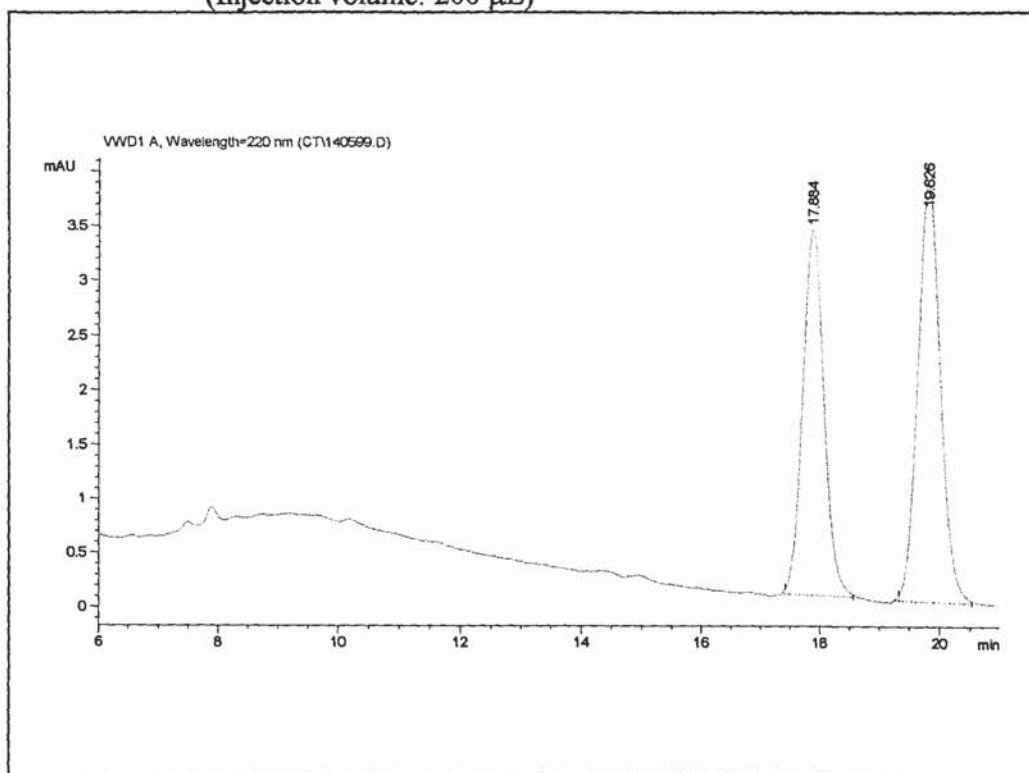
FIGURE 5.12 **1-OH MDZ (0.05 μg/mL) and diazepam (20ng/200μL)**
(Injection volume: 200 μL)
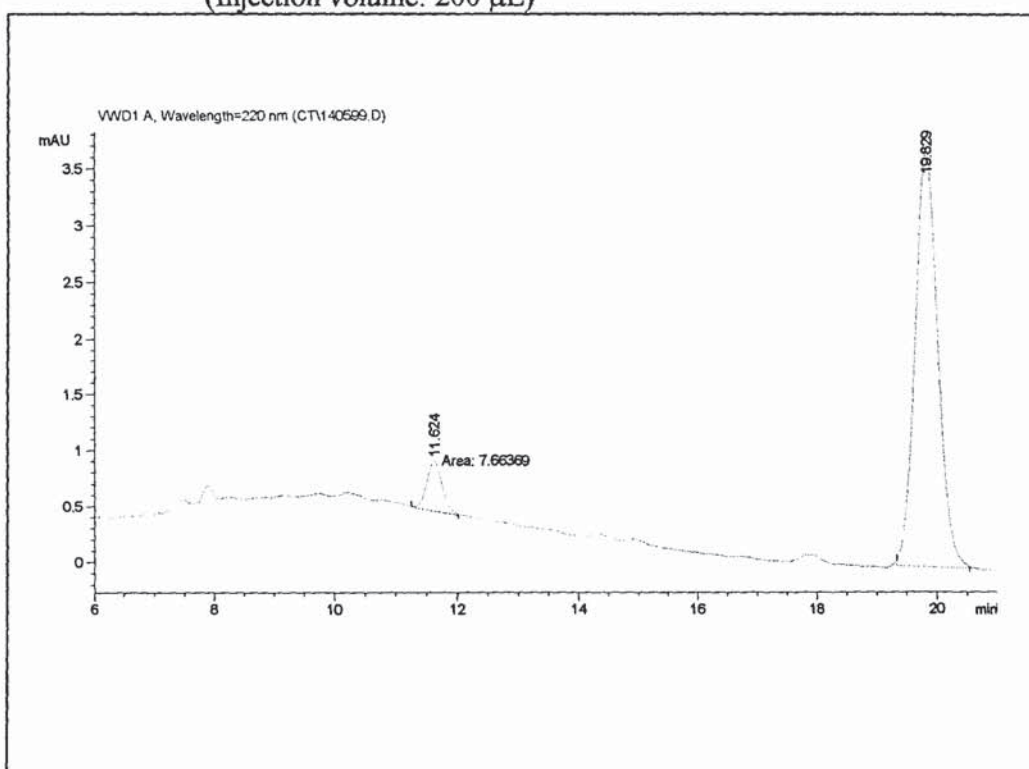
FIGURE 5.13 **4-OH MDZ (0.05 µg/mL) and diazepam (20ng/200µL)**
(Injection volume: 200 µL)
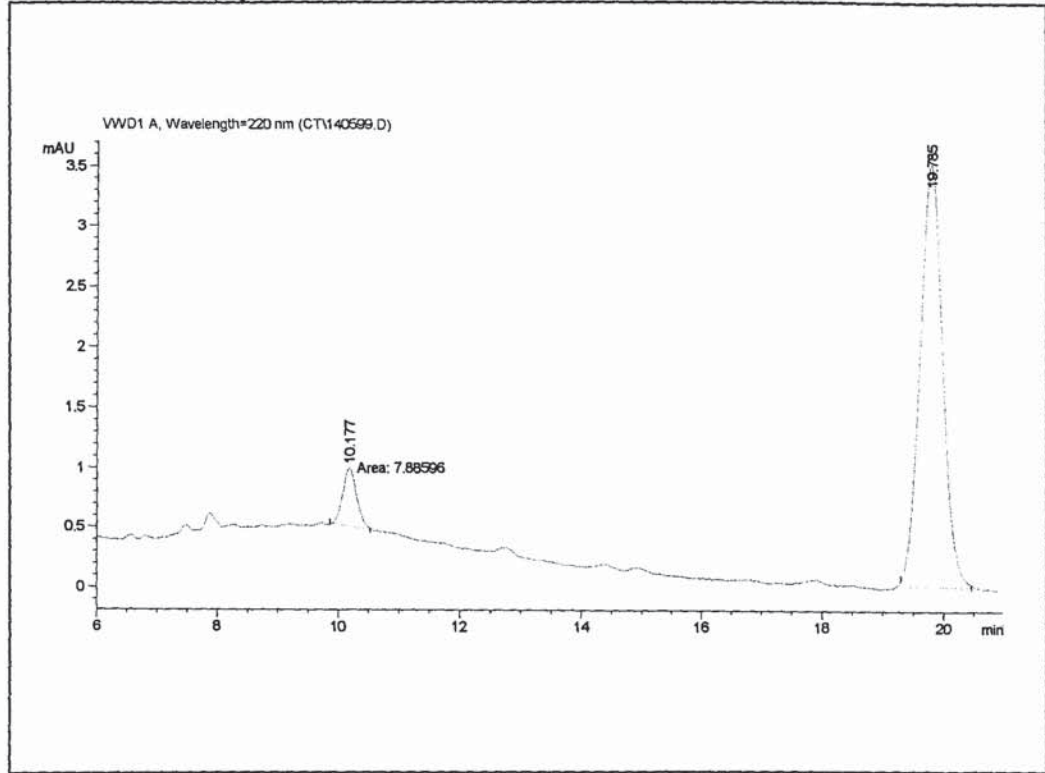
FIGURE 5.14 **Calibration graph of MDZ in HBSS, pH 7.42**

$$y = 0.0811x - 0.1125$$
$$R^2 = 0.9935$$

122
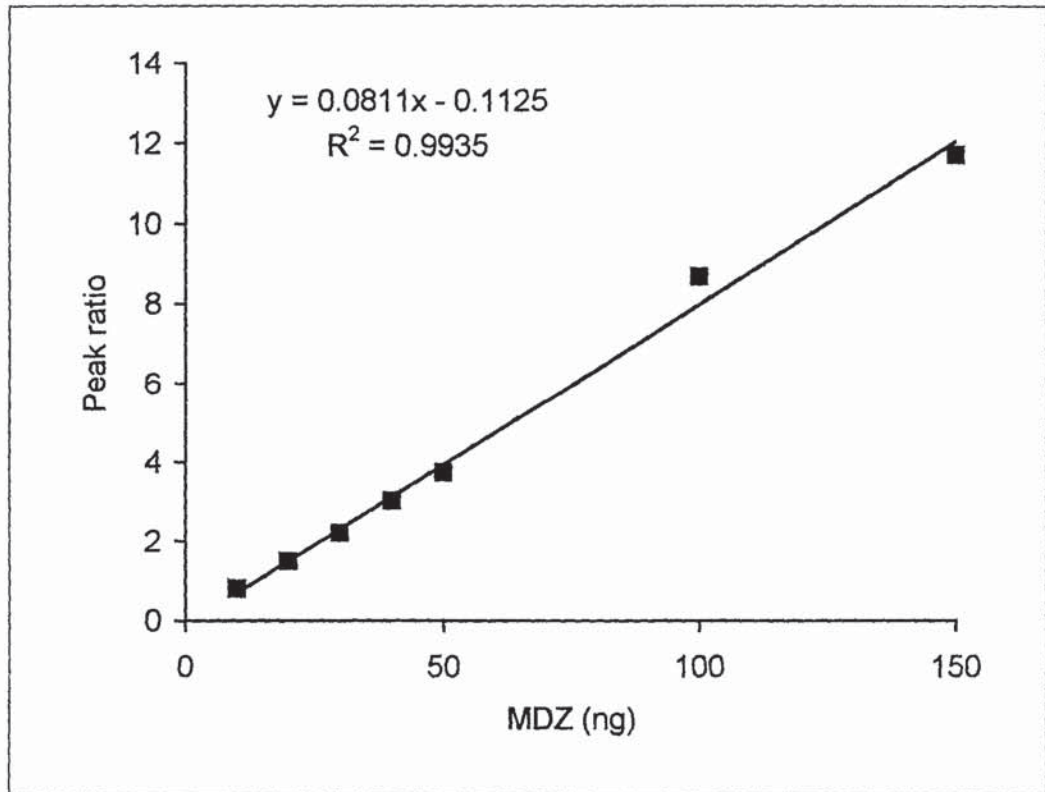
FIGURE 5.15 **Calibration graph of 1-OH MDZ in HBSS, pH 7.42**

$y = 0.0069x - 0.005$
$R^2 = 0.9935$
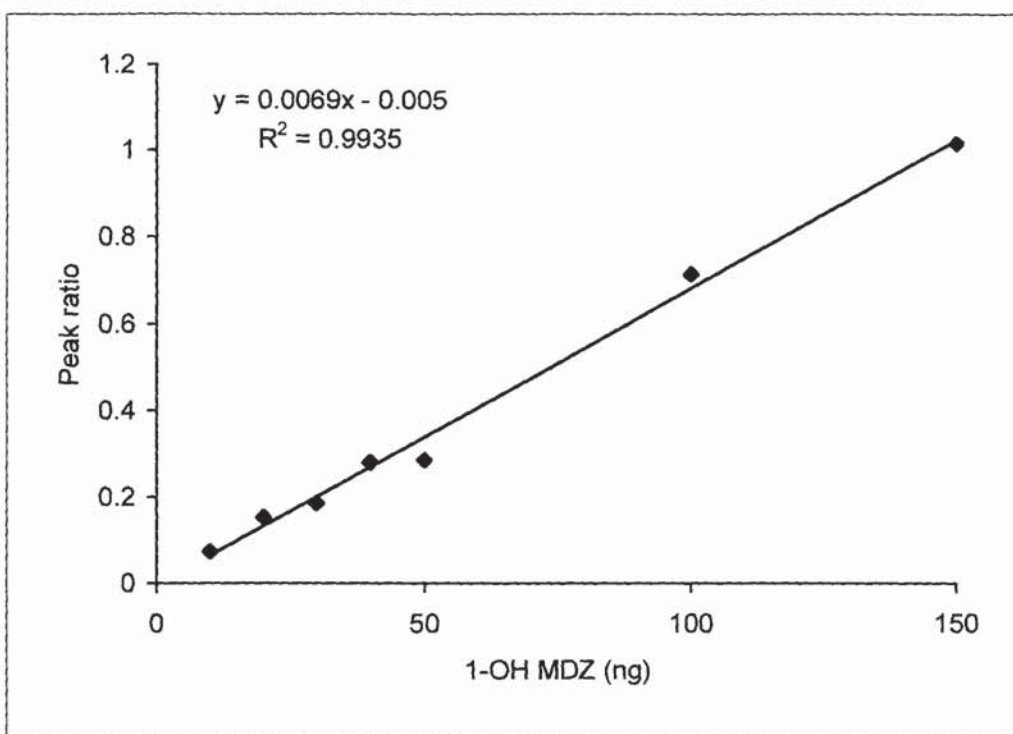
FIGURE 5.16 **Calibration graph of 4-OH MDZ in HBSS, pH 7.42**

$y = 0.0066x + 0.0209$
$R^2 = 0.9999$

123
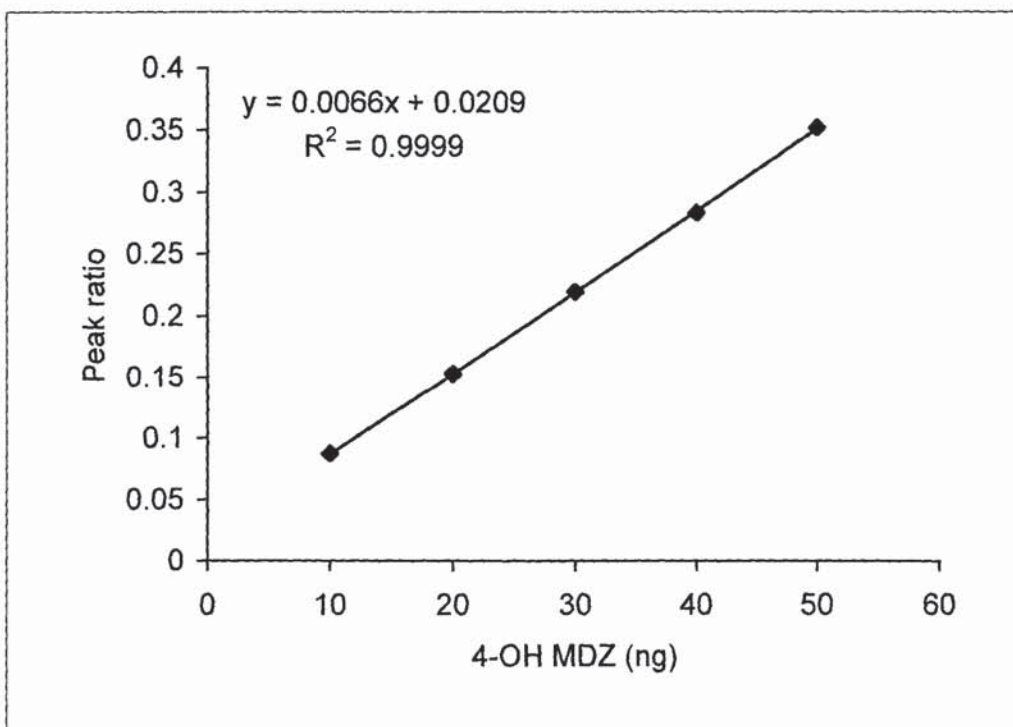
5.3.4 EXTENT OF MIDAZOLAM METABOLISM AS A FUNCTION OF TIME

The reported Km values for MDZ metabolism by microsomes prepared from human intestinal cells are 3.8, 3.7 and 4.5 μM for the duodenum, jejunum and ileum respectively [Paine *et al.*, 1997]. A shortage of MDZ as a CYP3A4 substrate might result in its unjustified rate and extent of metabolism, and, therefore would underestimate the true metabolic capacity of treated cells. Therefore, based on the findings by Paine *et al.*, (1997), a concentration of 4 μM of MDZ was used in all experiments to ensure saturable kinetics.

As shown in figures 5.17 and 5.18, only 1-OH MDZ metabolite was detected in the basolateral chamber of parent and Type I Caco-2 cells after 1 week of exposure to 0.25 μM 1α, 25-dihydroxyvitamin D_3 in contrast with the generation of both 1-OH MDZ and 4-OH MDZ by CYP3A4 after 2 weeks of treatment of the cells with 0.25 μM 1α, 25-dihydroxyvitamin D_3 (figure 5.9). The accumulation of 1-OH MDZ was at all times higher in the parent compared with Type I Caco-2 cells (figure 5.19A), indicating a higher metabolic activity as a result of either higher CYP3A4 content or higher enzyme activity or both in the parent cells. The rate of accumulation of the 1-OH MDZ in the basolateral chamber, as calculated from the slope of the graph (figure 5.19A), was 0.144 $\pm$ 0.007 and 0.079 $\pm$ 0.003 nmol/min/mg protein respectively for parent and Type I Caco-2 cells. Interestingly, the transepithelial transport rate of MDZ was almost identical for both cell types (0.238 $\pm$ 0.011 and 0.231 $\pm$ 0.010 nmol/min/mg protein for parent and Type I Caco-2 cells) (figure 5.19 B). Midazolam had to diffuse from the donor chamber into the cells where it was metabolised by CYP3A enzymes situated in the intracellular smooth endoplasmic reticulum before both parent and metabolite drugs could diffuse to the extracellular medium. This result indicates that for the same transcellular rate of MDZ transport, more MDZ was metabolised in the parent Caco-2 cells.

FIGURE 5.17 Formation and transport of 1-OH MDZ at 60 minutes in parent cells

(As found in the basolateral chamber of parent Caco-2 cells after 1 week of exposure to 0.25 μM 1α, 25-dihydroxyvitamin D_3)
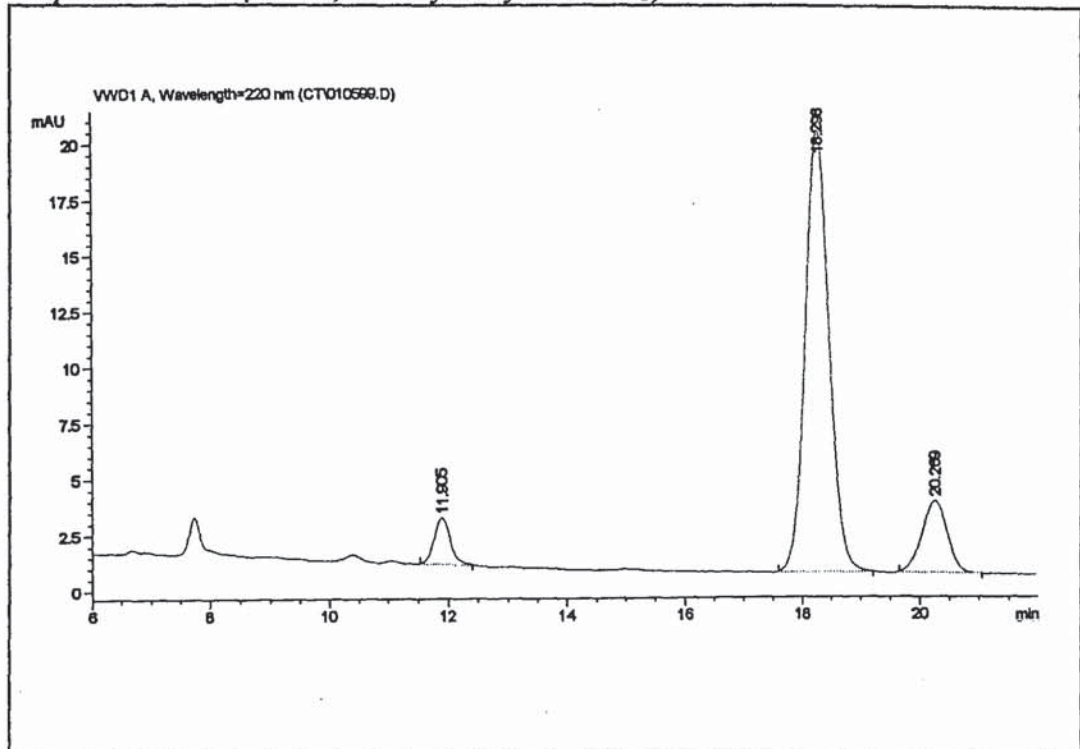
FIGURE 5.18 Formation and transport of 1-OH MDZ at 60 minutes in Type I cells

(As found in the basolateral chamber of Type I Caco-2 cells after 1 week of exposure to 0.25 μM 1α, 25-dihydroxyvitamin D_3)
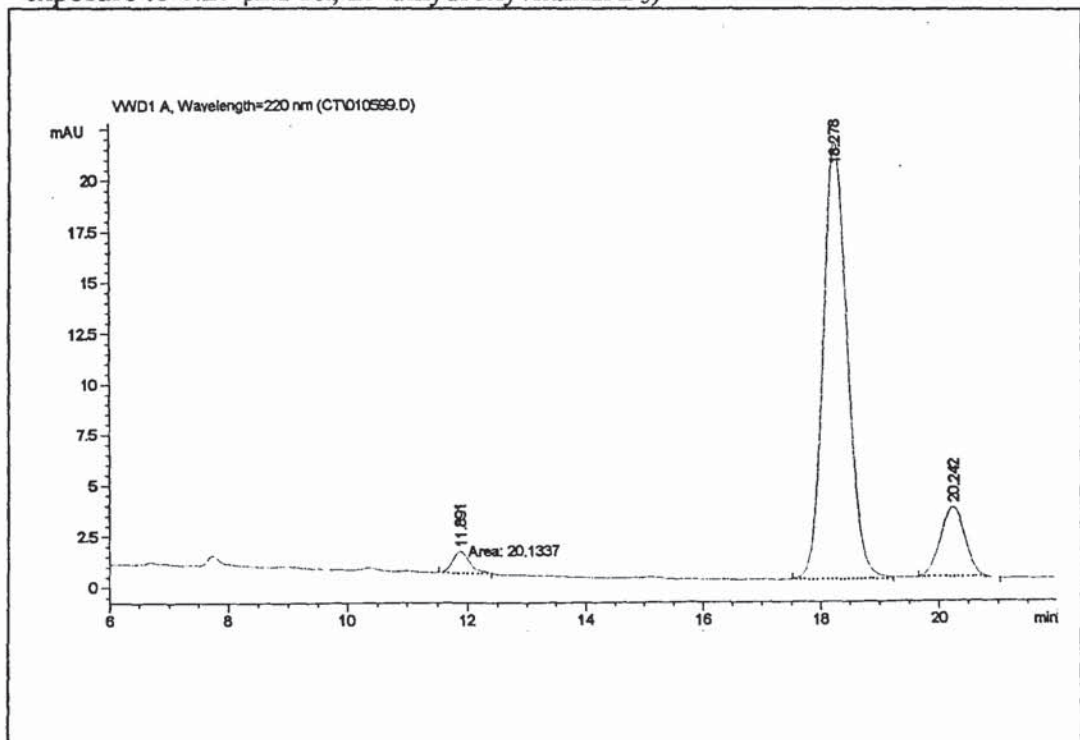
FIGURE 5.19 **Accumulation of 1-OH MDZ and MDZ basolaterally after 1 week**

Parent (#139) and Type I (#75) Caco-2 cells were incubated with 4.0 μM MDZ in M2 (pH 7.42) apically. A volume of 0.5 mL was withdrawn from the basolateral chamber for the analysis of MDZ, its metabolites and fluorescein at 15, 30, 45 and 60 minutes and immediately replaced with fresh, equal volume. Results were expressed as nmol/mg protein (mean ± sd, n=3).

A.   Accumulation of 1-OH MDZ
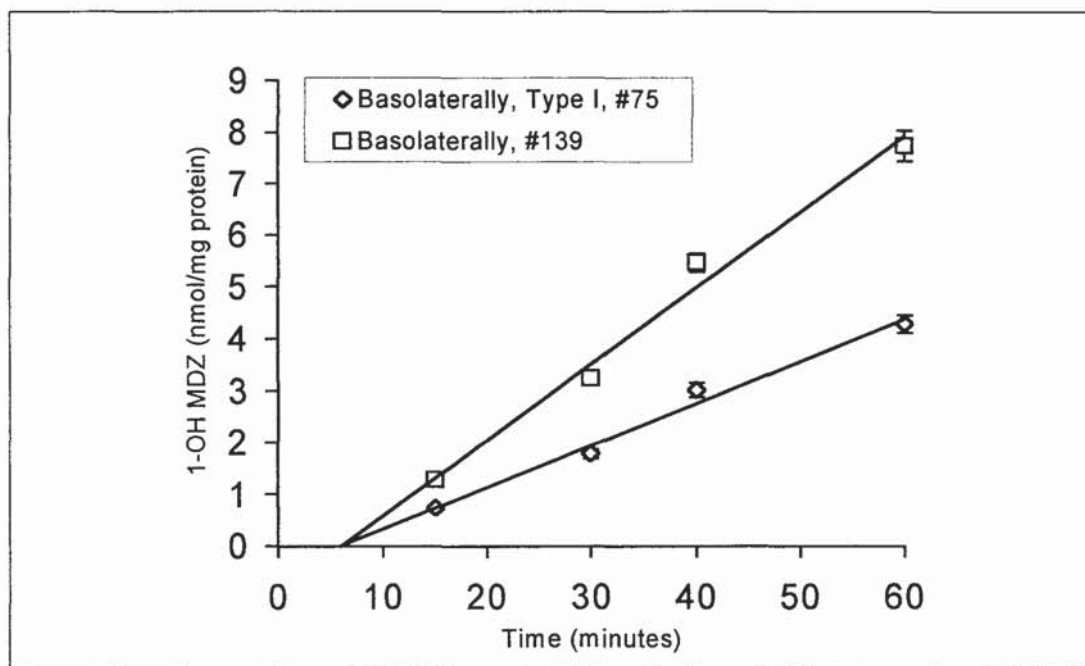
B.   Accumulation of MDZ
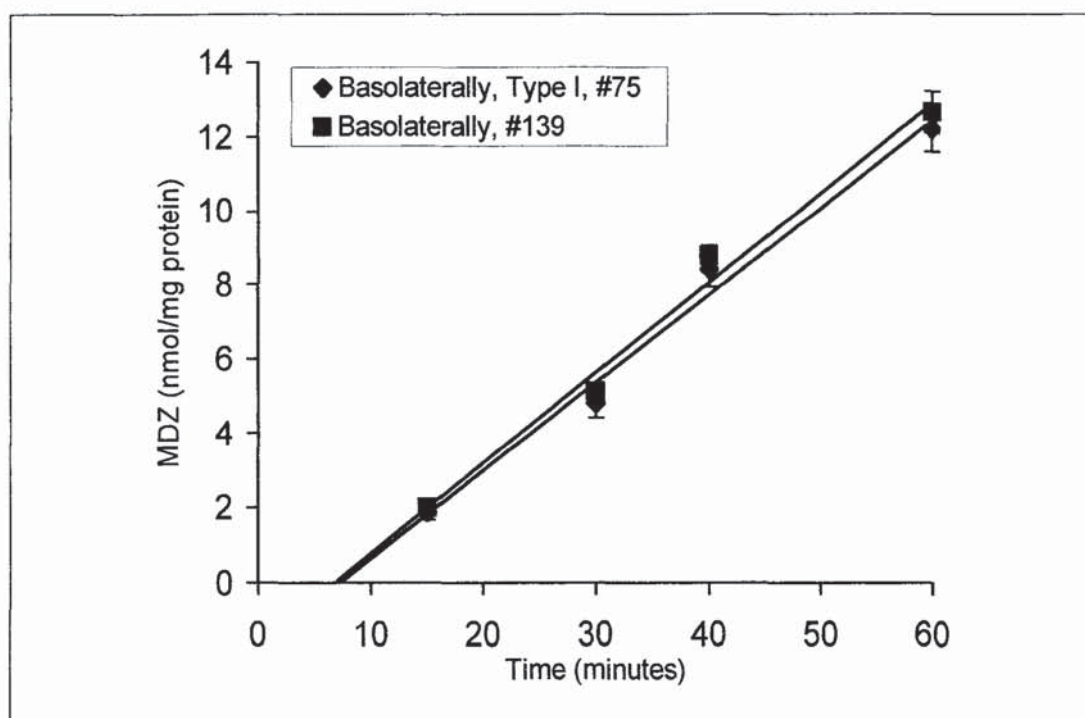
TABLE 5.1   **Rates of MDZ metabolism with/without 100 μM (±)verapamil in Type I and parent Caco-2 cells**

Parent (#139, #149) and Type I Caco-2 cells (#75, #83) were incubated with 4.0 μM MDZ in M2 (pH 7.42) in the apical or basolateral chamber. At pre-determined times, 0.5 ml of M2 was withdrawn from the receiver chamber and immediately replaced with a fresh, equal volume of transport medium (n=3). Volumes of 200 and 150 μL were subjected to HPLC and fluorescence analysis and the rates of accumulation of MDZ and its metabolites, and the transport of fluorescein (mean ± sd, n=3) in nmol/min/mg protein were determined

Length of exposure	Cell type	Direction	100 μM (±)Vera-pamil	1-OH MDZ	4-OH MDZ	MDZ	Fluores-cein
1 week	I, #75	A-B	-	0.079 ± 0.003		0.231 ± 0.010	0.063 ± 0.015
	# 139		-	0.144 ± 0.007		0.238 ± 0.011	0.035 ± 0.010
2 weeks	I, #75	A-B	-	0.257 ± 0.020		0.412 ± 0.017	0.370 ± 0.213
	#139		-	1.057 ± 0.046	0.087 ± 0.004	0.484 ± 0.039	0.103 ± 0.003
	I, #75		+	0.119 ± 0.019		0.516 ± 0.018	0.350 ± 0.250
	#139		+	0.378 ± 0.022		0.573 ± 0.027	0.102 ± 0.023
2 weeks	I, #83	B-A	-	0.316 ± 0.073	0.060 ± 0.007	0.372 ± 0.021	0.120 ± 0.032
	#149		-	0.931 ± 0.026	0.156 ± 0.004	0.396 ± 0.018	0.093 ± 0.010
	I, #83		+	0.085 ± 0.006		0.357 ± 0.020	0.189 ± 0.083
	#149		+	0.285 ± 0.015		0.460 ± 0.009	0.118 ± 0.006

5.3.5 KINETIC PROFILES OF THE FORMATION OF MIDAZOLAM METABOLITES

Since it has been reported that both MDZ and its 1-OH metabolite are preferentially distributed in the apical compartment, regardless of the input location of the parent drug, [Schmiedlin-Ren *et al.*, 1997, Fisher *et al.*, 1999], investigation of MDZ metabolism in the course of its transport from the apical-to-basolateral compartment (A-B), or *vice versa* (B-A), was conducted. The rates of apical and basolateral accumulation of 1-OH MDZ were similar in Type I Caco-2 cells (a rate of 0.257 ± 0.020 *vs.* 0.316 ± 0.073 nmol/min/mg protein respectively, figure 5.20A), indicating that 1-OH MDZ was transported predominantly by passive diffusion out of the cells. Similarly, there was no significant difference ($p > 0.05$) between the two rates of transport of MDZ in either direction in Type I cells (a value of 0.412 ± 0.017 *vs.* 0.372 ± 0.021 nmol/min/mg protein, figure 5.21A).

In contrast, faster rates of 1-OH MDZ accumulation both apically and basolaterally were detected at all times in parent Caco-2 cells (rates of 0.931 ± 0.026 and 1.057 ± 0.046 nmol/min/mg protein respectively) (figure 5.20B), implying a higher metabolising capacity of the parent cells than Type I cells. The rate of transepithelial transport of MDZ was slightly higher in the A-B direction (0.484 ± 0.039 nmol/mg protein) as compared to that in the reverse direction (0.396 ± 0.018 nmol/min/mg protein) in parent Caco-2 cells (figure 5.21 B). Therefore, more MDZ was available intracellularly for its metabolism and resulted in a faster basolateral accumulation of 1-OH MDZ as seen in figure 5.20B.

FIGURE 5.20 **Accumulation of 1-OH MDZ after two weeks of treatment in Type I and parent Caco-2 cells**

Parent (#139 and 149) and Type I (#75 and 83) Caco-2 cells were incubated with 4.0 μM MDZ in M2 (pH 7.42) apically or basolaterally. A volume of 0.5 mL was withdrawn from either the basolateral or apical chamber at 15, 30, 45, 60 and 90 minutes and immediately replaced with fresh, equal volume. Results were expressed as nmol/mg protein (mean ± sd, n=3).

A.   1-OH MDZ accumulation in Type I cells
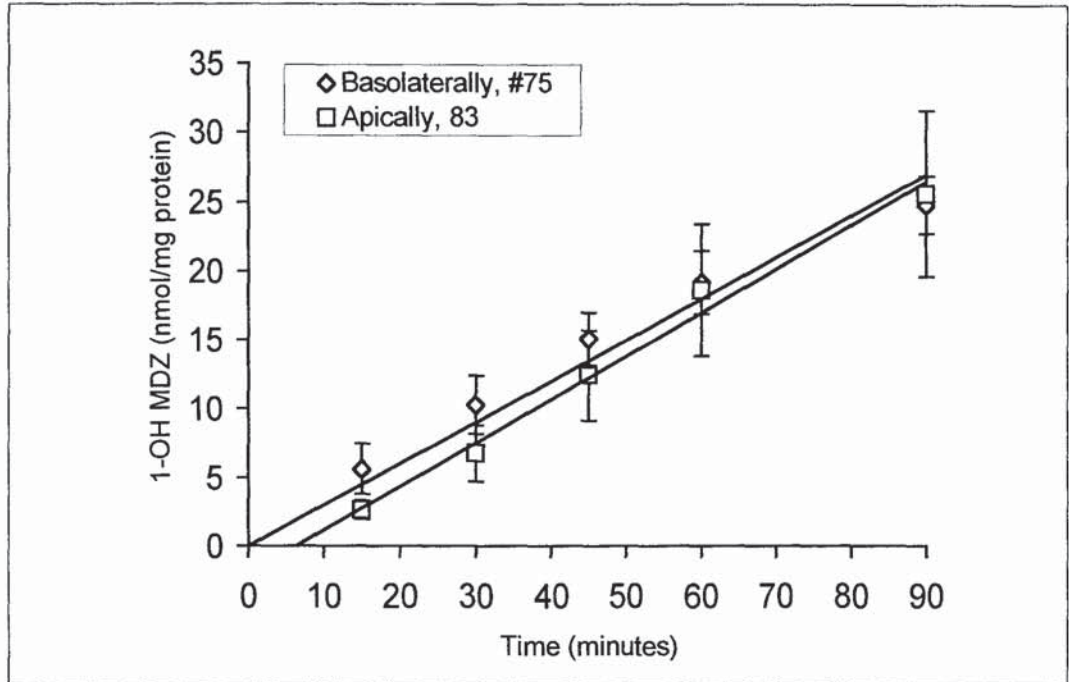
B.   1-OH MDZ accumulation in parent cells
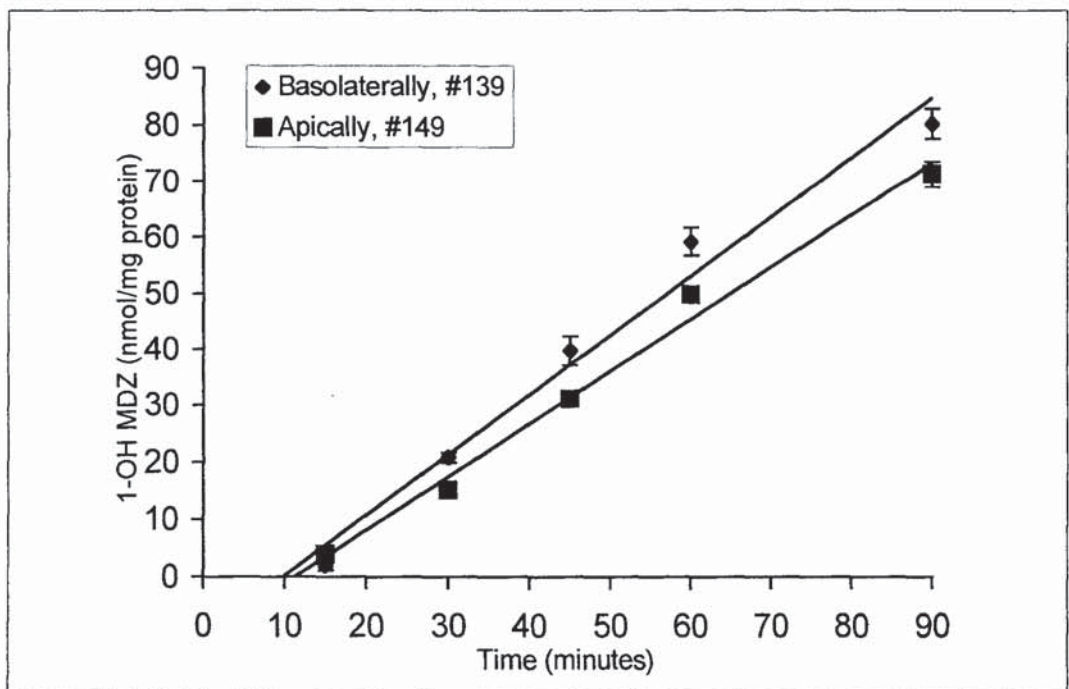
FIGURE 5.21 **Accumulation of MDZ after two weeks of treatments**
Parent (#139 and 149) and Type I (#75 and 83) Caco-2 cells were incubated with 4.0 µM MDZ in M2 (pH 7.42) apically or basolaterally. A volume of 0.5 mL was withdrawn from either the apical or basolateral chamber at 15, 30, 45, 60 and 90 minutes and immediately replaced with fresh, equal volume. Results were expressed as nmol/mg protein (mean ± sd, n=3).

A. Accumulation of MDZ in Type I cells
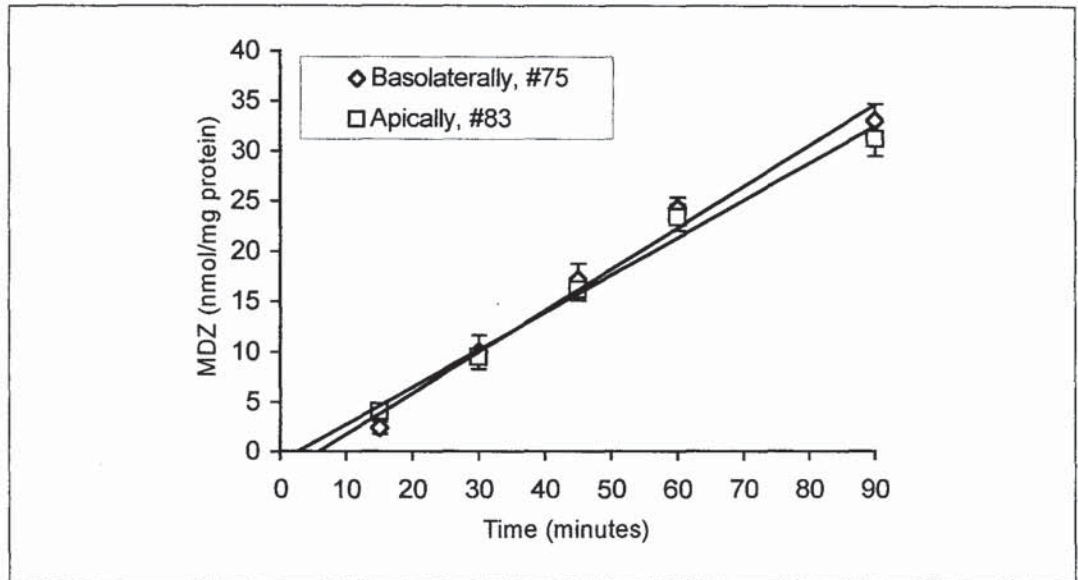
B. Accumulation of MDZ in parent cells
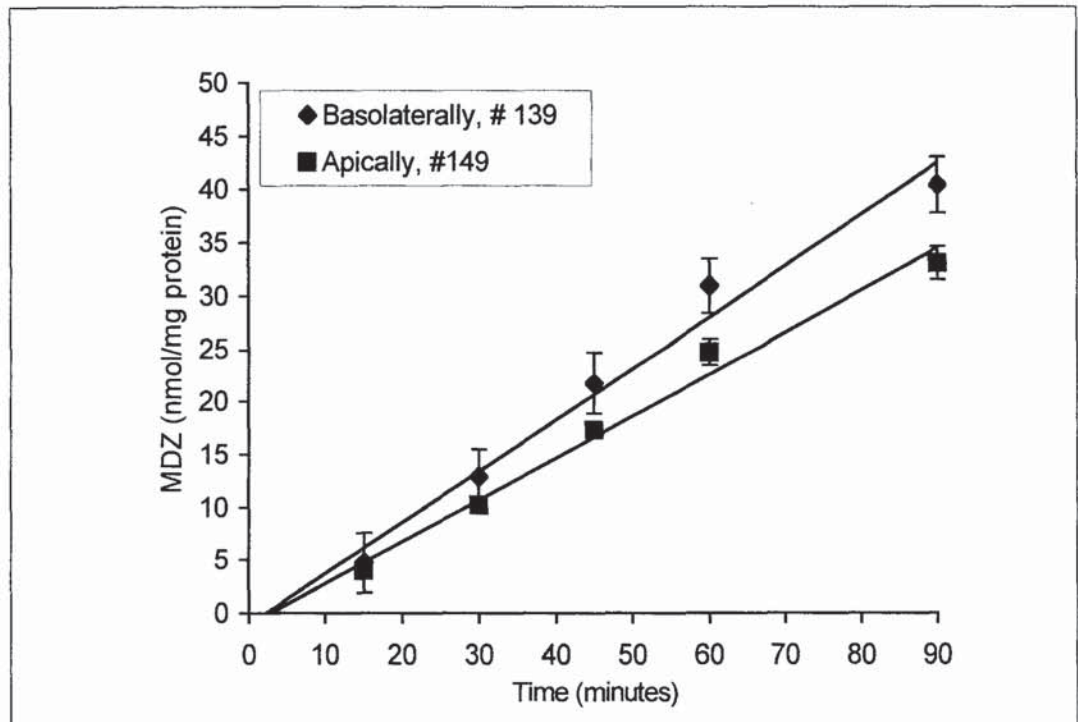
(±)Verapamil is an inhibitor of both P-glycoprotein and CYP3A4 [Watkins, 1997]. To confirm that 1-OH MDZ is not a substrate for P-gp, both verapamil and

midazolam were mixed thoroughly in M2 prior to adding it to either apical or basolateral compartment. The quantity of 1-OH MDZ was assessed in the receiver chambers as described previously. As shown in figure 5.22, 100 μM (±)verapamil suppressed the formation of 1-OH MDZ in both cell types, especially in parent Caco-2 cells, as a result of its binding to CYP3A4 and competitively inhibited midazolam metabolism. However, the rate of accumulation of 1-OH MDZ was still higher in the basolateral chamber of both Type I and parent Caco-2 cells, (rates of apical accumulation of 0.085 ± 0.006 and 0.285 ± 0.015 vs. those of basolateral accumulation, 0.119 ± 0.019 and 0.378 ± 0.022 nmol/min/mg protein for Type I and parent Caco-2 cells respectively), indicating that there was no involvement of P-gp in transporting 1-OH MDZ out of the cells, but rather, a dominant passive diffusion. Similarly, since (±)verapamil binds to CYP3A4, its presence resulted in a higher unbound intracellular MDZ concentration, which effectively increased MDZ concentration gradient between the cells and the surrounding extracellular media, leading to its increased transepithelial transport rates in either direction in both Type I and parent Caco-2 cells (Figure 5.23; Table 5.1). In Type I cells, there was a slight decrease in the rate of MDZ transport in the B-A direction in the presence of (±)verapamil compared with that in its absence (Table 5.1). However, this change, was not statistically significant ($p > 0.05$, two tailed Student t-test for unpaired mean sample data).

FIGURE 5.22 **Accumulation of 1-OH MDZ in the presence of 100 μM (±)verapamil after two weeks of treatment in Type I and parent Caco-2 cells.**

Parent (#139 and 149) and Type I (#75 and 83) Caco-2 cells were incubated with 4.0 μM MDZ with 100 μM (±)verapamil in M2 (pH 7.42) apically or basolaterally. A volume of 0.5 mL was withdrawn from either the apical or basolateral chamber at 15, 30, 45, 60 and 90 minutes and immediately replaced with fresh, equal volume. Results were expressed as nmol/mg protein (mean ± sd, n=3)

A.   1-OH MDZ accumulation in Type I cells, with 100 μM (±)verapamil
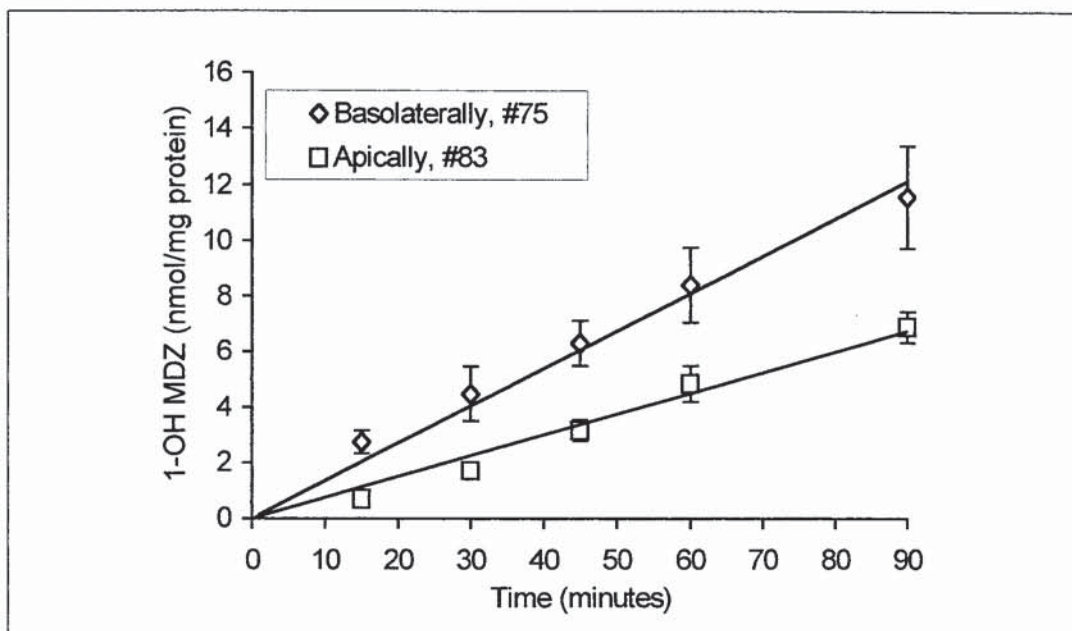
B.   1-OH MDZ accumulation in parent cells, with 100 μM (±)verapamil
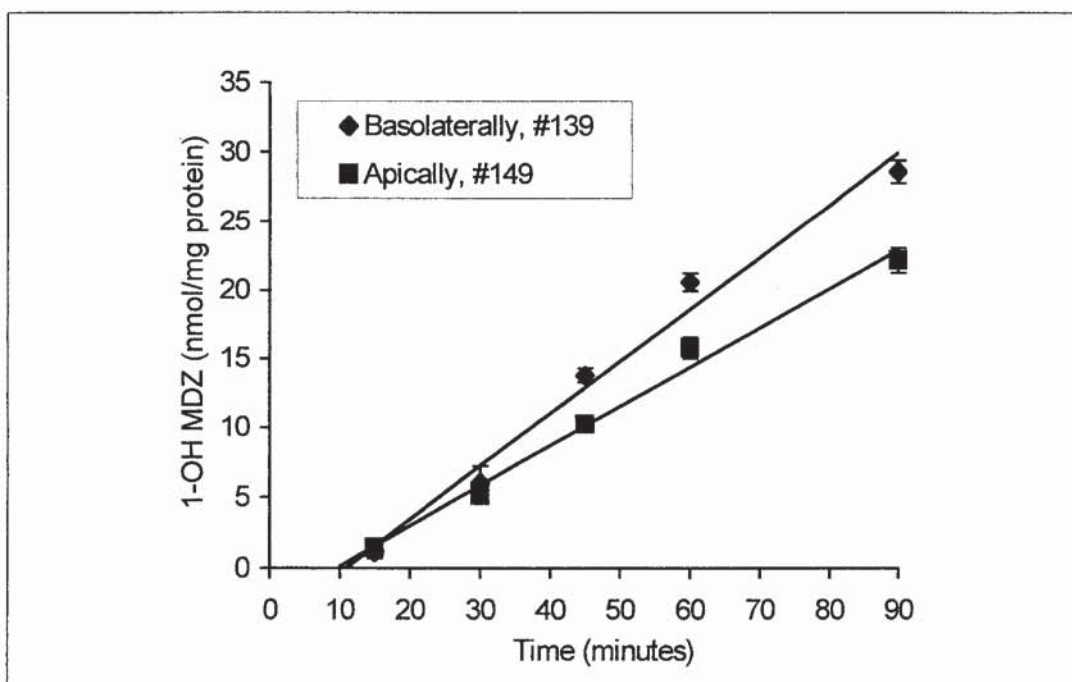
FIGURE 5.23 **Accumulation of MDZ in the presence of 100 μM (±)verapamil after two weeks of treatment in Type I and parent Caco-2 cells**
Parent (#139 and 149) and Type I (#75 and 83) Caco-2 cells were incubated with 4.0 μM MDZ with 100 μM (±)verapamil in M2 (pH 7.42) apically or basolaterally. A volume of 0.5 mL was withdrawn from either the apical or basolateral chamber at 15, 30, 45, 60 and 90 minutes and immediately replaced with fresh, equal volume. Results were expressed as nmol/mg protein (mean ± sd, n=3).

A.   MDZ accumulation in Type I cells, with 100 mM (±)verapamil
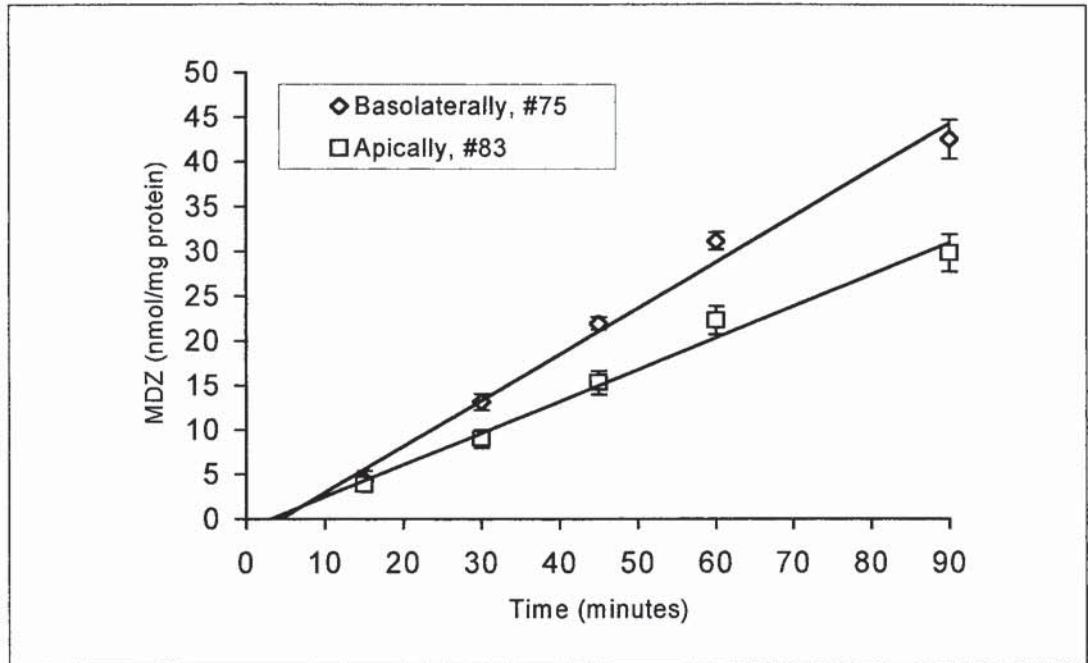
B.   MDZ accumulation in parent Caco-2 cells, with 100 mM (±)verapamil
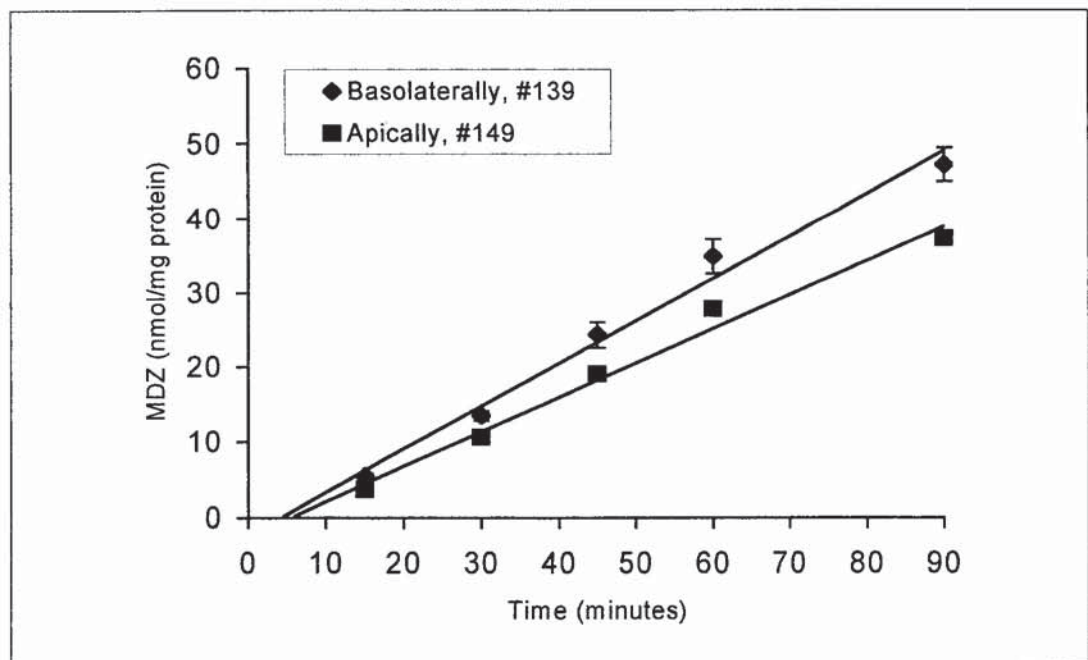
4-OH MDZ was only detected in the basolateral compartment of parent Caco-2 cells (rate of accumulation: 0.087 ± 0.004 nmol/min/mg protein) when MDZ was transported in the A-B direction (figure 5.24 A) in the absence of ($\pm$)verapamil. However, when MDZ was transported in the reverse (B-A) direction, 4-OH MDZ was accumulated in the apical chambers of both Type I and parent Caco-2 cells (values of 0.060 ± 0.007 and 0.156 ± 0.004 nmol/min/mg protein) (figure 5.24 A and B). Interestingly, its rate of accumulation in the apical chamber was almost twice as fast as that in the basolateral chamber in parent Caco-2 cells (figure 5.24 B). In the presence of ($\pm$)verapamil, no 4-OH MDZ was found in either chamber regardless of the direction of transport of MDZ (figure 5.25).

Transepithelial transport of fluorescein as a paracellular marker was run in parallel with MDZ for each experiment. Results in Table 5.1 indicate that there was no positive correlation between the transport of fluorescein and those of MDZ and 1-OH MDZ or 4-OH MDZ, indicating that MDZ, with a molecular weight of 342 and a calculated log P of 3.27 (Computer generated C logP, Biobyte Corp, CA, USA) diffuses transcellularly rather than paracellularly. Since the metabolites were formed intracellularly before they diffused out of the cells, their rates of accumulation were also unrelated to the fluorescein transepithelial flux.

In the absence of ($\pm$)verapamil, the rates of accumulation of 1-OH MDZ in the receiver compartments for both cell types were at least 4000-fold higher (table 5.1) than reported previously (75.9 pmol/min/g protein) [Schmiedlin-Ren et al., 1997], regardless of the direction of transport of the parent drug. Higher expression of cellular CYP3A4 at the protein level, relatively shorter experiments conducted in serum-free medium and direct analysis of the samples without any extraction may all contribute to the differences. Fisher et al., (1999b) reported that the formation of 1-OH MDZ (in pmol) in treated Caco-2 cells in serum-free, 1α, 25-dihydroxyvitamin D_3-free medium decreased with time, with the maximum formation at 2 hours. The results reported here were obtained from experiments conducted for 90 minutes.

FIGURE 5.24 **Accumulation of 4-OH MDZ after two weeks of treatment in**

Type I (A) and parent Caco-2 cells (B)

Parent (#139 and 149) and Type I (#75 and 83) Caco-2 cells were incubated with 4.0 μM MDZ with 100 μM (±)verapamil in M2 (pH 7.42) apically or basolaterally. A volume of 0.5 mL was withdrawn from either the apical or basolateral chamber at 15, 30, 45, 60 and 90 minutes and immediately replaced with fresh, equal volume. Results were expressed as nmol/mg protein (mean ± sd, n=3).

A.   4-OH MDZ accumulation in Type I cells
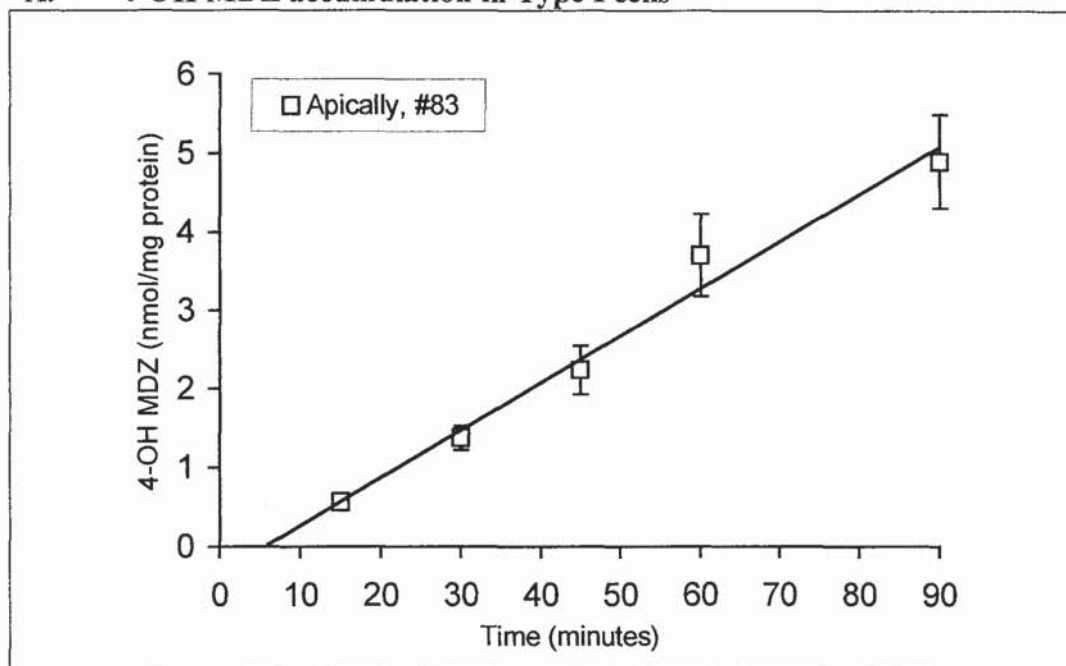
B.   4-OH MDZ accumulation in parent Caco-2 cells
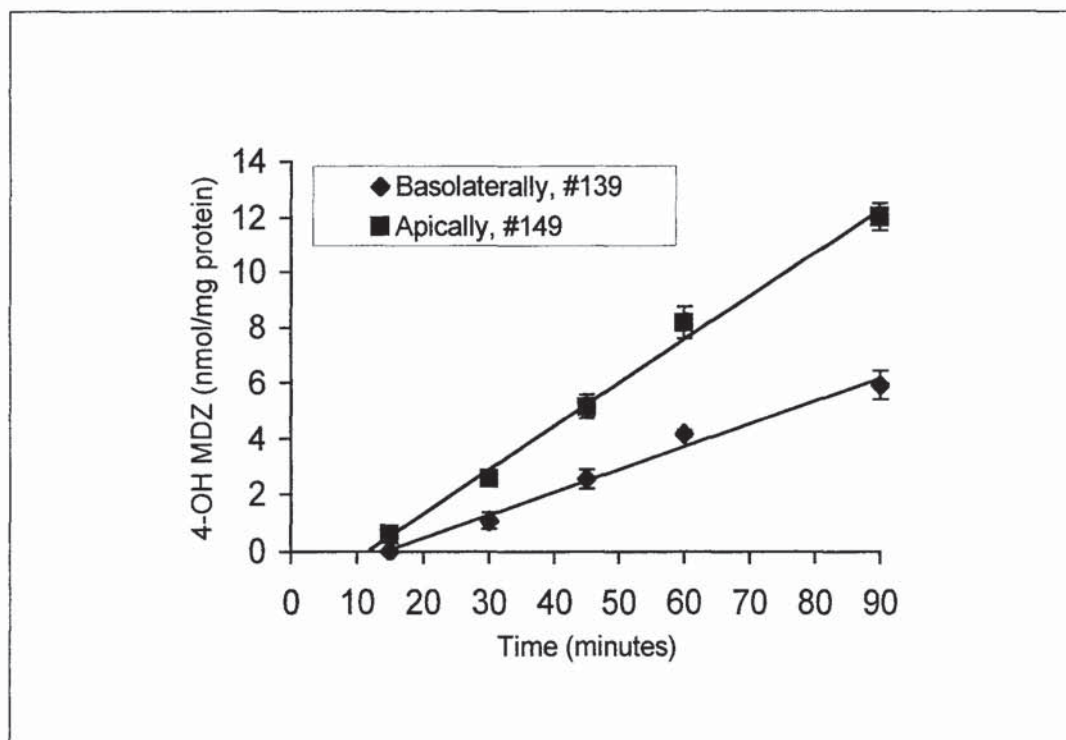
FIGURE 5.25 **Accumulation of MDZ metabolites at 90 minutes apically or basolaterally**
Parent (#139 and #149) and Type I cells (#75 and #83) were incubated with 4.0 μM midazolam in M2 (pH 7.42) apically or basolaterally. At 90 minutes post-incubation, the receiver phase was withdrawn and subjected to HPLC analysis. Results were expressed as MDZ metabolites (nmol/mg protein) in triplicate (mean ± sd). TI: Type I cells (#75 or 83); P: Parent Caco-2 cells (#139 or 149): V: 100 μM (±)verapamil; 1, 2, 3, 4: Basolateral accumulation; 5, 6, 7, 8: Apical accumulation
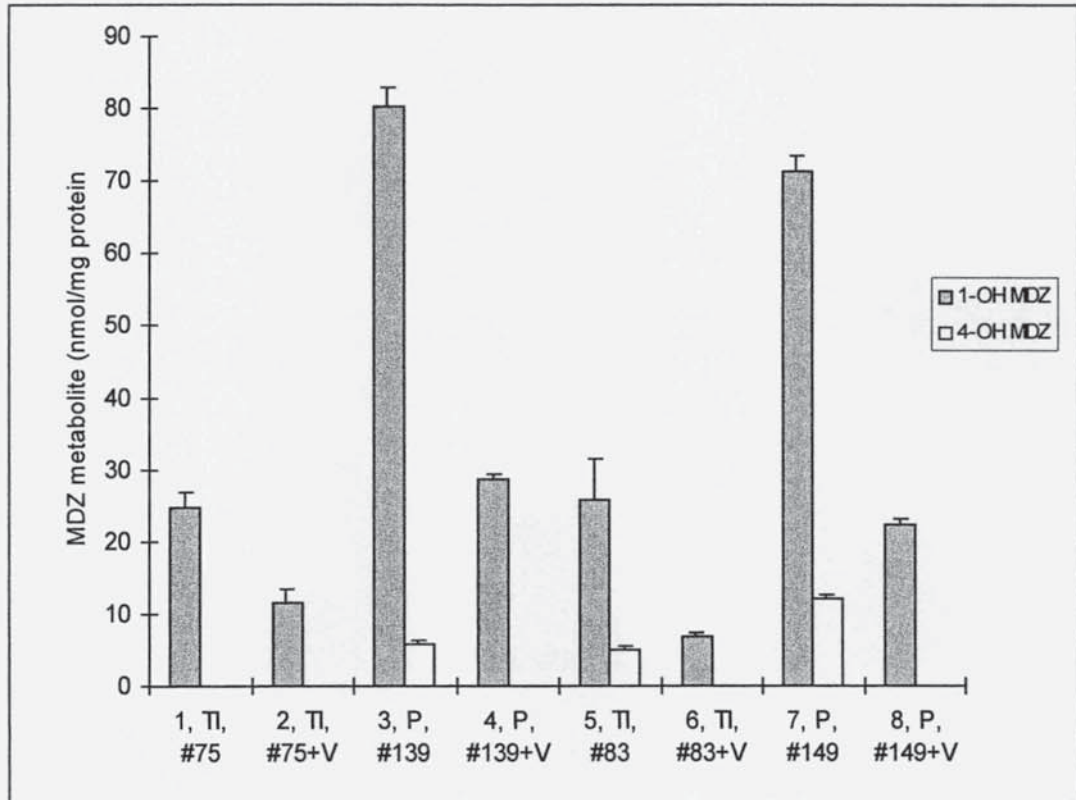
In theory, the rates of accumulation of MDZ metabolites in the receiver chamber depend on

(i)   the rate of diffusion of MDZ into the cells

(ii)   the rate at which it is metabolised intracellularly

(iii)   the rates at which MDZ metabolites diffuse into the receiver chambers and

(iv)   whether the metabolites are effluxed into the apical compartment by P-gp

MDZ binds extensively to extracellular protein as reported previously [Fisher *et al.*, 1999a]. The free fraction of MDZ in an experimental transport medium containing either 5%v/v FCS or 4g/mL human serum albumin after 4 hour incubation period was 3.3% of the original value [Fisher *et al.*, 1999a]. Binding of MDZ to human serum albumin in the receiver chamber elevated its concentration

gradient between the cells and the receiver compartment, therefore encouraging an accelerated diffusion through the cell monolayer and reducing its intracellular metabolism to about ~ 20% [Fisher *et al.*, 1999a]. Thus, the extensive metabolism of MDZ observed here was partly as a result of its abundant supply at the enzyme active sites in serum-free M2 transport medium.

The inter- and intra-variation of MDZ metabolism in humans was assessed by incubating it with microsomes, prepared from different sections of the intestinal mucosa of one foot long, that were sampled along the entire small intestine from six individuals. The median maximum rate of MDZ 1-hydroxylation decreased from the duodenum to jejunum to ileum (644 *vs.* 426 *vs.* 68 pmol/min/mg protein) [Paine *et al.*, 1997]. The rates of MDZ 1-hydroxylation reported in this chapter range from 257 ± 20 to 1057 ± 46 pmol/min/mg protein, in any direction of transport and in both cell types, accommodate for these reported *in vivo* values. This indicates that these two cell culture models, under conditions as described above, can be used to predict realistic *in vivo* metabolism of drug candidates by intestinal CYP3A.

Type I Caco-2 cells have been specifically cultured to distinguish and recognise any specific P-gp interactions (Chapter 4). Preferential apical accumulation of 4-OH MDZ indicates the involvement of P-gp in its distribution. This is supported, in part, by the fact that 4-OH MDZ apical accumulation was inhibited in the presence of ($\pm$)verapamil, a common substrate for both P-gp and CYP3A enzymes. In addition, the concentrations of cellular metabolites are more likely to equate to those in the receiver chambers. Passively diffused 1-OH MDZ had a much larger accumulation in the receiver chamber than its 4-OH metabolite (figure 5.28), implying a higher cellular concentration and yet, its accumulation was similar in both apical and basolateral chambers for both cell types. In contrast, 4-OH MDZ was preferentially sorted into the apical compartment, despite its much smaller concentration gradient. Therefore, the chance of 4-OH being accumulated apically by passive diffusion, preferentially (in Type I) or in a larger quantity found apically than that in the basolateral chamber in parent Caco-2 cells was highly unlikely.

Future experiments will involve the bi-directional transepithelial transport of 4-OH MDZ and 1-OH MDZ (as a control) through Type I cells in the presence and absence of (±)verapamil to confirm the above finding.

5.4   CONCLUSIONS

In conclusion, both cell models metabolise MDZ extensively (from a range of 257 ± 20 to 1057 ± 46 pmol/min/mg protein). Their spectrum of rates of cellular 1-hydroxylation of MDZ is similar to those observed using microsomes prepared from the human small intestine. Therefore, they can potentially be used as effective diagnostic tools of human origin for the studies of the interplay between efflux and intestinal metabolism as parts of the complex oral drug absorption process, and are useful predictive models for *in vitro-in vivo* drug metabolism and interactions.

CHAPTER SIX

THE EXPRESSION OF AMINO-ACID AND DI-/TRIPEPTIDE TRANSPORTERS IN DOXORUBICIN-EXPOSED CACO-2 CELLS*

ABSTRACT

The activities of the amino-acid and di-/tripeptide (DTS) transporters were assessed in Caco-2 cells that had been exposed to doxorubicin to enhance P-glycoprotein (P-gp) expression (Type I cells). With the same donor Gly-L-Pro concentration, the apparent permeability coefficient of Gly-L-Pro in non-exposed (parent) Caco-2 cells was more than triple that of doxorubicin-exposed (Type I) cells (25.041 ± 0.285 *vs*. 7.420 ± 0.166 x 10^{-5} cm/sec/mg protein). The presence of a DTS competitive inhibitor, SQ 29852, which markedly decreased Gly-L-Pro transport in the parent Caco-2 cells (Papp: 14.00 ± 0.724 x 10^{-5} cm/sec/mg protein), had little effect on that of Type I cells (Papp: 5.870 ± 0.161 x 10^{-5} cm/sec/mg protein).

Similarly, the apparent permeability coefficient of L-Pro in parent Caco-2 cells was one and a half times that in Type I Caco-2 cells (Papp of 24.223 ± 0.837 x 10^{-5} *vs*. 16.800 ± 0.546 x 10^{-5} cm/sec/mg protein respectively). The presence of 1 mM L-alanine decreased the cellular accumulation of L-Pro in both cell types.

In conclusion, Caco-2 cells with enhanced P-gp expression and/or activity (Type I cells) possessed a decreased cellular activity of other membrane transporters, namely the amino acid and di-/tripeptide transporters.

6.1 INTRODUCTION

The amino-acid transporters are transmembrane proteins with different amino-acid compositions and numbers of membrane-spanning domains depending on their types. For examples, it was shown that basic amino-acids such as lysine, arginine and orthinine were transported by a basic amino-acid transporter which had 662 amino acid residues and was predicted to have 14 hydrophobic membrane-spanning domains in *Xenopus laevis* oocytes [Wang *et al.*, 1991]. In contrast, a cDNA for rabbit intestinal Na^+-dependent glutamate transporter, referred to as EAAC1 was isolated and shown to encode a 524 amino-acid protein, was predicted to have 10 membrane-spanning domains [Hediger *et al.*, 1995]. Of relevance in this chapter is the intestinal imino-acid system which under physiological conditions, accepts exclusively imino-acids such as proline, hydroxyproline and N-methylamino-isobutyric acid and requires inwardly directed Na^+ and Cl^- gradients as the driving forces [Ganapathy *et al.*, 1994]. In human foetal jejunal and ileal brush border membrane vesicles, the uptake of L-Pro was mediated by the imino-acid system and stimulated in the presence of an inward Na^+-gradient although a small, non-specific accumulation of L-Pro was also observed [Stevens *et al.*, 1984; Malo *et al.*, 1991]. Similarly, its uptake in the brush border membrane vesicles prepared from the guinea pig ileum was Na^+-dependent and increased with increasing concentration of Na^+ ions in the external medium [Hayashi *et al.*, 1980]. Recently, functional expression of the rabbit intestinal Na^+/L-proline cotransporter had been demonstrated in *Xenopus laevis* oocytes [Urdaneta *et al.*, 1998]. This imino-acid transport system transported L-proline and 4-hydroxyproline but not L-alanine, neither cationic nor anionic amino-acids. In the absence of Na^+ ions, there was no uptake of L-proline. Its uptake was also inhibited in the presence of 4-hydroxyproline [Urdaneta *et al.*, 1998].

The amino-acid transporter for L-Pro (the structure is shown in table 6.1) in Caco-2 cells shares some similar characteristics with those of the mamalian intestinal imino-acid transporter. L-Proline uptake into Caco-2 cells is Na^+-dependent and reduced when Na^+ transport is inhibited [Nicklin *et al.*, 1992]. However, the transporter also shows some differences such as its strong binding affinity to amino-acids such as L-alanine, L-serine and α-aminoisobutyric acid and to others such as glycine, D-proline, valine and γ-aminoisobutyric acid of varying affinities. This indicates that the L-Pro amino-acid transporter in Caco-2 cells has

similar features with the A amino-acid transport system [Nicklin *et al.*, 1992]. The A (alanine preferring system) transports dipolar α-amino and imino-acids and their translocation is dependent on Na^+ gradient [Ganapathy *et al.*, 1994]. The efficiency of the amino-acid transporter is reduced when cellular protein synthesis and metabolism are inhibited [Nicklin *et al.*, 1992].

At the nanomolar concentration range, the active uptake of L-Pro by the amino-acid transporter in Caco-2 cells accounted for about two third of the total uptake (at 37°C and pH 7.4). Surprisingly, its uptake was also dependent on the concentration gradient of H^+ ions between the cells and the external medium with maximum uptake being observed at an external pH 5.0 [Nicklin *et al.*, 1992]. Vectorial transport (apical-to-basolateral) of L-Pro across the Caco-2 monolayers, was also H^+-coupled and was enhanced in the presence of an external apical acidic (pH 6.0) condition [Thwaites *et al.*, 1993c]. It was also demonstrated that its uptake into Caco-2 cells was accompanied by a rise of intracellular pH [Thwaites *et al.*, 1993c].
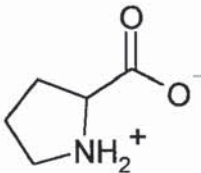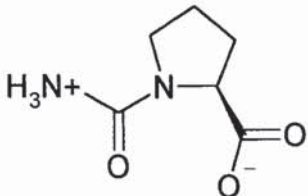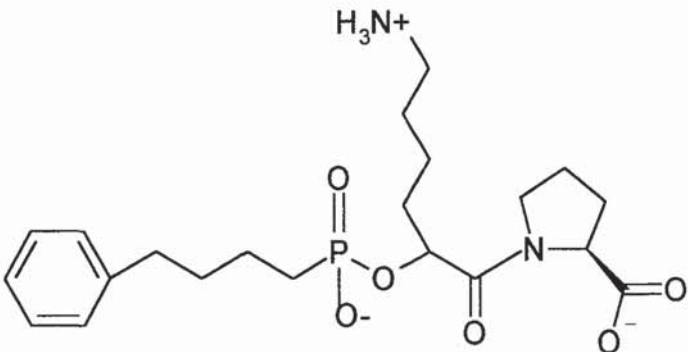
The coupling of the di-/tripeptides to H^+ rather than Na^+ by the di-/tripeptide transporter (DTS) is an important distinction between intestinal peptide transport and amino acid transport [Ganapathy and Leibach, 1985]. A H^+-coupled peptide transporter, PepT1 had been cloned from rabbit and human intestine [Fei *et al.*, 1994; Liang *et al.*, 1995]. The cDNA encodes 707 and 708 amino-acid residues for rabbit and human PepT1, respectively, with twelve putative membrane-spanning regions and an unusually large hydrophilic loop having several N-glycosylation sites. The transport of [^{14}C]Glycylsarcosine by human PepT1 in *Xenopus laevis* oocytes was enhanced in the presence of an inwardly directed H^+-gradient and was associated with an intracellular acidification [Liang *et al.*, 1995].

In addition to the transport of di-/tripeptides, that of other substrates such as the peptidomimetic drugs angiotensin-converting enzyme inhibitors (ACE inhibitors) captopril, lisinopril and SQ 29852 was also mediated by the DTS system in rat intestine [Hu and Gordon, 1988; Friedman and Amidon, 1989]. The absorption of L-Glycylproline (Gly-L-Pro) and SQ 29852 (the structures of which are shown in table 6.1) have been shown to be mediated by the DTS in Caco-2 cells [Nicklin *et al.*, 1996; Moore *et al.*, 1996; Morrison *et al.*, 1996]. Uptake of Gly-L-Pro into Caco-2 cells is concentration dependent (Km = 0.19 mM and Vmax = 0.29 µmol/min) [Moore *et al.*, 1996] and inhibited by SQ 29852 [Chong *et al.*,

1996]. Cellular uptake of SQ 29852 is mediated by a major saturable pathway (Km = 0.91 ± 0.11 mM, ~ 90% at 1 mM) and a minor passive component (k_d = 32.3 ± 6.6 ng/10^6 cells/20 min) and is inhibited by other dipeptides such as L-Ala-L-Pro (Ki = 2.96 mM) and L-Phe-Gly (Ki = 3.84 mM) but not by cephalosporins such as cephalexin. In contrast, SQ 29852 transport from the cells to the basolateral medium is retarded such that the passive paracellular route controls the overall transepithelial transport which results in the latter being non-saturable and increases with increasing apical concentration of SQ 29852 [Nicklin et al., 1996].

The objective of this chapter was to characterise and assess the expression of active amino-acid and DTS transporters in Caco-2 cells that have been continuously exposed to doxorubicin to enhance P-glycoprotein (P-gp) expression. The results contribute to the overall characterisation of a higher P-gp-expressing Caco-2 cell line as described in chapter 4.

TABLE 6.1   **Structures of L-Pro, Gly-L-Pro and SQ 29852**

| L-Pro |
| Gly-L-Pro |
| SQ 29852 |

142

6.2 MATERIALS AND METHODS

6.2.1 MATERIALS

[^{3}H]Gly-L-Pro, [^{3}H]L-Pro, D-[^{14}C]mannitol and SQ 29852 were as described in section 2.1.2. Non-radioactive L-alanine, L-proline and Gly-L-Pro were purchased from Sigma (Poole, UK). All other materials that were required for the transport medium are as described in section 2.1.2.

6.2.2 METHODS

6.2.2.1 CELL CULTURE

Type I Caco-2 cells and those of passage number >90 (parent Caco-2 cells) were cultured on clear Costar™ polyester inserts at a density of 85,000 cells/cm^2. The cells were maintained in cell culture medium M1 (section 2.2.1.1) which was changed every other day. They were used for experiments at three weeks post-seeding.

6.2.2.2 TRANPORT STUDIES OF L-PRO AND GLY-L-PRO

The transport studies of Gly-L-Pro and L-Pro were described previously (sections 2.2.4.3 and 2.2.4.4). Transported quantities were expressed as pmol/mg protein (mean ± sd, n = 3).

6.3 RESULTS AND DISCUSSION

The objective of this chapter was to assess the activities of the amino-acid and di-/tripeptide (DTS) transporters in Caco-2 cells that had been exposed to doxorubicin to increase P-glycoprotein expression. The assessment was made by direct comparison of the transepithelial transport of an imino-acid, L-Proline (L-Pro) and a dipeptide, L-Glycylproline (Gly-L-Pro), between non-exposed (parent) and exposed (Type I) Caco-2 cells.

6.3.1 TRANSEPITHELIAL TRANSPORT AND CELLULAR ACCUMULATION OF GLY-L-PRO

The uptake of both L-Pro and Gly-L-Pro have been shown to be carrier-mediated in Caco-2 cells [Nicklin *et al.*, 1992; Moore *et al.*, 1996]. Caco-2 cells actively transported L-Pro across the apical cell membrane with a Km value of 5.28 mM [Nicklin *et al.*, 1992], therefore inclusion of 10 mM of non-radiolabelled L-Pro in the apical chamber in the presence of the transported substrate, [^{3}H]Gly-L-Pro, ensured saturation of the amino-acid carrier and hence, any radioactivity detected in the basolateral chamber was likely to reflect the transport of intact dipeptide molecules.

Linear increases in the transepithelial transport rates of Gly-L-Pro were observed in both parent and Type I Caco-2 cells over 30 minutes (figure 6.1). The calculated apparent permeability coefficients were $25.041 \pm 0.285 \times 10^{-5}$ cm/sec/mg protein (parent cells) and $7.420 \pm 0.166 \times 10^{-5}$ cm/sec/mg protein (Type I cells), indicating that Gly-L-Pro transport in the parent cells was more than three times that in Type I Caco-2 cells (table 6.1). However, the quantity of Gly-L-Pro transported by the paracellular route might vary due to cellular batch-to-batch variation, and that could under/overestimate the contribution of the DTS towards the observed transepithelial permeation coeffiecient of Gly-L-Pro. Figure 6.2 shows a higher transepithelial flux of a paracellular marker, mannitol, in the parent Caco-2 cells ($3.114 \pm 0.087 \times 10^{-5}$ vs. $1.530 \pm 0.085 \times 10^{-5}$ cm/sec/mg protein respectively). Different cell monolayers on permeable inserts were formed from heterogeneous cell colonies which might display different permeabilities to mannitol transport as observed in figure 6.2. However, the surface area represented by the tight junctional complexes for passive diffusion of Gly-L-Pro is relatively much smaller than that contributed to the total surface area of the monolayer by the cells themselves. Therefore, the reduced transport of Gly-L-Pro in Type I cells was likely to be due to a decreased DTS activity. The presence of 1 mM SQ 29852 reduced the transport of Gly-L-Pro in the parent cells to nearly half its original value (Papp: $14.000 \pm 0.742 \times 10^{-5}$ cm/sec/mg protein) whereas that of Type I cells was slightly decreased (Papp: $5.870 \pm 0.161 \times 10^{-5}$ cm/sec/mg protein) (figure 6.1 and table 6.2). This could be due to a decrease in Gly-L-Pro uptake in the presence of a DTS inhibitor, SQ 29852, which resulted in a decrease transport. Indeed, cellular Gly-L-Pro accumulation after 30 minutes of its transepithelial

transport was significantly decreased ($p < 0.05$) in the presence of SQ 29852 (to ~ 42% and ~23% of the original values in parent and Type I Caco-2 cells) (figure 6.3). In the absence of SQ 29852, cellular accumulation of Gly-L-Pro in parent and Type I Caco-2 cells was 12.845 ± 0.521 and 3.044 ± 0.201 pmol/mg protein respectively after 30 minutes of transport (figure 6.3), implying a higher DTS activity in the parent cells. Washing the cells twice before cellular solubilisation reduced the non-specific binding of Gly-L-Pro to the cellular surface from 5.0 –9.0 (1st wash) to 1.2-1.8 pmol/mg protein (2nd wash), (figures 6.4 and 6.5), demonstrating that one wash could reduce ~76-80% non-specifically bound Gly-L-Pro to the cell surface. Thus, much higher radioactivity found with solubilised cells than that associated with the 2nd wash was most likely attributed to Gly-L-Pro binding tightly to the DTS or found within the cells which was therefore could not be washed off as in the case of non-specifically adsorbed Gly-L-Pro.

TABLE 6.2 Apparent permeability coefficients of Gly-L-Pro and mannitol in parent and Type I Caco-2 cells

Parent (#143) and Type I Caco-2 cells (#78) were incubated with 50 nM [^{3}H]Gly-L-Pro and 1 μM D-[^{14}C]mannitol with and without 1 mM SQ 29852 in the apical chamber. Transport of Gly-L-Pro was conducted at 37°C along a pH gradient (apical pH: 6.0 and basolateral pH: 7.4). Results were expressed as cm/sec/mg protein, mean ± sd, n=3. Asterisks (*, **) denote significant difference (p<0.05 and p<0.01) between Papp of Gly-L-Pro in the absence of SQ 29852 of parent cells *vs.* those achieved under each set of conditions as outlined in the table (One-way ANOVA with Dunnett multiple comparison post-test).

Compound	Cell type	1mM SQ 29852	Papp x 10^5 (cm/sec/mg protein)
Gly-L-Pro	#143	-	25.041 ± 0.285
		+	14.00 ± 0.724**
	Type I, #78	-	7.420 ± 0.166**
		+	5.870 ± 0.161**
Mannitol	#143	-	3.114 ± 0.087
		+	1.820 ± 0.036**
	Type I, #78	-	1.530 ± 0.085**
		+	1.220 ± 0.081**

146

FIGURE 6.1 **Transepithelial transport of Gly-L-Pro with/out 1mM SQ 29852**

Gly-L-Pro (50 nM) was transported from the apical chamber (apical pH: 6.0 and basolateral pH: 7.4). Results were expressed as pmol/mg protein, mean ± sd, n=3.
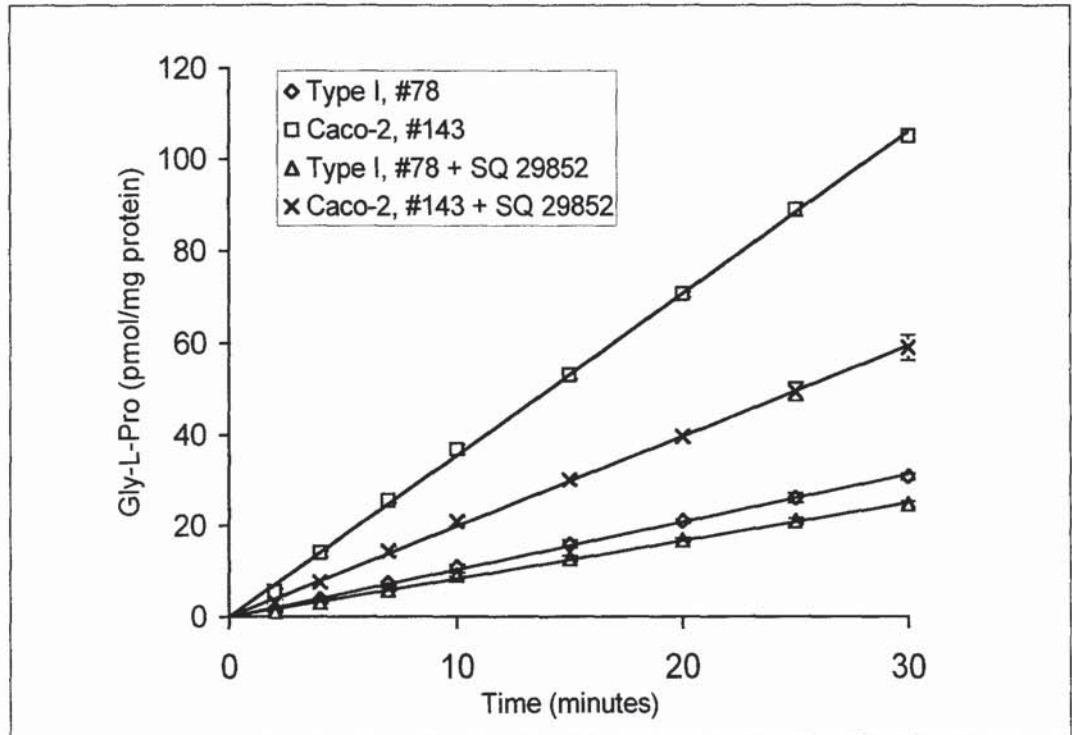
FIGURE 6.2 **Transepithelial transport of mannitol**

Results are expressed as pmol/mg protein, mean ± sd, n=3.
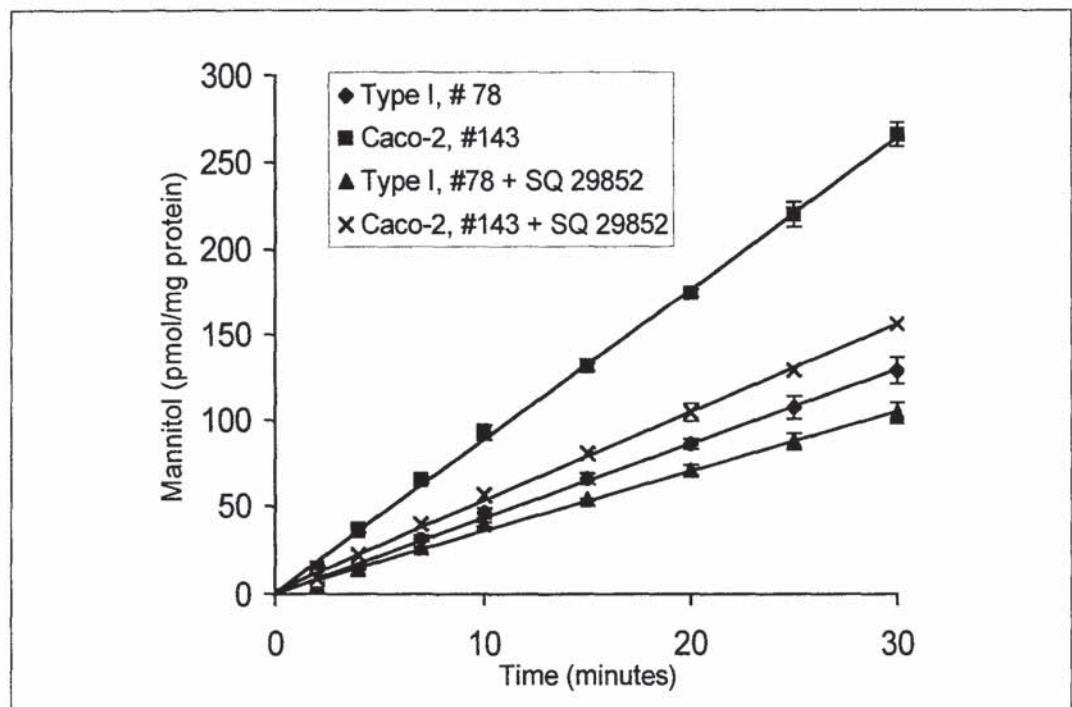
FIGURE 6.3 Cellular accumulation of Gly-L-Pro after 30 minutes

Caco-2 cells were incubated with 1% v/v Triton-X 100 at 37°C overnight after sodium azide washes. Results are expressed as amounts of Gly-L-Pro, pmol/mg protein, mean ± sd, n=3. Asterisk (*) denotes significant difference ($p < 0.05$) between Gly-L-Pro accumulation in Caco-2 cells, #143 *vs.* those obtained under each set of experimental conditions as stated in chart (One-way ANOVA with Dunnett multiple comparison post-test).
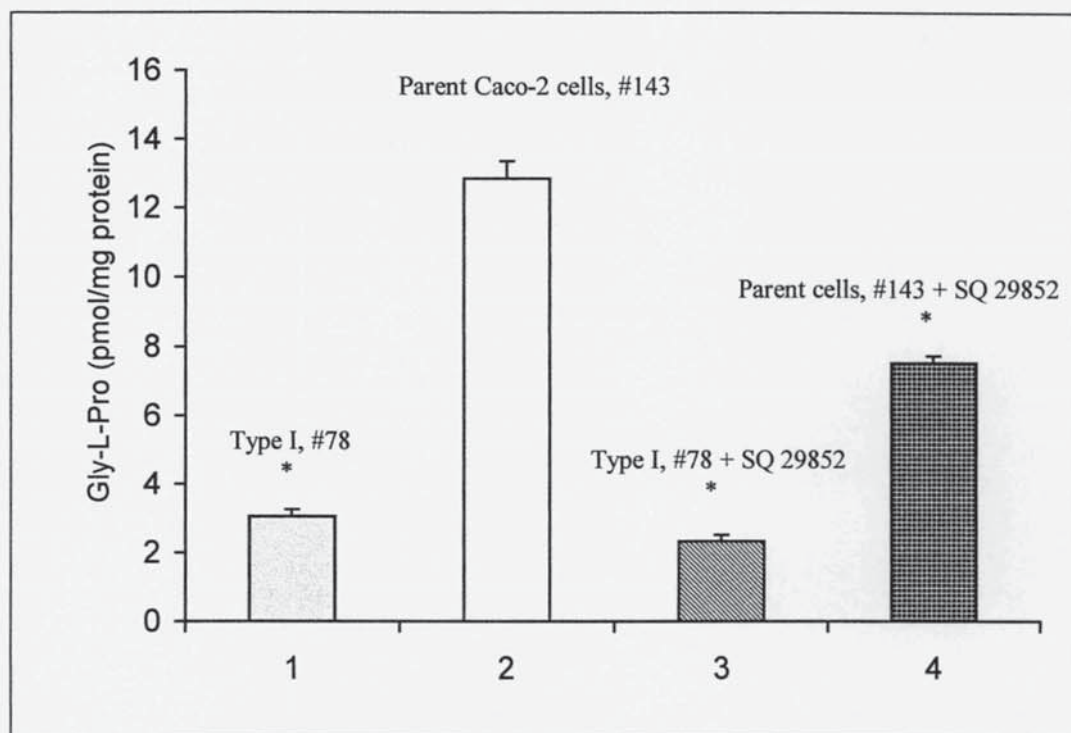
FIGURE 6.4 Gly-L-Pro associated with 1st sodium-azide (0.05%w/v) wash
At the end of the experiment, Caco-2 cells were washed twice from both the apical and basolateral chambers with ice–cold sodium azide (0.05% w/v). Results are expressed as amounts of Gly-L-Pro, pmol/ mg protein, mean ± sd, n=3.
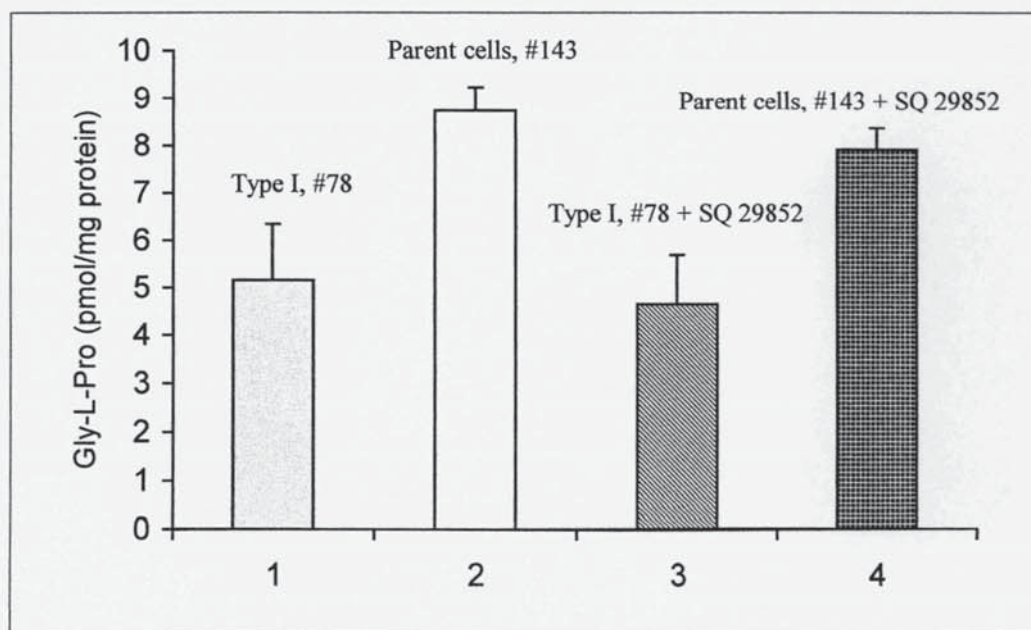
FIGURE 6.5 **Gly-L-Pro associated with 2nd sodium-azide (0.05%w/v) wash**
Results are expressed as amounts of Gly-L-Pro, pmol/mg protein, mean ± sd, n=3.
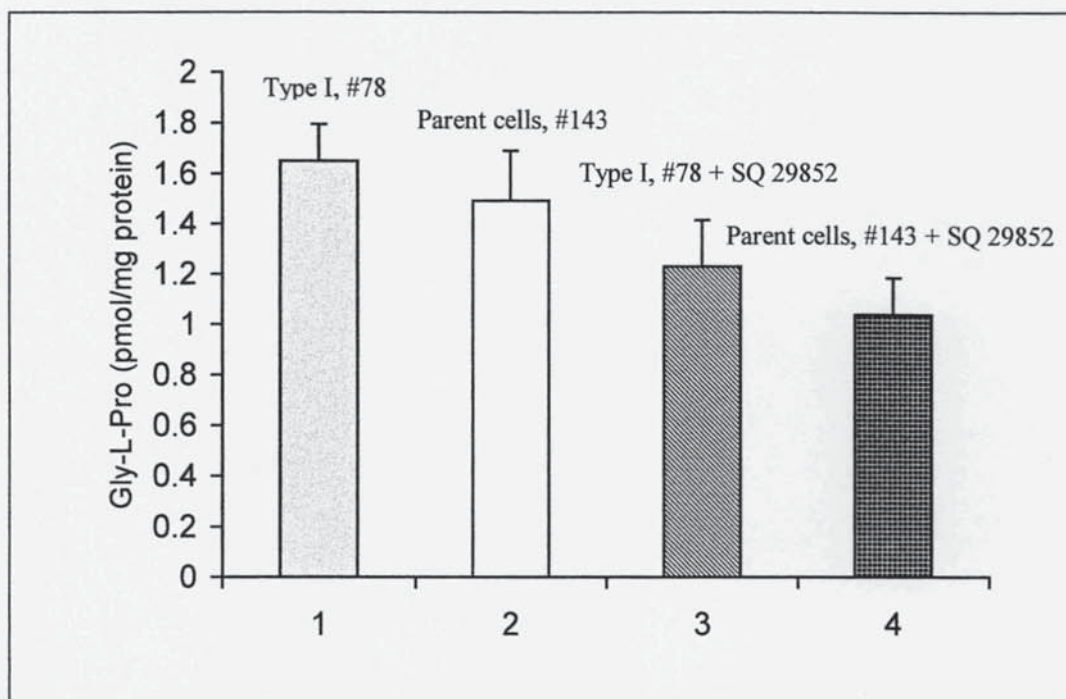
6.3.2 TRANSEPITHELIAL TRANSPORT AND CELLULAR ACCUMULATION OF L-PRO IN CACO-2 CELLS

Linear transepithelial transport of L-Pro was observed in both cell types over 30 minutes. Faster L-Pro transport was seen in parent Caco-2 cells compared with that in Type I cells (a value of 24.223 ± 0.837 x 10^{-5} *vs.* 16.800 ± 0.546 x 10^{-5} cm/sec/mg protein) (figure 6.6, table 6.3). The result could be partly attributed to a higher paracellular flux of L-Pro in the parent cells which displayed a higher mannitol transepithelial permeability than Type I cells (figure 6.7). However, based on the argument raised in section 6.3.1, higher transport of L-Pro in parent Caco-2 cells was most likely due to its higher activity of the amino-acid transporter. The presence of 1 mM L-alanine decreased L-Pro permeability to 11.400 ± 0.572 x 10^{-5} and 15.600 ± 0.256 x 10^{-5} cm/sec/mg protein respectively (figure 6.8) in parent and Type I cells respectively whilst mannitol fluxes also decreased as a result of batch to batch cellular variation (figure 6.9). Cellular accumulation studies revealed that the presence of L-alanine decreased the accumulation of L-Pro from 17.644 ± 0.731 to 13.894 ± 0.326 pmol/mg protein in parent cells (figure 6.10). Cellular accumulation of L-Pro in Type I cells with or without the presence of L-alanine was significantly lower than that in the parent

cells (p<0.05) (figure 6.10), implying a decreased activity of the amino-acid transport system in Type I compared with parent cells. Washing the cell monolayers twice resulted in a decrease in non-specific binding of L-Pro from ~ 5-9 pmol/mg protein (1st wash) to ~ 2-5 pmol/mg protein (2nd wash) (figures 6.11 and 6.12).

Brasitus *et al.*, (1989) reported that the change in membrane fluidity as a consequence of fatty acid composition was associated with kinetic changes in D-glucose transport by rat proximal intestinal membrane vesicles. The insertion of extra twelve-transmembrane domains P-glycoprotein molecules in the cell membrane of doxorubicin-exposed Caco-2 cells might affect the membrane fluidity which in turn affected the activity of the cellular amino-acid transport system. Alternatively, selection and/or induction of heterogeneous Caco-2 cells with doxorubicin as described in chapter 4 simply selected out colonies of cells with enhanced P-gp activity and/or expression but with lower activity of the di-/tripeptide and amino-acid transporters.

TABLE 6.3   **Apparent permeability coefficients of L-Pro and mannitol in parent and Type I Caco-2 cells**

Parent (#143 and #155) and Type I Caco-2 cells (#78 and #88) were incubated with 50 nM [^{3}H] L-Pro and 1 μM D-[^{14}C]mannitol with and without 1 mM L-alanine in the apical chamber. Transport of L-Pro was conducted at 37°C along a pH gradient (apical pH: 6.0 and basolateral pH: 7.4. Results were expressed as cm/sec/mg protein, mean ± sd, n=3. Asterisks (*, **) denote significant difference (p<0.05 and p<0.01) between Papp of L-Pro in the absence of L-alanine of Caco-2 cells, #143 *vs.* those achieved under each set of conditions as outlined in the table (One-way ANOVA with Dunnett multiple comparison post-test).

Compound	Cell type	1mM L-alanine	Papp x 10^5 (cm/sec/mg protein)
L-Pro	#143	-	24.223 ± 0.837
		+	11.400 ± 0.572**
	Type I, #78	-	16.800 ± 0.546**
		+	15.600 ± 0.256**
Mannitol	#143	-	2.594 ± 0.130
		+	0.817 ± 0.085**
	Type I, #78	-	1.850 ± 0.083**
		+	1.050 ± 0.025**

FIGURE 6.6 **Transepithelial transport of L-Pro**
L-Pro (50 nM) was transported from the apical chamber, apical pH: 6.0 and basolateral pH: 7.4. Results were expressed as pmol/mg protein, mean ± sd, n=3.
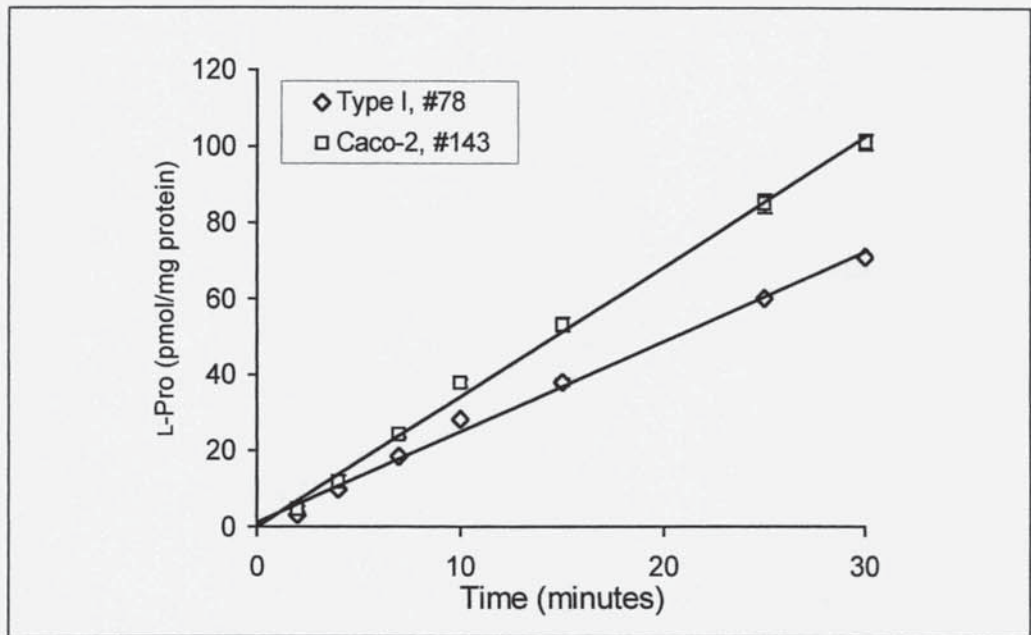


FIGURE 6.7 **Transepithelial transport of mannitol**
Mannitol (1 μM) was transported from the apical chamber, apical pH: 6.0 and basolateral pH: 7.4, in the presence of 50 nM [^{3}H]L-Pro. Results were expressed as pmol/mg protein, mean ± sd, n=3.
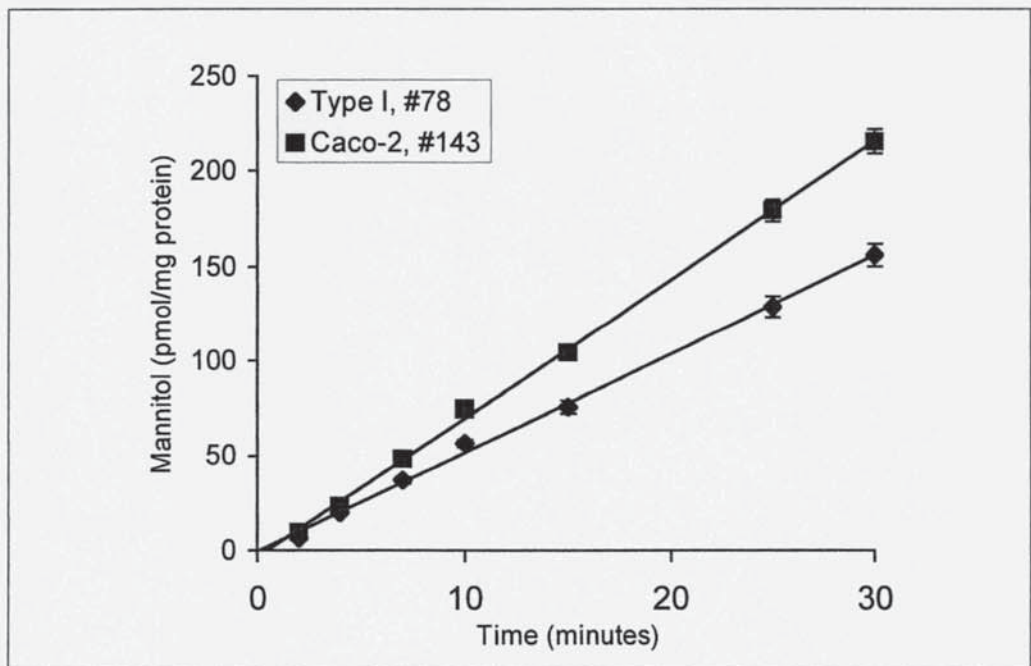
FIGURE 6.8   **Transepithelial transport of L-Pro with 1 mM L-alanine**
L-Pro (50 nM) was transported in the presence of 1mM L-alanine, apical pH: 6.0
and basolateral pH: 7.4. Results were expressed as pmol/mg protein, mean ± sd,
n=3.
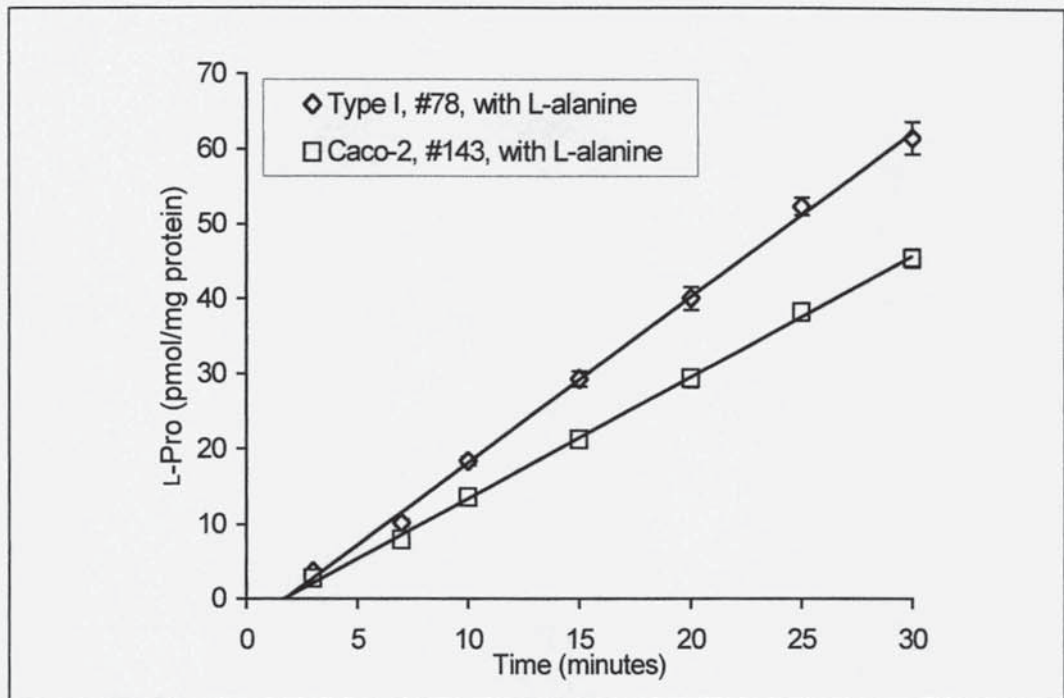
FIGURE 6.9   **Transepithelial transport of mannitol with 1mM L-alanine**
Mannitol (1 μM) was transported with 1 mM L-alanine and 50 nM [^{3}H]L-Pro,
apical pH: 6.0 and basolateral pH: 7.4. Results were expressed as pmol/mg
protein, mean ± sd, n=3.
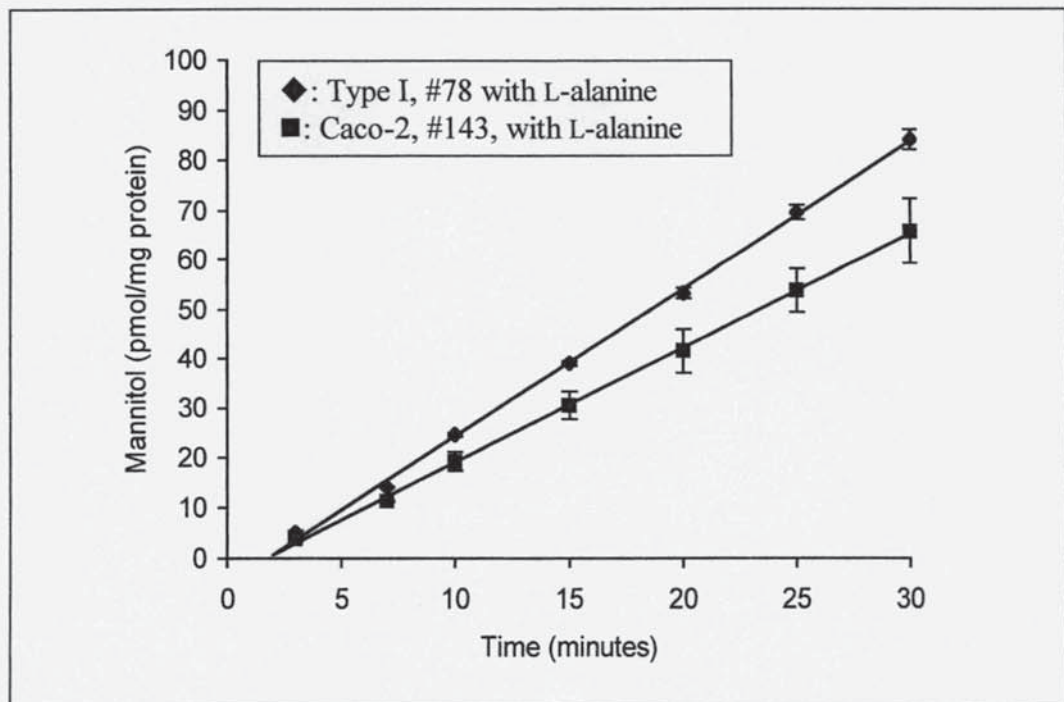
FIGURE 6.10 **Cellular accumulation of L-Pro after 30 minutes**
Caco-2 cells were incubated with 1% v/v Triton-X 100 at 37°C overnight after two sodium azide washes. Results are expressed as L-Pro (pmol/mg protein), mean ± sd, n=3. Asterisk (*) denotes significant difference ($p < 0.05$) between L-Pro accumulation in Caco-2 cells, #143 *vs.* those obtained under each set of conditions as stated in chart (One-way ANOVA with Dunnett multiple comparison post-test).
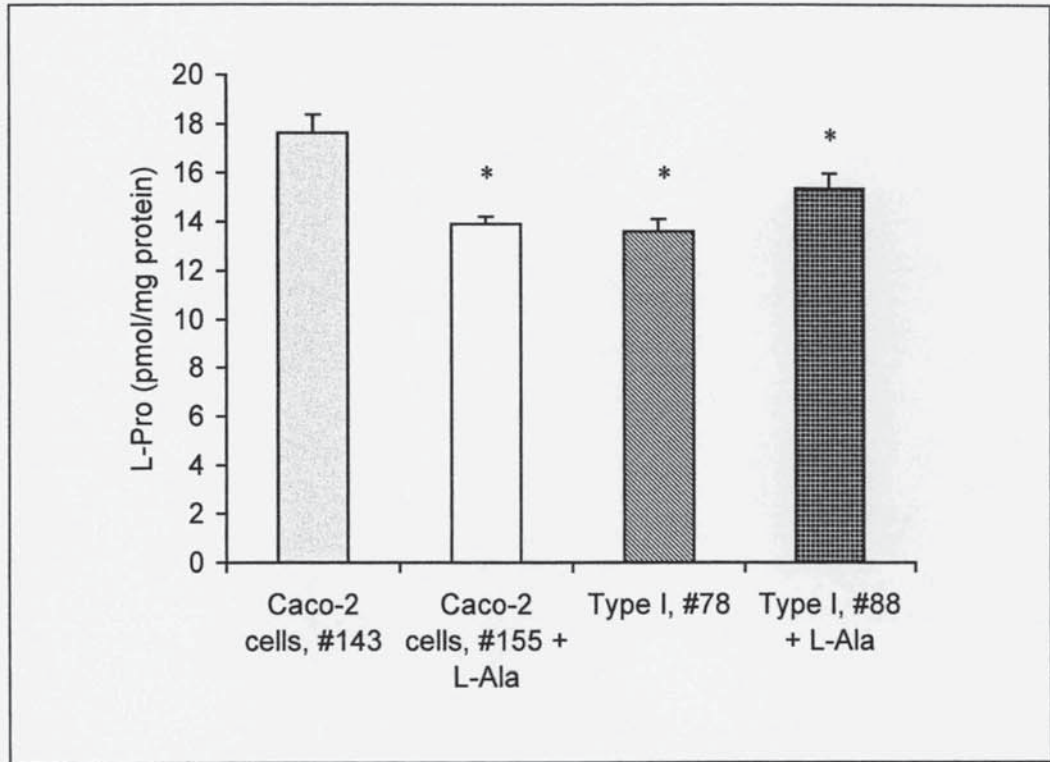
FIGURE 6.11 **L-Pro associated with 1st sodium-azide (0.05%w/v) wash**
At the end of the experiment, Caco-2 cells were washed twice from both the apical and basolateral chambers with ice–cold sodium azide (0.05% w/v). Results are expressed as amounts of L-Pro (pmol/ mg protein of cells), mean ± sd, n=3.
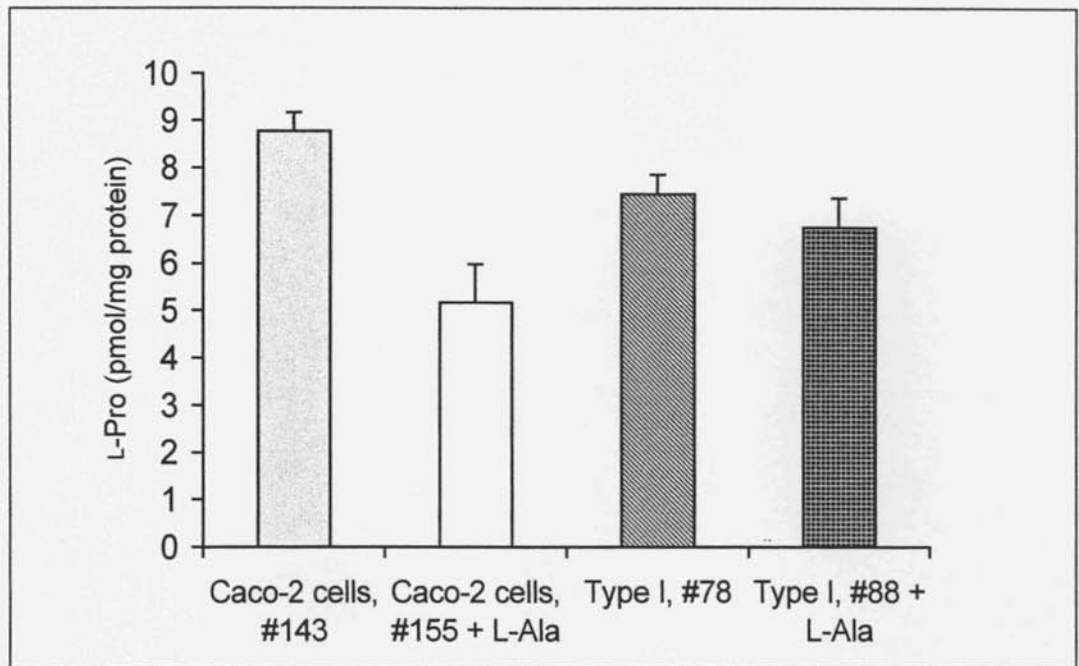
FIGURE 6.12 **L-Pro associated with 2nd sodium-azide (0.05%w/v) wash**
Results are expressed as amounts of L-Pro (pmol/ mg protein of cells), mean ± sd, n=3.
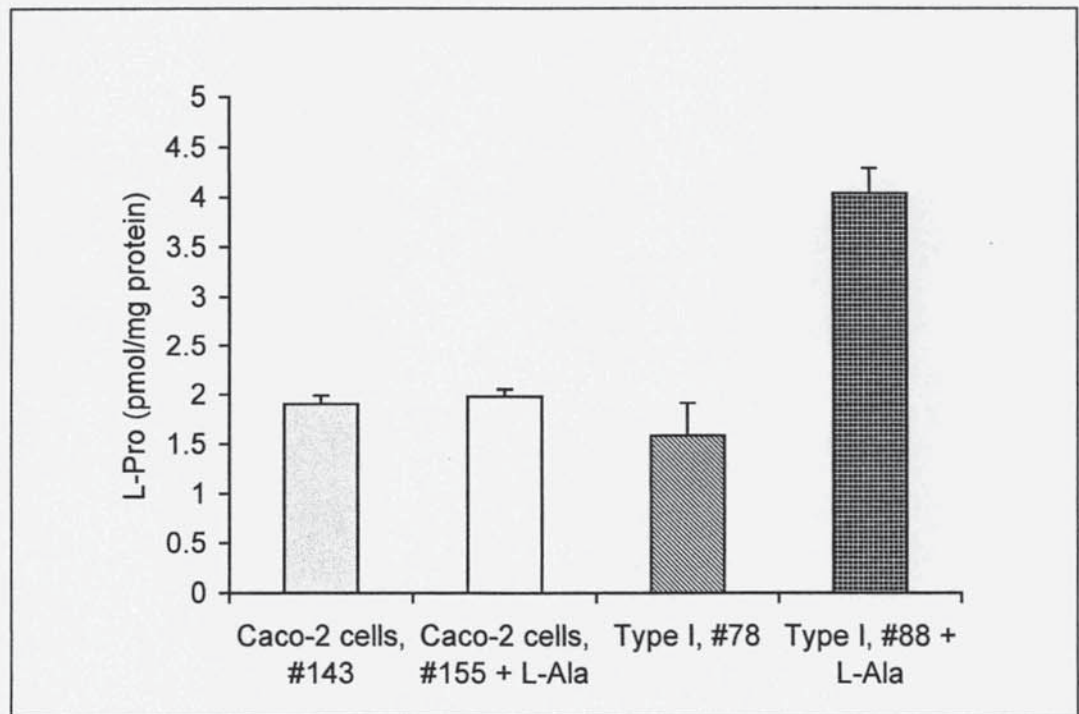
6.4 CONCLUSIONS

Although Type I Caco-2 cells were useful in the recognition of drug candidate-P-gp interactions, their enterocyte-like characteristics diminish as reflected by a lower DTS and amino-acid transport activity. This indicates the need for different cell culture systems to confidently model the interactions between the chemical compounds and cell membrane proteins accordingly, in the process of high throughput screening of new chemical entities.

CHAPTER SEVEN

CONCLUSIONS

ABSTRACT

In this chapter, the heterogeneity of the Caco-2 cell model and its applications in intestinal efflux and phase I metabolism studies are discussed.

The heterogeneity of Caco-2 cells [Artursson *et al.*, 1991] leads to their variable phenotypic characteristics which affect the reproducibility between different research groups. This heterogeneous nature is further potentiated by various protocols used to maintain stock cultures which undoubtedly lead to the prevalent formation of different sub-populations of Caco-2 cells. Whilst this variation makes data extrapolation from one laboratory to another difficult, it gives rise to the opportunistic formation of different populations of cells with different levels of expression of:

(i)   alkaline phosphatase

(ii)   P-glycoprotein, and

(iii)   different activities of the di-/tripeptide transporter (Chapter 3)

Based on their characteristics, Caco-2 cells can be chosen rationally

(i)   to suit the drug screening and interactions of different groups of orally-administered compounds absorbed by different mechanisms, or

(ii)   for further development of the cell model.

Highly P-gp expressing Caco-2 cells have been developed through stepwise selection of the cells of passage number >90 (from Novartis) with doxorubicin (Chapter 4). This newly-developed cell line (Type I) possessed approximately twice as much P-gp protein than the non-exposed cells (a value of 213 ± 54.35 % *vs.* 100 ± 16.05 %; section 4.3.1). Functional studies of P-gp in the doxorubicin-exposed Caco-2 cells revealed that they restricted the transepithelial transport of vincristine in the apical-to basolateral direction whilst facilitating its transport in the reverse direction more effectively than the non-exposed cells (section 4.3.2 and table 4.1). Moreover, they accumulated less vincristine than the non-exposed cells (272.89 ± 11.86 *vs.* 381.39 ± 61.82 fmol/mg protein, section 4.3.4). There was no apparent evidence of the co-existence of another member of the ATP-binding drug efflux pumps, the multidrug resistance protein (MRP), in doxorubicin-exposed (Type I) cells to account for the above-listed observations (section 4.3.2). Stopping exposing Type I cells to doxorubicin for more than 28 days decreased their expression of P-gp protein (a value of 135 ± 20.03 % *vs.* 100 ± 13.34% of non-exposed cells; section 4.3.1). In addition, discontinuous doxorubicin exposure resulted in little variances in the transepithelial fluxes of vincristine in both directions in previously exposed-cells compared with those of non-exposed cells (section 4.3.2 and table 4.1).

Due to the overlapping substrates and the co-location of P-gp and a Phase I-metabolising enzyme, cytochrome P450 3A4 (CYP3A4) in the intestinal epithelial cells, it has been proposed that they might function synergistically to limit the absorption of xenobiotics [Watcher et al., 1995]. The possibility of the co-ordinated regulation of CYP3A and P-gp gene expression in cancer cells has also been raised. This is due to the close proximity of their gene loci on the chromosomes and the observation that CYP3A4 possesses a p53 binding motif whilst binding of a p53 tumour suppressor gene down-regulates P-gp production [Watcher et al., 1995]. Increased CYP3A4 protein expression in Caco-2 cells has been demonstrated by exposing them to 0.25 μM 1α, 25-dihydroxyvitamin D$_3$ (an expression of 76.2 ± 7.6 vs. 14.96 ± 8.008 pmol/mg protein of non-exposed control cells) (section 5.3.2). Doxorubicin-exposed (Type I) cells that had been treated with 0.25 μM 1α, 25-dihydroxyvitamin D$_3$ metabolised midazolam poorly and less extensively than non-exposed cells that had been treated with the same conditions, suggesting that there was no such co-regulation of P-gp and CYP3A4 in Caco-2 cells (sections 5.3.4 and 5.3.5). However, there was evidence which suggested that CYP3A metabolised midazolam into 1- and 4-hydroxymidazolam, the latter might be a P-gp substrate and was effluxed apically, thus supporting the hypothesis of their synergistic roles (section 5.3.5).

As part of the cell line characterisation, doxorubicin-exposed (Type I) cells were found to be less effective in translocating L-proline and glycyl-L-proline across the cell monolayers (sections 6.3.1 and 6.3.2). Changes in cell membrane fluidity as a result of having extra P-gp molecules might affect the functional activities of other membrane transporters such as the amino-acid transporter and the di-/tripeptide transporter (Chapter 6). Alternatively, doxorubicin exposure could result in the selection of Caco-2 cells with enhanced P-gp activity and lower functional activities of the di-/tripeptide and amino-acid transporters from the heterogeneous parent cell line.

During this project, the following aims have be achieved:

- a realisation that Caco-2 cells of different origin may possess different phenotypic characteristics. This information is useful in the rational selection of different populations of Caco-2 cells to develop more advanced cellular intestinal models and to screen various drugs, the absorption of which is mediated by different mechanisms.

- the development and characterisation of a highly-P-gp expressing Caco-2 cell model which is useful for the prediction of the intestinal absorption of drug candidates *in vitro*. This model may contribute to a fast and simple, cost-effective, successful screening of new chemical entities that are P-gp substrates, to select lead compounds with desirable absorption properties, and achieve reliable studies of drug interactions and quantitative structure activity relationships (QSAR).

- successful induction of CYP3A expression in Caco-2 cells by 1α, 25-dihydroxyvitamin D_3 where the level of CYP3A protein expression and catalytic activity closely mirror those of human small intestinal tissues. This is an advanced step in the optimisation of the existing Caco-2 cell model to achieve a more intestinal-like cellular model. The results from such a drug-screening model reflect more accurately a variety of potentially complex factors encountered during the oral administration of drug candidates and hence their bioavailability *in vivo*

- an added proof that there was no co-regulation of CYP3A and P-gp in Caco-2 cells although they may have synergistic roles in limiting the absorption of xenobiotics.

Like with any other models, limitations are realised and may be improved by:

- investigation of the expression of P-gp (as a result of doxorubicin exposure) and CYP3A4 expression (as the result of 1α, 25-dihydroxyvitamin D_3 exposure) and their co-regulation at the message (mRNA) level. This study will complement the functional studies of P-gp (chapter 4) and CYP3A4 (chapter 5) as well as to provide further explanation for the behaviour of Caco-2 cells under such treatment conditions.

- prolongation of the exposure of Type I cells to doxorubicin of increasing concentration to enhance the cellular level of expressed P-gp. Smaller populations of cells may be exposed to doxorubicin (limited dilution method) to facilitate the selection process of more homogeneously higher-P-gp expressing cells. Alternatively, genetic engineering of the Caco-2 cell line to obtain high expression of both P-gp and 3A4 can also be investigated.

160

- both enterocyte-like phenotypic and functional characteristics may change with prolonged exposure, therefore, although the model may give a good prediction of drug candidates-P-gp interactions, other active transport activities of the cell line may be suppressed. Therefore, either a scaling factor is required or perhaps, different Caco-2 cell models are required to screen drug candidates accordingly.

- co-culture of the highly P-gp-expressing Caco-2 cells with a mucus-producing carcinoma cell line such as HT-29 to achieve a more enterocyte-like model.

Not only the results from such studies as outlined above contribute to the understanding of the cellular regulation processes, which in turn, may lead to a better manipulation of the cell line to achieve desirable properties, the time, human resources and cost of drug screening using such an advanced intestinal model will also be lowered as a consequence.

REFERENCES

ADIBI, S. (1997). The oligopeptide transporter (PEPT1) in human intestine: biology and function. *Gastroenterology*, **113**: 332-340.

ALSENZ, J., STEFFEN, H. and ALEX, R. (1998). Active apical secretory efflux of the HIV protease inhibitors saquinavir and ritonavir in Caco-2 cell monolayers. *Pharmaceutical Research*, **15**: 423-428.

AMASHEH, S., WENZEL, U., BOLL, M., DORN, D., WEBER, W. M., CLAUSS, W. and DANIEL, H. (1997). Transport of charged dipeptides by the intestinal H^+/peptide symporter PEPT1 expressed in *Xenopus laevis* oocytes. *Journal of Membrane Biology*, **155**: 247-256.

ANDERLE, P., NIEDERER, E., RUBAS, W., HILGENDORF, C., SPAHN-LANGUTH, H., WUNDERLI-ALLENSPACH, H., MERKLE, H. P. and LANGGUTH, P. (1998). P-glycoprotein (P-gp) mediated efflux in Caco-2 cells monolayers: The influence of culturing conditions and drug exposure on P-gp expression levels. *Journal of Pharmaceutical Sciences*, **87**: 757-762.

AOYAMA, T., YAMANO, S., WAXMAN, D. J., LAPENSON, D. P., MEYER, U. A., FISCHER, V., TYNDALE, R., INABA, T., KALOW, W., GELBOIN, H. V. and GOZALEZ, F. J. (1989). Cytochrome P-450 hPCN3, a novel cytochrome P-45 IIIA gene product that is differentially expressed in human liver. cDNA and deduced amino acid sequence and distinct specificities of cDNA-expressed hPCN1 and hPCN3 for the metabolism of steroid hormones and cyclosporine. *Journal of Biological Chemistry*, **264**: 10338-10395.

ARIMORI, K and NAKANO, M. (1998). Drug exorption from blood into the gastrointestinal tract. *Pharmaceutical Research*, **15**: 371-376.

ARTURSSON, P. (1990). Epithelial transport of drugs in cell culture.I: a model for studying the passive diffusion of drugs over intestinal absorptive (Caco-2) cells. *Journal of Pharmaceutical Sciences*, **79**: 476-482.

ARTURSSON, P. (1991a). Cell cultures as models for drug absorption across the intestinal mucosa. *Critical Reviews in Therapeutic Drug Carrier Systems*, **8**: 305-330.

ARTURSSON, P. and KARLSSON, J. (1991b). Correlation between oral drug absorption in humans and apparent drug permeability coefficients in human intestinal epithelial (Caco-2) cells. *Biochemical and Biophysical Research Communications*, **175**: 880-885.

ARTURSSON, P., PALM, K. and LUTHMAN, K. (1996). Caco-2 monolayers in experimental and theoretical predictions of drug transport. *Advanced Drug Delivery Reviews*, **22**: 67-84.

ASPEREN, J. V., MAYER, U., TELLINGEN, O. V. and BEIJNEN, J. H. (1997). The functional role of P-glycoprotein in the blood-brain barrier. *Pharmaceutical Sciences*, **86**: 881-884.

AUGUSTIJNS, P. F., BRADSHAW, T. P., GAN, L-S., HENDREN, R. W. and THAKKER, D. R. (1993). Evidence for a polarised efflux system in Caco-2 cells capable of modulating cyclosporin A transport. *Biochemical and Biophysical Research Communications,* **197**: 360-365.

BAIN, L. J and LEBLANC, G. A. (1996). Interaction of structurally diverse pesticides with the human MDR1 gene product P-glycoprotein. *Toxicology and Applied Pharmacology,* **141**: 288-298.

BALDINI, N., SCOTLANDI, K., SERRA, M., SHIKATA, T., ZINI, N., OGNIBENE, A., SANTI, S., FERRACINI, R. and MARALDI, N. M. (1995). Nuclear immunolocalisation of P-glycoprotein in multidrug-resistant cell lines showing similar mechanisms of doxorubicin distribution. *European Journal of Cell Biology,* **68**: 226-239.

BARTHE, L., BESSOUET, M., WOODLEY, J. F. and HOUIN, G. (1998). The improved everted gut sac: a simple method to study intestinal P-glycoprotein. *International Journal of Pharmaceutics,* **173**: 255-258.

BELLAMY, W. T. (1996). P-glycoproteins and multidrug resistance. *Annual Review of Pharmacology and Toxicology,* **36**: 161-183.

BLAIS, A., BISSONNETTE, P. and BERTELOOT, A. (1987). Common characteristics for Na^+-dependent sugar transport in Caco-2 cells and human foetal colon. *Journal of Membrane Biology,* **99**: 113-125.

BOLGER, M. B., HAWARTH, I. S., YEUNG, A. K., ANN, D., GRAFENSTEIN, H. V., HAMM-ALVAREZ, S., OKAMOTO, C. T., KIM, K-J., BASU, S. K., WU, S. and LEE, V. H. L. (1998). Structure, functional and molecular modeling approaches to the study of the intestinal dipeptide transporter PEPT1. *Journal of Pharmaceutical Sciences,* **87**: 1286-1291.

BRASITUS, T. A., DUDEJA, P. K., BOLT, M. J. G., SITRIN, M. D. and BAUM, C. (1989). Dietary triaglycerol modulates sodium-dependent D-glucose transport, fluidity and fatty acid composition of rat small intestinal brush-border membrane. *Biochimica et Biophysica Acta,* **979**: 177-186.

BRAYDEN, D. (1997). Human intestinal epithelial cell monolayers as presreens for oral drug delivery. *Pharmaceutical News,* **4**:11-15.

BRETSCHNEIDER, B., BRANDSCH, M. and NEUBERT, R. (1999). Intestinal transport of β-lactam antibiotics: Analysis of the affinity at the H^+/peptide symporter (PEPT1), the uptake into Caco-2 cell monolayers and the transepithelial flux. *Pharmaceutical Research,* **16**: 55-61.

BRUGGEMANN, E. P., CURRIER, S. J., GOTTESMAN, M. M. and PASTAN, I. (1992). Characterisation of the azidopine and vinblastine binding site of P-glycoprotein. *Journal of Biological Chemistry,* **267**: 21022-21026.

BUCHLER, M., KONIG, J., BROM, M., KARTENBECK, J., SPRING, H., HORIE, T. and KEPPLERS, D. (1996). cDNA cloning of the hepatocyte canalicular isoform of the multidrug resistance protein, cMrp, reveals a novel conjugate export pump deficient in hyperbilirubinemic mutant rats. *Journal of Biological Chemistry*, **271**: 15091-15098.

CARRIERE, V., LESUFFLEUR, T., BARBAT, A., ROUSSET, M., DUSSAULX, E., COSTET, P., De WAZIERS, I., BEAUNE, P. and ZWEIBAUM, A. (1994). Expression of cytochrome P450 3A in HT29-MTX cells and Caco-2 clone TC7. *FEBS letters*, **355**: 247-250.

CHAMBERS, T. C., POHL, J., RAYNOR, R. L. and KOU, J. F. (1993). Identification of specific sites in human P-glycoprotein phosphorylated by protein-kinase-C. *Journal of Biological Chemistry*, **268**: 4592-4595.

CHANTRET, I., BARBAT, A., DUSSAULX, E., BRATTAIN, M. G. and ZEWIBAUM, A. (1988). Epithelial polarity, villin, expression and enterocytic differentiation of cultured human colon carcinoma cells: A survey of twenty cell lines. *Cancer Research*, **48**: 1936-1942.

CHEN, C., CHIN, J. E., UEDA, K., CLARK, D. P., PASTAN, I., GOTTESMAN, M. M. and RONINSON, I. B. (1986). Internal duplication and homology with bacterial transport proteins in the mdr1 (P-glycoprotein) gene from the multidrug-resistant human cells. *Cell*, **47**: 381-389.

CHEN, G., DURAN, G. E., STEGER, K. A., LACAYO, N. J., JAFFREZOU, J. P., DUMONTET, C. and SIKIC, B. I. (1997). Multidrug-resistant human sarcoma cells with a mutant P-glycoprotein, altered phenotype and resistance to cyclosporins. *Journal of Biological Chemistry*, **272**: 5974-5982.

CHONG, S., DANDO, S., SOUCEK, K. and MORRISON, R. A. (1996). *In vitro* permeability is not quantitatively predictive of *in vivo* absorption for peptide-like drugs absorbed *via* the dipeptide transporter system. *Pharmaceutical Research*, **13**: 120-123.

COLE, S. P. C., BHARDWAJ, G., BERLACH, J. H., MACKIE, J. E., GRANT, C. E., ALMQUIST, K. C., STEWART, A. J., KURZ, E. U., DUNCAN, A. M. V. and DEELEY. R. G. (1992). Overexpression of a transporter gene in a multidrug-resistant human lung cancer cell line. *Science*, **258**: 1650-1654.

CRESPI, C. L., PENMAN, B. W. and HU, M. (1996). Development of Caco-2 cells expressing high levels of cDNA-derived cytochrome P4503A4. *Pharmaceutical Research*, **13**: 1635-1641.

DANTZIG, A. H and BERGIN, L. (1990). Uptake of the cephalosporin, cephalexin, by a dipeptide transport carrier in the human intestinal cell line, Caco-2. *Biochimica et Biophysica Acta*, **1027**: 211-217.

DECKER, C. J., LAITINEN, L. M., BRIDSON, G. W., RAYBUCK, S. A., TUNG, R. D. and CHATURVEDI, P. R. (1998). Metabolism of amprenavir in liver microsomes: Roles of CYP3A4 inhibitions of drug interactions. *Journal of Pharmaceutical Sciences*, **87**: 803-807.

DeWAZIER, I., CUGNENC, P. H., YANG, C. S., LEROUX J. P. and BEAUNE, P. H. (1990). Cytochrome P450 isozymes, epoxide hydrolases and glutathione S-transferases in rat and human, hepatic and extrahepatic tissues. *Journal of Pharmaceutical Experimental and Therapeutics*, **253**: 187-194.

DEY, S., RAMACHANDRA, M., PASTAN, I., GOTTESMAN, M. M. and AMBUDKAR, S. V. (1997). Evidence for two non-identical drug-interaction sites in the human P-glycoprotein. *Proceedings of National Academy of Sciences, USA*, **94**: 10594-10599.

DOIGE, C. A and SHAROM, F. J. (1992). Transport properties of P-glycoprotein in plasma membrane vesicles from multidrug-resistant Chinese hamster ovary cells. *Biochimica et Biophysica Acta*, **1109**: 161-171.

DOPPENSCHMITT, S., SPAHN-LANGGUTH, H., REGARDH, C. G. and LANGGUTH, P. (1999). Radioligand-binding assay employing P-glycoprotein-over-expressing cells: Testing drug affinities to the secretory intestinal multidrug transporter. *Pharmaceutical Research*, **15**; 1001-1006.

DUENSING, T. D and SLATE, D. L. (1994). Intracellular expression of P-glycoprotein in a human colon tumour cell line. *Anticancer Research*, **14**: 13-20.

EDDY, E. P., WILSON, G. and HILDAGO, I. J. (1993). Uptake of glycyl-L-proline in Caco-2 cells involves multiple transport mechanisms. *Pharmaceutical Research*, **10**: S207.

EMI, Y., TSUNASHIMA, D. T., OGAWARA, K., HIGAKI, K. and KIMURA, T. (1997). Role of P-glycoprotein as a secretory mechanism in quinidine absorption from rat small intestine. *Journal of Pharmaceutical Sciences*, **87**: 295-299.

ENDICOTT, J. A and LING, V. (1989). The biochemistry of P-glycoprotein-mediated multidrug resistance. *Annual Review of Biochemistry*, **58**: 137-71.

FEI, Y-J., KANAI, Y., NUSSBERGER, S., GANAPATHY, V., LEIBACH, F. H., ROMERO, M. F., SIGH, S. K., BORON, W. F. and HEDIGER, M. A. (1994). Expression cloning of a mammalian proton-coupled oligopeptide transporter. *Nature*, **368**: 563-566.

FERRY, D., RUSSELL, M. A. and CULLEN, M. H. (1992). P-glycoprotein possesses a 1, 4-dihydropyridine-selective drug acceptor site which is allosterically coupled to a vinca-alkaloid-selective binding site. *Biochemical and Biophysical Research Communications*, **188**: 440-445.

FISHER, J. M., WRIGHTON, S. A., CALAMIA, J. C, SHEN, D. D., KUNZE, K. L. and THUMMEL, K. E. (1999a). Midazolam metabolism by modified Caco-2 cell monolayers: Effects of extracellular protein binding. *Journal of Pharmacology and Experimental Therapeutics*, **289**: 1143-1150.

FISHER, J. M., WRIGHTON, S. A., WATKINS, P. B., SCHMIEDLIN-REN, P., CALAMIA, J. C., SHEN, D. D., KUNZE, K. L. and THUMMEL, K. E. (1999b). First-pass midazolam metabolism catalysed by 1α, 25-dihydroxyvitamine D3-modified Caco-2 cell monolayers. *Journal of Pharmacology and Experimental Therapeutics*, **289**: 1134-1142.

FOGH, J., FOGH, J. M. and ORFEO, T. (1977). One hundred and twenty-seven cultured human tumour cell lines producing tumours in nude mice. *Journal of National Cancer Institute*, **59**: 221-226.

FRIEDMAN, D.I and AMIDON, G.L. (1989). Intestinal absorption mechanism of dipeptide angiotensin converting enzyme inhibitors of the lysyl-proline type: Lisinopril and SQ 29852. *Journal of Pharmaceutical Sciences*, **78**: 995-998.

GAN, L-S. L., MOSELEY, M. A., KHOSLA, B., AUGUSTIJNS, P. F., BRADSHAW, T. P., HENDREN, R. W. and THAKKER, D. R. (1996). CYP3A-like cytochrome P450-mediated metabolism and polarised efflux of cyclosporin A in Caco-2 cells. Interaction between the two biochemical barriers to intestinal transport. *Drug Metabolism and Disposition*, **24**: 344-349.

GANAPATHY, V and LEIBACH, F. H. (1985). Intestinal peptide transport energized by a proton gradient?. *American Journal of Physiology*, **249**: G153-G160.

GANAPATHY, V., BRANDSCH, M. and LEIBACH, F. H. (1994). *Physiology of the gastrointestinal tract*. Johnson. L. R. (ed), 3rd edition, Raven Press, New York, pp 1773-1794.

GANAPATHY, V and LEIBACH, F.H. (1996). Peptide transporters. *Current Opinion in Nephrology and Hypertension*, **5**: 395-400.

GARRIDO, C., CHAUFFER, B., PINARD, D., TIBAUT, F., GENNE, P., ASSEM, M. and DIMANCHE-BOITREL, M-T. (1995). Circumvention of confluence-dependent resistance in a human multidrug-resistant colon-cancer cell line. *International Journal of Cancer*, **61**: 873-879.

GEORGES, E., BRADLEY, G., GARIEPY, J. and LING V. (1990). Detection of P-glycoprotein isoforms by gene specific monoclonal antibodies. *Proceedings of National Academy of Sciences, USA*, **87**: 152-156.

GERVOT, L., CARRIERE, V., COSTET, P., CUGNENC, P-H., BERGER, A., BEAUNE, P. H. and De WAZIERS, I. (1996). CYP3A5 is the major cytochrome P450 3A expressed in human colon and colonic cell lines. *Enviromental Toxicology and Pharmacology*, **2**: 381-388.

GOODFELLOW, H. R., SARDINI, A., RUETZ, S., CALLAGHAN, R., GROS, P., MCNAUGHTON, P. A. and HIGGINS, C. F. (1996). Protein kinase C-mediated phosphorylation does not regulate drug transport by the human multidrug resistance P-glycoprotein. *Journal of Biological Chemistry*, **271**: 13668-13674.

GORSKI, J. C., HALL, S. D., JONES, D. R., VANDENBRANDEN, M. and WRIGHTON, S. A. (1994). Regioselective biotransformation of midazolam by members of the human cytochrome P450 3A (CYP3A) subfamily. *Biochemical Pharmacology*, **47**: 1643-1653.

GOTTESMAN, M. M and PASTAN, I. (1988). The multidrug trnasporter, a double-edged sword. *Journal of Biological Chemistry*, **263**: 12163-12166.

GRASSET, E., PINTO, M., DUSSAULX, E., ZWEIBAUM, A. and DESJEUX, J.F. (1984). Epithelial properties of human colonic carcinoma cell line Caco-2: electrical parameters. *American Journal of Physiology*, **247**: C260-C267.

GREENBERGER, L. M. (1993). Major photoaffinity drug labelling sites for iodoaryl azidoprazosin in P-gp are within or immediately C-terminal to, transmenbrane domains 6 and 12. *Journal of Biological Chemistry*, **268**: 11471-11425.

GROMEZ, D. Y., WACHER, V. J., TOMLANOVICH, S. J., HERBERT, M. F. and BENET, L. Z. (1995). The effects of ketoconazole on the intestinal metabolism and biovailabilty of cyclosporine. *Clinical Pharmacology and Therapeutics*, **58**: 15-29.

GUILFOILE, P. G and HUTCHINSON, C. R. (1991). A bacterial analogue of the mdr gene of mammalian tumour cells is present in *Streptomyces peuceticus*, the producer of daunorubicin and doxorubicin. *Proceedings of National Academy of Sciences, USA*, **88**: 8553-8557.

HAEHNER, B. D., GORSKI, C. J., VANDERBRANDEN, M., WRIGHTON, S. A., JANARDAN, S. K., WATKINS, P. B. and HALL, S. D. (1996). Bionormal distribution of renal CYP 3A activity in humans. *Molecular Pharmacology*, **50**: 52-59.

HAMILTON, G., COSENTINI, E. P., TELEKY, B., KOPERNA, T., ZACHERI, J., RIEGLER, M., FEIL, W., SCHIESSEL, R. and WENZI, E. (1993). The multidrug-resistance modifiers verapamil, cyclosporin A and tamoxifen induce an intracellular acidification in colon carcinoma cell lines in vitro. *Anticancer Research*, **1993**: 2059-2064.

HAYASHI, K., YAMAMOTO, S-I., OHE, K., MIYOSHI, A., KAWASAKI, T. (1980). Na$^+$-gradient dependent transport of L-proline and analysis of its carrier system in brush border membrane vesicles of the guinea-pig ileum. *Biochimica et Biophysica Acta*, **601**: 654-663.

HAYMAN, M., CRAIN-DENOYELLE, A-M., NATH, S. K. and DESJEUX, J-F. (1990). Quantification of protein transcytosis in the human colon carcinoma cell line Caco-2. *Journal of Cellular Physiology*, **143**: 391-395.

167

HEDIGER, M. A., KANAI, Y., YOU, G. and NUSSBERGER, S. (1995). Mammalian ion-coupled solute transporters. *Journal of Physiology*, **482**: 7S-17S.

HIDALGO, I. J., RAUB, T and BORCHARDT, R.T. (1989). Characterisation of the human colon carcinoma cell line (Caco-2) as a model system for intestinal epithelial permeability. *Gastroenterology*, **96**: 736-749.

HIDALGO, I. J and BORCHARDT, R.T. (1990). Transport of bile acids in a human intestinal epithelial cell line, Caco-2. *Biochimica et Biophysica Acta*, **1035**: 97-103.

HIDALGO, I. J., BHATNAGAR, P., LEE, C-P., MILLER, J., CUCULLINO, G. and SMITH, P. L. (1995). Structural requirements for interaction with the oligopeptide transporter in Caco-2 cells. *Pharmaceutical Research*, **12**: 317-319.

HIGASHIKAWA, F., MURAKAMI, T., KANEDA, T., KATO, A. and TAKANO, M. (1999). Dose-dependent intestinal and hepatic first-pass metabolism of midazolam, a cytochrome P450 3A substrate with differently modulated enzyme activity in rats. *Journal of Pharmacy and Pharmacology*, *51*: 67-72.

HIGGINS, C. F. and GOTTESMAN, M. M. (1992). Is the multidrug transporter a flippase? *Trend in Biological Sciences*, **17**: 18-21.

HIGGINS, C. F., CALLAGHAN, R., LINTON, K. J., ROSENBERG, M. F. and FORD, R. C. (1997). Structure of the multidrug resistance P-glycoprotein. *Seminars in Cancer Biology*, **8**: 135-142.

HOLBROOK, P. (1989). Ph.D. thesis, Aston University, UK.

HORIO, M., CHIN, K. V., CURRIER, S. J., GOLDENBERG, S., WILLIAMS, C., PASTAN, I., GOTTESMAN, M. M. and HANDLER, J. (1988). Transepithelial transport of drugs by the multidrug transporter in cultured Madin-Darby Canine Kidney cell epithelia. *Journal of Biological Chemistry*, **264**: 14880-14884.

HOSKIN, J., DEHERDT, S. V., MOORE, R. E. and BUMOL, T. F. (1993). The development and characterisation of vinca alkaloid-resistant Caco-2 human colorectal cell lines expressing mdr-1. *International Journal of Cancer*, **53**: 680-688.

HOSOYA, K-I., KIM, K-J. and LEE, V.H.L. (1996). Age dependent expression of P-glycoprotein gp170 in Caco-2 cell monolayers. *Pharmaceutical Research*, **13**: 885-890.

HU, M and GORDON, A. L. (1988). Passive and carrier-mediated intestinal absorption components of captopril. *Journal of Pharmaceutical Sciences*, **77**: 1007-1011.

HU, M., ZHENG, L., CHEN, J., LIU, L., DANTZIG, A. and STRATFORD Jr, R. E. (1995a). Peptide transporter function and prolidase activities in Caco-2 cells: A lack of coordinated expression. *Journal of Drug Targeting*, **3**: 291-300.

HU, M., ZHENG, L., CHEN, J., LIU, L., ZHU, Y., DANTZIG, A.H., STRATFORD JR, R.E. (1995b). Mechanism of transport of quinapril in Caco-2 cell monolayers: Comparison with cephalexin. *Pharmaceutical Research*, **12**: 1120-1125.

HUNTER, J., HIRST, B. H. and SIMMONS, N. L. (1993a). Drug absorption limited by P-glycoprotein-mediated secretory drug transport in human intestinal epithelial Caco-2 cell layers. *Pharmaceutical Research*, **10**: 743-749.

HUNTER, J., JEPSON, M. A., TSURUO, T., SIMMONS, N.L. and HIRST, B.H. (1993b). Functional expression of P-glycoprotein in apical membranes of the human intestinal Caco-2 cells. Kinetics of vinblastine secretion and interaction with modulators. *Journal of Biological Chemistry*, **268**: 14991-14997.

KARTNER, N., RIORDAN, J. R. and LING, V. (1983). Cell surface P-glycoprotein associated with multidrug resistance in mammalian cell lines. *Science*, **221**: 1285-1288.

KEPPLER, D and KONIG, J. (1997). Expression and localisation of the conjugate export pump encoded by the MRP2 (cMRP/cMOAT) gene in the liver. *FASEB Journal*, **11**: 509-516.

KOLARS, J. C., AWNI, W. M., MERION, R. M. and WATKINS, P. B. (1991a). First-pass metabolism of cyclosporin by the gut. *Lancet*, **338**: 1488-1490.

KOLARS, J. C., SCHMIEDLIN-REN, P., SCHUETZ, J., GHOSH, M., DOBBINS, W. O. and WATKINS, P. B. (1991b). Expression of P4503A4 in duodenal mucosa: Interpatient variability and regulation in cultured explants. *Gastroenterology*, **100**: A221.

KOLARS, J. C., SCHMIEDLIN-REN, P., DOBBINS, W. O., SCHUETZ, J. D., WRIGHTON, S. A. and WATKINS, P. B. (1992a). Heterogeneity of cytochrome P450IIIA expression in rat gut epithelia. *Gastroenterology*, **102**: 1186-1198.

KOLARS, J. C., STETSON, P. L., RUSH, B. D., RUWART, M. J., SHMIEDLIN-REN, P., DUELL, E. A., VOORHEES, J. J. and WATKINS, P. B. (1992b). Cyclosporine metabolism by P450IIIA in rat enterocytes-another determinant of oral bioavailability?. *Transplantation*, **53**: 596-602.

KOLARS, J. C., SCHMIEDLIN-REN, P., SCHUETZ, J. D., FANG, C. and WATKINS, P. B. (1992c). Identication of rifampicin-inducible P450IIIA4 (CYP3A4) in human small bowel enterocytes. *Journal of Clinical Investigation*, **90**: 1871-1878.

LAMPIDIS, T. J., KOLONIAS, D., PODONA, T., ISAREAL, M., SAFA, A. R., LOTHSTEIN, L., SAVARAJ, N., TAPIERO, H. and PRIEBE, W. (1997). Circumvention of P-gp Mdr as a function of anthracycline lipophilicity and charge. *Biochemistry*, **36**: 2679-2685.

LANG, C. C., BROWN, R. M., KINIRONS, M. T., DEATHRIDGE, M. A., GUENGERICH, F. P., KELLEHER, D., O'BRIAIN, D. S. and GHISHAN, F. K. (1996). Decreased intestinal CYP3A in celiac disease: Reversal after successful gluten-free diet: A potential source of interindividual variability in first-pass drug metabolism. *Clinical Pharmacology Therapeutics*, **59**: 41-46.

LEIBACH, F.H and GANAPATHY, V. (1996). Peptide transporters in the intestine and the kidney. *Annual Review Nutrition*, **16**: 99-119.

LEIER, I., JEDLITSHKY, G., BUCHOLZ, U., COLE, S. P. C., DEELEY, R. G. and KEPPLER, D. (1994). The MRP gene encodes an ATP-dependent export pump for leukotriene C_4 and structurally related conjugates. *Journal of Biological Chemistry*, **269**: 27807-27810.

LENNERNAS, H., PALM, K., FAGERHOLM, U. and ARTURSSON, P. (1996). Comparison between active and passive drug transport in human intestinal epithelial (Caco-2) cells in vitro and human jejunum in vivo. *International Journal of Pharmaceutics*, **127**: 103-107.

LI, G., and KLOTZ, U. (1990). Inhibitory effect of omeprazole on the metabolism of midazolam *in vitro*. *Arzneimittelforschung*, **40**: 1105-1107.

LIANG, R., FEI, Y-J., PRASAD, P. D., RAMAMOORTHY, S., HAN, H., YANG-FENG, T. L., HEDIGER, M. A., GANAPATHY, V. and LEIBACH, F. H. (1995). Human intestinal H^+/peptide cotransporter: Cloning, functional expression and chromosomal localisation. *Journal of Biological Chemistry*, **270**: 6456-6463.

LING, K. J., LEESON, G. A., BURMASTER, S. D., HOOK, R. H., REITH, K. and CHENG, L. K. (1995). Metabolism of terfenadine associated with CYP3A(4) activity in human hepatic microsomes. *Drug Metabolism and Disposition*, **23**: 631-636.

LITMAN, T., ZEUTHEN, T., SKOVSGAARD, T. and STEIN, W. D. (1997a). Structure-activity relationships of P-glycoprotein interacting drugs: kinetic characterisation of their effects on ATPase activity. *Biochemica et Biophysica Acta*, **1361**: 159-168.

LITMAN, T., ZEUTHEN, T., SKOVSGAARD, T. and STEIN, W. D. (1997b). Competitive, non-competitive and cooperative interactions between substrates of P-glycoprotein as measured by its ATPase activity. *Biochemica et Biophysica Acta*, **1361**: 169-176.

LIU, R and SHAROM, F. J. (1997). Fluorescence studies of the nucleotide binding domains of the P-glycoprotein multidrug transporter. *Biochemistry*, 36: 2836-2843.

LOE, D. W., ALMQUIST, K. C., COLE, S. P. C. and DEELEY, R. G. (1996). ATP-dependent 17 β-oestradiol 17-(β-D-glucuronide) transport by multidrug resistance protein (MRP)- Inhibition by cholestatic steroids. *Journal of Biological Chemistry*, **271**: 9693-9689.

LOE, D. W., DEELEY, R. G. and COLE, S. P. C. (1998). Characterisation of vincristine transport by the Mr 190, 000 multidrug resistance protein (MRP): Evidence for cotransport with reduced glutathione. *Cancer Research*, **58**: 5130-5136.

LOO, T. W and CLARKE, D. M. (1993). Functional consequences of proline mutations in the predicted transmembrane domains of P-glycoprotein. *Journal of Biological Chemistry*, **268**: 3143-3149.

LOWN, K. S., KOLARS, J. C., THUMMEL, K. E., BARNETT, J. L., KUNZE, K. L., WRIGHTON, S. A. and WATKINS, P. B. (1994). Interpatient heterogeneity in expression of CYP3A4 and CYP3A5 in small bowel. Lack of prediction by the erythromycin breath test. *Drug Metabolism and Disposition*, **22**: 947-955.

LOWN, K. S., KOLARS, J. C., GHOSH, M., SCHMIEDLIN-REN, P. and WATKINS, P, B. (1996). Induction of MDR1 expression in normal rat and human intestine *in vivo*. *Gastroenterology*, **10**: A344.

LOWN, K. S., BAILEY, D. G., FONTANA, R. J., JANARDAN, S. K., ADAIR, C. H., FORTLAGE, L. A., BROWN, M. B., GOU, W. and WATKINS, P. B. (1997a). Grapefruit juice increases felodipine oral bioavialability in humans by decreasing intestinal CYP3A protein expression. *Journal of Clinical Investigation*, **99**: 2545-2553.

LOWN, K. S., MAYO, R. R., LEICHTMAN, A .B., HSIAO, H-L., TURGEON, D. K., SCHMIEDLIN-REN, P., BROWN, M. B., GUO, W., ROSSI, S. J., BENET, L. Z. and WATKINS, P. B. (1997b). Role of intestinal P-glycoprotein (mdr1) in interpatient variation in the oral bioavailability of cyclosporine. *Clinical Pharmacology and Therapeutics*, **62**: 248-260.

MALO, C. (1991). Multiple pathways for amino acid transport in brush border membrane vesicles isolated from the human foetal small intestine. *Gastroenterology*, **100**: 1644-1652.

MARINO, A. M., CHONG, S., DANDO, S. A., KRIPALAMI, K. J., BATHALA, M. S. and MORRISON, R. A. (1995). Distribution of the dipeptide transporter system along the gastrointestinal tract of rats based on absorption of a stable and specific probe, SQ 29852. *Journal of Pharmaceutical Science*, **85**: 282-286.

McKINNON. R. A., BURGESS, W. M., HALL., P., ABDUL-AZIZ, Z. and MAMANUS, M. E. (1992). Metabolism of food-derived heterocyclics amines in humans and rabbit tissues by P4503A proteins in the presence of flavonoids. *Cancer Research*, **52**: 2108s-2113s.

MECHETNER, E. B., SCHOTT, B., MORSE, B. S., STEIN, W. D., DRULEY, T., DAVIS, K. A., TSURUO, T. and RONINSON, I. B. (1997). P-glycoprotein fubction involves conformational transitions detectable by differential immunoreactivity. *Proceedings of National Academy of Sciences, USA*, **94**: 12908-12913.

MOFFAT, A. C. in Clarke's isolation and identification of drugs in pharmaceuticals, body fluids and post-mortem materials, 2nd edition (1986), Moffat, A. C., Jackson, J. V., Moss, M. S., and Widdop, B. (Eds.), The Pharmaceutical Press, London, pp785.

MOORE, V. A., CHONG, S., DANDO, S. A., LAU, W., IRWIN, W, J., TIMMINS, P. and MORISON, R. A. (1996). Systematic evaluation of the structural requirements for the intestinal dipeptide transporter system. *Pharmaceutical Research*, **12**: S301.

MORRISON, R.A., CHONG, S., MARINO, A., WASSERMAN, M. A., TIMMINS, P., MOORE, V. A. and IRWIN, W. J. (1996). Suitability of enalapril as a probe of the dipeptide transporter system: In vitro and in vivo studies. *Pharmaceutical Research*, **13**: 1078-1082.

MUTHIAH, R and SEETHARAM, B. (1987). [^{57}Co]Cyanocobalamin uptake by human colon adenocarcinoma cell line (Caco-2). *Journal of Cell Biology*: **105**: 235a.

NERURKAR. M. M., BURTON, P. S. and BORCHARDT, R. T. (1996). The use of surfactants to enhance the permeability of peptides through Caco-2 cells by inhibition of an apically polarised efflux system. *Pharmaceutical Research*, **13**: 528-534.

NG, W. F., SARANGI, F., ZASTAWNY, R. L., VEINOT, D. L. and LING, V. (1989). Identification of members of the P-glycoprotein multigene family. *Molecular Cell Biology*, **9**: 1224-1232

NICKLIN, P. L., IRWIN, W. J., HASSAN, I. F. and MACKAY, M. (1992). Proline uptake by monolayers of human intestinal absorptive (Caco-2) cells in vitro. *Biochimica et Biophysica Acta*, **1104**: 283-292.

NICKLIN, P. L., IRWIN, W. J., TIMMINS, P. and MORRISON, R. A. (1996). Uptake and transport of the ACE-inhibitor ceronapril (SQ 29852) by monolayers of human intestinal absorptive (Caco-2) cells in vitro. *International Journal of Pharmaceutics*, **140**: 175-183.

NIV, Y., BYRD, J. C., HO, S. B., DAHIYA, R and KIM, Y. S. (1992). Mucin synthesis and secretion in relation to spontaneous differentiation of colon cancer cells *in vitro*. *International Journal of Cancer*, 50: 147-152.

PAINE, M. F., KHALIGHI, M., FISHER, J. M., SHEN, D. D., KUNZE, K. L., MARSH, C. L., PERKINS, J. D. and THUMMEL, K. E. (1997). Characterisation of intestinal and intra-intestinal variations in human CYP3A-dependent metabolism. *Journal of Pharmacology and Experimental Therapeutics*. **283**: 1552-1562.

PALACIN, M., ESTEVEZ, R., BERTRAN, J. and ZORZANO, A. (1998). Molecular biology of mammalian plasma membrane amino acid transporters. *Physiological Reviews*, **78**: 969-1038.

PARKINSON, A. Biotransformation of xenobiotics (Chapter 6) in Casarett & Doull's Toxycology, the basic science of poisons, 5th edition (1996), Klaassen, C. D (edi), McGraw-Hill, USA, pp113-186.

PETERS, W. H and KREMERS, P. G. (1989). Cytochromes P450 in the intestinal mucosa of man. *Biochemical Pharmacology*, **38**: 1535-1538.

PINTO, M., ROBINE-LEON, S., APPAY, M. D., KEDINGER, M., TRIADOU, N., DUSSAULX, E., LACROIX, B., SIMON-ASSMANN, P., HAFFEN, K., FOGH, J. and ZWEIBAUM, A. (1983). Enterocyte-like differentiation and polarization of the human colon carcinoma cell line Caco-2 in culture. *Cell Biology*, **47**: 323-330.

PRASAD, R., DE WERGIFOSSE, P., GOFFEAU, A. and BALZI, E. (1995). Molecular cloning and characterisation of a novel gene of *Candida albicans*, CDR1, conferring multiple drug resistance to drugs and antifungals. *Current Genetics* **27**; 320-329.

PRUEKSARITANONT, T., GORHAM, L.M., HOCHMAN, J.H., TRAN, L.O. and VYAS, K. (1996). Comparative studies of drug metabolising enzymes in dog, monkey, and human small intestines, and in Caco-2 cells. *Drug Metabolism and Disposition*, **24**: 634-642.

RAEISSI, S.D., GUO, Z., DOBSON, G.L., ARTURSSON, P. and HILDAGO, I.J. (1997). Comparison of CYP3A activities in a subclone of Caco-2 cells (TC7) and human intestine. *Pharmaceutical Research*, **14**: 1019-1025.

RAEISSI, S. D., LI, J. and HIDALGO, I. J. (1998). The role of an α-amino group on H^+-dependent transepithelial transport of cephalosporins in Caco-2 cells. *Journal of Pharmacy and Pharmacology*, **51**: 35-40

RAJENDRAN, V. M., ANSARI, S. A., HARIG, J. M., ADAMS, M., KHAN, A. H. and RAMASWAMY, K. (1985). Transport of glycyl-l- proline by human intestinal brush border membrane vesicles. *Gastroenterology*, **89**: 1298-1304.

RAO, U. S and SCARBOROUGH, G. A. (1994). Direct demonstration of high affinity interactions of immunosuppressant drugs with the drug binding site of the human P-glycoprotein. *Molecular Pharmacology*, **45**: 773-776.

RAVIV, Y., POLLARD, H. B., BRUGGEMAN, E. P., PASTAN, I. and GOTTESMAN, M. M. (1990). Photosensitised labelling of a functional multidrug transporter in living drug resistant tumour cells. *Journal of Biological Chemistry*, **265**: 3975-3980.

ROSENBERG, M. F., CALLAGHAN, R., FORD, R. C. and HIGGINS, C. F. (1997). Structure of the multidrug resistance P-glycoprotein to 2.5 nm resolution determined by electron microscopy and image analysis. *Journal of Biological Chemistry*, **272**: 10685-10694.

SAFA, A. R., STERN, R. K., CHOI, K., AGRESTI, M., TAMAI, I., MEHTA, N. D. and RONINSON, I. B. (1990). Molecular basis of preferential resistance to colchicine in multidrug-resistant human cells conferred by Gly-185 to Val-185 substitution in P-glycoprotein. *Proceedings of National Academy of Sciences, USA*, **87**: 7225-7229.

SCHINKEL, A. H., SMIT, J. J. M., TELLIGEN, O. V., BEIJNEN, J. H., WAGENAAR, E., DEEMTER, L. V., MOL, C. A. A. M., VAN DER VALK, M, A., ROBANUS-MAANDAG, E. C., TE RIELE, H. P. J., BERNS, A. J. M. and BORST, P. (1994). Disruption of the mouse mdr1a P-glycoprotein gene leads to a deficiency in the blood-brain barrier and to increased sensitivity to drugs. *Cell*, **77**: 491-502.

SCHMIEDLIN-REN, P., THUMMEL, K. E., FISHER, J. M., PAINE, M. F., LOWN, K. S. and WATKINS, P. B. (1997). Expression of enzymatically active CYP3A4 by Caco-2 cells grown on extracellular matrix-coated permeable supports in the presence of $1\alpha,25$-dihydroxyvitamin D_3. *Molecular Pharmacology*, **51**: 741-754.

SCHOEMAKERS, R. G., STEVEHOUWER, M. C. and TUKKER, J. J. (1999). Structure-transport relationship for the intestinal small-peptide carrier: Is the carbonyl group of the peptide bond relevant for transport. *Pharmaceutical Research*, **16**: 62-68.

SCHUETZ, E. G., SCHUETZ, J.D., GROGAN, W. M., TOTH, A. N., TOTH, G. F., RAUCY, J., GUZELIAN, O., GIONELA, K. and WATLINGTON, C. O. (1992). Expression of cytochrome P450 3A in amphibian, rat and human kidney. *Archives of Biochemistry and Biophysics*, **294**: 206-214.

SCHUETZ, J. D., BEACH, D. L. and GUZELIAN, P. S. (1994). Selective expression of cytochrome P450 CYP3A mRNAs in embryonic and adult human liver. *Pharmacogenetics*, **4**: 11-20.

SCHUETZ, E.G., BECK, W. T. and SCHUETZ, J. D. (1996). Modulators and substrates of P-glycoprotein and cytochrome P4503A coordinately up-regulate these proteins in human colon carcinoma cells. *Molecular Pharmacology*, **49**: 311-318.

SENIOR, A. E., AL-SHAWI, M. K. and URBATSCH, I. L. (1995). The catalytic cycle of P-glycoprotein. *FEBS letters*, **377**: 285-289.

SHAROM, F. J., YU, X. and DOIGE, C. A. (1993). Functional reconstitution of drug transport and ATPase activity in proteoliposomes containing partially purified P-glycoprotein. *Journal of Biological Chemistry*, **268**, 24197-24202.

SHAROM, F. J., YU, X., DIDIODATA, G. and CHU, J. W. K. (1996). Synthetic hydrophobic peptides are substrates for P-glycoprotein and stimulate drug transport. *Biochemistry Journal*, **320**: 421-428.

SHAROM, F. J., LU, P., LIU, R. and YU, X. (1998). Linear and cyclic peptides as substrates and modulators of P-glycoprotein: Peptide binding effects on drug transport and accumulation. *Biochemistry Journal*, **333**: 621-630.

SHERWOOD, L. Human physiology from cells to systems, 3rd edition (1997), Lewis. P. (Ed), Wadsworth Publishing Company, Minneapolis, pp 546-600.

SHIMADA, T and HOSHI, T. (1988). Na^+-dependent elevation of the acidic cell surface pH (microclimate pH) of rat jejunal villus cells induced by cyclic nucleotides and phorbol ester: possible mediators of the regulation of the Na^+/H^+ antiporter. *Biochimica et Biophysica Acta*, **937**: 328-334.

SHIMADA, T., YAMAZAKI, H., MIMURA, M., INUI, Y. and GUENRICH, P. (1994). Inter-individual variations in human liver cytochrome P450 enzymes involved in the oxidation of drugs, carcinogens and toxic chemicals: Studies with liver microsomes of 30 Japanese and 30 Caucasians. *Journal of Pharmacology and Experimental Therapeutics*, **270**: 414-423.

SKETT, P., TYSON, C., GUILLOUZO, A. and MAIER, P. (1995). Report on the international workshop on the use of human in vitro liver preparations to study drug metabolism in drug development. *Biochemical Pharmacology*, **50**: 280-285.

SMIT, J. J. M., SCHINKEL, A. H., OUDE ELFERINK, R. P. J., GROEN, A. K., WAGENAAR, E., DEEMTER, L. V., MOL, C. A. A. M., OTTENHOFF, R., VAN DER LUGT, N. M. T., VAN RRON, M. A., VAN DER VALK, M. A., OFFERHAUS, G. J. A., BERNS, A. J. M. and BORST. P. (1993). Homozygous disruption of the murine mdr2 P-glycoprotein gene leads to a complete absence of phospholipid from bile and to liver disease. *Cell*, 75: 451-462.

SPARREBOOM, A., ASOEREN, J. V., MAYER, U., SCHINKEL, A. H., SMIT, J. W., MEIJER, D. K. F., BORST, P., NOOIJEN, W. J., BEIJNEN, J. H. and TELLINGEN, O. V. (1997). Limited oral bioavailability and active epithelial excretion of paclitaxel (Taxol) caused by P-glycoprotein in the intestine. *Proceedings of National Academy of Sciences, USA*, **94**: 2031-2035.

SPATZENEGGER, M and JAEGER, W. (1995). Clinical importance of hepatic cytochrome P450 in drug metabolism. *Drug Metabolism Reviews*, **27**: 397-417.

STEEL, A., NUSSBERGER, S., ROMERO, M. F., BORON, W. F., BOYD, C. A. R. and HEDIGER, M. A. (1997). Stoichiometry and pH dependence of the rabbit proton-dependent oligopeptide transporter PEPT1. *Journal of Physiology*, **498**.3: 563-569.

STEVENS, B. R., KAUNITZ, J. D. and WRIGHT, E. M. (1984). Intestinal transport of amino acids and sugars: Advances using membrane vesicles. *Annual Review of Physiology*, **46**: 417-33.

STRYER, L. Biochemistry, 3rd edition (1988). W.H.Freeman and Company, New York, pp188.

TAMAI, I., SAHEKI, A., SAITOH, R., SAI, Y., YAMADA, I. and TSUJI, A. (1997). Nonlinear intestinal absorption of 5-hydroxytryptamine receptor antagonist caused by absorptive and secretory transporters. *Journal of Pharmacology and Experimental Therapeutics*. **283**: 108-115.

TERAO, T., HISANAGA, E., SAI, Y., TAMAI, I. and TSUJI, A. (1996). Active secretion of drugs from the small intestinal epithelium in rats by P-glycoprotein functioning as an absorption barrier. *Journal of Pharmacy and Pharmacology*, **48**: 1083-1089.

THIEBAUT, F., TSURUO, T., HAMADA, H., GOTTESMAN, M. M., PASTAN, I. and WILLINGHAM, M.C. (1987). Cellular localisation of the multidrug-resistance gene product P-glycoprotein in normal human tissues. *Proceedings of National Academy of Sciences, USA*, **84**: 7735-7738.

THIEBAUT, F., TSURUO, T., HAMADA, H., GOTTESMAN, M. M., PASTAN, I. and WILLINGHAM, M. C. (1989). Immunohistochemical localisation in normal tissues of different epitopes in the multidrug transport protein P170: Evidence for localization in brain capillaries and crossreactivity of one antibody with a muscle protein. *Journal of Histochemistry and Cytochemistry*, **37**: 159-164.

THUMMEL, K. E and WILKINSON, G. R. (1998). *In vitro* and *in vivo* drug interactions involving human CYP3A. *Annual Review of Pharmacology and Toxicology*, **38**: 389-430.

THWAITES, D. T., BROWN, C. D. A., HIRST, B. H. and SIMMONS, N. L. (1992). Transepithelial glycylsarcosine transport in intestinal Caco-2 cells mediated by expression of H^+-coupled carriers at both apical and basal membranes. *Journal of Biological Chemistry*, **268**: 7640-7642.

THWAITES, D. T., BROWN, C. D. A., HIRST, B. H. and SIMMONS, N. L. (1993a). H^+-coupled dipeptide (glycylsarcosine) transport across apical and basal borders of human intestinal Caco-2 cell monolayers display distinctive charcteristics. *Biochimica et Biophysica Acta*, **1151**: 237-245.

THWAITES, D. T., McEWAN, G. T. A., BROWN, C. D. A., HIRST, B. H. and SIMMONS, N. L. (1993b). Na^+-independent, H^+-coupled transepithelial β-Alanine absorption by human intestinal Caco-2 cell monolayers. *The Journal of Biological Chemistry*, **268**: 18438-18441.

THWAITES, D. T., McEWAN, G. T. A., COOK, M. J., HIRST, B. H. and SIMMONS, N. L. (1993c). H^+ coupled (Na^+-independent) proline transport in human intestinal (Caco-2) epithelial cell monolayers. *FEBS letters*, **333**: 78-82.

TRIADOU, N., BATAILLE, J. and SCHMIT, Z. (1983). Logitudinal study of the human intestinal brush border membrane proteins. *Gastroenterology*, **85**: 1326-1332.

TSUJI, A., SIMANJUNTAK, M. T., TAMAI, I. and TERASAKI, T. (1990). pH-dependent intestinal transport of monocarboxylic acids: Carrier-mediated and H+-cotransport mechanism versus pH-partition hypothesis. *Journal of Pharmaceutical Sciences*, **79**: 1123-1124.

TSUJI, A and TAMAI, I. (1996). Carrier-mediated intestinal transport of drugs. *Pharmaceutical Research*, **13**: 963-977.

UEDA, K., OKAMURA, N., HIRAI, M., TANIGAWARA, Y., SAEKI, T., KIOKA, N., KOMANO, T. and HORI, R. (1992). Human P-glycoprotein transports cortisol, aldosterone and dexamethasone but not progesterone. *Journal of Biological Chemistry*, **267**: 24248-24252.

URBATSCH, I. L., SANKARAN, B., BHAGAT, S. and SENIOR, A. E. (1995a). Both P-glycoprotein nucleotide binding sites are catalytically active. *Journal of Biological Chemistry*, **270**: 26956-26961.

URBATSCH, I. L., SANKARAN, B., WEBER, J. and SENIOR, A. E. (1995b). P-glycoprotein is stably inhibited by vanadate-induced strapping of nucleotide at a single catalytic site. *Journal of Biological Chemistry*, **270**: 19383-19390.

URDANETA, E., BARBER, A., WRIGHT, E. M. and LOSTAO, M. P. (1998). Functional expression of the rabbit intestinal Na^+/L-proline cotransporter (IMINO system) in *Xenopus laevis* oocytes. *Journal of Physiological Biochemistry*, **54**: 155-160.

VREE, T. B., BAARS, A. M., BOOIJ, L. H. D. and DRIESSEN, J. J. (1981). Simultaneous determination and pharmacokinetics of midazolam and its hydroxymetabolites in plasma and urine of and and dog by mean of high performance liquid chromatography. *Artzneimittelforschung*, **31**: 2215-2219.

WALTER, E and KISSEL, T. (1994). Transepithelial transport and metabolism of thyrotropin-releasing hormone (TRH) in monolayers of a human intestinal cell line (Caco-2): Evidence for an active transport component. *Pharmaceutical Research*, **11**: 1575-1579.

WANG, H., KAVANAUGH, M. P., ALAN NORTH, R. and KABAT, D. (1991). Cell-surface receptor for ecotropic murine retroviruses is a basic amino-acid transporter. *Nature*, **22**: 729-731.

WATANABE, T., INABA, M. and SUGIYAMA, Y. (1989). Saturable process involved in active efflux of vincristine as a mechanism of multidrug resistance in P388 leukaemia cells. *Pharmaceutical Research*, **6**: 690-696.

WATCHER, V. J., WU, C-Y. and BENET, L. Z. (1995). Overlapping substrate specificities and tissue distribution of cytochrome P450 3A and P-glycoprotein: Implications for drug delivery and activity in cancer chemotherapy. *Molecular Carcinogenesis*, **13**: 129-134.

WATKINS, P. B., WRIGHTON, S. A., SCHUETZ, E. G., MOLOWA, D. T. and GUZELIAN, P. S. (1987). Identification of glucocorticoid-inducible cytochromes P-450 in the intestinal mucosa of rats and man. *Journal of Clinical Investigation*, **80**: 1029-1036.

WATKINS, P. B. (1994). Interpatient heterogeneity in expression of CYP3A4 and CYP3A5 in small bowel. Lack of prediction by the erythromycin breath test. *Drug Metabolism and Disposition*, **22**: 947-955.

WATKINS, P. B. (1997). The barrier function of CYP3A4 and P-glycoprotein in the small bowel. *Advanced Drug Delivery Reviews*, **27**: 161-170.

WENZEL, U., THWATES, D. T. and DANIEL, H. (1995). Stereoselective uptake of β-lactam antibiotics by the intestinal peptide transporter. *British Journal of Pharmacology*, **116**: 3021-3027.

WILKINSON, G.R. (1997). The effects of diet, ageing and disease-states on pre-systemic elimination and oral drug bioavailability in humans. *Advanced Drug Delivery Reviews*, **27**: 129-159.

WILLIGHAM, M. C., RICHERT, N. C., CORNWELL, M. M., TSURUO, T., HAMADA, H., GOTTESMAN. M. M. and PASTAN, I. H. (1987). Immunocytochemical localization of P170 at the plasma membrane of multidrug-resitant human cells. *Journal of Histochemistry and Cytochemistry*, **35**: 1451-1456.

WILS, P., PHUNG-BA, V., WARNERY, A., LECHARDEUR, D., RAEOSSI, S., HILDAGO, I. J. and SCHERMAN, D. (1994). Polarised transport of docetaxel and vinblastine mediated p-glycoprotein in human intestinal epithelial cell monolayers. *Biochemical Pharmacology*, **48**: 1528-1530.

WOODLEY, J.F. (1994). Enzymatic barriers for GI peptides and protein delivery. *Critical Reviews in Therapeutic Drug Carrier Systems*, **11**: 61-95.

WOOSLEY, R. L. (1996). Cardiac actions of antihistamines. *Annual Review of Pharmacology and Toxicology*, **36**: 233-252.

WRIGHTON, S. A., RING, B. J., WATKINS, P. B. and VANDENBRADEN, M. (1989). Identification of a polymorphically expresed member of the human cytochrome P-450III family. *Molecular Pharmacology*, **36**: 97-105.

WRIGHTON, S. A., BRIAN, W. R., SARI, M-A., IWASAKI, M., GUENGERICH, F. P., RAUCY, J. L., MOLOWA, D. T. and VANDENBRADEN, M. (1990). Studies on the expression and metabolic capabilities of human liver cytochrome P450IIIA5 (HLp3). *Molecular Pharmacology*, **38**: 207-213.

WRIGHTON, S. A and RING, B. J. (1994). Inhibition of human CYP3A catalysed 1'-hydroxymidazolam formation by ketoconazole, nifedipine, erythromycin, cimetidine and nizatidine. *Pharmaceutical Research*, **11**: 921-924.

WU, C-Y., BENET, L. Z., HEBERT, M. F., GUPTA, S. K. and ROWLAND, M. (1995). Differentiation of absorption and firs-pass gut and hepatic metabolism in humans: Studies with cyclosporin. *Clinical Pharmacology and Therapeutics*, **58**: 492-497.

YANG, C. P-H., GOEI DE PINHO, S., GREENBERGER, L. M., ARCECI, R. J. and HORWITZ, S. B. (1989). Progesterone interacts with P-glycoprotein in multidrug-resistant cells and in the endometrium of gravid uterus. *Journal of Biological Chemistry*, **264**: 782-788.

ZAMAN, G. J. R., FLENS, M. J., VAN LEUSDEN., M. R., DE HAAS, M., MULDER, H. S., LANKELMA, J., PINEDO, H. M., SCHEPER, R. J., BAAS, F., BROXTERMAN, H. J. and BORST, P. (1994). The human multidrug resistance-associated protein MRP is a plasma membrane drug efflux pump. *Proceedings of National Academy of Sciences, USA*, **91**: 8822-8826.

ABBREVIATIONS

ACE	Angiotensin-converting enzyme
A-B	Apical-to-basolateral
B-A	Basolateral-to-apical
BCA	Biocinchoninic acid
BSA	Bovine serum albumin
°C	Degree Celcius
Ci	Curie
cm	Centimetre
CO_2	Carbon dioxide
CPM	Counts per minute
CsA	Cyclosporin A
CYP3A4	Cytochrome P450 3A4
kDa	Kilodalton
DMEM	Dulbecco's Modified Eagle Medium
DMSO	Dimethylsulphoxide
2,4-DNP	2,4-dinitophenol
DPM	Decays per minute
EDTA	Ethylenediaminetetraacetic acid
FCS	Foetal calf serum
FITC	Fluorescein isothyanate
fmol	Femtomole
g	Gravitational force
GI	Gastrointestinal
HBSS	Hank's balanced salt solution
HEPES	N-[2-hydroxyethyl]piperazine-N'-[2-ethanesulphonic acid]
HPLC	High performance liquid chromatography
K_d	Diffusion rate constant
Km	Michaelis constant
M	Molar
MES	2-[N-morpholino]ethanosulphonic acid
mg	Milligram
MDZ	Midazolam
min	Minute

mol	Mole
MW	Molecular weight
NEAA	Non-essential amino acids
nmol	Nanomole
1-OH MDZ	1-hydroxymidazolam
4-OH MDZ	4-hydroxymidazolam
O_2	Oxygen
Papp	Apparent permeability coefficient
PBS	Phosphate buffered saline
P-gp	P-glycoprotein
pmol	Picomol
PMSF	Phenylmethylsulphonide fluoride
PVDF	polyvinylidene difluoride
se	Standard deviation of the population mean
sd	Standard deviation of sample mean
SDS	Sodium dodecyl sulphate
TBS	Tris-buffered saline
TBST	Tris-buffered saline Tween
TDS	Di-/tripeptide transport system
TX-100	Triton-X 100
Vmax	Maximum velocity
%	Percentage
µL	Microlitre
µm	Micrometre
µM	Micromolar
Ω	Ohm

LIST OF PUBLICATIONS TO DATE

TRAN, C. D. H., CONWAY, B. R., TIMMINS, P. and IRWIN, W. J. (1999). 1α, 25-Dihydroxyvitamin D_3 increased cytochrome P450 3A4 protein expression in Caco-2 cells on Costar collagen-coated inserts but did not up-regulate P-glycoprotein (P-gp) function in doxorubicin-exposed Caco-2 cells. *Journal of Pharmacy and Pharmacology*, **51** (Suppl): 155.

TRAN, C. D. H., TIMMINS, P., CONWAY, B. R. and IRWIN, W. J. (1999). Non-parallel expression of cytochrome P450 3A and P-glycoprotein in Caco-2 cells. Poster presentation, Annual meeting of American Association of Pharmaceutical Scientists (New Orleans, USA, 14-18 November, 1999).

TRAN, C. D. H., TIMMINS, P., CONWAY, B. R. and IRWIN, W. J. (1999). Lower expression of di-/tripeptide transporter in doxorubicin-exposed Caco-2 cells. Poster presentation, Annual meeting of American Association of Pharmaceutical Scientists (New Orleans, USA, 14-18 November, 1999).